Water Spray Suppression and Intensification of High Flash Point Hydrocarbon Pool Fires

by

San-Ping Ho

A Dissertation

Submitted to the Faculty

of the

WORCESTER POLYTECHNIC INSTITUTE

in partial fulfillment of the requirements for the

Degree of Doctor of Philosophy

in

Fire Protection Engineering

By

August 2003

APPROVED:

Professor Robert G. Zalosh, Major Advisor

Professor John Woycheese, Co-Advisor

Dr. Hong-Zeng Yu, Co-Advisor, FMGlobal

Professor David A. Lucht, Department Head

ABSTRACT

The primary purpose of this research was to quantify fire suppression and fire intensification phenomena for water spray application to high flash point hydrocarbon oil pool fires. Test data and analyses of the phenomena include the drop size distribution and application and delivered densities of various water sprays, and spray-induced oil cooling and oil splattering for mineral seal oil and for cooking oil 30-cm diameter pool fires. Four different types of tests were conducted as described below.

A Dantec Particle Dynamic, phase Doppler, Analyzer was used to measure the water drop sizes and velocities generated by 13 selected nozzles and sprinkler heads. Most measurements were made 0.91 m (3 ft) below the nozzles/sprinklers, since this was the location of the center of the hydrocarbon pool in later fire tests. The correlations for the volume-median drop diameter, $d_{w,}$ were of the form $\frac{d_w}{D} = \frac{C}{We_n^m}$, where D is the nozzle orifice and We_n is the spray Weber number based on D and the nozzle velocity.

A ring burner was designed and constructed for uniformly heating oil pool surfaces from above and igniting them. The resulting oil temperatures while the oil was heated to its flash point satisfied the one-dimensional transient heat conduction model for a semi-infinitely thick solid with a shallow heated layer near the surface. Water sprays actuated when the oil surface temperature reached its flash point rapidly cooled the heated layer and caused mixing with the cooler oil below.

Fire suppression tests were conducted to determine the relationship between required water spray density, drop size, and oil temperature in order to achieve suppression. A data correlation using non-dimensional parameters was developed to quantify the fire suppression criteria for the high flash point oil fires. Oil pool fires with the higher flash point oils, such as the 291^{o}C flash point soybean oil, could be suppressed with much lower water densities than those of the lower flash point (137^{o}C) mineral seal oil. However, if the water spray drop sizes are sufficiently small, the lower flash point oil fires can also be extinguished with lower spray densities. The NFPA 15

specified critical water density (0.30 gpm/ft^2, 12 mm/min) to extinguish high flash point pool fires is only valid for mineral seal oil when the drop size is lower than about 300 μm. It is valid with larger drop sprays only when the flash point of the oil is higher than $190^{\circ}C$ according to the correlation developed here.

Spray-induced pool fire intensification tests were conducted under a fire products calorimeter for measuring heat release rates. Supplemental oil vaporization rate tests were also conducted to determine the contributions of oil vaporization and oil splattering to the intensified fire. Results showed that vaporization could only account for between 1% and 1.7% of the heat release rate in intensified mineral seal oil fires, and less than 1% of the heat release rate in intensified soybean oil fires. The remainder is due to spray-induced oil splattering, which increased with increasing drop Weber number as well as increased oil temperature. The heat release rate is enhanced by factor from 2.12 to 5.55 compared to the heat release rate of free burning cooking oil. For mineral seal oil, this ratio is in the range 0.92 to 1.25 for the spray conditions tested. Correlations with the dimensionless factors of $\frac{\Delta H_w}{C_{pl}(T_{fluid}-100)}$ and the Weber number of the water spray were also developed to quantify the ratio of the splattered oil to applied spray density.

Acknowledgements

Highly appreciates to Professor Robert Zalosh for leading me to the fire protection research. His high standards have challenged me a better career in the future. His encouragements and helps are so important for me to achieve this degree. I would also like to thank Dr. Hong-Zeng Yu for helping me about the theory and tests in FMGlobal these three years. His excellent sprinkler technology helps me to understand more about water spray and fire suppression. Professor Woycheese is also highly appreciated for his words in the dissertation.

Dr. Paul Croce, Mr. Jeffrey Newman, Dr. H.C. Kung, Patricia Beaulieu, Blair Swinnerton, Daniel Zielinski, and the staff in FMGlobal Research are all highly appreciated for their supports, helps and words in my dissertation.

To my parents, parents in law, wife, and family for their fully support. Especially my wife takes good care of my three kids so many years. Her sacrifice contributes so much to my achievement.

TABLE OF CONTENTS

LIST OF FIGURES

LIST OF TABLES

1 Introduction

Water spray is widely used for protecting combustible liquid pool fires. Combustible liquids are defined as liquids having a flashpoint at or above 37.8 ^{o}C (100 $^{\circ}$F) for a closed cup test. They are further classified as Class II, Class IIIA, and Class IIIB [43]. A Class II liquid is defined as any liquid that has a flash point at or above 37.8 ^{o}C (100 ^{o}F) and below 60 ^{o}C (140 ^{o} F). A Class IIIA liquid has a flash point at or above 60 ^{o}C (140 ^{o}F), but below 93 ^{o}C (200 ^{o}F). Class IIIB liquids have a flash point at or above 93 ^{o}C (200 ^{o}F) and are the liquids that will be addressed in this dissertation.

Typical Class IIIB liquids are cooking oils, lubricating oils, transformer oils, residual fuel oil, heat transfer fluids, and various liquids used in chemical processing plants. The flash points for some of these oils are listed in Table 1.1.

Table 1.1 Flash points for typical combustible oils.

Materials	Transformer oil (*1)	Cooking oil (Peanut oil)(*2)	Fatty acid (*3)	Mineral seal oil (*4)
Flash point , $^{\circ}C$ ($^{\circ}F$)	146-300 (295-572)	282 (540)	138-204 (280-400)	137 (280)

*1: Data from FMGlobal Data Sheet 5-4 and NFPA 325

*2: Data from NFPA 325

*3 Data from Procter and Gamble OL-700C Material Safety Data Sheet

*4 Data from Gulf Mineral Seal Oil Material Safety Data Sheet

For most transformer oil fires, an explosion ruptures the transformer, and causes the transformer oil to burn on the unheated substrate, such as transformer pad. Per NFPA 15 paragraph 7.4.4.3.1 the water shall be applied at a net rate not less than 10.2 mm/min (0.25 gpm/ft^2) on the projected area of rectangular prism envelope for the transformer and its appurtenances, and not less than 6.1 mm/min (0.15 gpm/ft^2) on the expected nonabsorbing ground surface area of exposure. For most lubricating oil fires, a spray of oil from a ruptured oil line is ignited by contact with a hot

surface, such as a hot bearing. Unburned oil forms a pool, which is exposed to the heat flux of the spray fire and if eventually causes a pool fire. The water spray density to control the fire per NFPA 15 paragraph 7.3.3 for this scenario is 12.2 mm/min (0.30 gpm/ft^2). If automatic sprinklers are used, a discharge density of 8.1 mm/min (0.2 gpm/ft^2) over the room area is currently recommended in FMGlobal Data Sheet 5-4 [19] .

A fryer cooker fire is one example of a cooking oil fire. An explosion of oil vapor could occur in the duct because the oil is heated to close to its flash point and a lot of vapor is sucked into the duct. The burner of the oil heat source could ignite the leak oil or the oil could autoignite, resulting in a pool fire. FMGlobal Data Sheet 7-20 [20] , revision 1.1, recommended that oil cookers be protected with ¼-in. orifice or smaller open, stainless steel, wide-angle (120^o or greater) discharge water spray nozzles at a 20.4 mm/min (0.5 gpm/ft^2) density.

NFPA 34 [44] requires that dipping and coating processes using Class IIIB fluids should be located only in buildings that are protected throughout by an automatic sprinkler system. If these processes are located in an unsprinklered building, a sprinkler system must be installed to protect the processing area. NFPA 30 [43] also requires that an approved automatic fire extinguishing system protect tank storage of Class IIIB liquids inside a building. These codes specify requirements such as sprinkler water density and water supply. The water density is required from 8.1mm/min (0.2 gpm/ft^2) to 12.2 mm/min (0.3 gpm/ft^2) for different rack storage of combustible IIIB liquid per NFPA 30.

The fire extinguishment mechanism of high flash point non-water miscible fluid pool fire depends on the heat transfer between water drops and combustible liquid near the burning surface, water vaporization on the oil surface, water boiling vaporization, and oil splattering. Effective heat transfer rate between water droplets and fuel liquid will enhance the extinguishments of combustible liquid fire. As water vaporizes on the fuel surface, it absorbs heat and helps to extinguish the fire. Water boiling vaporization will enhance the heat removed from the oil, but more splattering of the fuel surface will intensify the fire. Based on test results of mineral seal oil and soybean cooking oil, these four factors will play important roles for fire extinguishment. In order to design an effective spray system for fire suppression, this

extinguishment mechanism depending on the fuel density, fuel viscosity, surface tension, water drop velocity, water drop particle size, and water flux when the water spray is applied to a deep fuel pool is discussed in this research.

The mineral seal oil and cooking oil pool fires were selected for test purposes, because they are representative of class IIIB hydrocarbon liquid pool fires that are often difficult to extinguish using water sprays. The flash point of mineral seal oil, $137^{\circ}C$ $(280^{\circ}F)$, is slightly higher than the minimum flash point $93\ ^{\circ}C$ $(200^{\circ}F)$ for class IIIB combustible liquid and the flash point of cooking oil is $291^{\circ}C$ $(556^{\circ}F)$ is much higher than the minimum flash point.

The Mineral seal oil (CAS Number 64742-46-7) was obtained from the Citgo Petroleum Corporation (Product Number 2540), and is described in the Citgo Material Safety Data Sheet (MSDS) as a hydrotreated petroleum middle distillate. The soybean oil (cooking oil) was obtained from Ashland Chemical Company, and is described in the MSDS as fatty acid vegetable oil of secret composition. The mineral seal oil advises use of foam, water fog, or water spray for large fires, but contains that the foam/water may cause frothing and may not achieve extinguishment. The soybean oil MSDS advises that water of foam may cause violent frothing.

2 Literature Review

2.1 Droplet Impact on Solid and Liquid Surface

Worthington [72] used a droplet of milk into water to observe the splash and described the development of the splash phenomena. He found that the droplet produced a crown-like crater and a tall rebounding column as shown in Figure 2.2.

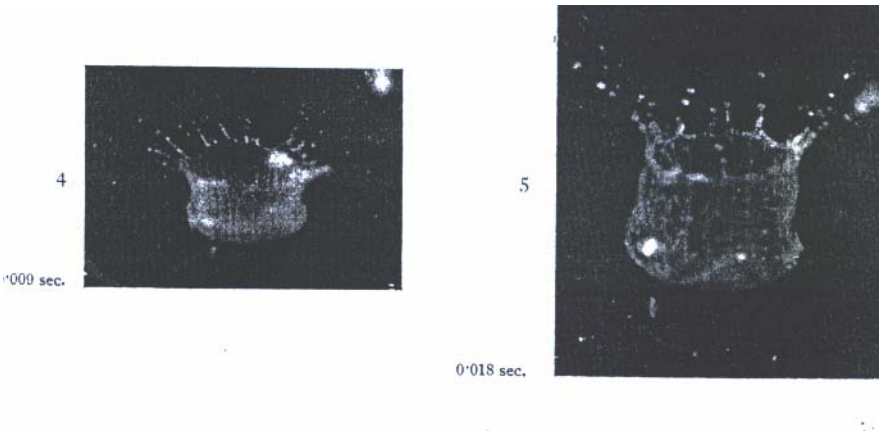

Figure 2.2 The crater and rebounding column for a droplet of milk into water.

Wachters, et al., [9] performed an analysis of the splashing impact of droplets of different liquids in diameters of 2-3 mm against a hot (about $400\,^{o}C$) dry wall. They used a single dimensionless number, Weber number (We= $\frac{\rho u^2 d}{\sigma}$), to describe the disintegration process of drops after impact. For drops of We <30, no splash were observed; a drop in the range 30<We<80, broke after it bounced back from the wall; and, for drops of We > 80, splash occurred.

Bernardin [4] states that drop velocity and surface temperature are two important parameters governing the impact behavior. He observed water drops impinging on a polished surface, and defined four distinct heat transfer regimes of the boiling curve: single-phase regime, nucleate boiling regime, transition boiling regime, and film boiling regime.

A single water drop striking on the wetted solid surface was investigated by Cossaii et al [9]. They found that another parameter in addition to the Weber number would affect the splash

scenario. They also identified that the Ohnesorge number (Oh=$\frac{\mu}{(d\sigma\rho)^{1/2}}$) appears to play an important role in defining the splash morphology in addition to the influence of the film thickness and liquid viscosity on the splash. Four phases can be identified for evolution of the splash: 1) crown formation and jetting, 2) rim instability and jet formation, 3) break-up of the jets and formation of secondary droplets, and 4) crown collapsing period. For high viscosity liquid droplets, secondary droplets were observed to detach only after full development of the crown, and the droplets could begin to detach from jets even during the crown-collapsing period in their tests.

Shiraz, et al., [61] derived the droplet splashing correlation when a molten tin droplet was dropped on a stainless steel surface as shown on Figure 2.2. The number of fingers of the crown is proportional to $\sqrt{\frac{We\sqrt{\mathrm{Re}}}{48}}$, if $\frac{We}{\sqrt{\mathrm{Re}}} >> 1$, and We>>12.

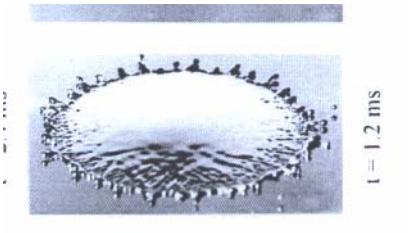

Figure 2.2 Splash scenario for molten tin droplet on a stainless steel surface.

Zhang, et al., [79] studied the splat morphology and rapid solidification for molybdenum droplets impacting on molybdenum, mild steel, and glass substrate. They developed a correlation between the splat flattening ratio and the Reynolds ($\frac{\rho u d}{\mu}$) and Jakob number ($Ja = c_s(T_f - T_{sub})/h_f$).

Macklin, et al., [33] found that a larger Weber number produces a thinner corona and an increase of the liquid volume in the corona. They also found that the total volume of secondary droplets

might reach 2 to 4 times the volume of the impinging drop. This suggests that a large quantity of hydrocarbon droplets can be generated from the impact of a water spray.

From the preceding review, it seems that most of the work has concentrated on single droplet dropped on a heated or unheated solid surface, or falling into water. The analysis of water spray on a heated oil pool has not been explored; that is examined in this research.

2.2 Flammable Liquids Fire Suppression Test

When water spray suddenly hit the surface of a burning combustible liquid with a low flash point and high boiling point, the rate of the fuel vaporization increased and created a rising fire ball as shown by Kokkala[28]. He also observed that a larger fire required a longer extinction time, and could remain uncontrolled indefinitely. For higher flash point liquids (about 126 $^{\circ}C$), the water spray may cool the fuel below the flash point and water vapor is produced to inhibit combustion. The droplet size and velocity were not measured during his tests. Kokkala also found different fire-spray interaction characteristics on liquid fuel surfaces as shown on Figure 2.3. Figure 2.3a shows shortened vertical flames because water spray cooling reduces the flammable liquid surface temperature and vaporization rate. Water spray with small drops and/or low velocity has more thermal effects than spray aerodynamic effects. Figure 2.3b shows flattened flames caused by the downward flow of air entrained into the spray overcoming the fire plume buoyancy. This is the interaction with large heavy water drops or a high velocity water spray. Figure 2.3c shows a wind-blown flame. Figure 2.3d shows an intensified flame associated with the sputtering of water droplets reaching the surface of a high flash point flammable liquid. Small water drops have a short sputtering time. Figure 2.3e shows what Kokkala calls ridge flames observed near extinction when most of the liquid surface is flame free. These ridge flames are observed with a high velocity, small droplet water spray. Figure 2.3f shows rim flames produced just prior to extinguishment because the container wall remains hot after the spray has cooled the free surface of the interior liquid.

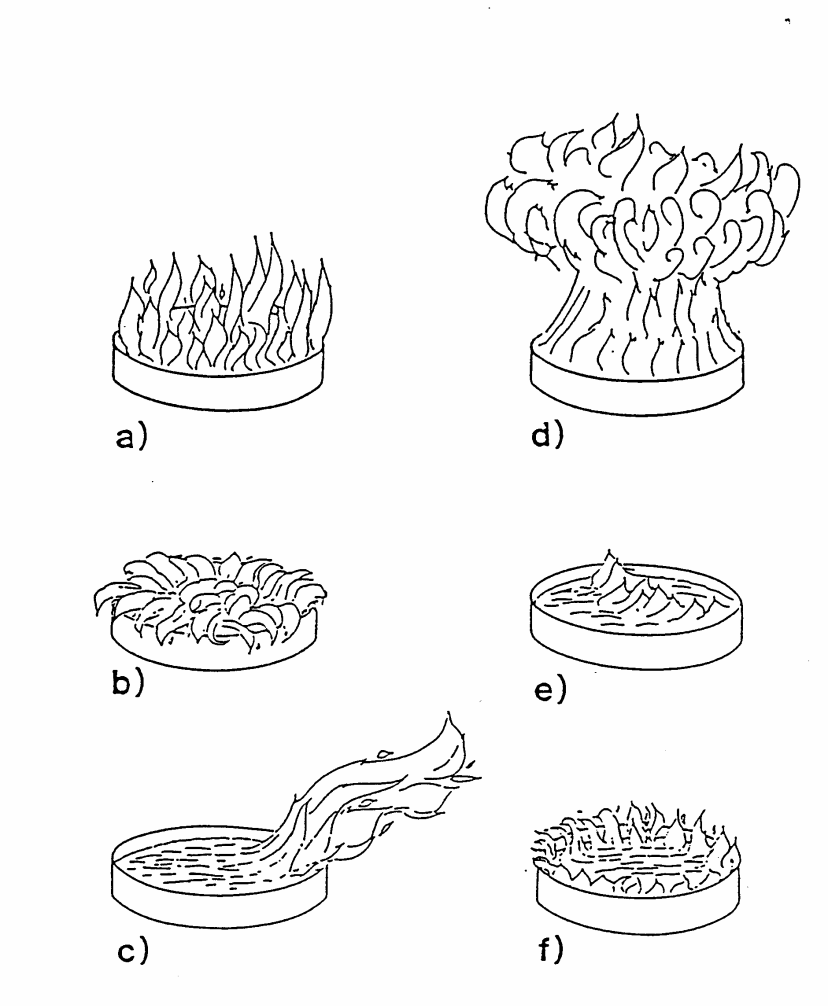

Figure 2.3 Characteristic flame shapes during water application: (a) shortened vertical flames, (b) flattened flames, (c) blown flames, (d) rising fire ball, (e) ridge flame, and (f) rim flame.

Rasbash [52–58] has run some high flash point pool fire tests with kerosene and transformer oil and he correlated the spray density required to cool the liquid surface to its flash point as shown in Equation 2-1. He also correlated the extinguishment time to the relationship between water densities, drop size, and oil flash point as shown on equation 2-2.

$$\dot{R}''_{cr,w} = Kd_w/(T_{FP} - T_w) \qquad (T_{FP} - T_w > 40^oC) \qquad 2\text{-}1$$

The constant K is between 6-12 gpm $^oC/ft^2 - mm$.

$$t_{ext} = 6.7 \times 10^5 \times \dot{R}_w''^{-2/3} d_w^{\,0.85} (T_{FP} - T_w)^{-5/3} \qquad (T_{FP} - T_w > 40^o C) \qquad \text{2-2}$$

Where:

$\dot{R}''_{cr,w}$: spray density required to cool the liquid surface to its flash point (gpm/ft^2)

d_w: water mass median diameter $(mm, d_w > 0.4mm)$

T_{FP}: flash point (^0C)

T_w: water temperature (^0C)

t_{ext}: fire extinguishment time (s)

$\dot{R}''_w$: applied water density (gpm/ft^2)

Nam [36] (2000) conducted extinguishment tests with three test mock-ups that simulated industrial oil cookers for 10 ft long by 8 ft wide, 20 ft long by 8 ft wide and 40ft long by 8ft wide dimensions. 0.5 gpm/ft^2 provides the best protection based on the extinction time for ¼ in. spray nozzles installed 30 in. above the oil surface. The temperature of the cooking oil was below its flash point ($460^\circ F$) when the fire was extinguished. He also found that inadequate water application intensified the high flash point pool fire because the vaporized water droplets below the pool surface and splashing water carry more fuel droplets into the air to intensify the fire.

Wang [68] (2002) conducted kerosene and alcohol pool fires and found that the fire was more difficult to extinguish for larger distance from 1 meter to 1.8 meter between fuel surface and the nozzle. He also found that a higher water density can suppressed the kerosene fire easier than the alcohol fire. He related the higher water density to a higher operating pressure but he did not really measure the required water density in his tests.

Kim et. al.[26]–[27] (1996, 1997) conducted an extensive series of laboratory tests with water spray applied to 15 cm diameter gasoline pool fires. Their water sprays had Sauter Mean Diameters in the range 30 μm to 72 μm depending on nozzle pressure. They observed fire suppression when the spray application density was greater than 6.5 ±0.5 mm/min (0.16 gpm/ft^2), and fire intensification with spray densities below this critical value. They surmise that spray cooling of the burning fuel surface is the dominant suppression mechanism, and that spray thrust aerodynamically spreads out the flame and enhances the burning rate at sub-critical water spray densities.

Eisenberg et al[17] conducted several small-scale tests that showed that the water spray would temporarily intensify the fire in a small fatty acid pool. The flashpoint of the test oil was 380^{o}F. In these tests, the pressure of the ¼-in. Bete nozzle was at 20 psig and the sample was put in a 4-in. pan, 5ft below the nozzle. The water spray eventually suppressed the fires.

Notarianni [45] reviewed the water mist fire suppression literatures. She pointed out that a practical system successfully extinguished hydraulic fluid and diesel oil fire in submarine compartments and smaller fires were harder to extinguish than larger fires for water mist systems in compartments, because the larger fires provided higher water vapor and CO_2 concentration in the compartments.

Although these previous research projects focused on some fire suppression phenomena and some quantitative analysis of the results, more detailed analysis and correlations are provided by this research to describe the suppression of high flash point pool fires.

2.3 Water Drop Size and Velocity Measurement and Analysis

Yao et al [73] described the relationship between the particle diameter and experimental terminal velocity. Hung [24] used the simplified steady state momentum conservation equation for the relationship of terminal velocity and drop size. They also used computational fluid dynamics to simulate the dynamics of spray droplets impacting on objects with a complex geometry.

Dundas [16] used photography to measure the drop size of different sprinkler heads. He used 30 data points from different spray and sprinkler heads to correlate the data as shown in equation 2-3.

$$\frac{d_w}{D} = \frac{1.413}{We_n^{0.328}} \qquad 2\text{-}3$$

Where:

d_w : water drop size (mm)

D: nozzle diameter (mm)

We_n : Weber number in the nozzle based on nozzle velocity

Yu [75][76] used a laser-illuminated optical array-imaging device to measure the drop size from 100 μm to 6400 μm. This is a better approach for measuring drop size than drop freezing and still photography. He found the volume median drop sizes are 860 μm, 1000 μm, and 1370 μm at 206-kpa pressures for a 12.7-mm standard sprinkler, a 13.5-mm large orifice sprinkler, and a 16.3-mm sprinkler, respectively. He also measured drop terminal velocities during the tests. The terminal velocities he obtained was close to but a little bit smaller than the results of Yao's tests.

Chan [7] also used the same instrument as Yu's to measure the particle size of ESFR sprinklers. He obtained a volume median drop size of 670 μm at 345 –kpa pressure for a K-14 ESFR sprinkler.

Widmann [70] used a Phase Doppler Interferometry (PDI) system to characterize the water sprays produced by four residential fire sprinklers. The measurements include characteristic sizes, mean velocity and liquid volume flux and the uncertainty analysis also showed the PDI can be used to accurately characterize the sprays produced by residential sprinkler.

Yu's [75][76] device can only measure 100 μm to 6400 μm of water drop sizes. The Dantec Phase Doppler Particle Analyzer (PDPA) can measure droplet sizes from 0.5 μm to 10,000 μm . This research included measurements of the velocities and drop sizes of 13 sprinklers and nozzles for fire suppression and oil suppression test analyses.

3 Thesis Scope and Approach

There are three objectives to be achieved in this thesis: to understand why and how water spray intensifies some combustible liquid pool fires and rapidly suppresses other pool fires; to develop quantitative criteria for predicting when intensification is expected and when suppression is expected; and to quantify fire intensification effects due to some water spray applications. In order to accomplish these objectives, a series of tests were designed as follows: Water drop size and velocity measurements, oil splattering tests and fire suppression tests. The water drop size and velocity are important parameters for this study, so they were measured by Dantec Particle Dynamic Analyzer before conducting fire suppression tests and the tests by spraying water drops onto a heated combustible liquid.

3.1 Measurement of Drop Size and Velocity

The Dantec Particle Dynamic Analyzer (PDA)[10][11] was used to measure water drop sizes and velocities of the Grinnell AM24, BETE WL 11/2 90°, Spraying Systems 1/8 GG full jet 2, 1/8HH-1.5, 1/8GG full jet 6SQ, 1/4GG full jet 10SQ, 3/8GG full jet 22, 3/8GG full jet 15, 3/8GG full jet 18SQ, 1/2GGfull jet 32, 1/2GG full jet 25, and 1/2GG full jet 29SQ nozzles. Appendix A shows the basic theory of particle size and velocity measurement for a PDA system and Appendix B photos 1 and 2 are the equipment pictures. The pan 91 cm (3 ft) under the nozzles was used to measure the water flux for different nozzles and different operating conditions.

Figure 3.1 shows the test layout. The height of the laser and receiving probe can be adjusted using the probe support. The nozzle location and height can be adjusted by the pipe support. A positive displacement pump or pressure tank was used to produce designed pressures for these nozzles. The vertical distance between the measurement point and the nozzle is 91 cm (3 ft for) all the measurements. Dantec PDA software was used to analyze the data online and also used to process the data for further analysis. These tests provided distributions of particle size and water density for these nozzles. Appendix B photos 3, 4, 5, and 6 are pictures for measuring water spray drop size and velocity by using the Dantec PDA system.

A humidifier was used to align the laser beam and get good reflection, refraction, or 2nd refraction signal. The refraction light is used for the measurement of water droplet in air based on Mie theroy. After the water discharged through the measurement zone, the PDA software was run to record the droplet size and velocity.

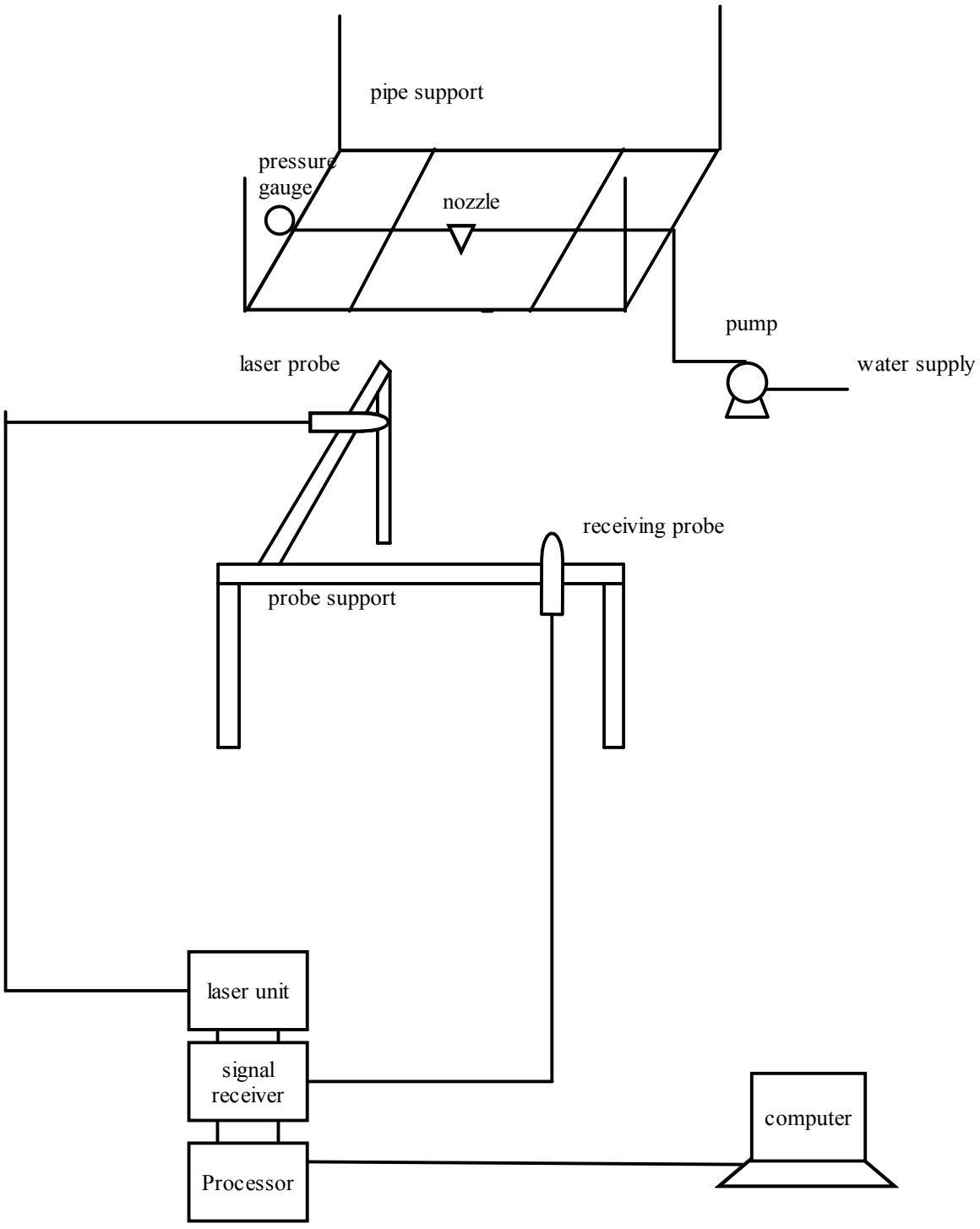

Figure 3.1 The layout for the measurement of particle size and velocity and water flux.

3.2 Oil Splattering Experiments

Oil splattering tests includes three series of tests. One is oil vaporization rate measurement at specific oil temperature and air velocities. The equipment setup is as shown in Figure 3.2. The 30.48 cm (12 in) oil pan was put on a heater and stirrer system and a load cell was inserted to measure the mass change under these tests. A temperature controller was used to control the temperature of the oil. Two thermocouples were inserted in the oil to check the temperature and one was used for the temperature controller. The load cell was used to measure the vaporization rates of mineral seal oil and cooking oil at specific temperature and air velocities. A fan located 91 cm (3 ft) from the center of the pan was used to provide horizontal wind velocities from 1m/s to 3.5 m/s by adjusting a motor controller. A spraying system 1/8 HH 1.5 spray nozzle located 91 cm (3 ft) above the center of the pan discharging air was used to provide vertical wind velocities from 1 m/s to 3.5 m/s by regulating the air pressure. Taylor Biram's Type Anemometer No.3132 measured these wind velocities.

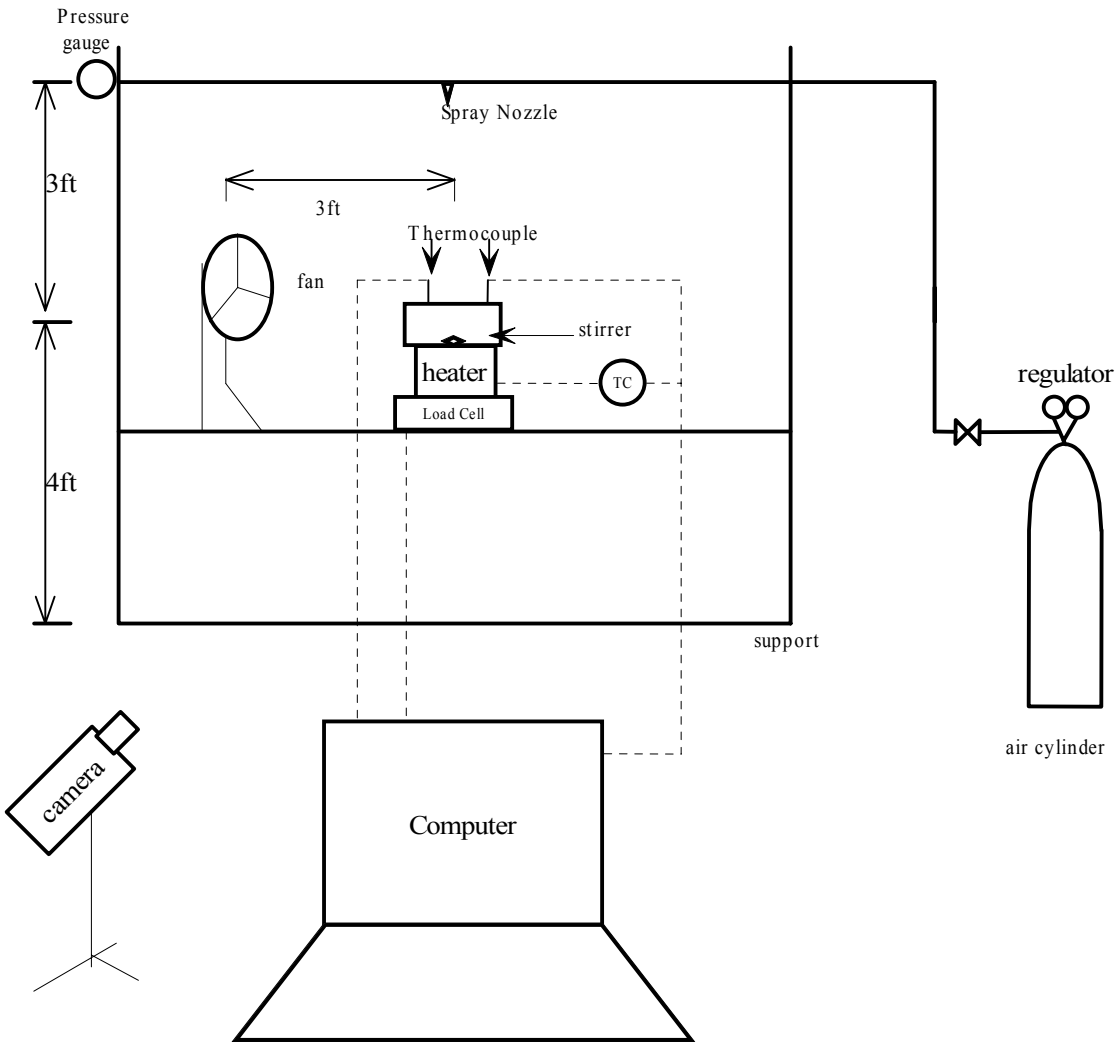

Figure 3.2 The equipment for oil vaporization rate measurement.

Another setup was used for oil splattering tests. Figure 3.3 shows the layout of the heated liquid splattering experiments for mineral seal oil and cooking oil. A heater inside the oil was used to heat the whole oil liquid to a specific temperature and then was removed. The six thermocouples were installed at different locations inside the steel pan, which is 30.48 cm (12-in.) diameter and 9.1 cm (3-in.) high. They were located at 5.1 cm (2in.) from the wall and 1.27 cm (½ in.), 2.54 cm (1 in.), 3.81 cm (1 ½ in.), 4.45 cm (1 ¾ in.), 5.1 cm (2 in.), 5.7 cm (2 ¼ in.) from the bottom of the pan. The oil was 3.81 cm (1 ½ in.) depth. A load cell was under the oil pan and covered by a metal cone to prevent water spray on the load cell. Two cameras were used to record the experimental results. One was used for the close-up view and another was used for overall view. A propane ring burner was used for pilot flame and installed 5.1 cm (2 in.) above the fuel

surface. Spray nozzles were installed 91 cm (3 ft) above the fuel surface and discharged specific flow rates, which were provided by a pump or pressure tank. Water was discharged after the burner was ignited.

Thermocouples were used to measure the fuel temperature during the entire course of the fire tests. Two heat flux gauges were set 91 cm (3ft) and 122 cm (4 ft) from the center of the pan and 30.48 cm (1ft) above the fuel surface. They were used to measure the radiant heat flux from the fire.

A Fire products collector was used to measure the heat release rate during some tests. The total heat release rate was calculated by equation 3-1 per ASTM E2058-01 as shown in appendix C. Carbon dioxide and carbon monoxide concentration are used to calculate the heat release rate for this fire products collector.

$$\dot{Q}_{chem} = [7.434 \times 10^{-2}(X_{co_2} - X_{co_{2,\infty}}) + 6.764 \times 10^{-3}(X_{co} - X_{co,\infty})](\frac{P_\infty \Delta P}{T_{gas}})^{1/2} \qquad 3\text{-}1$$

The third test series were to measure delivered densities. The equipment setup was the same as oil splattering tests but the tests procedure was changed as follows. The ring burner was ignited at propane flow rate of 0.85 (30), 1.13 (40), 1.42 (50), 1.70 (60), and 1.98 (70) m^3/hr (ft^3/hr) and water spray was discharged through the propane ring flame into the pan. The mass gain rate was obtained and used to calculate oil splattering rate in later analysis.

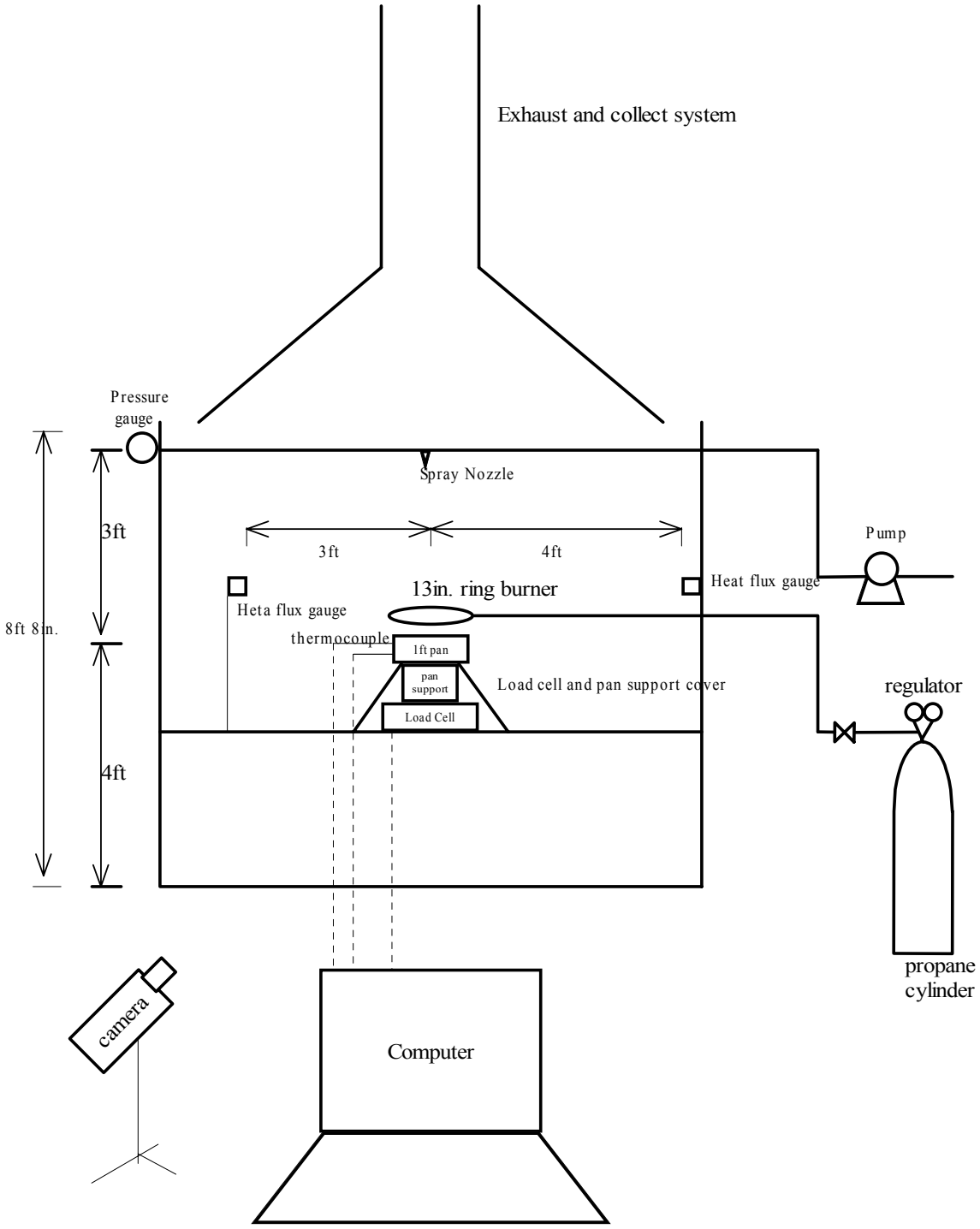

Figure 3.3 The layout of the heated liquid splattering experiments for mineral seal oil and cooking oil.

3.3 Fire Suppression Tests

Fire suppression tests include suppression and non-suppression tests. The layout is as shown in Figure 3.4. A 33 cm (13 in.) diameter propane burner 7.6 cm (3 in.) and 5.1 cm (2 in.) above the fuel surface was used to provide a heat flux source to heat the fuel surface and ignite the fuel for 137 $^{\circ}C$ flash point mineral seal oil and 291 $^{\circ}C$ flash point cooking oil. The burner was shut off and removed from the 30.48 cm (12 in.) diameter pan area when the oil was ignited on the surface. The fire sustained for 30 seconds to stabilize the burning and then water spray from 91 cm (3 ft) above the pan was discharged to the fire. The fire suppression process was observed and recorded for different nozzles and pressures that provided different water densities and drop sizes. Six thermocouples were installed at 5.1 cm (2 in.) from the wall and 1.27 cm (½ in.), 2.54 cm (1 in.), 3.81 cm (1 ½ in.), 4.45 cm (1 ¾ in.), 5.1 cm (2 in.), 5.7 cm (2-¼ in.) from the bottom of the pan. They were used to measure the fuel temperature during the entire course of the fire tests and the temperature profile of the oil was analyzed. If the fire was sustained for 2 minutes (before the oil was about to overflow the pan), the fire was deemed unsuppressed. The 30.48 cm (12 in.) diameter pan was within a 122 cm (4 ft) by 122 cm (4 ft) by 30.48cm (1 ft) large pan to prevent oil spread on the floor.

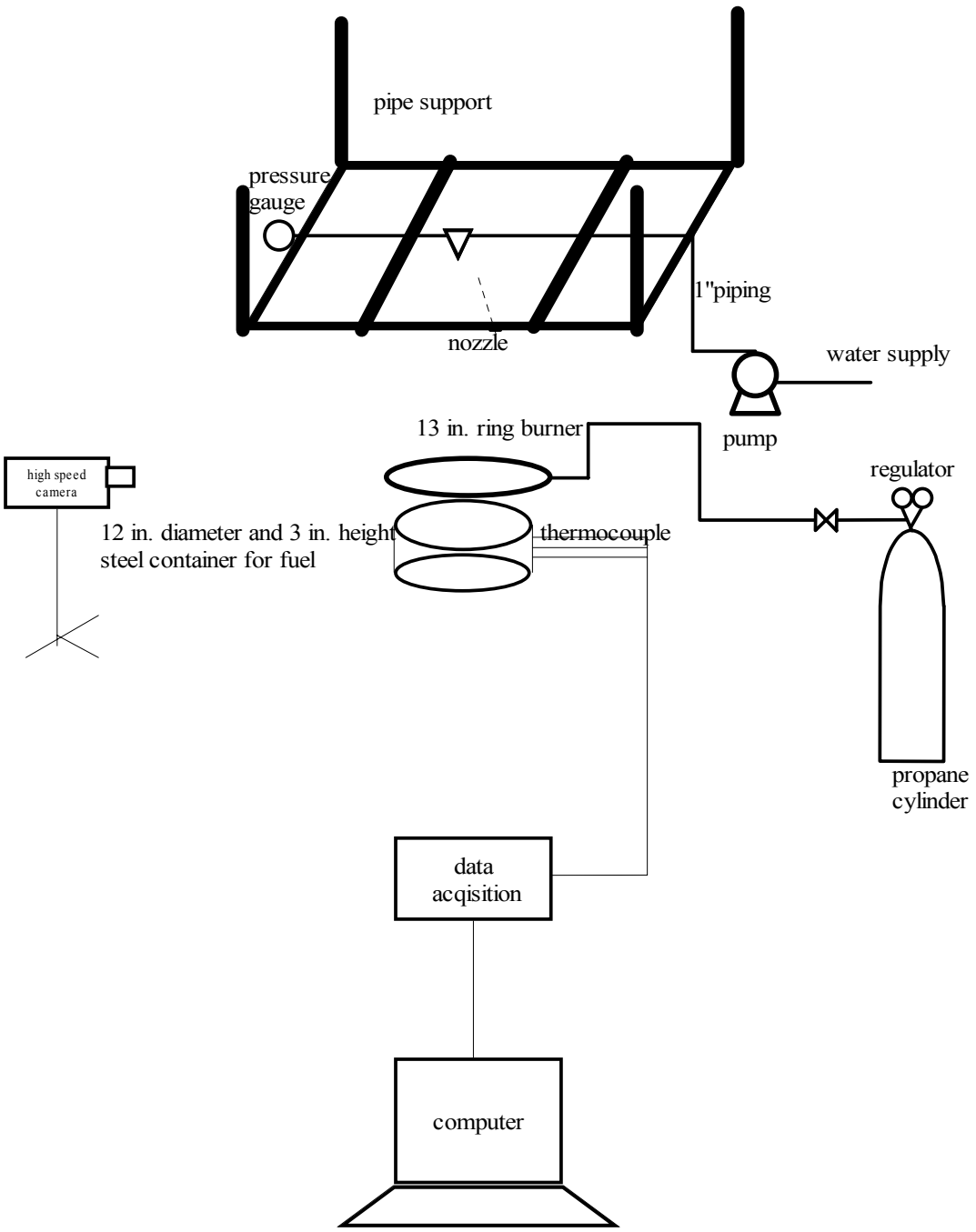

Figure 3.4 The layout for the splattering of heated oil when water discharge to the fuel.

4 Water Drop Size and Velocity Measurement

Water drop sizes, drop velocities and water fluxes were measured for the Grinnell AM24, BETE WL 11/2 90° , Spraying Systems 1/8 GG full jet 2, 1/8HH-1.5, 1/8GG full jet 6SQ, 1/4GG full jet 10SQ, 3/8GG full jet 22, 3/8GG full jet 15, 3/8GG full jet 18SQ, 1/2GGfull jet 32, 1/2GG full jet 25, and 1/2GG full jet 29SQ nozzles because these data are very important for further analysis of spray-surface interaction tests. The 100, 500, and 1000 μm glass bead tests show a good level of accuracy for these particle size measuring instruments.

Dundas [16] and Yu [75][76] used the correlation as equation 4-1 to predict volume median drop sizes for nozzles or sprinkler heads. The constant C was obtained to predict the particle size under different operating pressure. Yu's [75] result is as shown in Table 4.1. Chan [7] also used the same equipment to measure the drop size for ESFR K-14 sprinkler head. The constant C for the K-14 head is 1.78 as shown in Table 4.1.

$$\frac{d_w}{D} = \frac{C}{We_n^{1/3}} \qquad 4\text{-}1$$

Where: d_w is drop size (mm)

D is the orifice diameter (mm)

C is constant

We_n is Weber number based on water velocity at nozzle ($We_n = \frac{\rho_w u_n^2 D}{\sigma_w}$)

u_n = water velocity at nozzle

ρ_w = water density

σ_w = water surface tension

The drop sizes can be predicted from Equation 4-1, if the constant is obtained from the test data as shown in Table 4.1. When the operating pressure changes for a specific nozzle, Weber number also changes and equation Table 4.1 can be calculated to obtain the drop size for the operating pressure. Equation 4-1 is for the entire spray, and does not necessarily apply to a small area in a spray. Equation 4-2 is the modified equation to fit the test data in this research.

$$\frac{d_w}{D} = \frac{C}{We_n^m} \qquad 4\text{-}2$$

where: m is a constant for the specific nozzle

Table 4.1 Sprinkler constant C for different sprinkler heads from Yu and Chan.

Nozzle diameter (mm)	Water pressure (kPa)	Droplet size (mm)	Constant C
16.3(0.64in.)	206	1.66	4.3
13.5(17/32in.)	206	0.96	2.86
12.7(1/2in.)	206	0.86	2.33
19.1(0.75in)	345	0.67	1.78

A Dantec PDPA system was used for measuring the water drop sizes and velocities of these nozzles. The measured point was located at 0.91m (3ft) under the centerline of the nozzle. The following sections describe and discuss the details for each nozzle:

4.1 Spraying system 3/8GG 18SQ nozzle

Figure 4.1 shows the spraying system 3/8GG 18SQ nozzle. The 3/8 designation is the inlet connection pipe size, GG is nozzle type, 18 is the capacity that indicates a 1.8gpm flow rate at 10psi, and SQ is square type nozzle. The nozzle size D is 2.4 mm (0.094 in.). The drop size and velocity of this nozzle is as shown in Table 4.2. The cumulative distribution of particle size is based on test data. The PDA program provided 10% fraction volume diameter to 90% fraction volume diameter. The 10%, 50%, and 90% fraction volume diameter were listed in Appendix D. Rosin-Rammler correlation [10][11] as equation 4-3 is the data fit for reference to understand the trend of the fraction volume diameter. The actual fraction volume diameter should be obtained from the program to analyze data.

$$V_c = 1 - \exp[-(\frac{d_w}{x})^n] \qquad 4\text{-}3$$

where:

V_c is the percentage of volume fraction of water droplet

x , n are Rosin- Rammler constants from each test data

Equation 4-3 can be expressed as Equation 4-4 for spraying system 3/8GG18SQ nozzle that was operated at 69 kPa (10 psi) water pressure and the shape curve is as shown in Figure 4.2. X and n were calculated from PDPA program itself based on the test data fit.

$$V_c = 1 - \exp[-(\frac{d_w}{427})^{3.96}] \qquad 4\text{-}4$$

Five water pressures were used to produce different drop sizes and velocities for this nozzle. At higher pressure, smaller particle size and larger velocity were observed for this nozzle. Figure 4.3 shows linear regression from the test data by using Dantec PDPA system with constant C equal to 5.8 and the power of the Weber number equal to 1/3. The coefficient of determination

R^2 is 0.92 based on the measurement data. The drop size prediction correlation can be expressed as shown in Equation 4-5. This correlation is only available when the measured point was located at 0.91m (3ft) under the centerline of the nozzle.

$$\frac{d_w}{D} = \frac{5.8}{We_n^{1/3}} \qquad 4\text{-}5$$

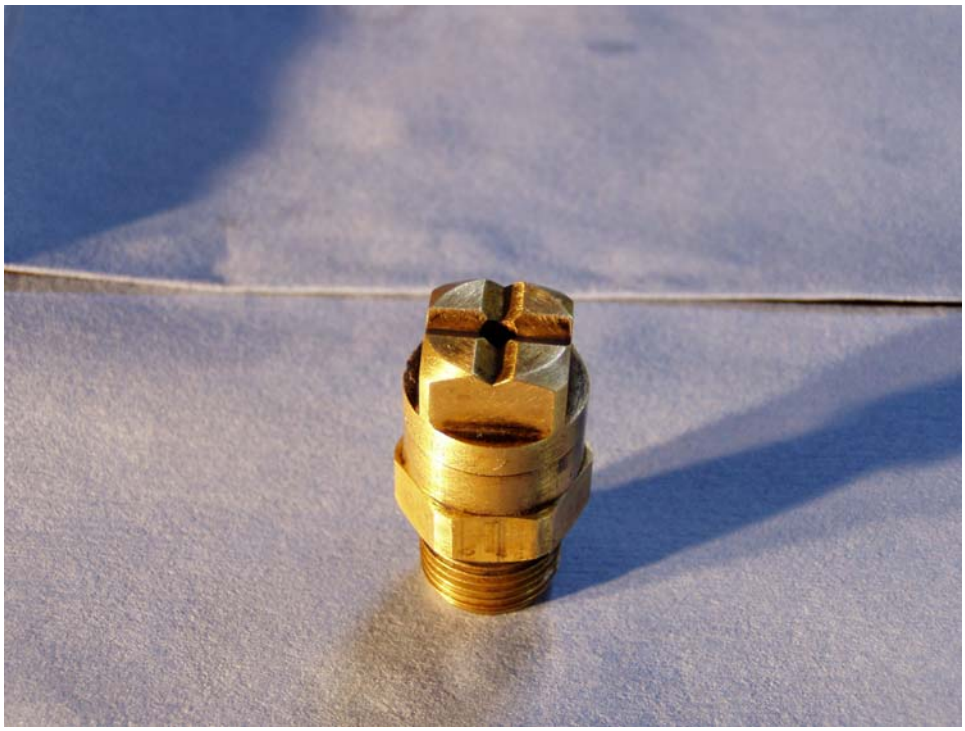

Figure 4.1 Spraying System 3/8GG, 18SQ Nozzle.

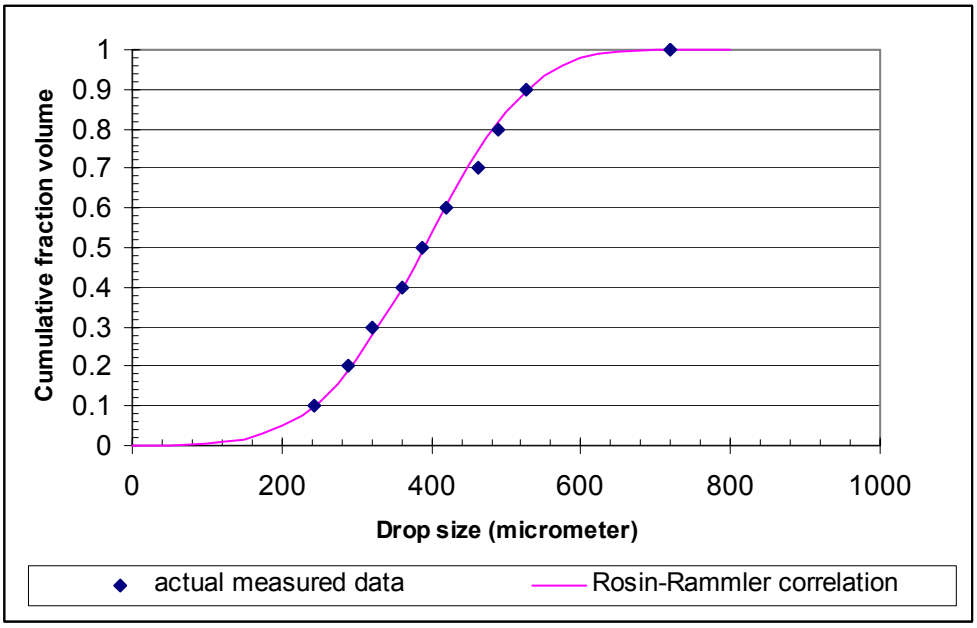

Figure 4.2 Rosin-Rammler curve and actual measured drop size distribution for Spraying System 3/8GG 18SQ nozzle at 10 psi water pressure.

Table 4.2 Water Drop Size, Velocity, and Rosin-Rammler Constants x and n Measured by Dantec PDA System and Water Density for Spraying System 3/8GG, 18SQ Nozzle at Different Operating Pressures.

Pressure , kpa(psi)	Dv,0.5 μm	Velocity m/s	x	n	Water Density mm/min(gpm/ft^2)
69 (10)	389	2.61	427	3.96	11 (0.27)
138 (20)	354	3.21	387	4.09	11.4 (0.28)
276 (40)	279	4.19	306	3.94	16.7 (0.41)
345 (50)	250	4.59	274	4.00	18.3 (0.45)
414 (60)	213	4.74	232	4.27	20.4 (0.50)

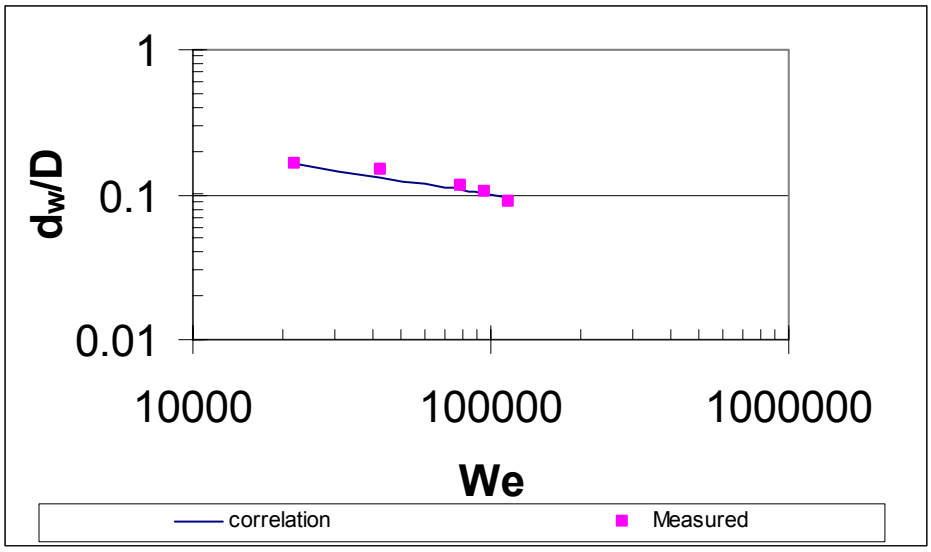

Figure 4.3 Particle Size Prediction at different Weber Number for Spraying System 3/8GG, 18SQ Nozzle.

4.2 The drop sizes and velocities measurement of Spraying System 1/8GG, 2 nozzle

Figure 4.4 shows the Spraying System 1/8GG 2 nozzle. The nozzle size D is 1 mm (0.04 in.) Three water pressures were used to produce different drop sizes and velocities for this nozzle as shown in Table 4.3. Figure 4.5 shows the linear regression data fit for the drop size prediction correlation shown in Equation 4-6. Coefficient of determination R^2 is 0.99.

$$\frac{d_w}{D} = \frac{2.05}{We_n^{1/4}} \qquad 4\text{-}6$$

Figure 4.4 Spraying System 3/8GG, 18SQ Nozzle.

Table 4.3 Water Drop Size, Velocity, and Rosin-Rammler Constants x and n Measured by Dantec PDA System and Water Density for Spraying System 1/8GG, 2 Nozzle at Different Operating Pressure.

Pressure , kpa (psi)	Dv,0.5 , μm	Velocity ,m/s	x	n	Water Density ,mm/min(gpm/ft^2)
172 (25)	197	2.71	214	4.38	7.7 (0.19)
345 (50)	164	4.08	179	4.46	8.6 (0.21)
517 (75)	152	4.47	165	4.55	9.8 (0.24)

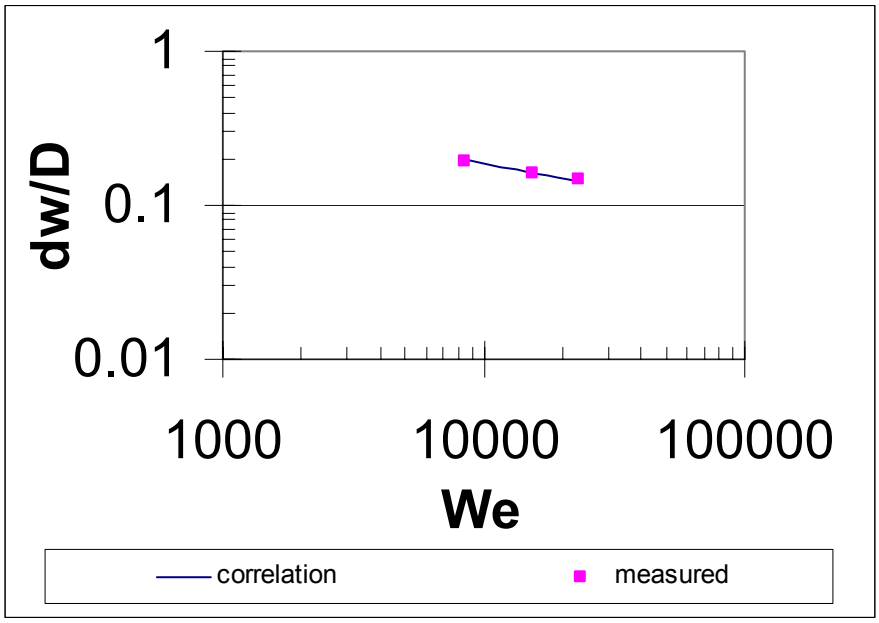

Figure 4.5 Particle size prediction at different Weber Number for Spraying System 1/8GG, 2 Nozzle.

4.3 The drop sizes and velocities measurement of spraying System 1/8GG, 6SQ Nozzle

Figure 4.66 shows the spraying system 1/8GG, 6SQ nozzle. The nozzle size D is 1.3 mm (0.05 in.). Two water pressures were used to produce different drop sizes and velocities for this nozzle as shown in Table 4.4. Figure 4.7 shows the linear regression data fit for drop size prediction correlation shown in Equation 4-7.

$$\frac{d_w}{D} = \frac{5.98}{We_n^{1/3}} \qquad 4\text{-}7$$

Figure 4.6 Spraying System 1/8GG, 6SQ Nozzle.

Table 4.4 Water Drop Size, Velocity, and Rosin-Rammler Constants x and n Measured by Dantec PDA System and Water Density for Spraying System 1/8GG, 6SQ Nozzle at Different Operating Pressure.

Pressure , kpa(psi)	Dv,0.5 , μm	Velocity ,m/s	x	n	Water Density ,mm/min(gpm/ft^2)
172 (25)	243	3.72	268	3.76	6.1 (0.15)
345 (50)	184	5.16	204	4.11	9 (0.22)

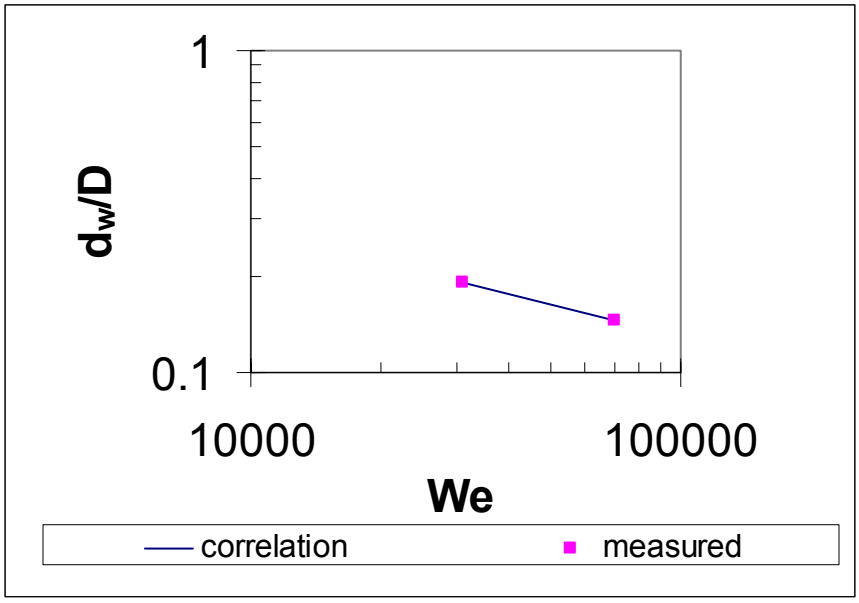

Figure 4.7 Particle size prediction at different Weber number for Spraying System 1/8GG, 6SQ nozzl

4.4 The drop sizes and velocities measurement of Spraying System 1/4GG, 10SQ nozzle

Figure 4.8 shows the spraying system 1/4GG, 10SQ nozzle. The nozzle size is 1.6 mm (0.0625 in.). Two water pressures were used to produce different drop sizes and velocities for this nozzle as shown in Table 4.5. Figure 4.9 shows the linear regression data fit for the drop size prediction correlation shown in Equation 4-8.

$$\frac{d_w}{D} = \frac{6.01}{We_n^{1/3}} \qquad 4\text{-}8$$

Figure 4.8 Spraying System 1/4GG, 10SQ nozzle.

Table 4.5 Water Drop Size, Velocity, and Rosin-Rammler Constants x and n Measured by Dantec PDPA System and Water Density for Spraying System 1/4GG, 10SQ Nozzle at Different Operating Pressure.

Pressure , kpa(psi)	Dv,0.5 μm	Velocity m/s	x	n	Water Density mm/min(gpm/ft^2)
172 (25)	335	3.05	354	4.17	11.8 (0.29)
345 (50)	260	4.69	281	4.49	16.3 (0.40)

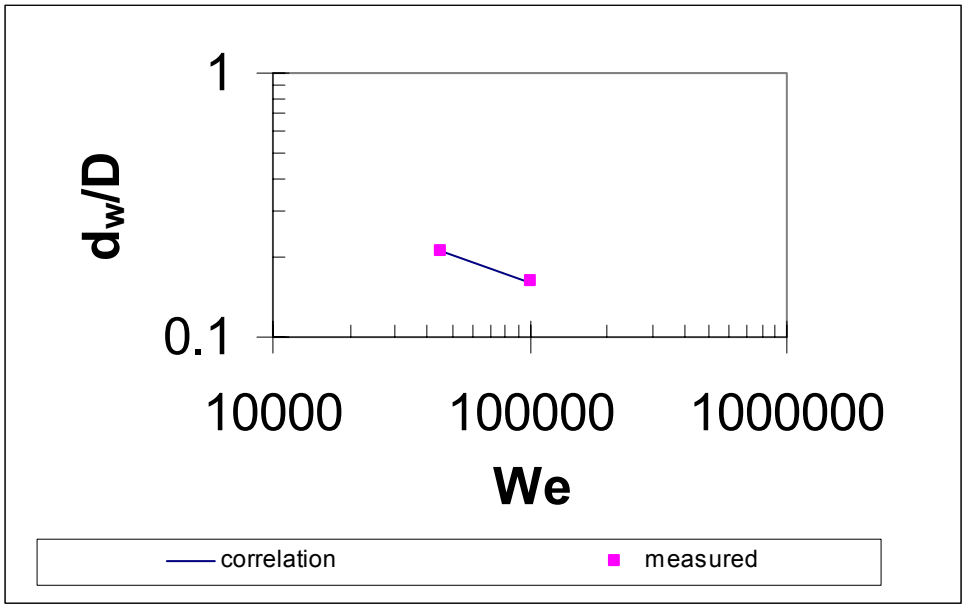

Figure 4.9 Particle size prediction for different Weber number for Spraying System 1/4GG, 10SQ nozzle.

4.5 The drop sizes and velocities measurement of Spraying System 3/8GG, 15 Nozzle

Figure 4.10 shows the spraying system 3/8GG, 15 nozzle. The nozzle size D is 2.4 mm (0.094 in.). Six water pressures were used to produce different drop sizes and velocities for this nozzle as shown in Table 4.6. Figure 4.11shows linear regression data fit for the drop size prediction correlation shown in Equation 4-9. Coefficient of determination R^2 is 0.94.

$$\frac{d_w}{D} = \frac{22.28}{We_n^{1/2}} \qquad 4\text{-}9$$

Figure 4.10 Spraying System 3/8GG, 15 nozzle.

Table 4.6 Water drop size, velocity, and Rosin-Rammler Constants x and n measured by Dantec PDPA System and water density for Spraying System 3/8GG, 15 nozzle at different operating pressure.

Pressure , kpa(psi)	Dv,0.5 μm	Velocity m/s	x	n	Water Density mm/min(gpm/ft^2)
69 (10)	415	2.57	452	4.23	14.3 (0.35)
138 (20)	360	2.7	394	3.98	15.9 (0.39)
206 (30)	242	3.5	264	4.19	17.1 (0.42)
276 (40)	237	3.63	260	4.14	17.5 (0.43)
345 (50)	202	4.66	220	4.11	18.3 (0.45)
414 (60)	186	5.28	203	4.11	20 (0.49)

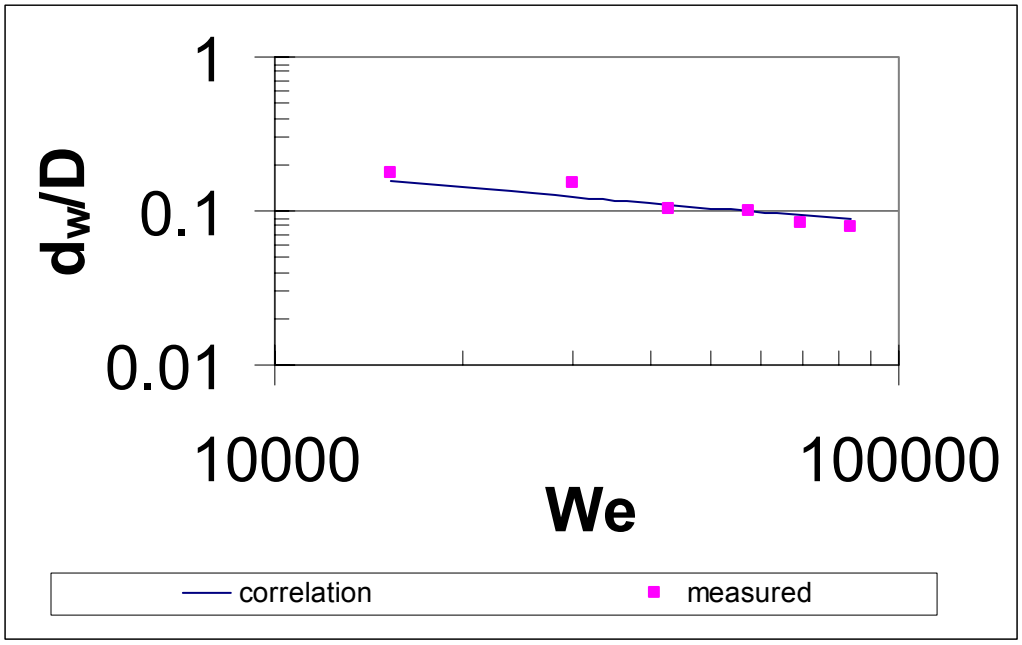

Figure 4.11 Particle size prediction at different Weber number for Spraying System 3/8GG, 15 nozzle.

4.6 The drop sizes and velocities measurement of spraying system 3/8GG, 22 nozzle

Figure 4.12 shows the spraying system 3/8GG, 22 nozzle. The nozzle size D is 2.8 mm (0.11 in.). Six water pressures were used to produce different drop sizes and velocities for this nozzle as shown in Table 4.7. Figure 4.13 shows linear regression data fit for the drop size prediction correlation shown in Equation 4-10. Coefficient of determination R^2 is 0.94.

$$\frac{d_w}{D} = \frac{8.32}{We_n^{2/5}} \qquad 4\text{-}10$$

Figure 4.12 Spraying System 3/8GG, 22 nozzle.

Table 4.7 Water drop sizes, velocities, and Rosin-Rammler constants x and n measured by Dantec PDA system and water density for Spraying System 3/8GG, 22 Nozzle at different operating pressure.

Pressure , kpa(psi)	Dv,0.5 μm	Velocity m/s	x	n	Water Density mm/min(gpm/ft^2)
69 (10)	425	2.3	468	3.81	4.9 (0.12)
138 (20)	375	2.7	413	3.8	6.5 (0.16)
206 (30)	330	2.8	363	4.89	7.3 (0.18)
276 (40)	268	2.9	289	4.85	8.6 (0.21)
345 (50)	237	3.32	257	4.56	10.2 (0.25)
414 (60)	227	3.46	246	4.51	13.9 (0.34)

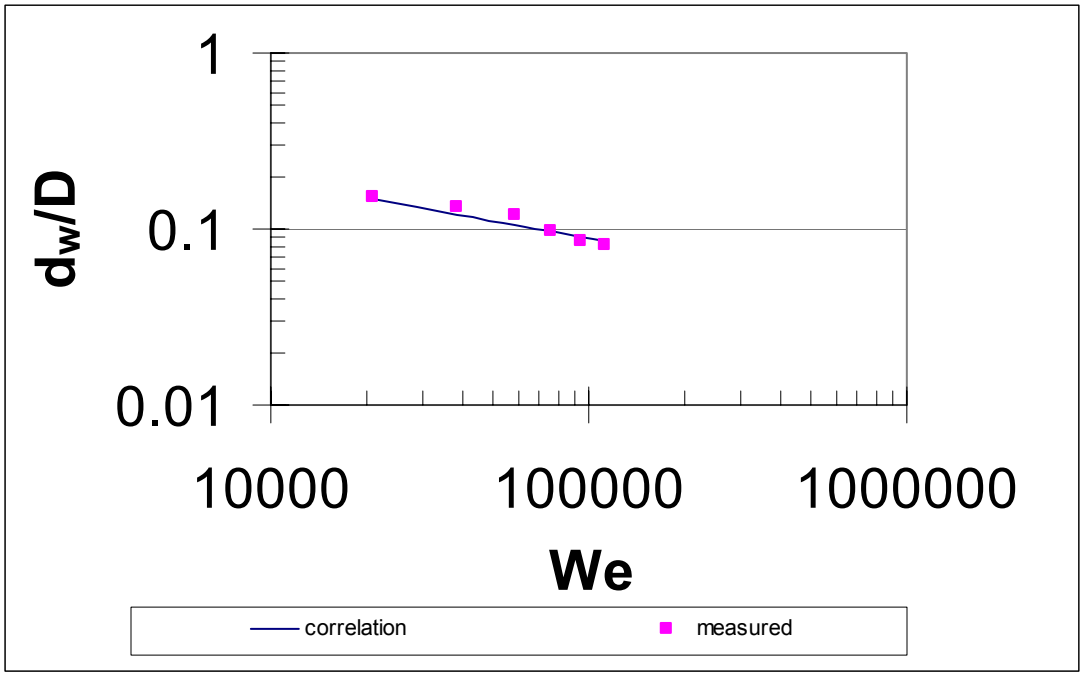

Figure 4.13 Particle size prediction at different Weber number for Spraying System 3/8GG, 22 nozzle.

4.7 The drop sizes and velocities measurement of spraying system 1/2GG, 25 nozzle

Figure 4.14 shows the spraying system 1/2GG, 25 nozzle. The nozzle size D is 3.2 mm (0.125 in.). Six water pressures were used to produce different drop sizes and velocities for this nozzle as shown in Table 4.8. Figure 4.15 shows linear regression data fit for the drop size prediction correlation shown in Equation 4-11. Coefficient of determination R^2 is 0.98.

$$\frac{d_w}{D} = \frac{851}{We_n^{0.85}} \qquad 4\text{-}11$$

Figure 4.14 Spraying System 1/2GG, 25 nozzle.

Table 4.8 Water drop sizes, velocities, and Rosin-Rammler constants x and n measured by Dantec PDA system and water densities for Spraying System 1/2GG, 25 Nozzle at different operating pressure.

Pressure , kpa(psi)	Dv,0.5 μm	Velocity m/s	x	n	Water Density mm/min(gpm/ft^2)
34.5 (5)	955	2.7	1041	4.23	23.2 (0.57)
69 (10)	672	3.05	724	3.77	18.3 (0.45)
103 (15)	459	3.08	499	4.46	18.3 (0.45)
138 (20)	333	3.19	359	4.88	22.4 (0.55)
172 (25)	317	3.49	344	4.6	20.4 (0.5)
206 (30)	264	3.69	288	4.61	16.7 (0.41)

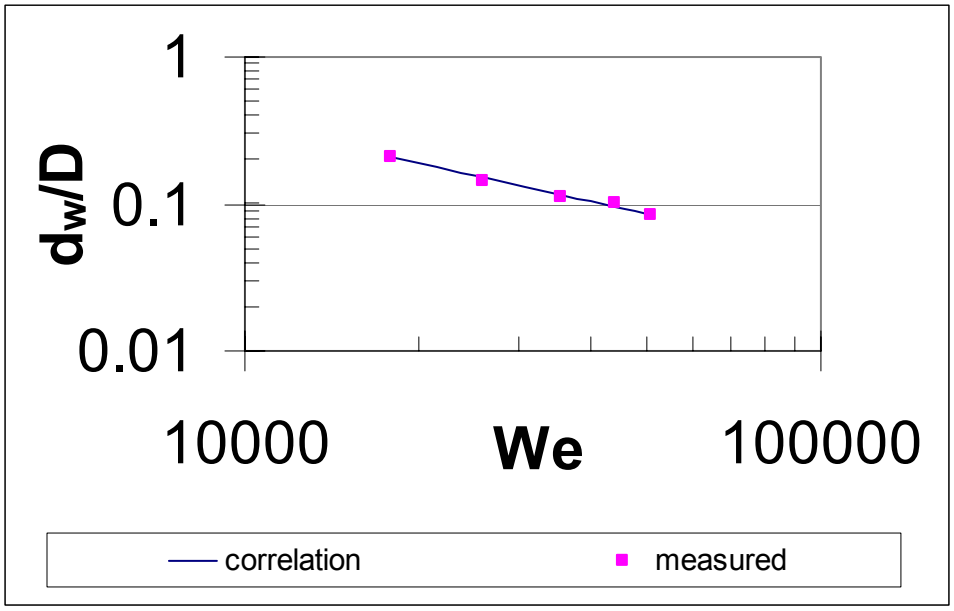

Figure 4.15 Particle size prediction at different Weber number for Spraying System 1/2GG, 25 nozzle.

4.8 The drop sizes and velocities measurement of Spraying System 1/2GG, 29SQ nozzle

Figure 4.16 shows the spraying system 1/2GG, 29SQ nozzle. The nozzle size D is 3.2 mm (0.125 in.). Six water pressures were used to produce different drop sizes and velocities for this nozzle as shown in Table 4.9. Figure 4.17 shows linear regression data fit for the drop size prediction correlation shown in Equation 4-13. Coefficient of determination R^2 is 0.98.

$$\frac{d_w}{D} = \frac{447}{We_n^{0.77}} \qquad 4\text{-}12$$

Figure 4.16 Spraying System 1/2GG, 29SQ nozzle.

Table 4.9 Water drop sizes, velocities, and Rosin-Rammler constants x and n measured by Dantec PDA System and water densities for Spraying System 1/2GG, 29SQ nozzle at different operating pressure.

Pressure , kpa(psi)	Dv,0.5 μm	Velocity m/s	x	n	Water Density mm/min(gpm/ft^2)
34.5 (5)	830	2.35	920	3.58	23.2 (0.57)
69 (10)	617	2.44	670	4.05	16.7 (0.41)
103 (15)	441	2.66	483	3.99	17.5 (0.43)
138 (20)	373	2.74	411	3.86	22.4 (0.55)
172 (25)	341	3.59	375	3.79	20.4 (0.5)
206 (30)	296	4.43	325	3.92	16.7 (0.41)

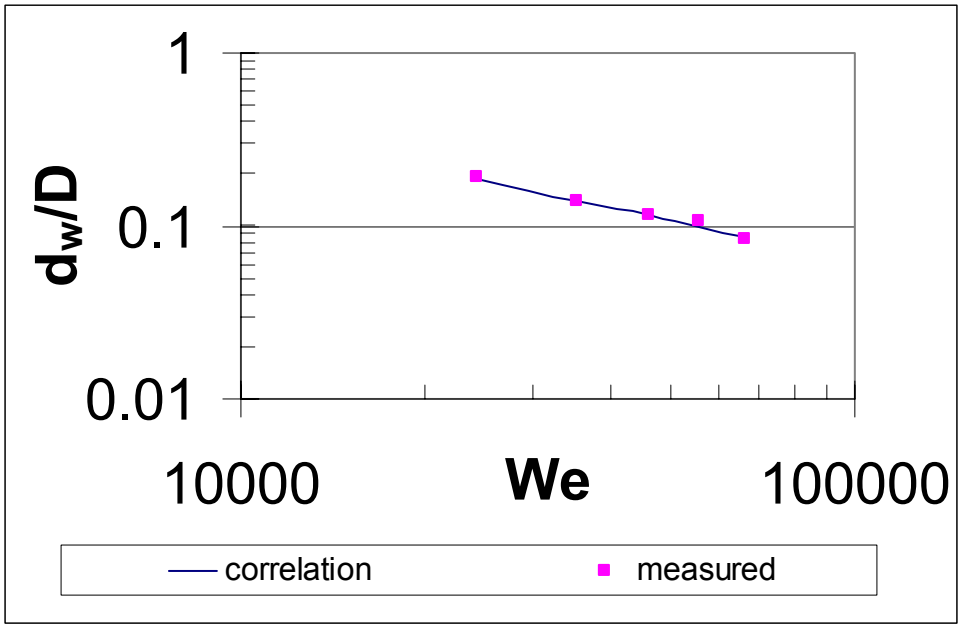

Figure 4.17 Particle size prediction at different Weber number for Spraying System 1/2GG, 29SQ nozzle.

4.9 The drop sizes and velocities measurement of spraying system 1/2GG, 32 nozzle

Figure 4.18 shows the spraying system 1/2GG, 32 nozzle. The nozzle size D is 3.6 mm (0.14 in.). Six water pressures were used to produce different drop sizes and velocities for this nozzle as shown in Table 4.10. Figure 4.19 shows linear regression data fit for the drop size prediction correlation as shown in Equation 4-13 . Coefficient of determination R^2 is 0.99.

$$\frac{d_w}{D} = \frac{363}{We_n^{0.76}} \qquad 4\text{-}13$$

Figure 4.18 Spraying System 1/2GG, 32 nozzle.

Table 4.10 Water drop sizes, velocities, and Rosin-Rammler constants x and n measured by Dantec PDA System and water Densities for Spraying System 1/2GG, 32 nozzle at different operating pressure.

Pressure , kpa(psi)	Dv,0.5 μm	Velocity m/s	x	n	Water Density mm/min(gpm/ft^2)
34.5 (5)	718	2.55	794	3.63	20.4 (0.5)
69 (10)	657	2.66	767	3.62	21.2 (0.52)
103 (15)	543	3.34	600	3.64	22.8 (0.56)
138 (20)	425	3.6	470	3.62	24 (0.59)
172 (25)	350	4.21	384	3.93	26.1 (0.64)
206 (30)	305	4.47	333	4.2	27.7 (0.68)

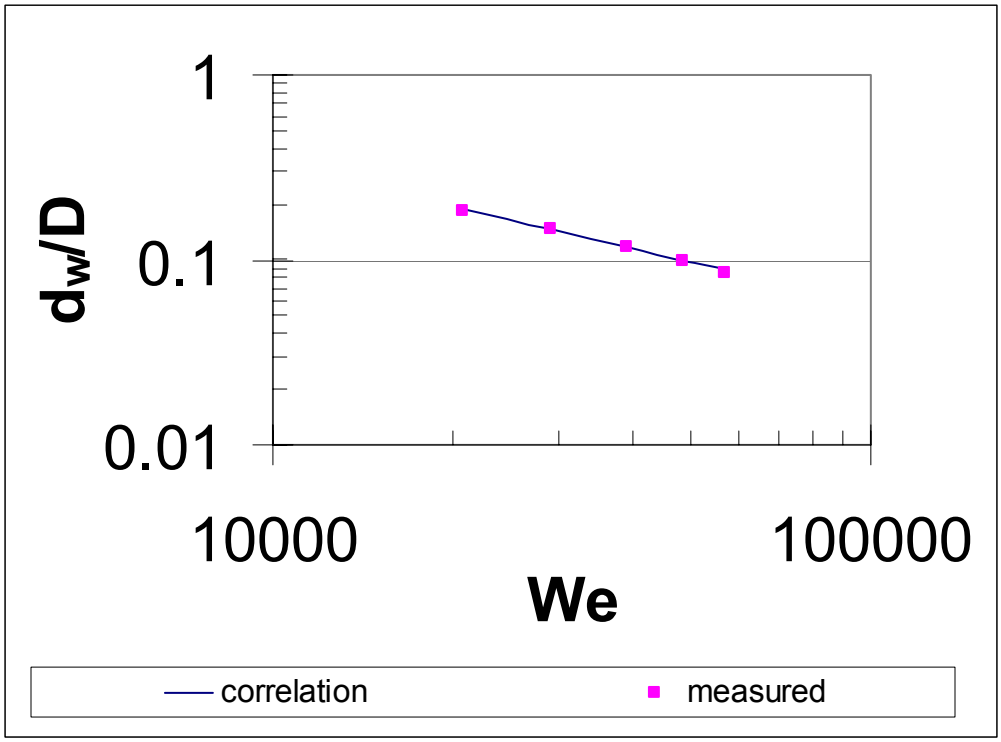

Figure 4.19 Modified particle size prediction for different Weber number for Spraying System 1/2GG, 32 nozzle.

4.10 The drop sizes and velocities measurement of Grinnell AM24 Nozzle

Figure 4.20 shows the Grinnell AM24 nozzle. The K value of this nozzle is 9,2 $\frac{lpm}{(bar)^{1/2}}$ ($0.64\frac{gpm}{(psi)^{1/2}}$) . The nozzle size D is 3.2 mm (0.125 in.). Four water pressures were used to produce different drop sizes and velocities for this nozzle as shown in Table 4.11. Figure 4.21 shows linear regression data fit for the drop size prediction correlation as shown in Equation 4-14. Coefficient of determination R^2 is 0.99.

$$\frac{d_w}{D} = \frac{724}{We_n^{0.76}} \qquad 4\text{-}14$$

Figure 4.20 Grinnell AM24 nozzle.

Table 4.11 Water drop sizes, velocities, and Rosin-Rammler constants x and n measured by Dantec PDA System and water Densities for Grinnell AM24 nozzle at different operating pressure.

Pressure , kpa(psi)	Dv,0.5 , μm	Velocity ,m/s	x	n	Water Density ,mm/min(gpm/ft^2)
172 (25)	1056	2.45	1170	3.4	17.5 (0.43)
345 (50)	769	3.39	850	3.4	15.1 (0.37)
517 (75)	450	4.18	498	4.03	17.1 (0.42)
690 (101)	368	4.68	396	3.94	17.5 (0.43)

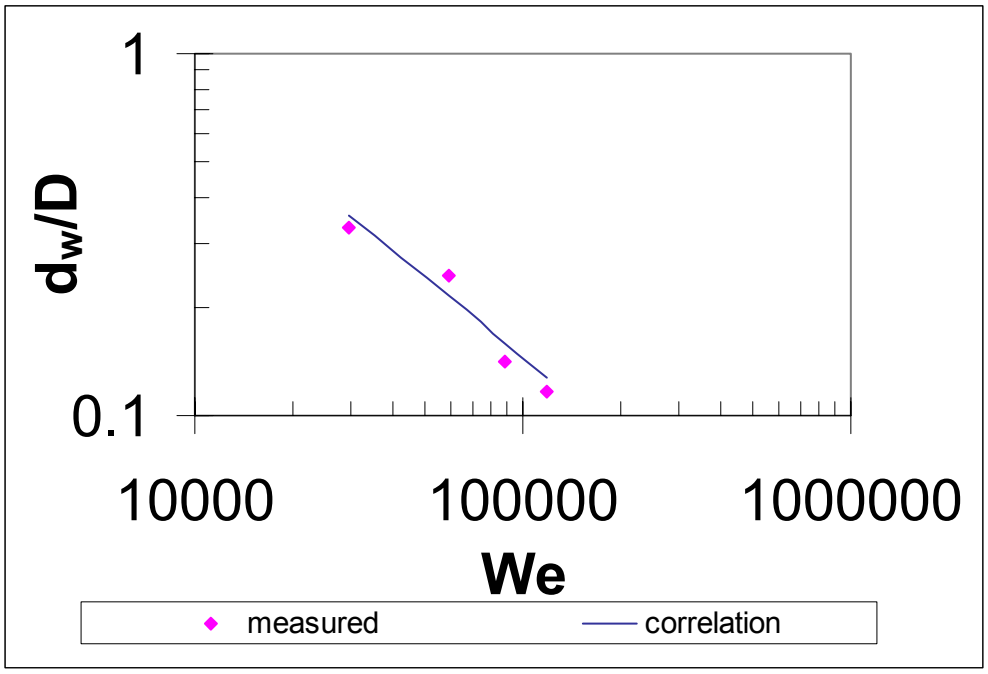

Figure 4.21 Particle size prediction at different Weber number for Grinnell AM24 nozzle.

4.11 The drop sizes and velocities measurement of BETE ¼ WL1 ½ nozzle

Figure 4.22 shows the BETE Fog Nozzle, Inc ¼ WL1 ½ nozzle. The K factor of this nozzle is 3,8 $\frac{lpm}{(bar)^{1/2}}$ $(0.265\frac{gpm}{(psi)^{1/2}})$. The nozzle size D is 2.8 mm (0.11 in.). Three water pressures were used to produce different drop sizes and velocities for this nozzle as shown in Table 4.12. Figure 4.23 shows linear regression data fit drop size prediction correlation can be expressed as shown in Equation 4-15. Coefficient of determination R^2 is 0.99.

$$\frac{d_w}{D} = \frac{0.132}{We_n^{0.074}} \qquad 4\text{-}15$$

Figure 4.22 Bete WL 11/2 nozzle.

Table 4.12 Water drop sizes, velocities, and Rosin-Rammler constants x and n measured by Dantec PDA System and water densities for Bete WL 11/2 Nozzle at different operating pressure.

Pressure , kpa(psi)	Dv,0.5 , μm	Velocity ,m/s	x	n	Water Density ,mm/min(gpm/ft^2)
172 (25)	189	3.2	205.78	4.41	2.85 (0.07)
517 (75)	174	4.63	188.1	4.81	7.3 (0.18)
862 (125)	168	6.26	181.5	4.91	9 (0.22)

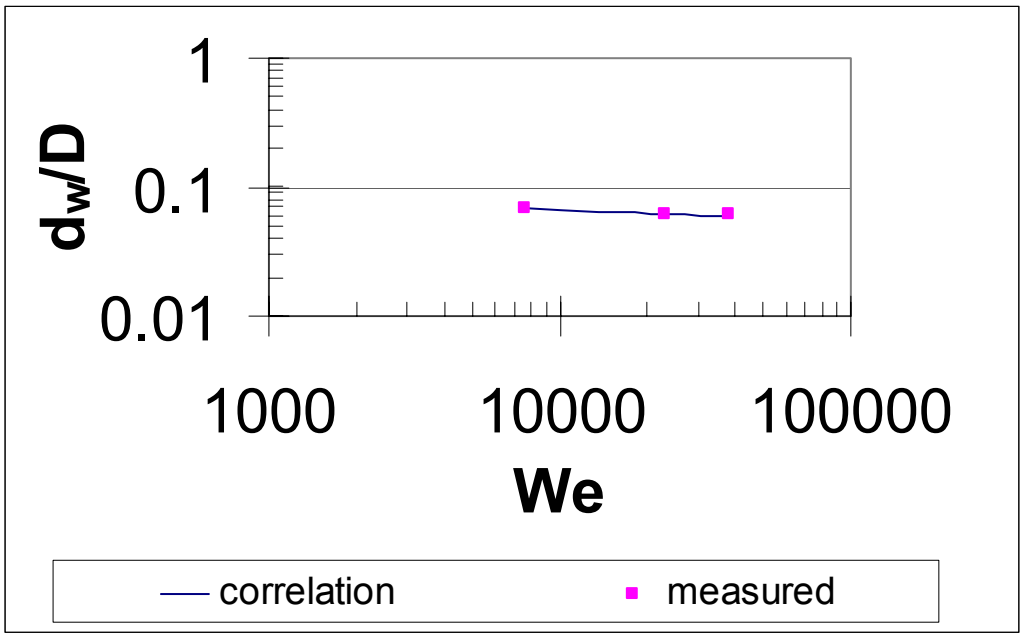

Figure 4.23 Particle size prediction at different Weber number for BETE 1/4WL 1 ½ nozzle.

4.12 The drop sizes and velocities measurement of Spraco 11-0620-01 nozzle

Figure 4.24 shows the Spraco 11-0620-01 nozzle. The meaning of the model Spraco 11-0620-01 is that the 11 stands for spray type, 06 is the flow rate code for this particular model at design pressure, 20 is the spray angle code at design pressure, and 01 is the connection code. The nozzle size D is 1.2 mm (0.046 in.). Two water pressures were used to produce different drop sizes and velocities for this nozzle as shown in Table 4.13. Figure 4.25 shows linear regression data fit drop size prediction correlation shown in Equation 4-16.

$$\frac{d_w}{D} = \frac{0.4}{We_n^{0.02}} \qquad 4\text{-}16$$

Figure 4.24 Spraco 11-0620-01 nozzle.

Table 4.13 Water drop size, velocities, and Rosin-Rammler constants x and n measured by Dantec PDA System and water densities for the model Spraco 110620-01 nozzle at different operating pressure.

Pressure , kpa(psi)	Dv,0.5 , μm	Velocity ,m/s	x	n	Water Density ,mm/min(gpm/ft^2)
345 (50)	116	2.61	125.4	4.76	3.3 (0.08)
517 (75)	115	3.37	124.1	4.78	4.5 (0.11)

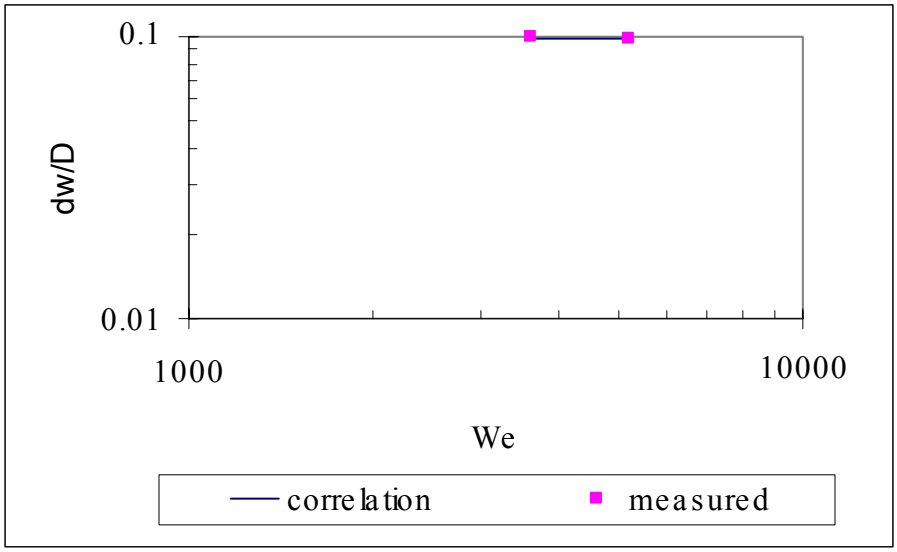

Figure 4.25 Particle size prediction at different Weber number for the model Spraco 11- 0620-01 nozzle.

4.13 The drop sizes and velocities measurement of Spraying System 1/8HH 1.5 nozzle

Figure 4.26 shows the Spraying System 1/8HH 1.5 nozzle and the nozzle size D is 1.2 mm (0.047 in.). The drop sizes and velocities of this nozzle are as shown in Table 4.14. This nozzle produced the smallest drops and spray densities of all the nozzles tested as shown in Table 4.10. Figure 4.27 shows linear regression data fit for the drop size prediction correlation shown in Equation 4-17.

$$\frac{d_w}{D} = \frac{1.8}{We_n^{1/3}} \qquad 4\text{-}17$$

Figure 4.26 Spraying System 1/8HH 1.5 nozzle.

Table 4.14 Water drop sizes, velocities, and Rosin-Rammler constants x and n measured by Dantec PDA System and water densities for Spraying System 1/8HH 1.5 nozzle at different operating pressure.

Pressure , kpa(psi)	Dv,0.5 , μm	Velocity ,m/s	x	n	Water Density ,mm/min(gpm/ft^2)
345 (50)	161	3	174	4.71	2.85 (0.07)
517 (75)	143	3.12	154.3	5.1	2.85 (0.07)

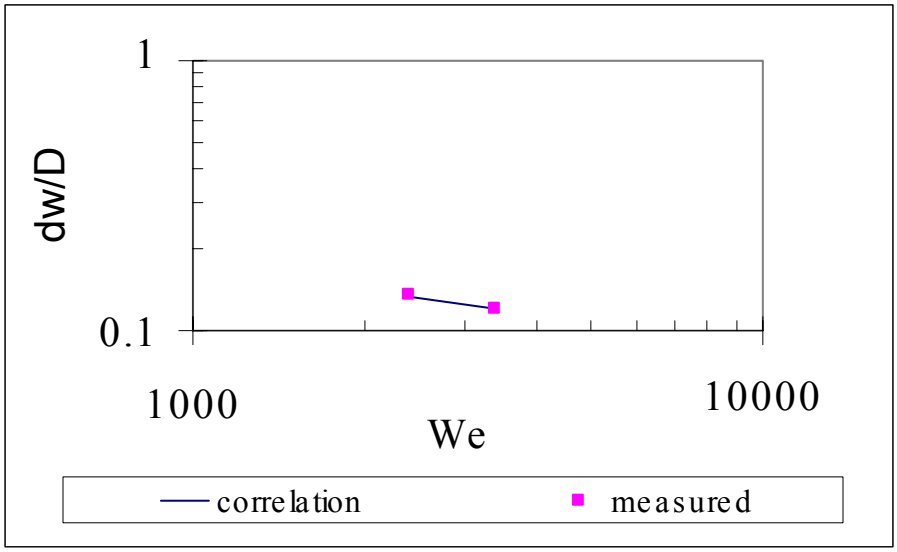

Figure 4.27 Particle size prediction for different Weber number for Spraying System nozzle.

4.14 Summary

Broad ranges of water densities (from about 3 to 28 mm/min) and drop sizes (from about 140 μm to 1100 μm) were obtained from these 13 nozzles as shown in Figure 4.28. These data can be applied to oil splattering quantification and the analysis of fire suppression tests based on tests requirements.

Local drop size measurement can not all apply the correlation $\frac{d_w}{D} = \frac{C}{We^{1/3}}$ from the measurement of this research. The larger orifice with lower operating pressure could cause higher water density in the center to produce larger droplets. The drop size should be measured at specific location for local application, if the spray is not used for whole spray application. The obtained correlations from this research are only applicable when the measured point was located at 0.91m (3ft) under the centerline of the nozzle.

The test data of 13 nozzles show that higher velocities and smaller drop sizes are obtained when the operating pressure increases. This information can be also used for other application such as water spray cooling hot surfaces, in addition to being used to help correlate the data in this dissertation.

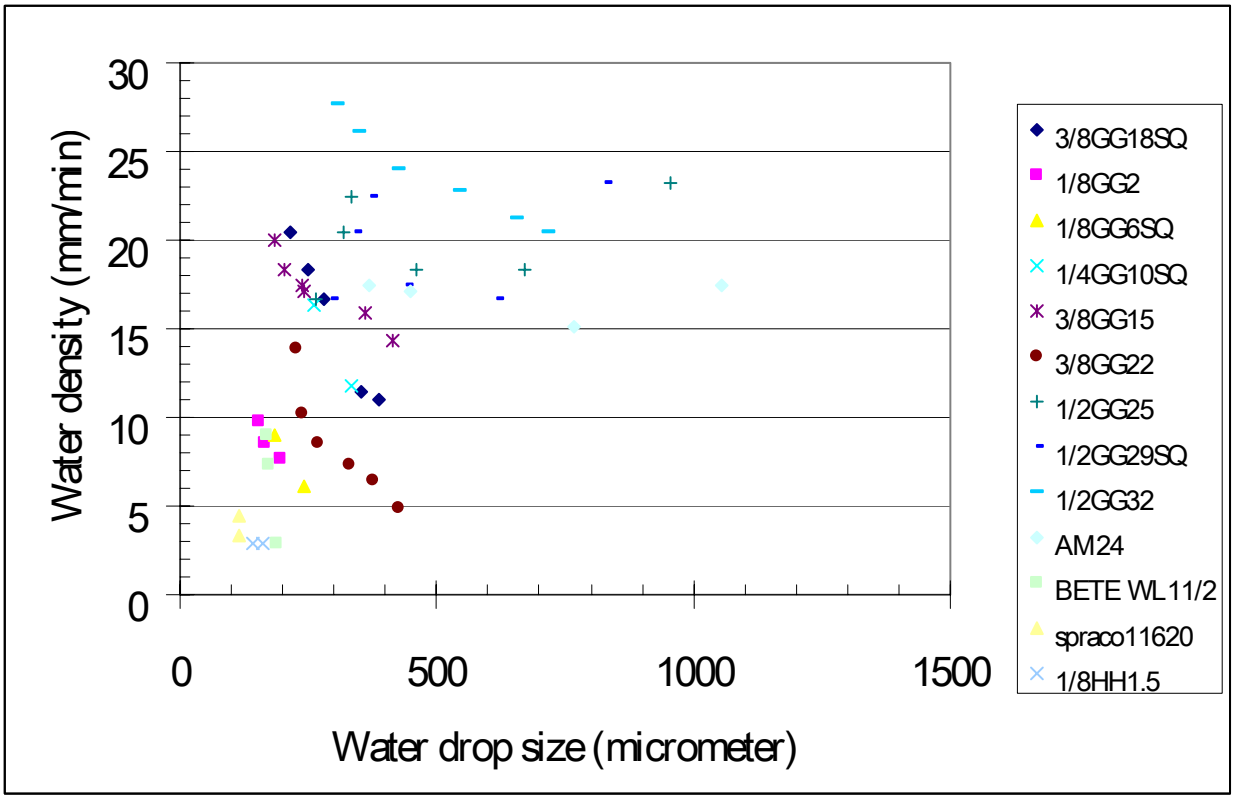

Figure 4.28 Water density and drop size distribution for selected nozzles.

5 Oil Heating and Ignition

Experiments described here simulate the scenario of a high flash point oil pool being exposed to a nearby fire. A radiant heat flux on the fuel surface can increase the oil surface temperature to its fire point in this scenario. A heat flux source is needed to heat the oil from its surface.

A 33 cm (13 in.) diameter propane ring burner was designed to heat and ignite high flash point oil it in this research. Figure 5.1 shows the propane ring burner heat the mineral seal oil and Figure 5.2 shows the oil ignited and burning. The following will discuss this burner; how it provides a uniform heat flux to the pool and ignites the pool.

Figure 5.1 Propane ring burner used by this research to heat oil.

Figure 5.2 The propane ring burner heated the oil and ignited it.

5.1 Surface heat flux measurement

A surface heat flux applied to heat the oil was designed to produce a uniform oil surface temperature. A propane ring burner was used to provide the surface heat flux. This heat flux depends on the propane flow rate and the distance between burner and fuel. The ring burner material is copper tubing. The diameter of the ring is 33cm (13 in.) including 84 0.13 cm (0.052 in.) diameter holes with 1.27 cm (0.5 in.) spacing. Three radiometers were used to measure the uniformity of the heat flux over the oil surface at different distances below the ring fire source. The first radiometer was located on the centerline of the ring. The second radiometer was located 8.89 cm (3½ in.) from the centerline. The third one was located 15.2 cm (6 in.) from the centerline. Three elevations were tested at 5.08 cm (2 in.), 7.62 cm (3 in.), and 10.2 cm (4 in.). The configuration is as shown in Figure 5.3. The gains for the radiometers are 4.7784 KW/m^2mV, 4.86381 KW/m^2mV, and 4.43641 KW/m^2mV for serial no.80181, no.108651, and no. 118941 of Medtherm Corporation.

The propane flow rate increased the heat flux measured in the center compared to the heat fluxes measured as a function of propane flow rate are shown in Figure 5.4, Figure 5.5 and Figure 5.6 for burner elevation of 5.08 cm (2 in.), 7.62 cm (3 in.) and 10.02 cm (4 in.), respectively. The three curves for the three radial positions coincide at the uniform heat flux point when the radiometers were located 5.08 cm (2 in.) below the propane ring fire, a uniform heat flux of 24.5 KW/m^2 was obtained as shown in Figure 5.4 when the propane flow rate is 1.8 m^3/hr (63.5 ft^3/hr). If the radiometers are located at 7.62 cm (3 in.) below the ring fire, the uniform heat fluxes are 12.7 kW/m^2, 13.5 kW/m^2, 14.5 kW/m^2 at 0.99 m^3/hr (35 ft^3/hr), 1.05 m^3/hr (37 ft^3/hr), and 1.13 m^3/hr (40 ft^3/hr) propane flow rate as shown in Figure 5.5. When the radiometers are located 10.2 cm (4 in.) below the ring fire, the uniform heat flux is 7.6 kW/m^2 for 0.71 m^3/hr (25 ft^3/hr) propane flow rate as shown in Figure 5.6. Thus, uniform heat fluxes can be obtained by adjusting the flow rate of propane for the ring burner and the height between the ring burner and oil surface.

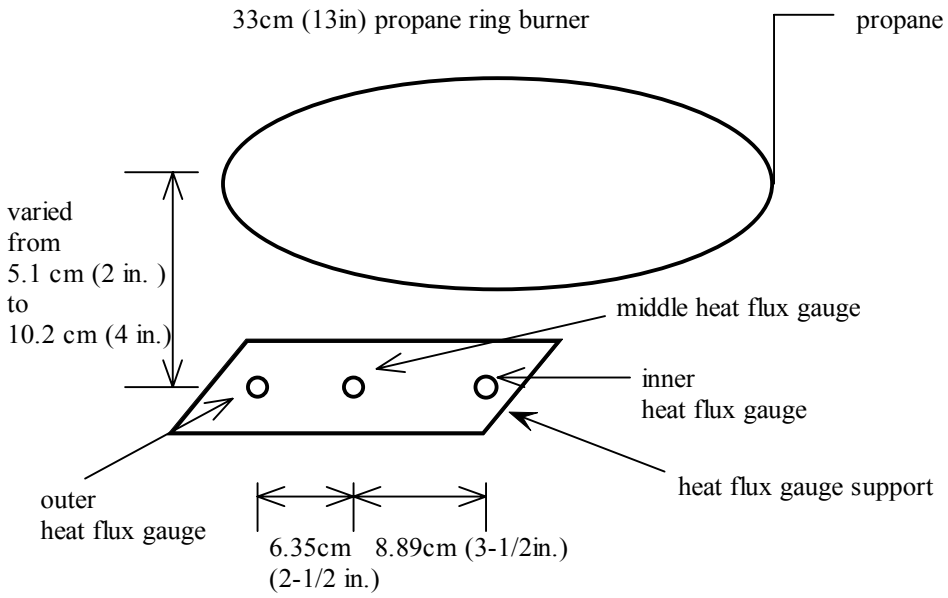

Figure 5.3 Configuration for uniform heat flux measurement.

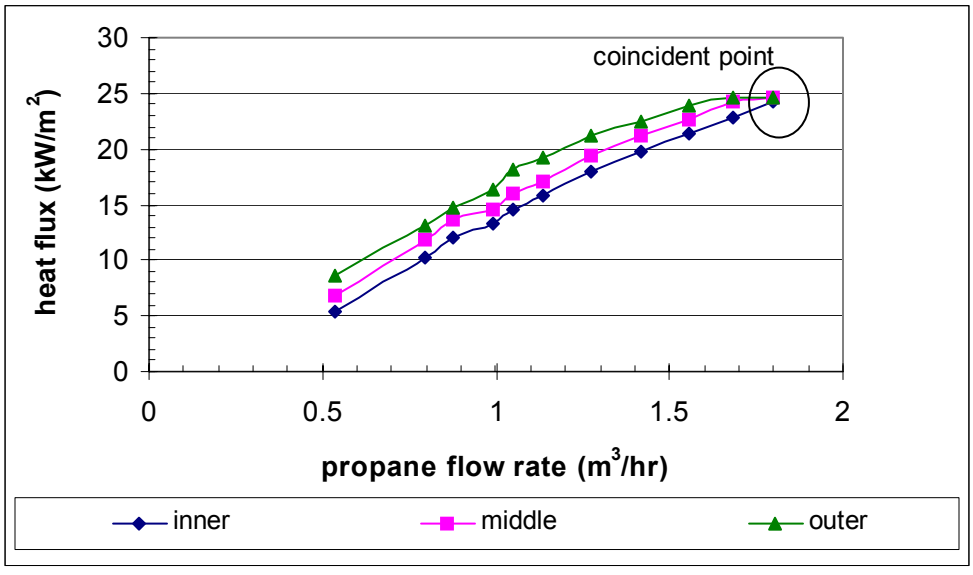

Figure 5.4 The relationship of heat flux and propane flow rate at burner 2 in above oil.

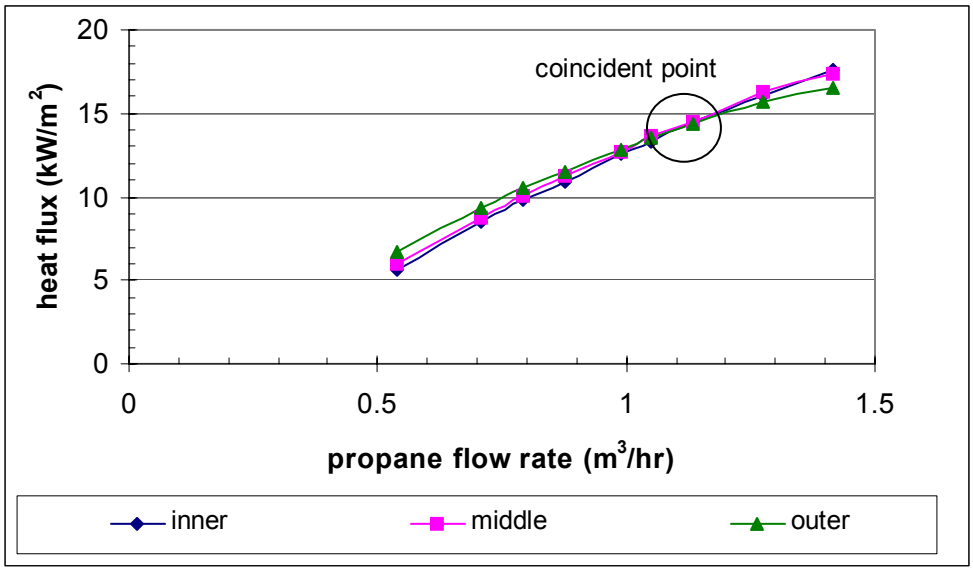

Figure 5.5 The relationship between heat flux and propane flow rate at burner 3 in. above the oil.

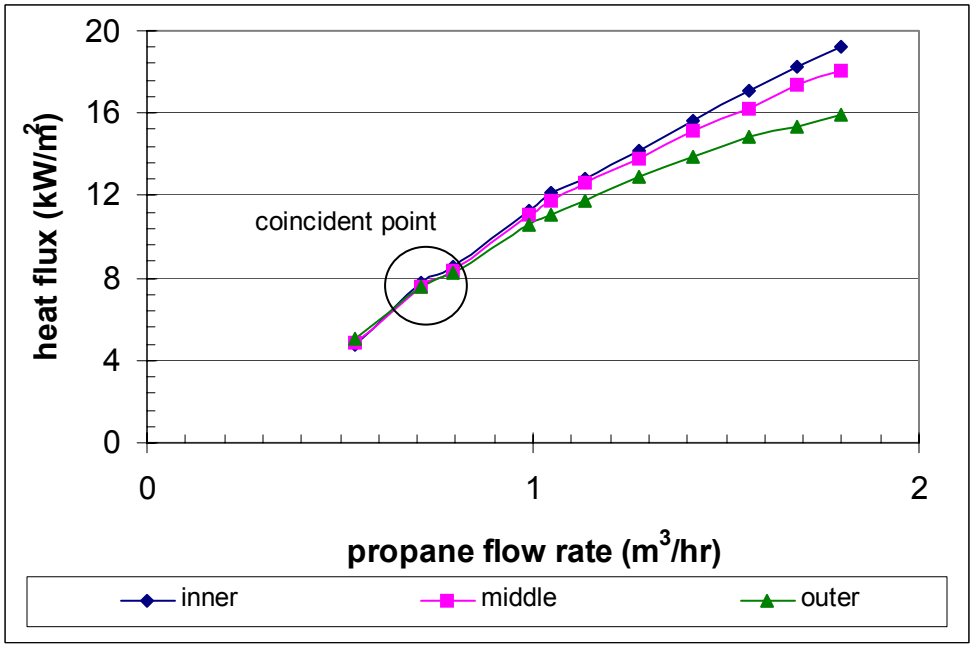

Figure 5.6 The relationship between heat flux and propane flow rate at burner 4 in above the oil.

5.2 Oil Heating

Figure 5.7 shows the temperature rises in the oil when a $14.5\,kW/m^2$ heat flux was used to heat the fuel and also shows that the temperature rise is very close between the thermocouples in the center and edge of the oil surface. A thermally thick behavior was observed and the result is consistent with the results of Putorti's [49] correlation as shown in equation 5-1 when $7.6\,kW/m^2$, $14.5\,kW/m^2$, $24.5\,kW/m^2$ heat fluxes were used to heat mineral seal oil surfaces to its flash point which is 137 ^oC. Figure 5.8 to Figure 5.10 show the measured temperature rise of the surface and the equation 5-1 predictions when the oil was exposed to 7.6 kW/m^2, 14.5 kW/m^2, and 24.5 kW/m^2 heat flux. The ignition times of predicted and measured are shown in Table 5.1. The thermal conductivity, density, heat capacity of mineral seal oil from Dr. Legzdins (personal communicate 2001) are $1.367\frac{W}{m^oK}$, $820\frac{kg}{m^3}$, and $1.92\frac{kJ}{kg^oC}$. The convective heat transfer coefficient is 10 $\frac{W}{m^{2\,o}K}$ in this correlation.

$$\dot{q}_e'' = [0.5(\frac{\pi k\rho_{oil}C}{t_{ig}})^{0.5} + 0.25\pi h_c](T_{fire} - T_o) \qquad 5\text{-}1$$

Where:

$\dot{q}_e''$ is external heat flux on the oil

k is thermal conductivity

ρ_{oil} is oil density

C is heat capacity

h_c is convective heat transfer coefficient

T_{fp} is the fire point of oil

Table 5.1 Comparison of actual applied heat flux and predicted heat flux using Putorti's equation.

Time to reach flash point	Actual applied heat flux (KW/m^2)	Predicted heat flux (KW/m^2)
377	7.6	7.8
137	14.5	13.2
39	24.5	24.0

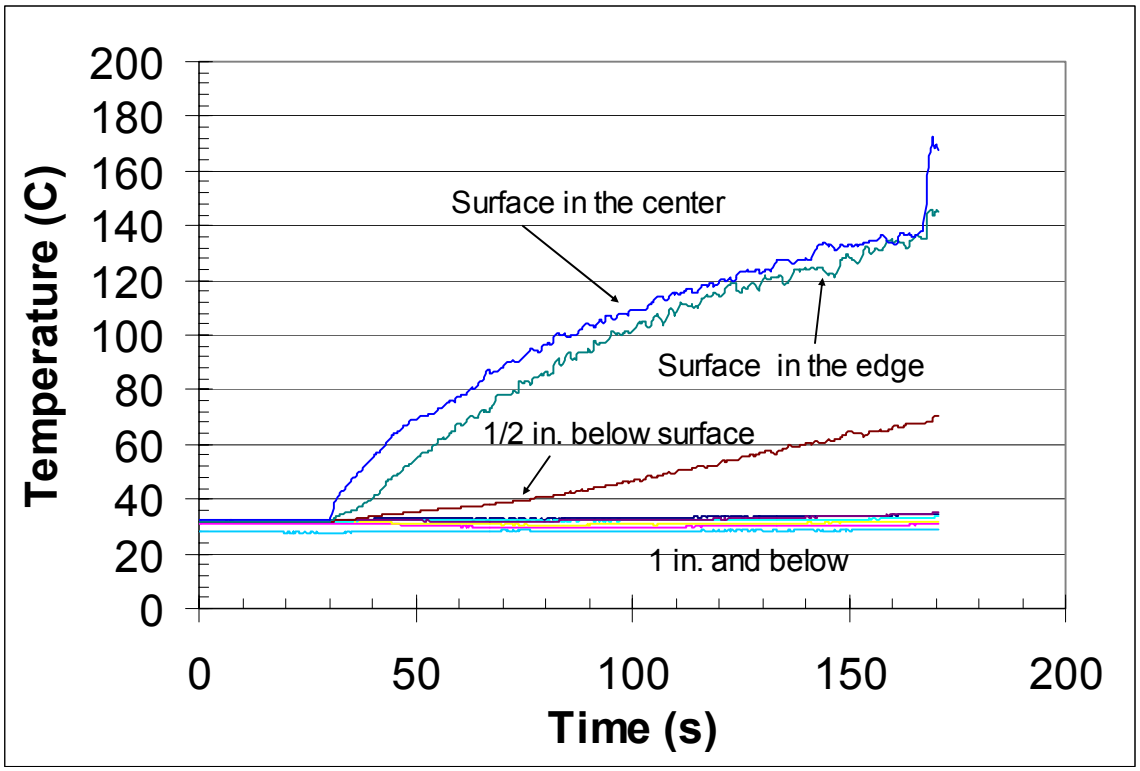

Figure 5.7 Temperature v.s. time when a 14.5 KW/m^2 heat flux was used to heat the mineral seal oil.

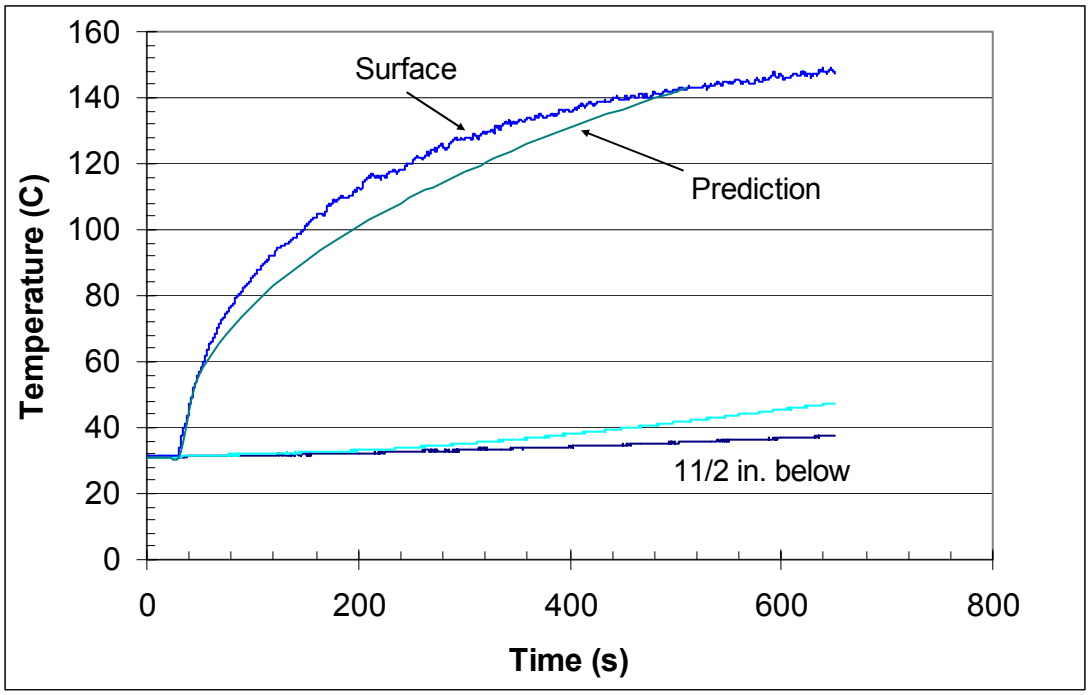

Figure 5.8 Surface temperature rise between oil heating and prediction at 7.6 KW/m^2 heat flux.

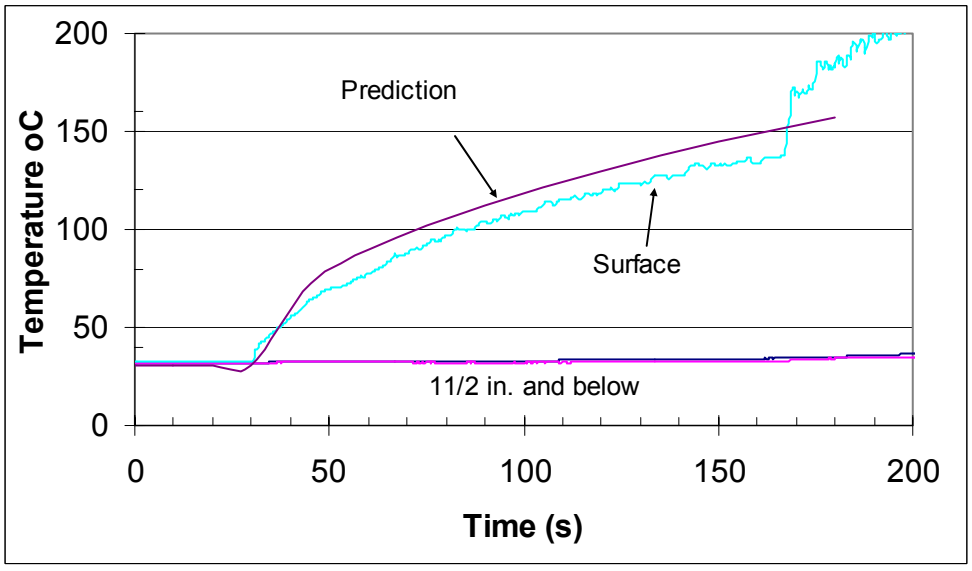

Figure 5.9 Surface temperature rise between oil heating and prediction at 14.5 KW/m^2 heat flux.

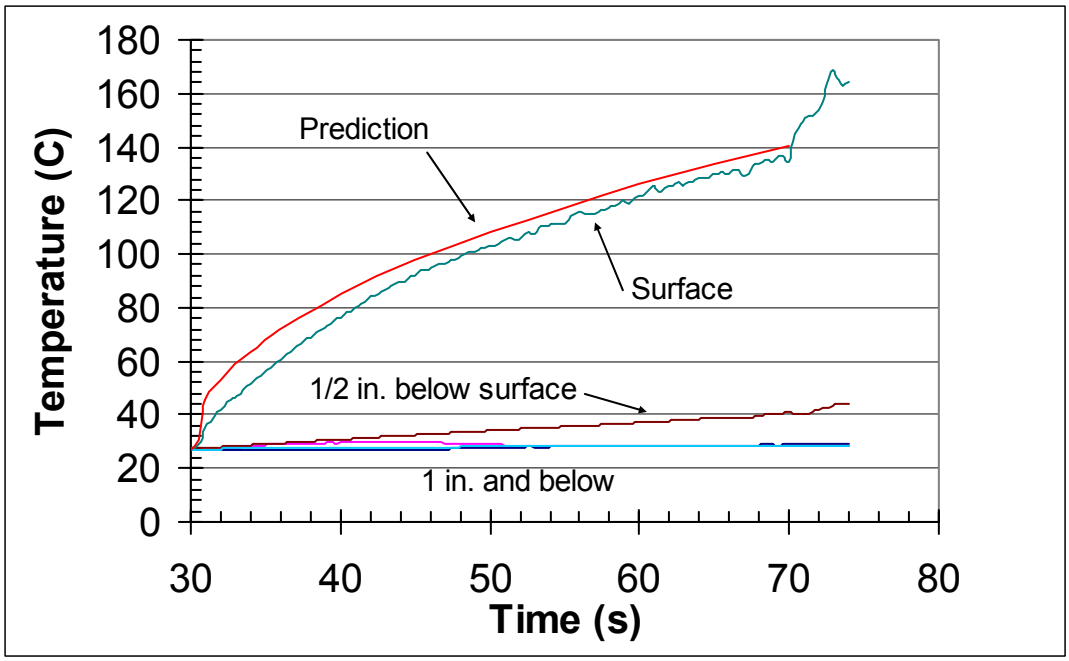

Figure 5.10 Surface temperature rise between oil heating and prediction at 24.5 KW/m^2 heat flux.

5.3 Summary

The propane ring burner can provide a uniform heat flux to heat and ignite oil. The heating produces a thermally thick temperature distribution and is predicted well using Putorti's correlation. $7.6\,KW/m^2$, $14.5\,KW/m^2$, $24.5\,KW/m^2$ heat fluxes can be obtained when the ring burner is 10.2 cm (4in.), 7.62 cm (3in.) and 5.08 cm (2in.) above the fuel surface propane flow rates are 0.71 m^3/hr (25 ft^3/hr), 1.13 m^3/hr (40 ft^3/hr), and 1.8 m^3/hr (63.5 ft^3/hr), respectively.

Thermally thick oil heating plays an important role for fire spread when the oil pool is heated and ignited by an exposing fire. This shows the hot oil layer only exists on a thin layer of the oil surface. If a water spray discharges onto this kind of oil fire, the water spray not only cools the oil but also mixes or enhances the heat transfer between the hot oil and cold oil to help extinguish the fire. This effect is observed in suppression experiments described in the following chapters.

6 Oil Splattering Quantification: Heat Release Rate Testing

Oil splattering is a very important factor for high flash point oil fire suppression. Little research has been done to quantify the oil splattering amount when water spray discharges onto oil or flaming oil. Preliminary and quantitative tests were conducted in this research to provide a better understanding for oil splattering.

6.1 Preliminary Tests

6.1.1 Water spray cooling effect on heated mineral seal oil surface

A 7 bar water spray of AM24 was discharged onto the oil heated to a surface temperature of $140^{\circ}C$ and produced immediate cooling of the oil surface. The oil temperature dropped $53^{\circ}C$ within two seconds at 7-bar nozzle pressure discharge. The result is as shown in Figure 6.1.

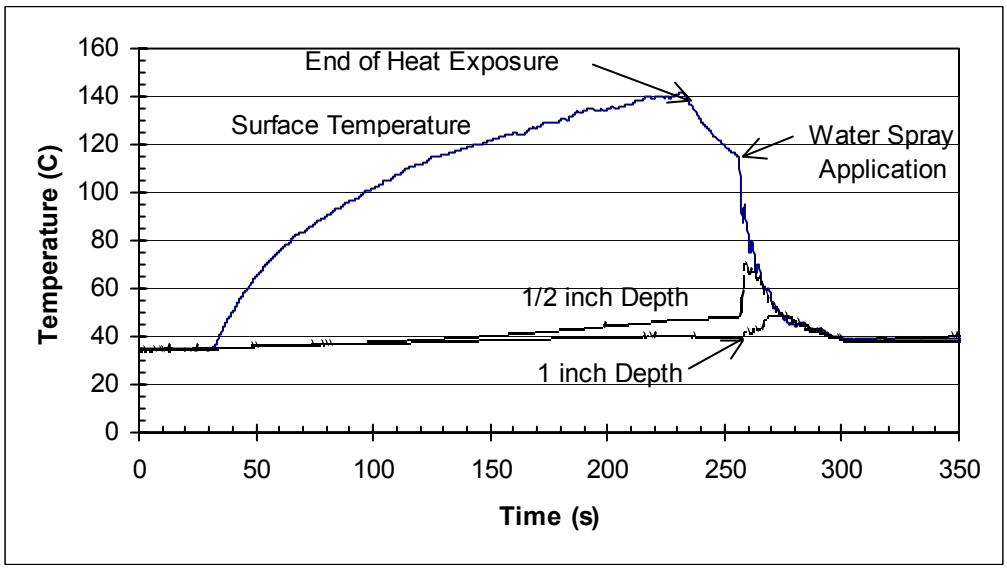

Figure 6.1 Oil temperatures measured with 14 kW/m^2 heat flux followed by water spray application.

6.1.2 Tests for splattering oils ignited by a pilot flame

A series of tests was conducted for mineral seal oil at different temperature and ignited with a pilot flame under the same water spray as shown in Table 6.1. The mineral seal oil was heated to specific temperatures below its flash point by using a heater under the oil pan. A propane ring burner was used for the pilot flame. The burner was ignited and the water spray was immediately discharged into the oil surface to prevent addition heating of the oil by the pilot flame. The pilot flame was removed after the water spray discharge ignited the oil splatter. The oil splatter flame was sustained for different durations based on oil temperatures. The results are as shown in Table 6.1 and Table 6.2 for mineral seal oil and cooking oil, respectively.

Mineral seal oil was ignited even though the oil temperature was at ambient temperature, $19^{\circ}C$. This proves the fire was caused by oil splattering because the oil temperature was well below its flash point, $137^{\circ}C$. The higher the oil temperature, the longer the duration of flaming because more oil splattering occurs at higher oil temperatures and the higher temperatures of the oil splattering droplets were also more easily vaporized and ignited. These results show that the oil splattering plays a very important role in high flash point pool fire intensification and suppression. Cooking oil tests showed similar results. The higher the oil temperature, the longer was the flame duration for cooking oil too. The splattered oil could not be ignited when the cooking oil temperature was below $215^{\circ}C$, because there were not enough splattering oil drops to ignite or to sustain the flame. A smaller drop size and water density were used for cooking oil because higher oil temperature caused too much oil splattering and too large a flame with the AM 24 sprinkler head in the cooking oil tests.

Table 6.1 Oil ignition duration for different mineral seal oil temperatures when water was applied to cause oil splattering and ignite.

Test No.	Nozzle Type	Pressure, kPa (psi)	Water Density mm/min (gpm/ft^2)	Drop Size ($D_{v,0.5}, \mu m$)	Temperature of Oil ($^{\circ}C$)	Remark
45	AM24	517 (75)	17.1 (0.42)	450	92	Oil ignited and 81 sec suppressed
47	AM24	517 (75)	17.1 (0.42)	450	70	Oil ignited and 58 sec suppressed
48	AM24	517 (75)	17.1 (0.42)	450	50	Oil ignited and 47 sec suppressed
49	AM24	517 (75)	17.1 (0.42)	450	19	Oil ignited and 5 sec suppressed

Table 6.2 Oil ignition duration for different cooking oil temperatures when water was applied to cause oil splattering and ignition.

Test No.	Nozzle Type	Pressure, kPa (psi)	Water Density mm/min (gpm/ft^2)	Drop Size ($D_{v,0.5}, \mu m$)	Temperature of Oil ($^{\circ}C$)	Remark
36	AM6	101.5	2.03 (0.05)	154	150	Oil not ignited
37	AM6	101.5	2.03 (0.05)	154	215	Oil ignited and 7 sec suppressed
38	AM6	101.5	2.03 (0.05)	154	240	Oil ignited and 21 sec suppressed
39	AM6	101.5	2.03 (0.05)	154	250	Oil ignited and 62sec suppressed
40	AM6	101.5	2.03 (0.05)	154	270	Oil ignited and not suppressed for 120 sec, flame out when water shut off

6.1.3 Observation of heated oil splattering under dyed water sprays and using an IR camera

Mineral seal oil was heated to 80 $^{\circ}C$ and a water spray was discharged onto the heated oil. Substantial oil splattering and water splash were observed as shown in Figure 6.2, when water spray containing green dye was discharged onto the 80 $^{\circ}C$ mineral seal oil. The water and oil could be distinguished from Figure 6.2 but the amount of oil splattering was hard to quantify from the photograph. The splattering oil streaked at large heights above the pan and over the side of the pan. The splatter streaks could provide larger oil surface area to vaporize and contribute more burning oils in a fire. The amount of streaked oil over the side of the pan is discussed in later chapters.

An IR camera was also used in an attempt to observe this oil splattering. The oil was heated to 80 $^{\circ}C$ as shown in Figure 6.3 and water was discharged onto the oil at 44 seconds as shown in Figure 6.4. The hot oil splattering was not observed during the test as shown in Figure 6.4, but the 80 $^{\circ}C$ oil was cooled to roughly uniform temperature of 30 $^{\circ}C$, as indicated by the color change of the oil between Figure 6.3 and Figure 6.4.

Figure 6.2 Green dye water spray discharged on heated oil.

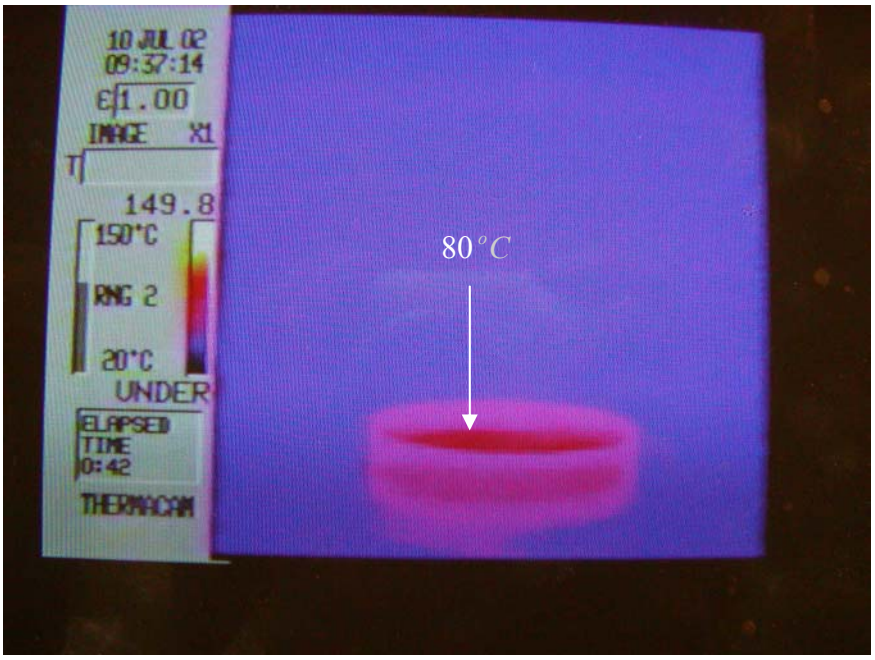

Figure 6.3 Heated oil at $80^{o}C$ observed by IR camera.

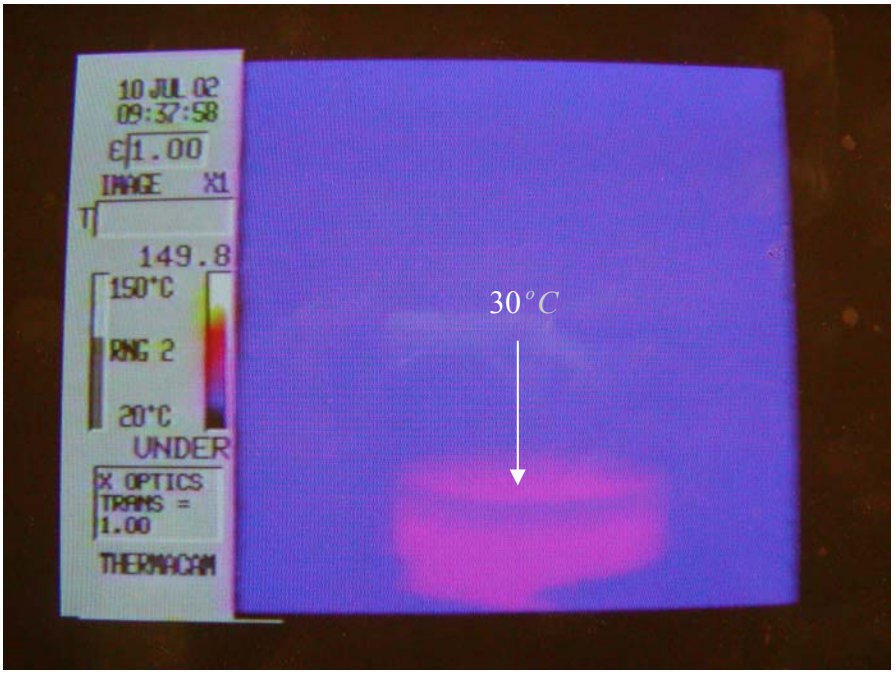

Figure 6.4 Water spray on heated oil at 44 seconds observed by IR camera.

6.2 Quantitative analysis of oil splattering contribution to a pool fire

The heat release rate measured in the fire products collector indicated the amount of splattered oil burned when water spray was discharged onto the heated oil surface. The rate of oil splattered should be a function of water drop size, velocity, spray density, oil surface tension, viscosity, oil density and other factors. The following Equation 6-1 is the chemical heat release rate in the fire products collector from the burning of splattered and vaporized oil. The combustion efficiency of oil vapor χ_v is assumed to equal the combustion efficiency of a free burn oil pool fire because the water spray fraction was probably small in the fire zone. The combustion efficiencies of free burning mineral seal oil and cooking oil pool fires are 0.76 and 0.98 from Tewarson [62] and Newman [41].

$$\dot{Q}_{chem} = (\chi_s \dot{m}_s'' + \dot{m}_v'') A \Delta H_{chem} \qquad 6\text{-}1$$

Where:

$\dot{m}_s''$ is the oil splattering rate per unit area

$\dot{m}_v''$ is the oil vaporization burning rate per unit area without splattering

A is cross section pan area

χ_s is the combustion fraction of the splattering oil, relative to that of oil vapor

ΔH_{chem} is the chemical heat of combustion for mineral seal oil ($\Delta H_{chem} = \chi_v \Delta H_T$)

$\dot{Q}_{chem}$ is chemical heat release rate measured in the fire products collector

The chemical heat release rate measured in the system is from burning rate of splattered oil and oil vaporization rate from the pool surface. Equation 6-1 has four unknowns $\chi_s, \dot{m}_s'', \dot{m}_v'', \Delta H_{chem}$ that are analyzed as follows:

The $\dot{m}_v''$ can be obtained by measuring the mass loss rate upon heating oil to a specific temperature and providing a downward wind velocity to simulate the spray induced air velocity. A horizontal velocity is also provided to obtain an oil vaporization rate for comparison with the

vaporization rate of the vertical wind. An evaporation rate of mineral seal oil at $130^{\circ}C$ obtained from a test without wind velocity is as shown in Figure 6.5. The evaporation rate is $0.19\frac{g}{m^2 s}$ for mineral seal oil heated to $130^{\circ}C$. Other vaporization rates are 0.084 $\frac{g}{m^2 s}$ and 0.034 $\frac{g}{m^2 s}$ for oil temperature of $110^{\circ}C$ and 90 $^{\circ}C$ respectively.

Experiments were also conducted in the advanced flammability measurements apparatus by Beaulieu[3] to obtain critical burning rates to sustain a flame, and heats of gasification of mineral seal oil and cooking oil. The critical burning rates per unit area are $2.1\frac{g}{m^2 s}$ and 4.6 $\frac{g}{m^2 s}$ for cooking oil and mineral seal oil and the heats of gasification of cooking oil and mineral seal oil are 0.8 kJ/g and 0.7 kJ/g. The vaporization rate at $130^{\circ}C$ is only 3 % of the critical burning rate without wind velocity. Vaporization rates with vertical wind and horizontal wind of mineral seal oil are as shown in Figure 6.6 and Table 6.3. The vaporization rates per unit area of mineral seal oil are linearly proportional to the vertical wind velocity for different temperature if the wind velocity is smaller than 3.3 m/s and can be expressed as equations 6-2 and 6-3. The vaporization rate is up to 6 % of the critical burning rate with wind velocity.

$$\text{At } 90\ ^{0}C: \dot{m}_v'' = 0.02u + 0.03 \quad (\text{u} < 3.3 \text{ m/s}) \tag{6-2}$$

$$\text{At } 110\ ^{0}C: \dot{m}_v'' = 0.06u + 0.06 \quad (\text{u} < 3.3 \text{ m/s}) \tag{6-3}$$

Where: $\dot{m}_v''$ is vaporization rate ($\frac{g}{s \cdot m^2}$)

u is vertical wind velocity (m/s)

The vaporization rate per unit area can also be estimated from the following theoretical equation.

$$\dot{m}_v'' = M_v k_g P_{sat} / RT_L \tag{6-4}$$

where: M_v is the vapor molecular weight (kg/kg-mole)

k_g is the mass transfer coefficient (m/min)

P_{sat} is the liquid saturation vapor pressure (Pa) at T_L

R is the ideal gas constant

T_L is the liquid temperature (^0K)

A correlation of mass transfer coefficient based on experimental data is provided by Mackay and Matsuga [32] as Equation 6-5. This equation shows the mass transfer coefficient is proportional to the 0.78 power of the horizontal wind velocity, but no correlation is found for vertical wind velocity.

$$k_g = 0.00482 N_{Sc}^{-0.67} u^{0.78} d_P^{-0.11} \qquad 6\text{-}5$$

Where

k_g is the mass transfer coefficient (m/s)

N_{sc} is the Schmidt number ($\frac{\nu}{D}$)

u is the wind velocity 10 m off the ground (m/s)

d_P is the diameter of the pool (m)

ν is the kinematic viscosity (m^2/s)

D is the diffusivity (m^2/s)

Mineral seal oil and cooking oil are blends of numerous hydrocarbons with varying vapor pressures as a function of temperature. If the composition and constituent vapor pressures were known the multi-component mass transfer coefficient could be calculated as described in the CCPS "Guidelines for Use of Vapor Cloud Dispersion Models, 2nd Edition, 1996" [1] and in the Wang M.S. thesis [69] .The vaporization rates of cooking oil are 0.008g/s, 0.014g/s, 0.024g/s, and 0.029g/s for vertical wind velocities 0 m/s, 1.6 m/s, 3.3 m/s, and 4.1 m/s at an oil temperature of 270^0C respectively as shown in Figure 6.7. The vaporization rate is also linearly proportional to vertical wind velocity for cooking oil.

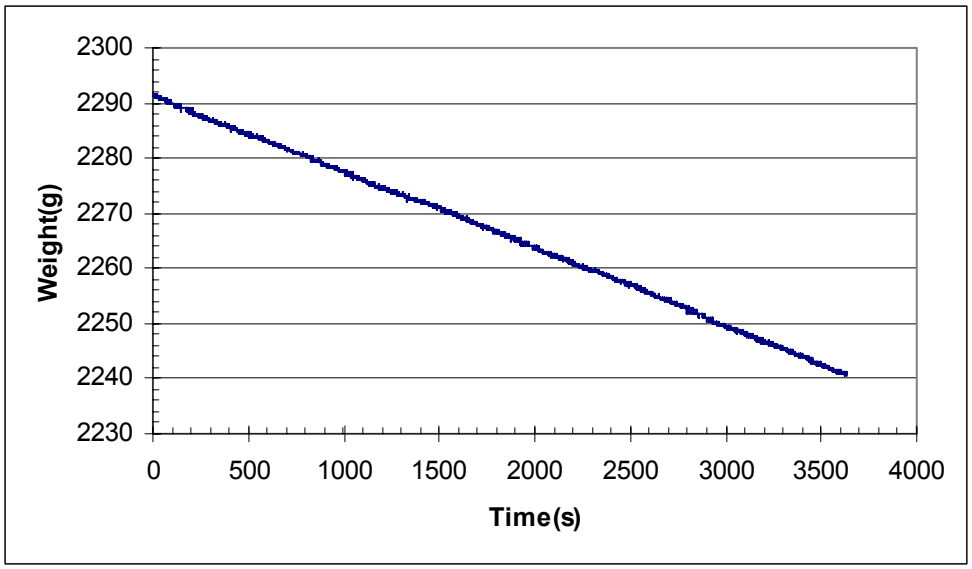

Figure 6.5 The weight v.s. time for the vaporization rate test of mineral seal oil at $130\,^{0}C$.

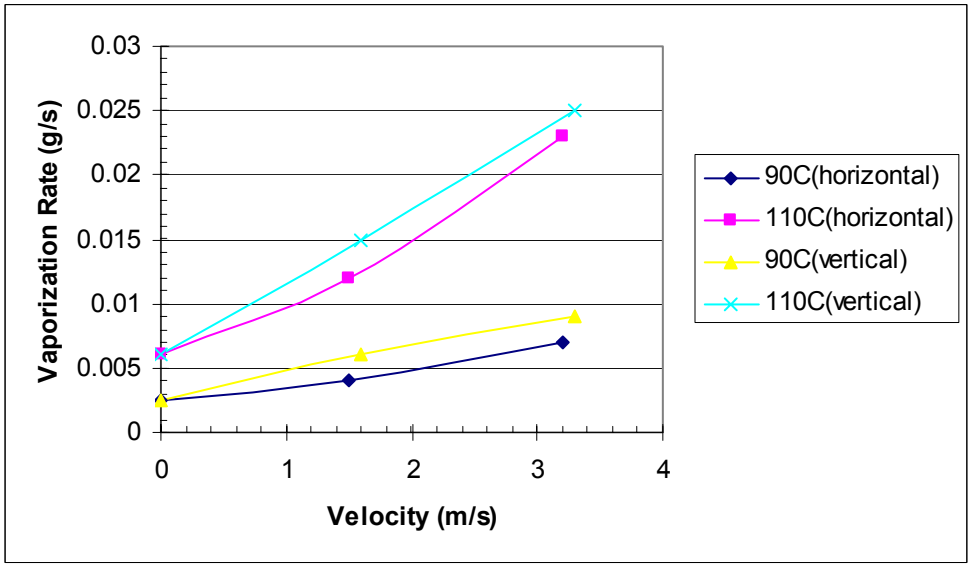

Figure 6.6 Vaporization rate v.s. velocity at different temperature for mineral seal oil.

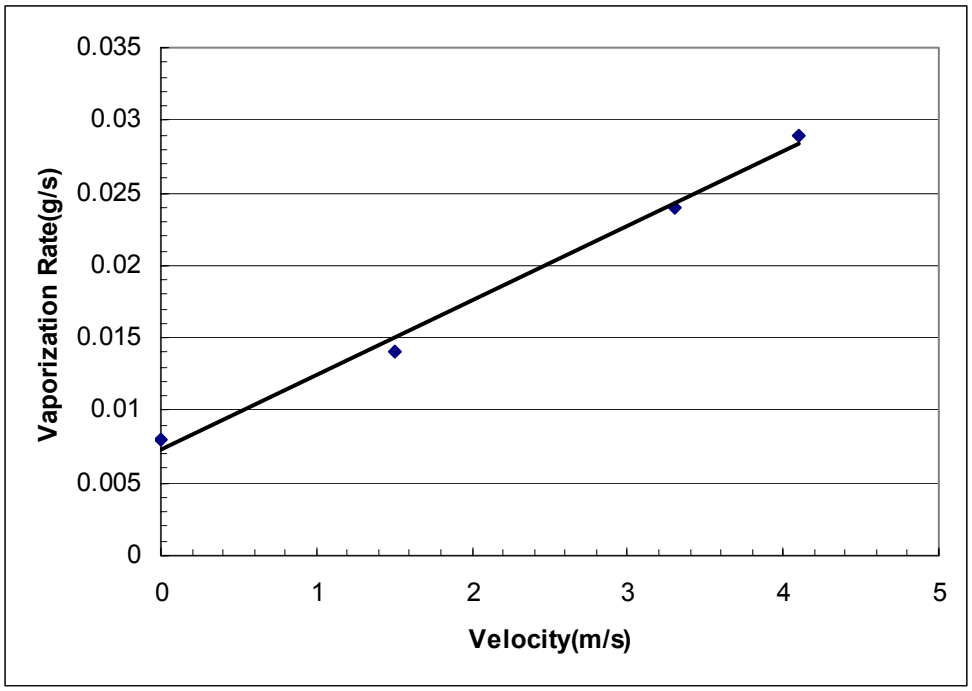

Figure 6.7 Vaporization rate v.s. vertical wind velocity for $270^{o}C$ cooking oil.

Table 6.3 Vaporization rate at different temperature and velocity for mineral seal oil.

Vaporization rate for horizontal wind			Vaporization rate for vertical wind		
Velocity (m/s)	Oil temperature $90^{\circ}C$	Oil temperature $110^{\circ}C$	Velocity (m/s)	Oil temperature $90^{\circ}C$	Oil temperature $110^{\circ}C$
0	0.0025 g/s	0.0061 g/s	0	0.0025 g/s	0.0061 g/s
1.5	0.004 g/s	0.012 g/s	1.6	0.006 g/s	0.015 g/s
3.2	0.007 g/s	0.023 g/s	3.3	0.009 g/s	0.025 g/s

The vaporization rates measured in these tests represent a combination of natural and forced convection with the relative contributions depending on the wind velocity. At zero wind velocity, there is only natural convection, but at velocities greater than 1,5 m/s, forced convection becomes dominant. The data indicate that vertical velocities produce larger vaporization rates

than horizontal velocities, perhaps because vertical velocities cause steeper velocity gradients at the liquid surface.

The chemical heat of combustion (ΔH_{chem}) can be obtained from pool fire free burns of mineral seal oil and cooking oil. The total heat release rate is the multiplication of mass burning rate, combustion efficiency, and heat of combustion for mineral seal oil. The equation is as follows:

$$\dot{Q}_{chem} = (\dot{m}'')A\chi\Delta H = \dot{m}''A\Delta H_{chem} \qquad 6\text{-}6$$

The chemical heat release rate can be obtained from data obtained in the fire products collector and the mass loss rate can be obtained by measuring the weight during the tests. The $\chi\Delta H$ or ΔH_{chem} can be obtained from equation 6-6. The chemical heat release rate and convective heat release rate can be calculated by the equations 6-7 and 6-8 using the fire products collector test data. The constant in equations 6-7 and 6-8 are modified for this specific equipment from ASTM E2058-01 as shown in appendix C. The chemical heat release rate obtained was 31 ± 2 kW in Figure 6.8 and the burning rate was recorded as 0.977 g/s from the mineral seal oil free burn test. The chemical heat of combustion can be calculated as 31.2 ± 2 kJ/g. The chemical heat release rate and burning rate of cooking oil are 29 ± 2 kW (as shown in Figure 6.9) and 0.85 g/s, respectively. The chemical heat of combustion of cooking oil can be obtained as 33 ± 2 kJ/g. These chemical heats of combustion are 32 kJ/g for mineral seal oil and 36 kJ/g for cooking oil from Tewarson [62] and Newman's [41] results.

$$\dot{Q}_{chem} = [7.434\times10^{-2}(X_{co_2} - X_{co_{2,\infty}}) + 6.764\times10^{-3}(X_{co} - X_{co,\infty})](\frac{P_\infty \Delta P}{T_{gas}})^{1/2} \qquad 6\text{-}7$$

$$\dot{Q}_{conv} = 3.3876(\frac{P_\infty \Delta P}{T_{gas}})^{1/2}(H_{(T_{gas})} - H_{(T_{amb})}) \qquad 6\text{-}8$$

where:

X_{co_2} the carbon dioxide concentration in the exhaust (ppm)

$X_{co_{2,\infty}}$ the carbon dioxide concentration in the atmosphere (ppm)

X_{co} the carbon monoxide concentration in the exhaust (ppm)

$X_{co,\infty}$ the carbon monoxide concentration in the atmosphere (ppm)

P_{∞} the atmosphere pressure (in. Hg)

ΔP the differential pressure in the exhaust (mmHg)

T_{gas} the temperature in the ambient (K)

T_{amb} the temperature in the exhaust (K)

$\dot{Q}_{chem}$ the chemical heat release rate (kW)

$\dot{Q}_{conv}$ the convective heat release rate (kW)

$H_{(T)}$ The enthalpy (kJ/kg) ($H_T = T + 6.7 \times 10^{-5} T^2 - 2590/T$)

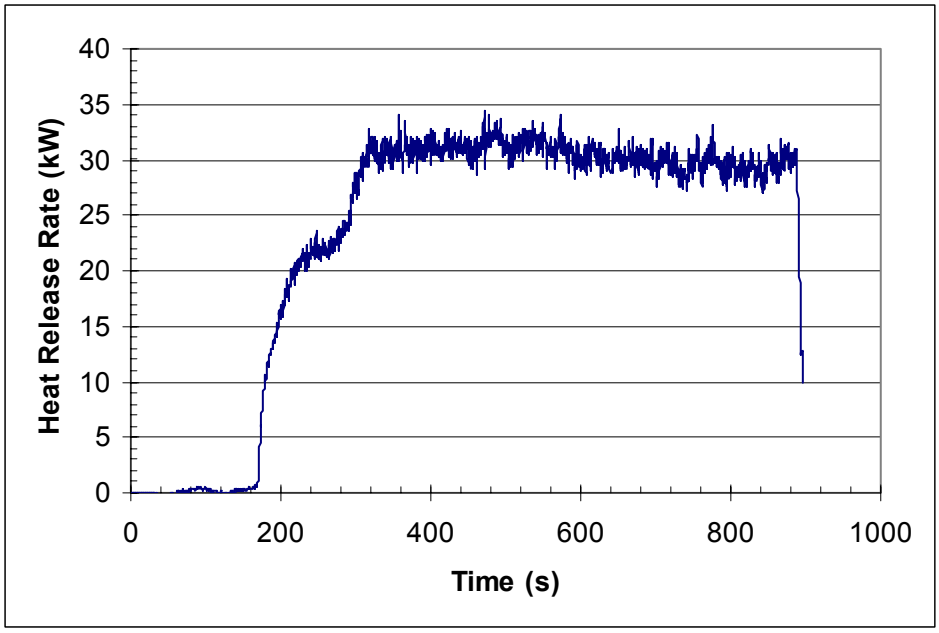

Figure 6.8 Chemical heat release rate for mineral seal oil free burn.

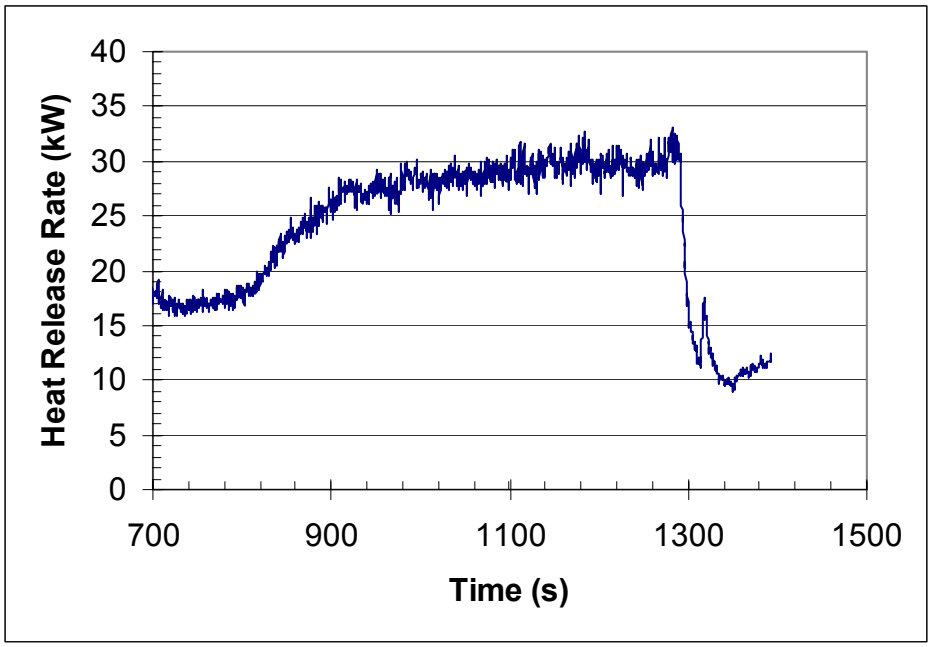

Figure 6.9 Chemical heat release rate for cooking oil free burn.

Another equation is required to solve the $\chi_s, \dot{m}''_s$. The mass loss rate is the sum of the splattered oil rate and oil vaporization rate as shown in equation 6-9. The mass loss rate can be obtained from equation 6-10 when water spray was discharged onto the oil. The mass change rate was measured during the test and $\dot{m}_{w,s}$ can be obtained from the delivered density test as shown in equation 6-11 from the delivered density test in later discussions. The $\dot{m}_{loss}$ can be calculated form equation 6-10 and χ_s can be calculated from equation 6-1.

$$\dot{m}_{loss} = (\dot{m}''_s + \dot{m}''_v)A \qquad 6\text{-}9$$

$$\dot{m}_{pan} = \dot{m}_{w,s} - \dot{m}_{loss} \qquad 6\text{-}10$$

$$\dot{m}_{w,s} = \dot{m}''_{dd}(\dot{Q})A \qquad 6\text{-}11$$

Where: $\dot{m}''_{dd}(\dot{Q})$ is the water delivered density at $\dot{Q}$ using the same nozzle and flow rate.

$\dot{m}_{w,s}$ is water gain rate in the pan

$\dot{m}_{pan}$ is mass change rate in the pan

$\dot{m}_{loss}$ is the oil loss rate in the pan

Equation 6-11 neglects any water loss due to vaporization and splashing. It is assumed that these losses only a small percentage of the delivered density since the water does not float on the liquid surface. The delivered density $\dot{m}''_{dd}(Q)$ can be obtained from water spray discharging through the propane ring burner. Ring burner fires using 1.42 m^3/hr (50 $ft^3/\min$), 1.70 m^3/hr (60 $ft^3/\min$), and 1.98 m^3/hr (70 $ft^3/\min$) flow rates of propane were used to simulate oil splattering fire sizes of 35kW, 40 kW, and 48kW respectively. 10 psi water from a 1/2GG29SQ nozzle, 10psi water from a 3/8GG15 nozzle, and 10psi water from a 3/8GG22 nozzle were used to discharge onto the propane burner at 1.42 m^3/hr (50 $ft^3/\min$), 1.70 m^3/hr (60 $ft^3/\min$), and 1.98 m^3/hr (70 $ft^3/\min$) flow rates. The chemical heat release rates remained the same 40kW for those nozzles when the flow rate of propane was maintained at 1.70 m^3/hr (60 $ft^3/\min$) as shown in Figures Figure 6.10 to Figure 6.12. The propane burner is a good simulation for different water densities discharging into different fire sizes. Other delivered densities for different fire sizes were also obtained and shown in Figure 6.13 and Table 6.4.

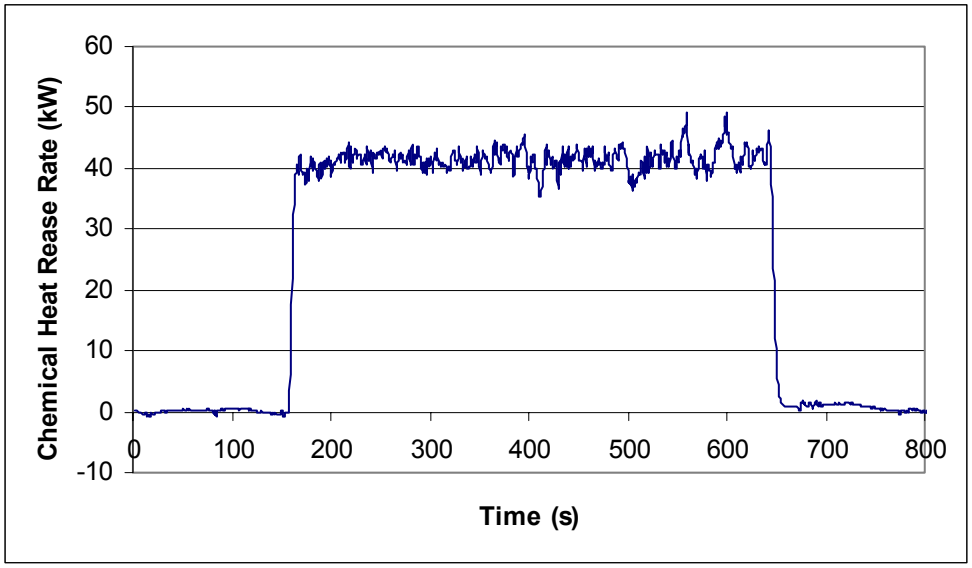

Figure 6.10 The chemical heat release rate v.s. time for 10 psi water of 3/8GG,18SQ nozzle on1.70 m^3/hr (60 $ft^3/\min$) propane burner.

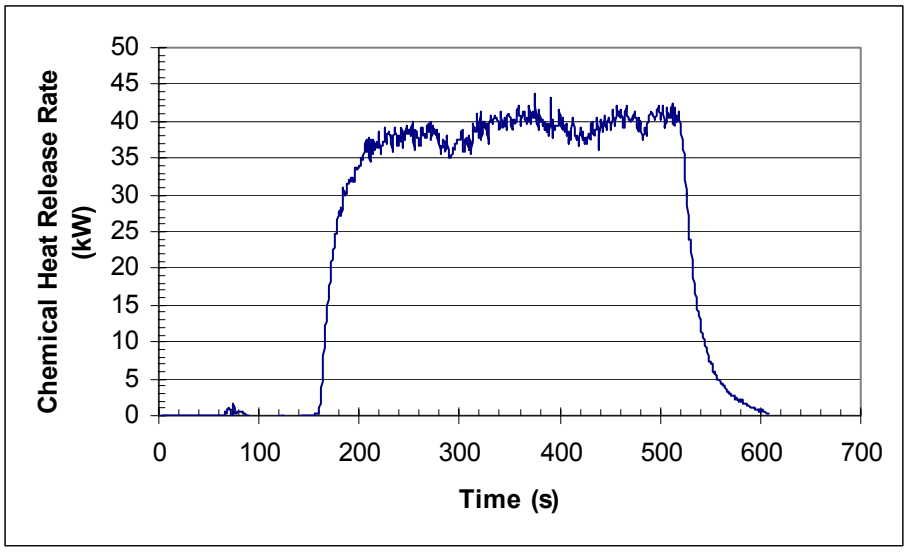

Figure 6.11 The chemical heat release rate v.s. time for 10 psi water of 3/8GG,15 nozzle on 1.70 m^3/hr (60 $ft^3/\min$) propane burner.

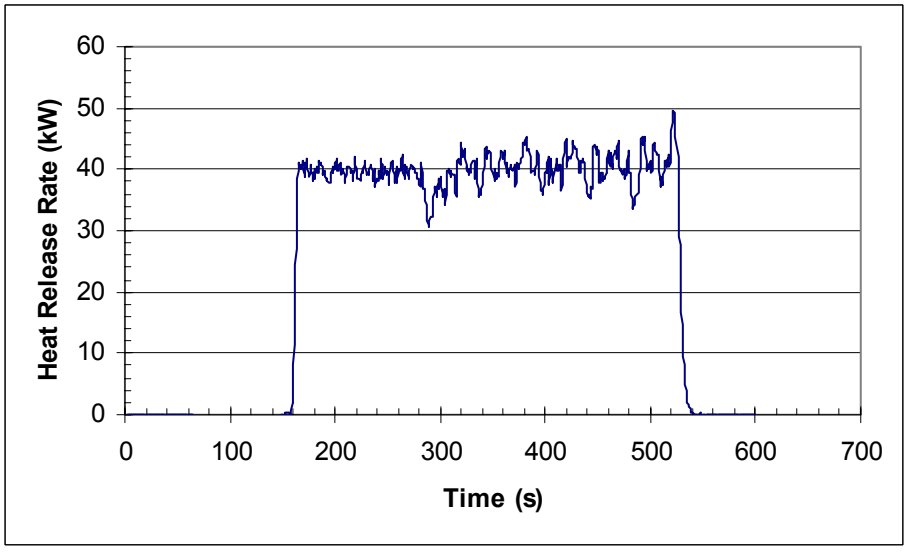

Figure 6.12 The chemical heat release rate v.s. time for 10 psi water of 1/2GG, 29SQ nozzle on 1.70 m^3/hr (60 $ft^3/\min$) propane burner.

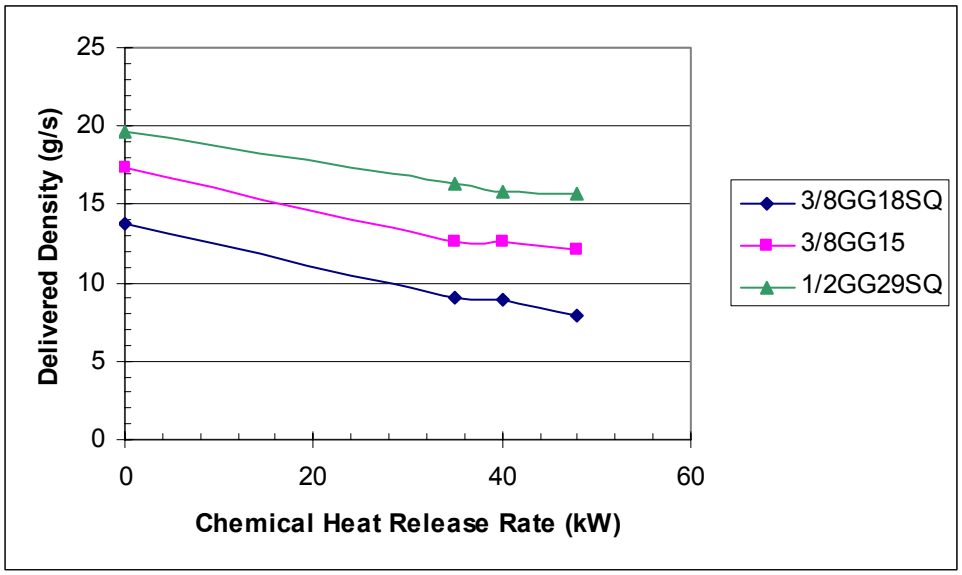

Figure 6.13 The delivered density v.s. chemical heat release rate for different nozzle.

Table 6.4 Delivered Density for different nozzles and different fire sizes.

$\dot{Q}_{chem}$ (kW)	10psi 3/8GG18SQ (g/s)	10psi 3/8GG 15 (g/s)	10psi 1/2GG29SQ (g/s)
0	13.8	17.3	19.6
35	9.03	12.6	16.3
40	8.94	12.6	15.8
48	7.9	12.1	15.8

Oil splattering quantification tests include water discharging onto $110^{o}C$ heated mineral seal oil, and igniting the oil by a ring burner pilot flame as described in chapter 3.2. The heat release rates measured in the fire products collector were 40kW, 37kW, and 30kW as shown in Figure 6.14 to Figure 6.16 when 10 psi from a 1/2GG 29SQ nozzle, 10 psi from a 3/8GG 15 nozzle, and 10 psi from a 3/8GG 18SQ nozzle water sprays were discharged onto mineral seal oil heated to $110^{o}C$. The mass gain rates are 12.3g/s, 9.7g/s, and 7.6g/s for 1/2GG29SQ nozzle, 3/8GG15 nozzle, and 3/8GG18SQ nozzle water discharge respectively. The vaporization rates can be obtained from

equation 6-3 as $0.15\frac{g}{m^2 s}$, $0.15\frac{g}{m^2 s}$, and $0.16\frac{g}{m^2 s}$ for these nozzle spray velocities at an oil temperature of $110^{o}C$. Rasbash[55] found that the smallest droplet velocity is equal to that of the entrained air in the spray. The smallest droplet velocities were found close to their mean velocities in these tests. The oil was cooled to $108^{o}C$ after the test. The oil mass loss rates can be obtained from Equations 6-10 and 6-11. The combustion fraction was obtained from Equation 6-1 if the vaporization rates data were obtained from vaporization tests and the mass loss rates of splattering oil were obtained from equation 6-10. Larger droplets caused more oil splattering and more burning oil contributed to the fire producing a larger heat release rate as shown on Table 6.5. The combustion efficiency is smaller for lager droplet water spray, and further analyses are conducted in chapter 7.

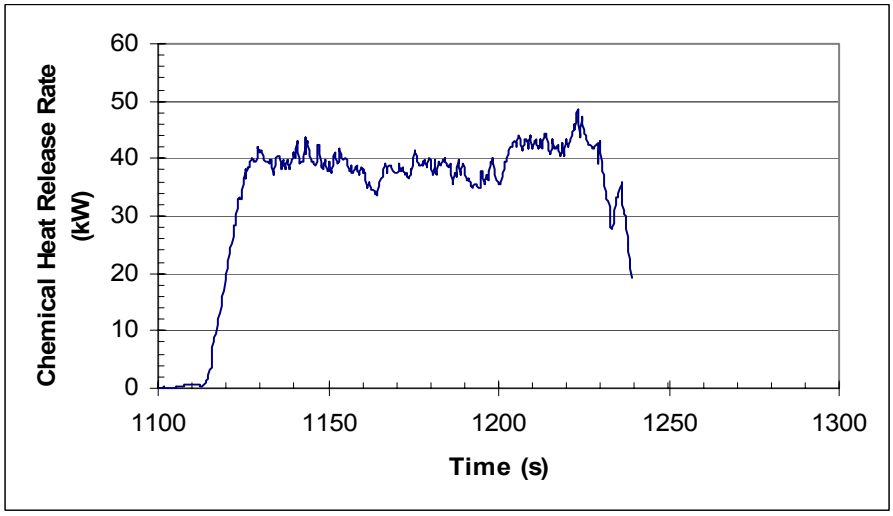

Figure 6.14 The chemical heat release rate v.s. time for 10 psi 1/2GG,29SQ nozzle on $110^{o}C$ mineral seal oil.

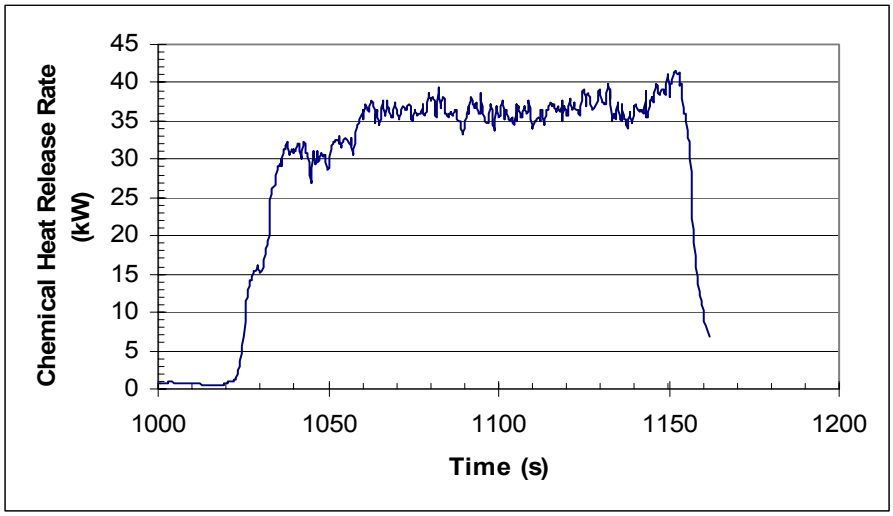

Figure 6.15 The chemical heat release rate v.s. time for 10 psi 3/8GG 15 nozzle on $110^{o}C$ mineral seal oil.

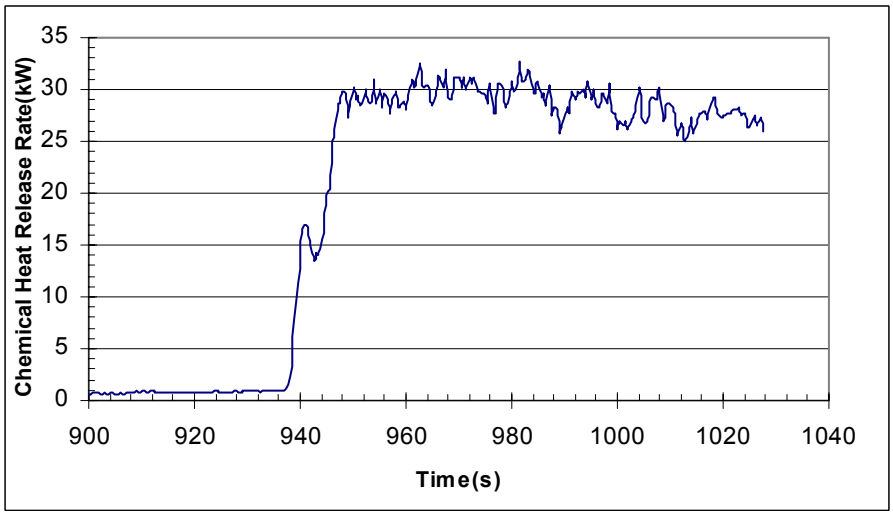

Figure 6.16 The chemical heat release rate v.s. time for 10 psi 3/8GG, 18SQ nozzle on $110^{o}C$ mineral seal oil.

Table 6.5 Oil splattering tests result for mineral seal oil at $110^{o}C$.

	Drop Size (μm)	Drop Velocity (m/s)	$\dot{m}''_w$ ($\frac{g}{s \cdot m^2}$)	$\dot{m}''_v$ ($\frac{g}{s \cdot m^2}$)	$\dot{m}''_s$ ($\frac{g}{s \cdot m^2}$)	χ_s	$\frac{\dot{m}''_v}{\dot{m}''_s \chi_s + \dot{m}''_v}$	$\frac{\dot{Q}}{Q_{freeburn}}$	$\frac{\dot{m}''_s}{\dot{m}''_w}$
10 psi 1/2GG 29SQ	617	2.44	265	0.15	46	0.37	0.01	1.25	0.17
10 psi 3/8GG1 5	415	2.57	238	0.15	39	0.40	0.012	1.16	0.16
10 psi 3/8GG 18SQ	389	2.61	185	0.16	25	0.51	0.017	0.92	0.13

The cooking oil was preheated to $270^{o}C$ with a heater inside the oil and 50psi water from a Spraco 110620 nozzle, 75psi water from a 1/8HH,1.5 nozzle, and 25psi water from a BETE WL1 1/2 nozzle were discharged onto the heated oil with a pilot flame by using a propane ring burner as shown in Figure 6.17 to Figure 6.19. The flame height increases with the drop size of the water spray. The oil was spread outside the pan causing a huge fire ball when 243 μm droplet diameter water sprays discharged onto cooking oil heated to $270^{o}C$ as shown in Figure 6.20. This fire size was beyond the collector capacity, and the heat release rate data cannot be used for further analysis of the test. The heat release rates of three other tests were successfully measured in the fire products collector as shown in Figure 6.21 to Figure 6.23. The splattered cooking oil heat release rates were several times larger than the splattered mineral seal oil heat release rates. The heat release rates decreased with time in Figure 6.22 and Figure 6.23 because the oil levels decreased very quickly and the larger ullage height reduced the liquid burning rate in a tank fire as described in chapter 8 of industrial fire protection engineering by Zalosh [77] . The cooking oil was cooled to $268^{o}C$ after the tests. Larger droplets caused large fire balls because oil splattered contributing to the fire. The mass loss rates are 7.6 g/s, 9.7 g/s, and 12.3 g/s for 50psi from a sprayco 110620 nozzle, 75psi from a 1/8HH1.5 nozzle, and 25psi from a BETE WL1 1/2 nozzle

of water discharge respectively. Cooking oil splattered significantly, and no water was collected inside hot oil. The mass change rate $\dot{m}_{pan}$ equaled to negative of the oil mass loss rate in Equation 6-10. The vaporization rates can be obtained as $0.2\ g/s\cdot m^2$, $0.3\ g/s\cdot m^2$, and $0.18\ g/s\cdot m^2$ for these nozzle test conditions from Figure 6.7. The combustion fraction can be obtained from equation 6-1 if the vaporization rate data were obtained from the vaporization tests and the mass loss rates of splattering oil were obtained from equations 6-10. Larger droplets caused more oil splattering and more burning oil contributed to the fire that showed a larger heat release rate as shown in Table 6-6. The heat release rate caused by $116\ \mu m$, $143\ \mu m$, and $189\ \mu m$ droplet water sprays are 2.12, 4.14, and 5.5 times the heat release rate of free burning cooking oil.

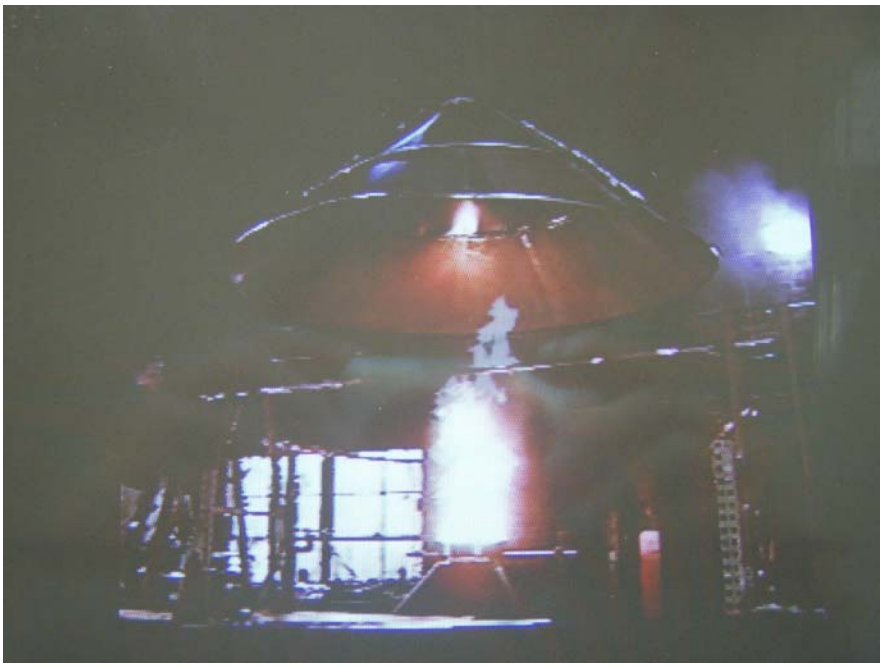

Figure 6.17 Cooking oil splattering fire for 50 psi Spraco 110620 water spray ($116\ \mu m$) on $270\ ^oC$ oil.

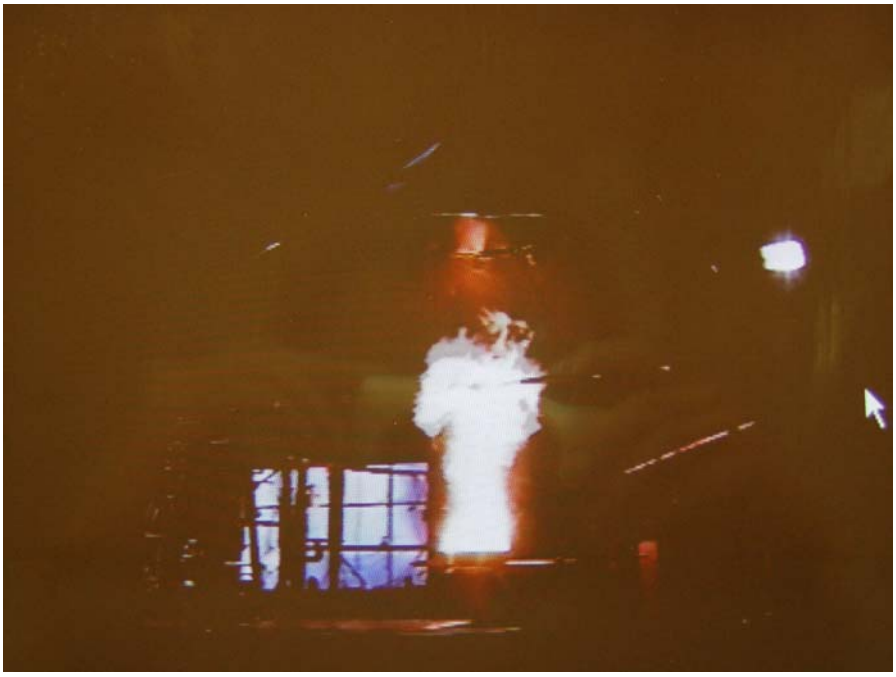

Figure 6.18 Cooking oil splattering fire for 75 psi 1/8HH1.5 nozzle water spray (143 μm) on 270 ^{o}C oil.

Figure 6.19 Cooking oil splattering fire for 25 psi BETE 1 1/2 water spray (189 μm) on 270 ^{o}C oil.

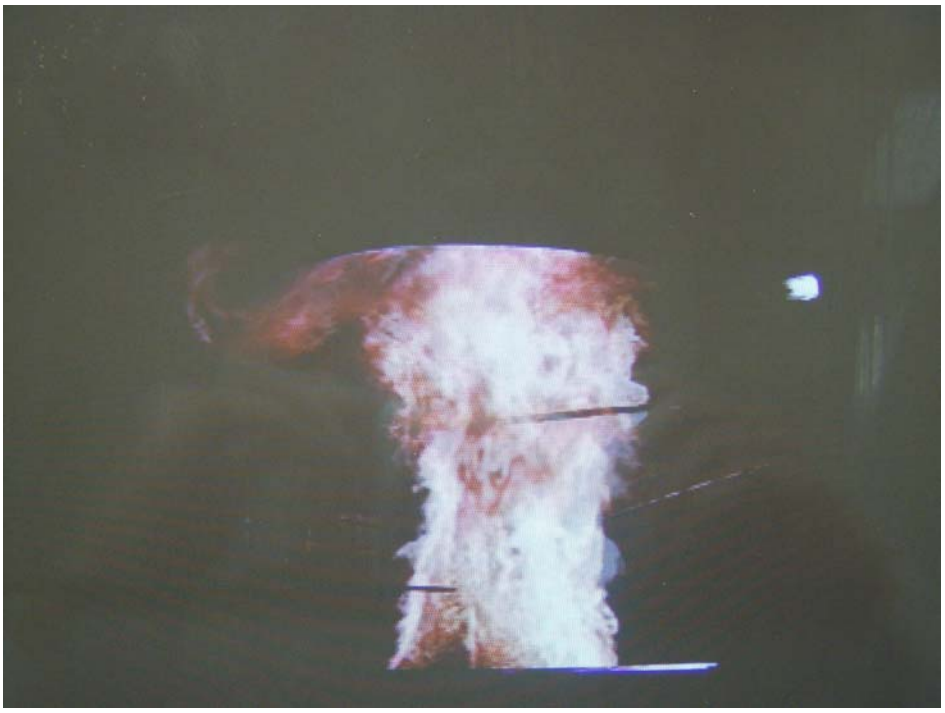

Figure 6.20 Cooking oil splattering fire for 20 psi Spraying System water spray (243 μm) on 270 ^{o}C oil.

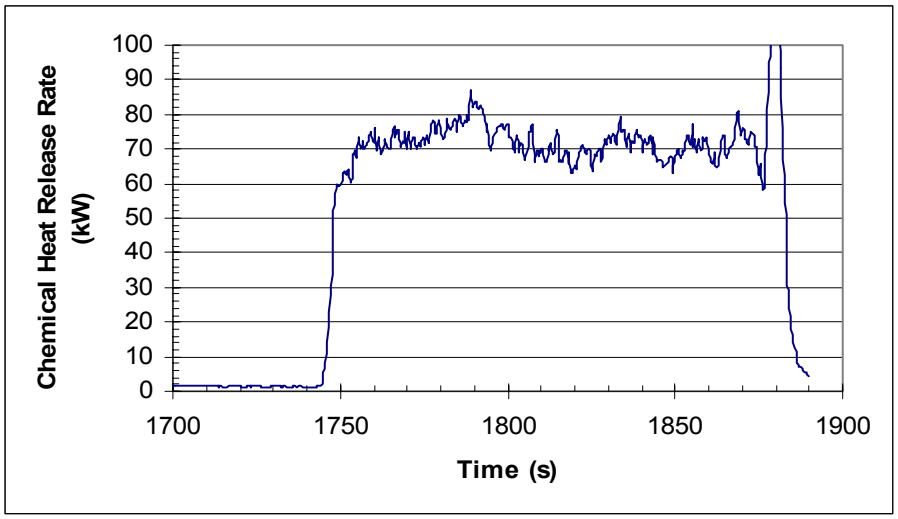

Figure 6.21 The heat release rate v.s. time for 50 psi spraco 110620 nozzle of water on 270 ^{o}C cooking oil.

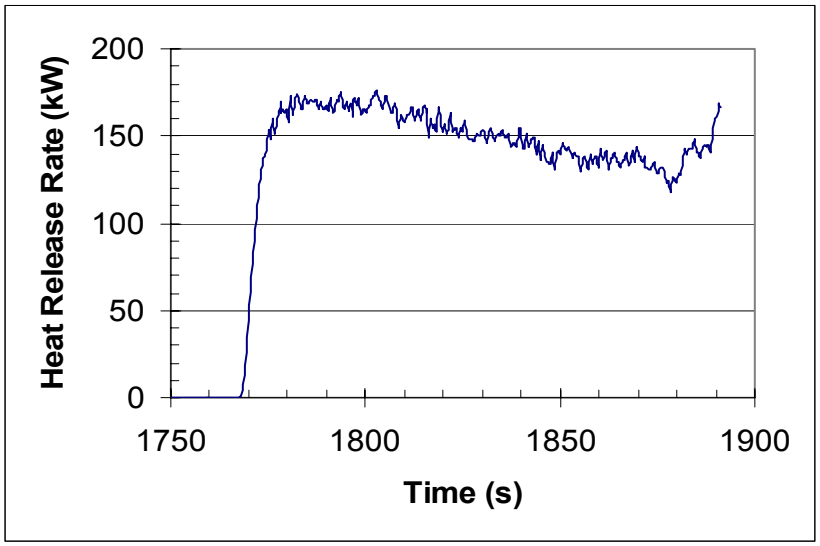

Figure 6.22 The heat release rate v.s. time for 75 psi 1/8HH1.5 nozzle of water on $270^{o}C$ cooking oil.

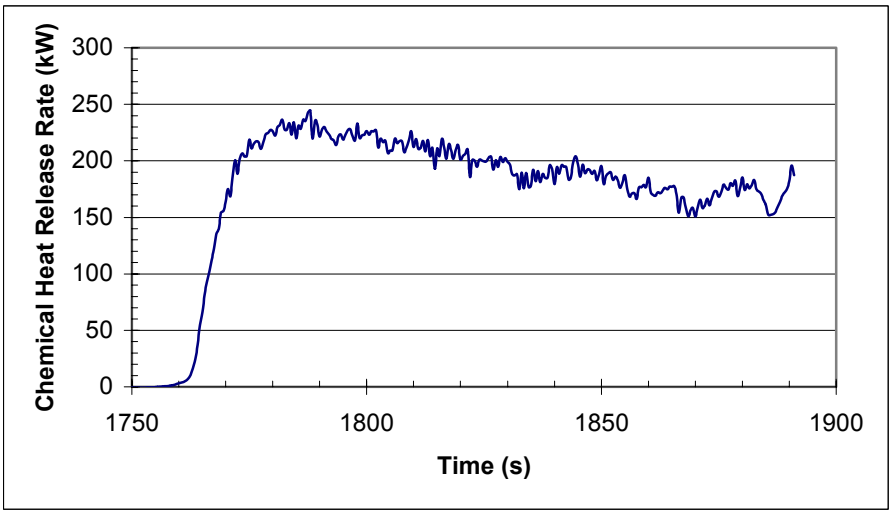

Figure 6.23 The heat release rate v.s. time for 25 psi BETE WL 1 1/2 nozzle of water on $270^{o}C$ cooking oil.

Table 6.6 Oil splattering tests result for cooking oil at $270^{o}C$.

	Drop Size (μm)	Drop Velocity (m/s)	$\dot{m}''_w$ $(\frac{g}{s \cdot m^2})$	$\dot{m}''_v$ $(\frac{g}{s \cdot m^2})$	$\dot{m}''_s$ $(\frac{g}{s \cdot m^2})$	χ_s	$\frac{\dot{m}''_v}{\dot{m}''_s \chi_s + \dot{m}''_v}$	$\frac{\dot{Q}}{Q_{freeburn}}$	$\frac{\dot{m}''_s}{\dot{m}''_w}$
50 psi Sprayco 11062	116	2.61	54	0.2	43	0.68	0.0088	2.12	0.79
75 psi 1/8HH1.5	143	3.12	48	0.3	80	0.7	0.0068	4.14	1.68
25 psi BETE WL 1 ½	189	2.48	48	0.18	114	0.67	0.003	5.55	2.39

6.3 Summary

A series of tests for mineral seal oil ignited by water spray with a pilot flame was conducted at different temperatures below the oil flash point of 137 $^{\circ}C$ (see Table 6.1). At higher oil temperatures, longer fire duration was obtained because more oil splattering occurred at higher oil temperatures causing sustained burning. However, the water spray induced splattering oil ignition even at room temperature.

Green dye water spray discharging onto heated oil was used to visualize and photograph splattering oil. The results showed that the oil splattering is generated oil sputter that reach 10 cm above the oil surface

Oil vaporization rates were measured at different air velocities and different temperatures for mineral seal oil and cooking oil. The vaporization rates of mineral seal oil and cooking oil are linearly proportional to vertical wind velocities for different temperatures if the wind velocities are smaller than 3.2 m/s. The vaporization rates of mineral seal oil are also proportional to horizontal wind velocity for mineral seal oil at different temperatures.

The delivered density can be obtained from water spray discharging through the propane ring burner. Ring burner fires using 1.42 m^3/hr (50 $ft^3/\min$), 1.70 m^3/hr (60 $ft^3/\min$), and 1.98 m^3/hr (70 $ft^3/\min$) flow rates of propane were used to simulate oil splattering fire sizes as 35kW, 40 kW, and 48kW respectively. 10psi water of 1/2GG29SQ nozzle, 10psi water of 3/8GG15, and 10psi water of 3/8GG22 were used to discharge into propane burner at 1.42 m^3/hr (50 $ft^3/\min$), 1.70 m^3/hr (60 $ft^3/\min$), and 1.98 m^3/hr (70 $ft^3/\min$) flow rates. The chemical heat release rates remained the same 40kW for these nozzles when the flow rate of propane was maintained at 1.70 m^3/hr (60 $ft^3/\min$).

Larger droplets caused more oil splattering and more burning oil contributing to fire that showed larger heat release rates collected in the hood and exhaust system for mineral seal oil and cooking oil. The heat release rate caused by 389 μm, 415 μm, 617 μm droplet water sprays are

0.92, 1.13, and 1.25 times the free burn heat release rate of the mineral seal oil pool fire. The heat release rate caused by 116 μm, 143 μm, 189 μm droplet water sprays are 2.12, 4.14, 5.5 times the free burn heat release rate of the higher temperature (270 $^{\circ}C$) burning cooking oil.

7 Intensification and Splattering Analysis

Oil splattering is a very important phenomenon for the intensification of high flash point pool fires. Previous research on the factors that affect splattering is reviewed briefly here. Worthington[72] dropped milk into water to observe the splash scenario. He observed that higher falling drop obtained a higher crater and a taller rebounding column because the higher falling drop provided a larger momentum onto the water. Manzello et al [34] found that the liquid splash was caused at higher Weber number if the pool temperature is lower. For 20 $^{\circ}C$ water pool, the critical Weber number to cause splash is 57. It is 38 for 94 $^{\circ}C$ water pool. They[34] also found the critical Weber number for jet breakup was independent of liquid depth. The amount of oil splattering is also found to depend on the Weber number of the water spray and oil temperature from this research. The larger Weber number of water spray and higher oil temperature caused more oil splattering for high flash point hydrocarbon pool fires. A more detailed discussion of the fire heat release rate test data in chapter 6 for mineral seal oil and cooking oil splattering related to Weber number is as follows.

7.1 Oil splattering for mineral seal oil

The heat release rate increases with Weber number and water density of the water spray for the bottom heated mineral seal oil splattering tests as shown in Figure 7.1. The ratio of oil splattering heat release rates to the free burn heat release rate is in the range 0.92 to 1.25 with a ratio of 1.0 occurring at a Weber number of 38, corresponding to a drop diameter of about 400 μm. The heat release rates were enhanced by the water spray when We > 38. The larger Weber number of the water spray caused more oil splattering of mineral seal oil as shown in Figure 7.2. The ratio of oil splattering mass flux to water density increases with Weber number of the water spray and reaches a constant 0.18; the curve can be expressed as equation 7-1 for mineral seal oil preheated to 110 $^{\circ}C$.

$$\frac{\dot{m}''_s}{\dot{m}''_w} = 0.18 - 41.25e^{-\frac{We}{5.4}} \qquad (T_{FP} = 137^{\circ}C \text{ and } 35<\text{We}<55) \tag{7-1}$$

Thus, the fire intensification is roughly linearly proportional to the spray density when We > 38. The combustion fraction (χ_s) of splattering mineral seal oil decreases with the Weber number of the water spray as shown in Figure 7.3. Figure 7-4 shows that the χ_s decreases with increasing spray density. The equation 7-2 can be used to obtain the combustion fraction based on the Weber number, and density of water spray for preheated mineral seal oil. The larger Weber number water sprays apparently caused more oil splattering outside the flaming area and reduced the combustion fraction.

$$\chi_s = 0.36 + (-0.0018\dot{m}''_w + 0.49)e^{-\frac{We}{(-23.8\dot{m}''_w + 5778)}}$$

$$(T_{FP} = 137^{\circ}C, 185\frac{g}{m^2 s} < \dot{m}''_w < 270\frac{g}{m^2 s} \text{ and } 35<\text{We}<55) \tag{7-2}$$

The heat release rate contributed by vaporization rate of the mineral seal oil also decreases with the Weber number of the water spray as shown in Figure 7.45. The contribution of vaporization rate to heat release rate is about 1 % to 1.7 % based on different Weber numbers of the water spray. The correlation can be expressed as equation 7-3 for the vaporization rate of mineral seal oil.

$$\frac{\dot{m}_v''}{\dot{m}_s''\chi_s + \dot{m}_v''} = 0.0116 + 3\times10^5 e^{-\frac{We}{2.07}} \quad (T_{FP} = 137^\circ C \text{ and } 35<\text{We}<55) \qquad 7\text{-}3$$

Oil splattering rate, vaporization rate, and combustion fraction can be calculated from equations 7-1, 7-2 and 7-3 for mineral seal oil at specific water densities and Weber numbers of the water spray. These data can be used to quantify oil splattering contribution in preheated mineral seal oil fire suppression tests.

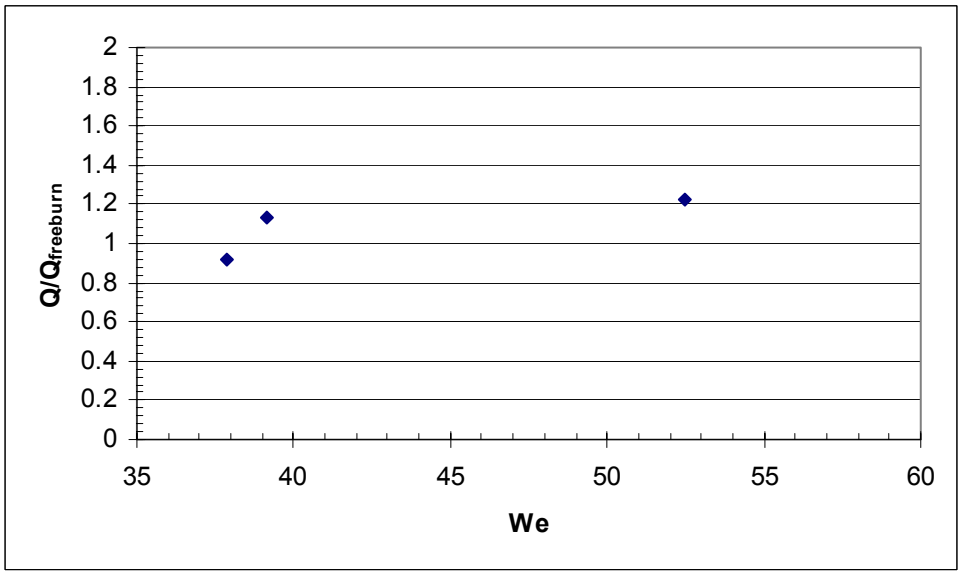

Figure 7.1 The ratio of heat release rate of spray induced oil splattering to oil free burn HRR for $110^\circ C$ mineral seal oil.

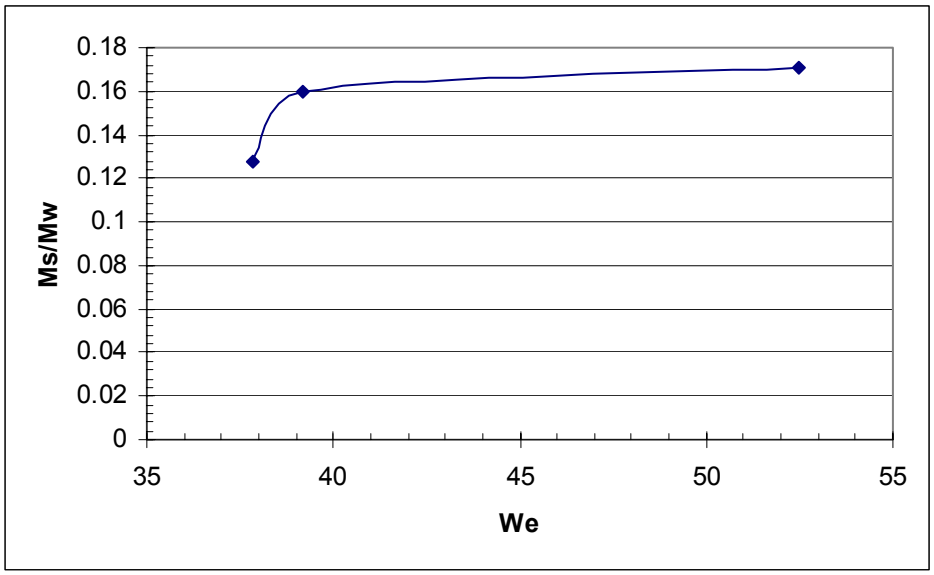

Figure 7.2 The ratio of oil splattering to water density for 110°*C* mineral seal oil.

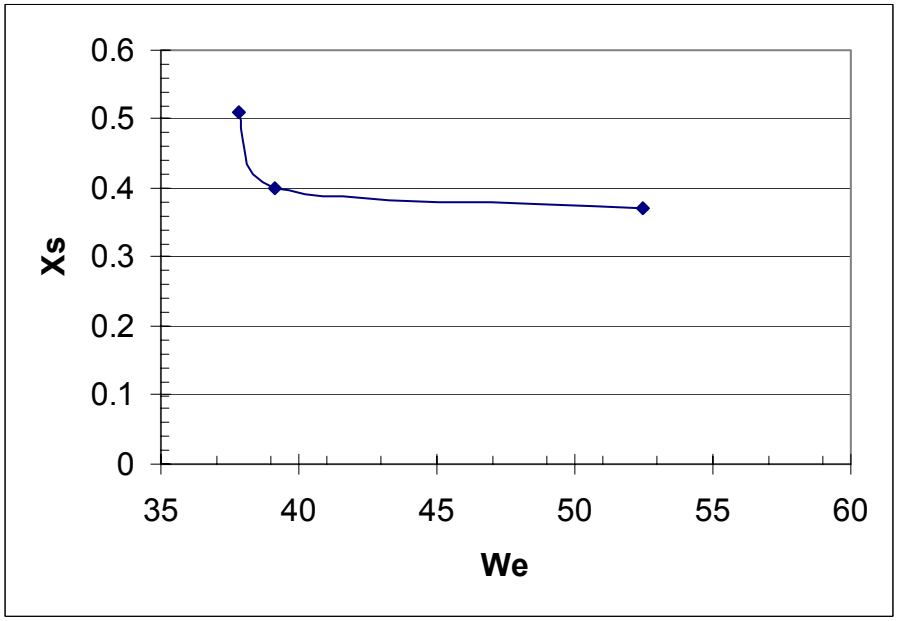

Figure 7.3 The combustion fraction v.s Weber number for 110°*C* mineral seal oil.

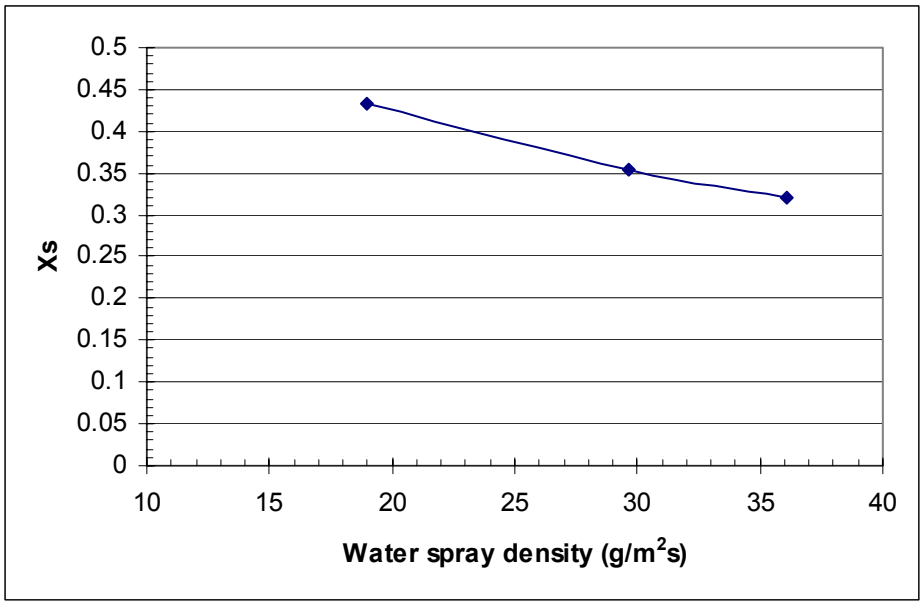

Figure 7.4 The combustion fraction v.s. water spray density for 110°*C* mineral seal oil.

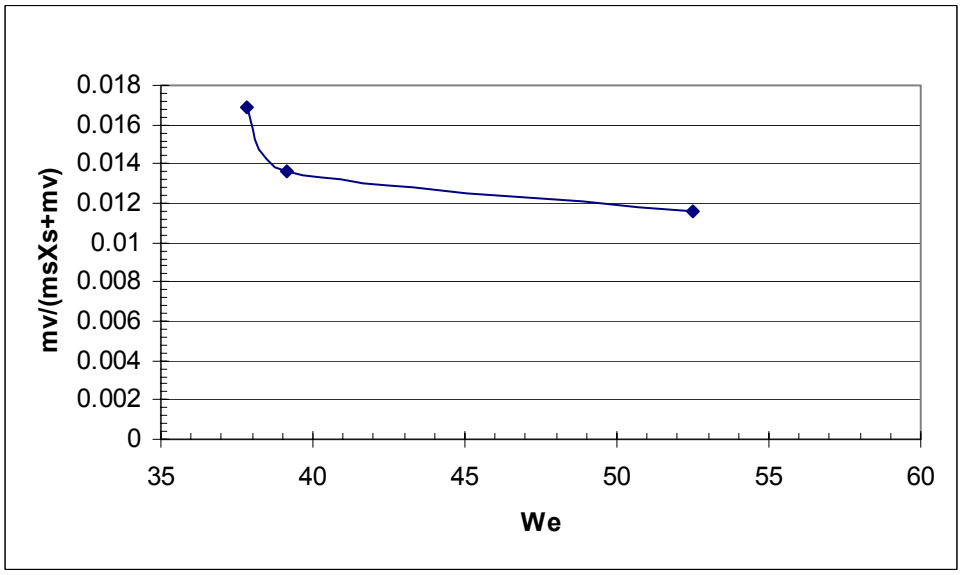

Figure 7.5 The ratio of vaporization rate to total oil burning rate for 110°*C* mineral seal oil.

7.2 Cooking oil splattering analysis

The flash point of cooking oil, 270^0C, is much higher than the boiling point of water. This temperature difference caused even more oil splattering when water spray was discharged onto the preheated cooking oil fire. The heat release rate is significantly greater for water spray on cooking oil than on mineral seal oil fires. The heat release rate is enhanced by factors from 2.12 to 5.55 compared to the heat release rate of free burning cooking oil as shown in Figure 7.6. This corresponding ratio is only 0.92 to 1.25 for mineral seal oil. The ratio factor in Figure 7.6 is close to 1 When Weber number is close to zero. This stands for the oil splattering caused by lower Weber number of water spray for cooking oil and mineral seal needs higher Weber number of water spray to cause oil splattering. The oil splattering of preheated cooking oil is very larger than the oil splattering of preheated mineral seal oil even though the spray density for the cooling oil (about 3 mm/min) was much less than the spray density for mineral seal oil (11 to 16 mm/min). The ratio of oil splattering mass flux to water density correlated to the Weber number of the water spray is as equation 7-4 and as shown in Figure 7.7.

$$\frac{\dot{m}''_s}{\dot{m}''_w} = 0.1We - 0.3 \qquad (T_{FP} = 270^\circ C \text{ and } 10<\text{We}<30) \tag{7-4}$$

The combustion fraction is constant, 0.68, for cooking oil as shown in Figure 7.8. The lower Weber number and water density of the water spray caused high combustion fraction for cooking oil tests, probably because the oil splatter consisted of smaller oil droplets. The higher Weber number tests could not be conducted because too much oil splattered outside the pan and the fire also spread to the metal cover as shown in Figure 6.20. The vaporization rate is less than 1 % because higher oil splattering contributing to fires is caused by water spray as shown in Figure 7.9 and the vaporization of oil is not as important compared as oil splattering for cooking oil. These data can be used to quantify oil splattering contribution in preheated cooking oil fire suppression tests.

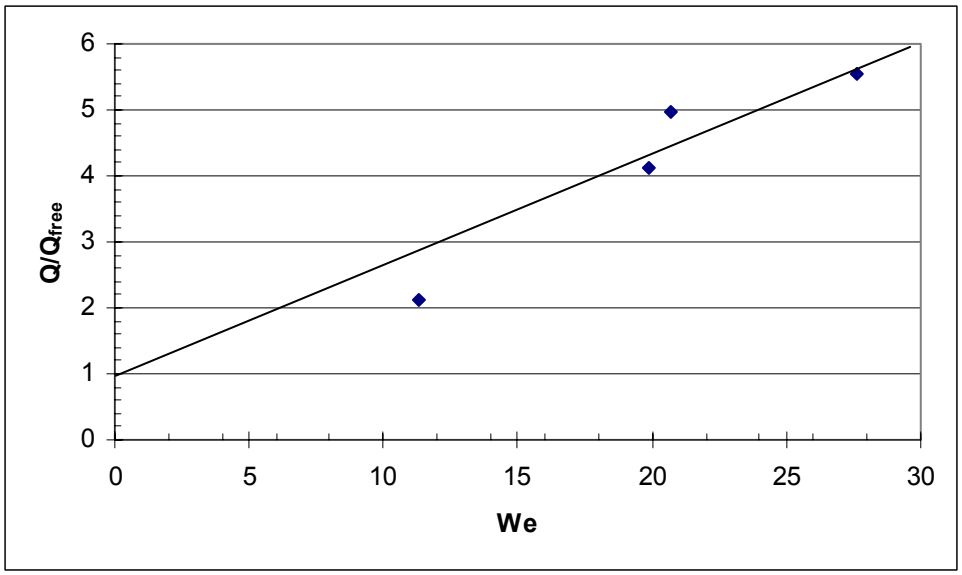

Figure 7.6 The ratio of heat release rate of oil splattering tooil free burn for 270 $^{\circ}C$ cooking oil.

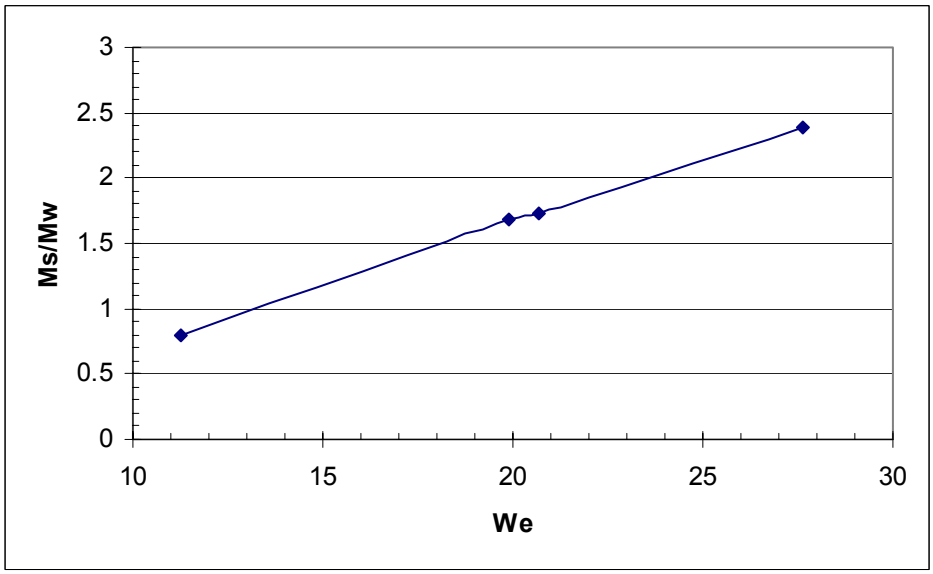

Figure 7.7 The ratio of oil splattering to water density for 270 $^{\circ}C$ cooking oil.

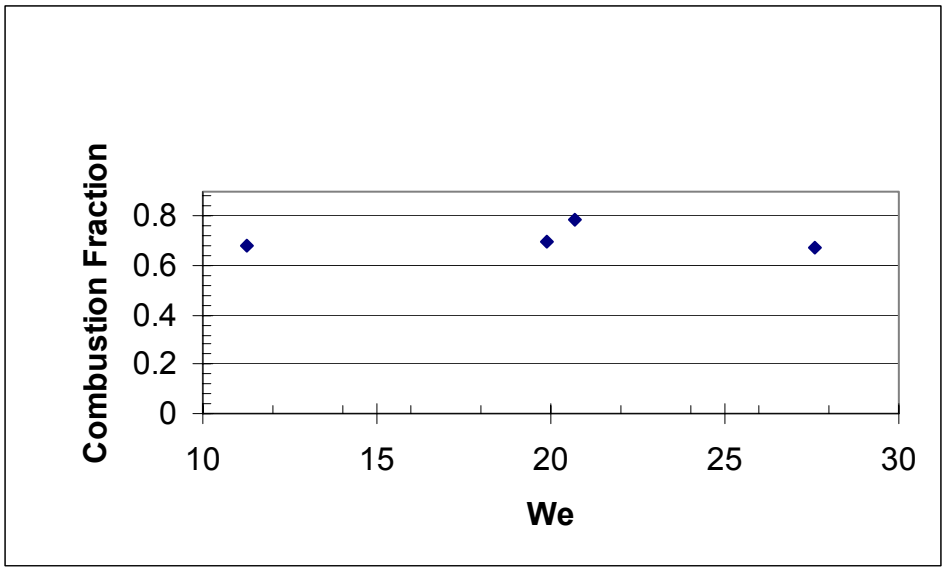

Figure 7.8 The combustion fraction v.s Weber number for 270 $^{\circ}C$ cooking oil.

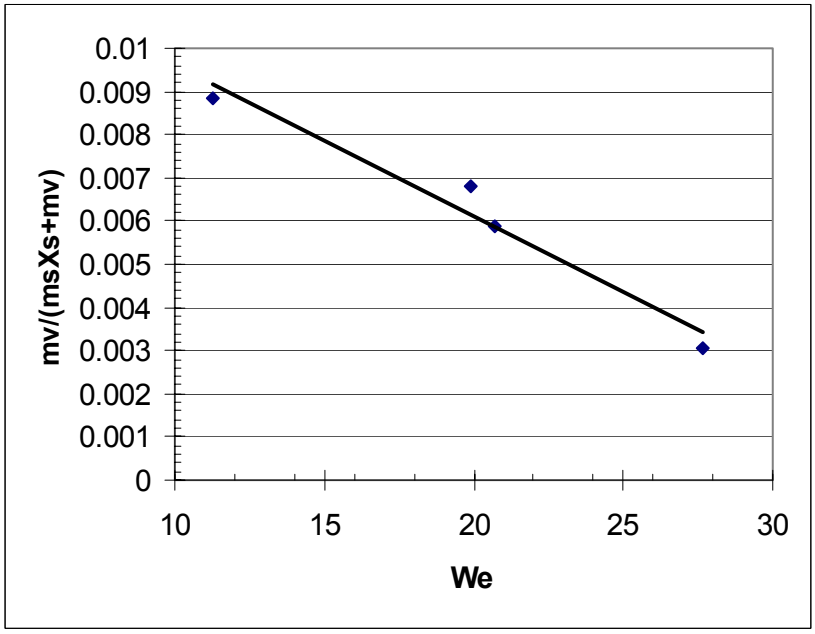

Figure 7.9 The ratio of vaporization rate to total oil burning rate for 270 $^{\circ}C$ cooking oil.

7.3 Quantitative analysis for oil splattering

Mineral seal oil and cooking oil were heated to close to their flashpoints which are higher than the boiling point of water for these oil splattering tests. Since the oil splattering is caused by water spray vaporization and water momentum, the higher oil temperature and higher Weber number of the water spray caused more water vaporization. Manzello et al[34] found that the liquid splash occurred at higher Weber number when the pool temperature is lower. The liquid splash occurred at a critical Weber number (We_c) of 57, for a 20$^\circ C$ liquid temperature and at We_c = 38 for a 94 $^\circ C$ liquid temperature. Figure 7.10 shows the ratio of splattered oil to water spray density for mineral seal oil and cooking oil when water spray was discharged onto the preheated oil with a pilot flame. Based on these discussions the ratio of splattered oil to water density can be expressed as the function of the dimensionless factor of $\frac{C_{pl}(T_{fluid}-100)}{\Delta H_w}$ and Weber number as shown in equation 7-5.

$$\frac{\dot{m}''_s}{\dot{m}''_w} = f_1(We - We_c(T_{fluid})) \qquad \text{for } T_{fluid} < 100^\circ C \qquad \text{7-5a}$$

$$\frac{\dot{m}''_s}{\dot{m}''_w} = f_2(\frac{C_{pl}(T_{fluid}-100)}{\Delta H_w}, We) \qquad \text{for } T_{fluid} > 100^\circ C \qquad \text{7-5b}$$

The tests conducted in this dissertation did not cover values of $T_{fluid} < 100^\circ C$, so there was no attempt to determine f_1. The function term of f_2 is discussed in this chapter.

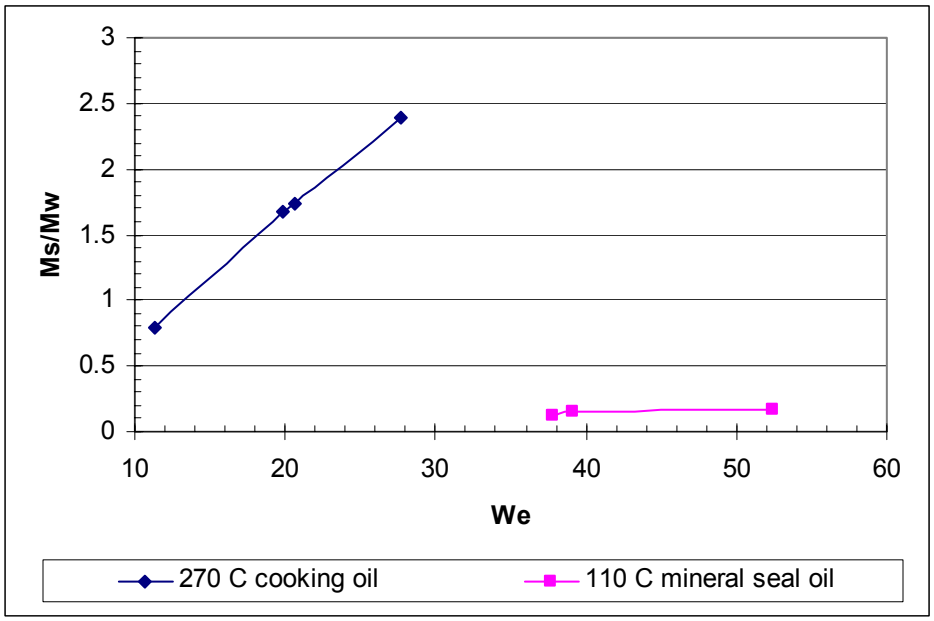

Figure 7.10 The ratio of oil spattering to water density at different oil temperature.

The ratios of oil splattering to water density were as shown in equation 7-1 and 7-4 for mineral seal oil and cooking oil.

$$\frac{\dot{m}''_{s,m}}{\dot{m}''_{w}} = 0.18 - 41.25e^{-\frac{We}{5.4}} \qquad \text{mineral seal oil} \qquad 7\text{-}1$$

$$\frac{\dot{m}''_{s,cooking}}{\dot{m}''_{w}} = 0.1We - 0.3 \qquad \text{cooking oil} \qquad 7\text{-}4$$

These two different type correlations could not be used to generate a uniformly valid generalized correlation. A generalized correlation is useful to estimate the oil splattering based on different oil temperature and Weber number of the water spray. If the correlation is modified to a linearly

correlation as equation 7-6 for mineral seal oil, the deviations are 4% to 12% compared with the mineral seal oil fire test data.

$$\frac{\dot{m}''_{s,m}}{\dot{m}''_{w}} = 0.002We + 0.06 \qquad 7\text{-}6$$

The ratio of oil spattering to water density can be generalized as equation 7-7 based on equations 7-4, 7-5 and 7-6.

$$\frac{\dot{m}''_{s}}{\dot{m}''_{w}} = f_1(\frac{\Delta H_w}{C_{pl}(T_{fluid}-100)})We - f_2(\frac{\Delta H_w}{C_{pl}(T_{fluid}-100)}) \qquad 7\text{-}7$$

f_1, f_2 are all assumed exponential functions and the equation 7-7 can be modified as equation 7-8.

$$\frac{\dot{m}''_{s}}{\dot{m}''_{w}} = -0.3 + c_1 e^{-\frac{C_2 \Delta H_w}{C_{Pl}(T_{fluid}-100)}} We + c_3 e^{-\frac{c_4 C_{pl}(T_{fluid}-100)}{\Delta H_w}} \qquad 7\text{-}8$$

The c_1, c_2, c_3, c_4 can be obtained as 0.13, 24.5 1.32 and 125 for equation 7-8 based on equations 7-4,7-5 and 7-6.

The equation 7-8 can be rewritten as equation 7-9.

$$\frac{\dot{m}_s''}{\dot{m}_w''} = -0.3 + 0.13e^{-\frac{24.5\Delta H_w}{C_{Pl}(T_{fluid}-100)}}We + 1.32e^{-\frac{125C_{pl}(T_{fluid}-100)}{\Delta H_w}} \quad 7\text{-}9$$

(10<We<55 and $T_{fluid} \geq 110^{\circ}C$)

Equation 7-9 can be used to prediction the splattered oils depending on water density, oil heat capacity, oil temperature, and Weber number of the water spray. Figure 7.11 shows the prediction curve for the ratio of oil splattering to water density from equation 7-9 and the test data from this research. The cooking oil was heated to $250^{o}C$ and 50 psi water spray from sprayco nozzle was discharged onto the oil to obtain the oil splattering. The ratio of the oil splattering to water density is 0.62 from the test. 0.68 is obtained from equation 7-9 in this specific condition. The error is 8% between the prediction and test data. This correlation is consistent for this test but still very limited to the conditions of this research. It is useful for understanding the trend of oil splattering. The higher temperature oil should have a better fit because the linear relationship with Weber number. More tests for different oils should be conducted in the future to compare with this correlation.

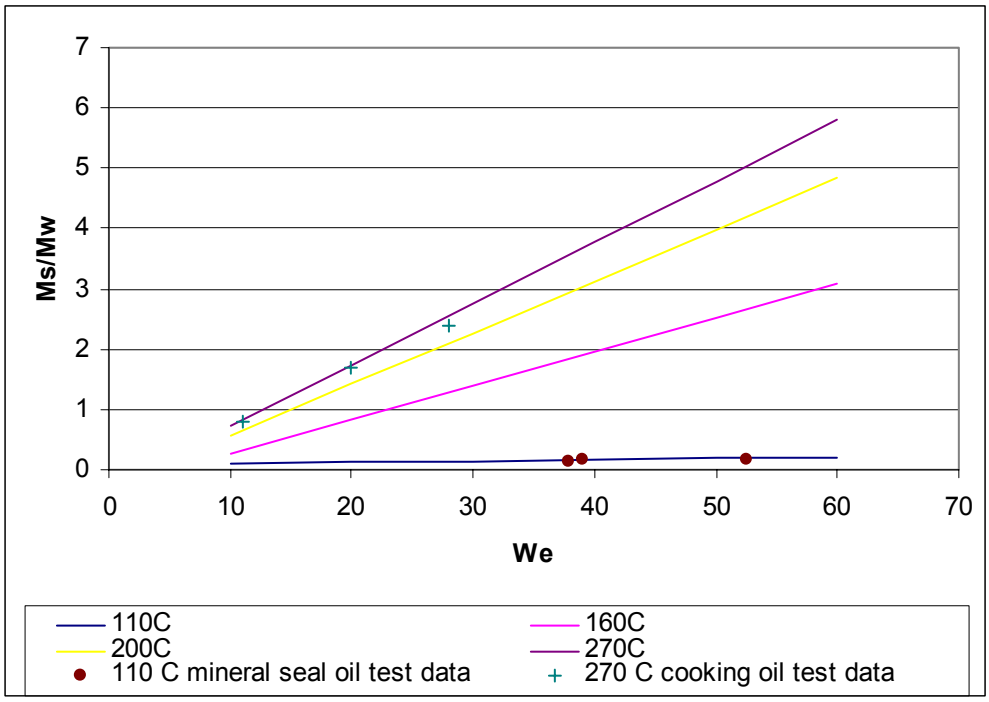

Figure 7.11 The prediction curve for the ratio of oil splattering to water density from equation 7-9 and the test data from this research.

7.4 Summary

Correlations of oil splattering rate, combustion fraction, vaporization rate, and heat release rate for water sprayed onto oil heated close to its flash point were obtained based on cooking oil and mineral seal test data. The general correlation for oil Splattering was developed depending on water density, oil heat capacity, oil temperature, and water spray Weber number. This correlation is still very limited to specific conditions from this research, but should demonstrate the trend of oil splattering.

The ratio of oil splattering to water density increases with increasing oil temperature and Weber number. The combustion fraction decreased with the Weber number for the mineral seal oil and was constant at 0.68 for cooking oil. The larger Weber number of water sprays caused more oil splattering outside the flaming area and reduced the combustion fraction for mineral seal oil tests. The vaporization rates are close between mineral seal oil and cooking oil when these high flash point oils were heated close to their flash point from this research. The fraction of the vaporization rate to the total oil burning rate of mineral seal oil is between 1% and 1.7%, and this fraction for cooking oil is less than 1% from the test data.

The heat release rate is enhanced by factor from 2.12 to 5.55 compared to the heat release rate of free burning cooking. For mineral seal oil, this ratio is only of 0.92 to 1.25. The oil splattering of cooking oil is much larger than the oil splattering of mineral seal oil with the same water density discharge because the flashpoint of the cooking oil is $291\,^{o}C$ higher than the flash point $137\,^{o}C$ of the mineral seal oil.

8 Pool Fire Suppression and Intensification Tests

High flash point liquids are very hard to ignite at ambient temperature. However several applications and fire scenarios cause high temperatures for high flash point oils such as transformer oil in a transformer or cooking oil in a fryer cooker. Figure 8.1 is a transformer oil fire, which is described in the FMGlobal[21]. It can spread to a big area without a fire suppression system and fire resistant barriers. The flash point of transformer oil is usually 146°C (295°F) to 300°C (572°F). Figure 8.2 is a simulated fryer cooker fire from Nam's technical report in FMGlobal[35]. The flash point of this cooking oil is 230°C (446°F).

High flash point liquid fires always can intensify with water application because they are heated to a temperature higher than the water boiling point of 100 °C (212°F). Fire suppression and intensification tests described in this chapter were conducted with two liquids with very different flash points. The flash point of mineral seal oil is 137°C (280°F) and the flash point of the soybean cooking oil is 291°C (556°F). The wide range of flash points aid in understanding high flash point pool fire suppression and intensification in this research. These oil fires were heated from their surfaces and ignited. These phenomena were different from chapters 6 and 7 that oils were preheated to specific temperatures for the whole oils. Two separate series of fire tests for mineral seal oil and cooking oil are discussed as follows.

Figure 8.1 Typical Transformer oil fire (from FMGlobal).

Figure 8.2 FMGlobal simulated fryer cooker fire (from FM Global).

8.1 Mineral seal oil fire suppression and intensification tests

Fire suppression tests started by heating the mineral seal oil with the ring burner until the oil ignited, and then removing the burner for 30 seconds to allow for a free burn period followed by unobstructed water spray discharge onto the burning oil, as shown in Figure 8.3. Experiments have been conducted with the Grinnell AM24, BETE WL 11/2 90^0 , Spraying Systems 1/8 GG full jet 2, 1/8HH-1.5, 1/8GG full jet 6SQ, 1/4GG full jet 10SQ, 3/8GG full jet 22, 3/8GG full jet 15, 3/8GG full jet 18SQ, 1/2GGfull jet 32, 1/2GG full jet 25, sprayco110620-01 and 1/2GG full jet 29SQ nozzles operating at various water pressures and with spray characteristics described in chapter 4. Thermocouples installed above and below the oil surface provided temperature data before and during water spray discharge. For AM24 nozzle, the burner was 7.62 cm above the fuel surface. For other nozzles, the burner was 5 cm above the fuel surface.

Temperature data for a suppression test with the minimum recommended nozzle pressure of 7.0 bars (101 psi) of AM 24 nozzle are shown in Figure 8.4. Ignition occurred at 340 seconds as indicated by the steep rise in the temperature above the oil surface. Water began discharging at 370 seconds, and the flame was almost extinguished within six seconds as indicated by the steep drop in the temperature above the oil surface. A small residual flame lingered near the edge of the pan for another 12 seconds before it was extinguished also. The oil surface temperature data in Figure 8.4 shows rapid cooling immediately upon water spray discharge.

Temperature data for a nonsuppression test with a nozzle pressure of 1.7 bars (25 psi) of AM24 are shown in Figure 8.5. The oil surface temperature immediately drops below the flash point upon water discharge at 285 seconds. The vapor space temperature above the oil surface also drops suddenly, but shows signs of redeveloping a higher temperature soon after water application. The flame went off when the water spray was shut because the oil temperature was below the oil flash point. The flame redeveloped at about 400 seconds as shown in Figure 8.5 because the pan temperature was still high enough to reignite the hot oil. Visual observations show the flame intensifying at water application in this test. Figure 8.6 shows the increased flame height associated with fire intensification. This is just the opposite of the decreased flame

height observed at 7 bars (101 psi), as shown in Figure 8.3. The minimum certified water pressure for shipboard applications with this nozzle is 7 bars (101 psi). Temperatures measured in other tests are shown in Appendix E.

Water spray flux measurements were made directly under the nozzle operating at 1.7 bars (25 psi), 3.4 bars (50 psi), 5.1 bars (75 psi) and at 7.0 bars (101 psi) for AM24. The measured fluxes were 17.5 mm/min ($0.43\ gpm/ft^2$) at 1.7 bars (25 psi), 15.1 mm/min ($0.37\ gpm/ft^2$) at 3.4 bars (50 psi), 17.1 mm/min ($0.42\ gpm/ft^2$) at 5.1 bars (75 psi) and 18.1 mm/min ($0.45\ gpm/ft^2$) at 7 bars (101 psi). These water fluxes are about 40% greater than the minimum design density of 12.2 mm/min ($0.3\ gpm/ft^2$) specified in NFPA 15 (2001) for the control of combustible liquid pool fires. The absence or occurrence of oil surface splattering determines whether or not the pool fire is suppressed at these high water spray fluxes. Small drop sprays produce rapid suppression, whereas large drop sprays produce fire intensification due to oil drops and jets emitted from the oil surface. Figure 8.7 shows that the larger water droplets of $1056\ \mu m$ at an operating pressure of 1.7 bars for AM24 nozzle caused significant oil splattering flame and the fire was not extinguished. Figure 8.8 shows that the droplet size of $368\ \mu m$ at an operating pressure of 7.0 bars for AM24 nozzle causes much less oil splattering flame and the fire was extinguished at 20 seconds. Figure 8.9 shows that small droplet size of $168\ \mu m$ at an operating pressure of 8.7 bars for Bete WL nozzle caused no mineral seal oil splattering and the fire was extinguished at 4 seconds. The oil splattering plays a very important role for high flash point fire extinguishment.

Figure 8.3 Water spray discharge onto burning oil at 7 bar for AM24 nozzle.

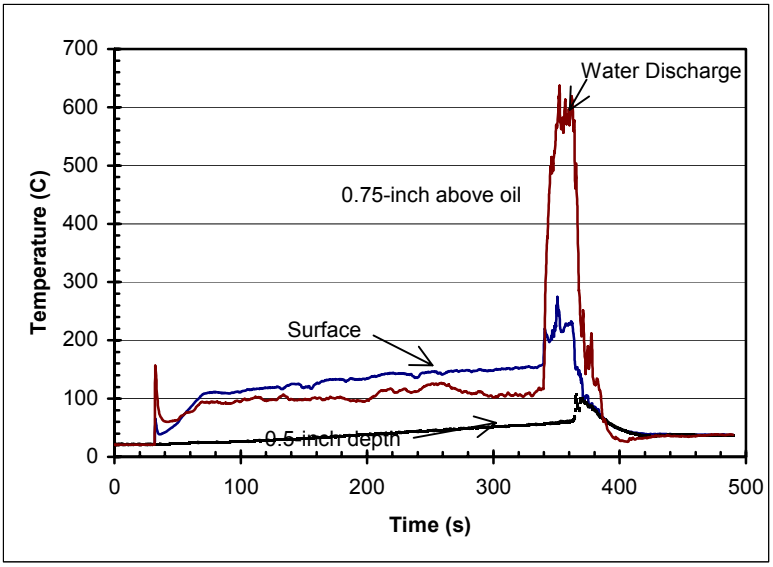

Figure 8.4 Temperatures measured during suppression test with nozzle pressure of 7 bars for AM24 nozzle.

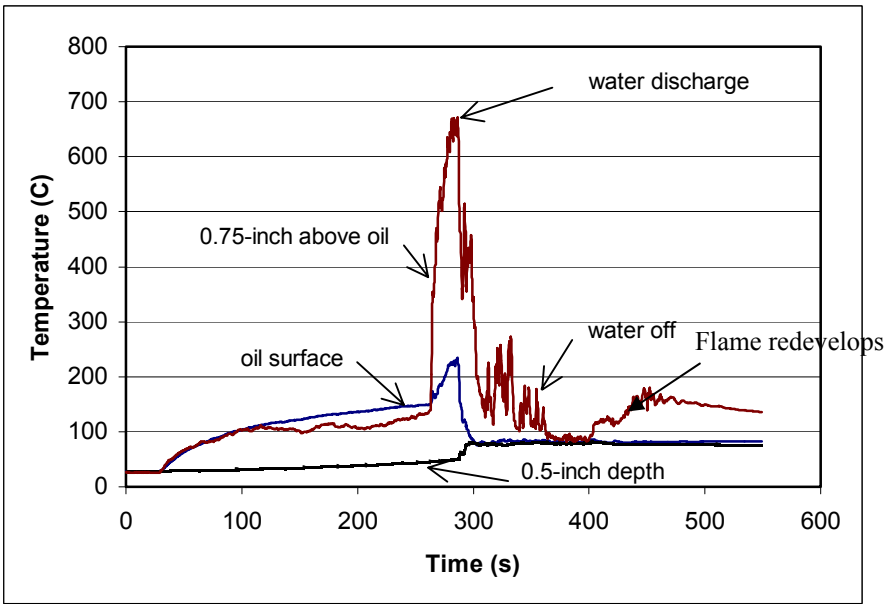

Figure 8.5 Temperatures measured during nonsuppression test at a pressure of 1.7 bars for AM24 nozzle.

Figure 8.6 Higher flame height after spray discharge at 1.7 bars for AM24 nozzle.

Figure 8.7 Burning oil with 1056 μm droplet water spray discharge

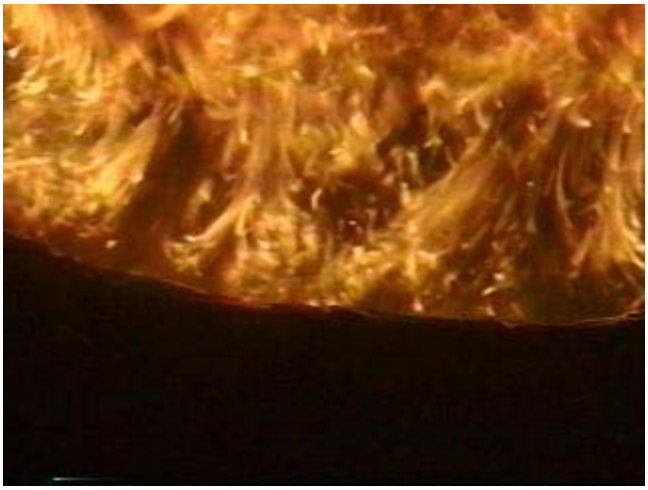

Figure 8.8 Burning oil with 368 μm droplet water spray discharge.

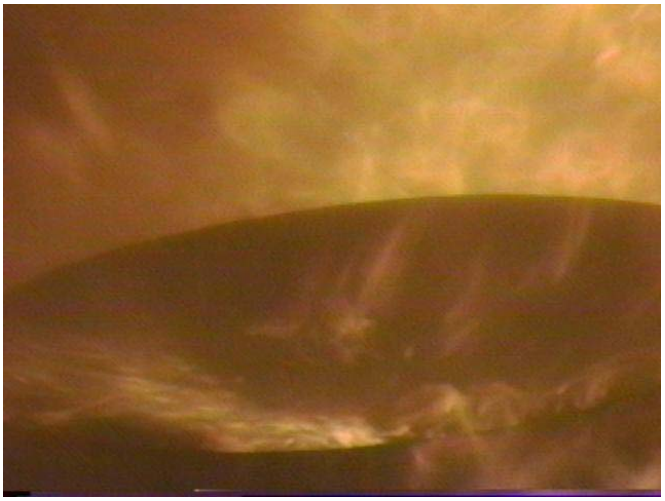

Figure 8.9 Burning oil with 168 μm water spray discharge.

All 49 fire tests are listed in Table 8.1 for mineral seal oil. 32 tests resulted in fire suppression and 17 tests were non-suppression. The nozzle type, water density, drop sizes, velocities and extinguishment time are also shown in the table and used for further analysis in Chapter 9. The smaller drop sizes and larger velocities, and shorter extinguishing times were obtained when the operating pressure increased for a specific nozzle. For a specific nozzle with lower water pressure such as AM24 nozzle at 172 kPa (25 psi) water pressure, the fire was intensified. The fire was temporarily intensified in the higher water pressure tests, such as 517 kPa (75 psi) for AM24 nozzle, but the fire size gradually became smaller after a period time of water discharge and eventually died out. The fire was intensified but blown outside the pan with high water pressure such as 690 kPa (101.5 psi) for AM24 nozzle. The fire died out very quickly in this condition.

Table 8.1 Fire suppression and non-suppression tests for mineral seal oil.

Test no.	Nozzle type	Water pressure, kPa(psi)	Water density, mm/min (gpm/ft^2)	Water drop size (μm)	Water drop mean velocity (m/s)	Remark
Test 2	AM24	690(101.5)	17.5(0.43)	368	4.7	Fire suppressed at 18 s
Test 4	AM24	172(25)	17.5(0.43)	1056	2.4	Fire not suppressed
Test 6	AM24	172(25)	17.5(0.43)	1056	2.4	Fire not suppressed
Test 19	AM24	517(75)	17.1(0.42)	450	4.2	Fire suppressed at 60 s
Test 20	AM24	517(75)	17.1(0.42)	450	4.2	Fire suppressed at 60 s

Test no.	Nozzle type	Water pressure, kPa(psi)	Water density, mm/min (gpm/ft^2)	Water drop size (μm)	Water drop mean velocity (m/s)	Remark
Test 21	AM24	345(50)	15.1(0.37)	368	3.4	Fire not suppressed
Fpc20	1/8HH-1.5	517(75)	2.85(0.07)	143	3.12	Fire suppressed at 35 s
Fpc21	1/8HH-1.5	345(50)	2.85(0.07)	161	3	Fire not suppressed
Fpc22	Bete WL 1 ½	862(125)	9(0.22)	168	6.26	Fire suppressed at 2 s
Fpc23	Bete WL 1 ½	517(75)	7.3(0.18)	174	4.63	Fire suppressed at 30 s
Fpc24	Bete WL 1 ½	172(25)	2.85(0.07)	189	3.2	Fire not suppressed
Fpc 26	1/8GG,2	172(25)	7.7(0.19)	197	2.71	Fire not suppressed
Fpc 27	1/8GG,2	345(50)	8.6(0.21)	164	4.08	Fire suppressed at 10 s
Fpc 28	1/8GG,2	517(75)	9.8(0.24)	152	4.47	Fire suppressed at 3 s
Fpc 30	1/8GG,6SQ	138(20)	6.1(0.15)	243	3.72	Fire not suppressed

Test no.	Nozzle type	Water pressure, kPa(psi)	Water density, mm/min (gpm/ft^2)	Water drop size (μm)	Water drop mean velocity (m/s)	Remark
Fpc 33	1/8GG,6SQ	345(50)	9(0.22)	184	5.16	Fire suppressed at 4 s
Fpc 36	1/4GG,10SQ	138(20)	11.8(0.29)	335	3.05	Fire not suppressed
Fpc 39	1/4GG,10SQ	345(50)	16.3(0.4)	260	4.69	Fire suppressed at 4 s
Fpc 42	3/8GG,18SQ	69(10)	11(0.27)	389	2.61	Fire not suppressed
Fpc 44	3/8GG,18SQ	138(20)	11.4(0.28)	354	3.21	Fire not suppressed
Fpc83	3/8GG,18SQ	276(40)	16.7(0.41)	279	4.19	Fire Suppressed at 35 s
Fpc 84	3/8GG,18SQ	345(50)	18.3(0.45)	250	4.59	Fire suppressed at 8 s
Fpc 85	3/8GG,18SQ	414(60)	20.4(0.50)	213	4.74	Fire suppressed at 5 s
Fpc 48	3/8GG,22	69(10)	4.9(0.12)	425	2.3	Fire not suppressed

Test no.	Nozzle type	Water pressure, kPa(psi)	Water density, mm/min (gpm/ft^2)	Water drop size (μm)	Water drop mean velocity (m/s)	Remark
Fpc 50	3/8GG,22	138(20)	6.5(0.16)	375	2.7	Fire not suppressed
Fpc 86	3/8GG,22	345(50)	10.2(0.25)	237	3.32	Fire suppressed at 15s
Fpc 87	3/8GG,22	414(60)	13.9(0.34)	227	3.46	Fire suppressed at 3 s
Fpc 53	1/2GG,32	206(30)	27.7(0.68)	305	4.47	Fire suppressed at 4 s
Fpc 54	1/2GG,32	172(25)	26.1(0.64)	350	4.21	Fire suppressed at 4 s
Fpc 55	1/2GG,32	138(20)	24(0.59)	425	3.6	Fire suppressed at 20 s
Fpc 56	1/2GG,32	103(15)	22.8(0.56)	543	3.34	Fire suppressed at 60 s
Fpc 58	1/2GG,32	69(10)	21.2(0.52)	657	2.66	Fire suppressed at 100 s

Test no.	Nozzle type	Water pressure, kPa(psi)	Water density, mm/min (gpm/ft^2)	Water drop size (μm)	Water drop mean velocity (m/s)	Remark
Fpc 59	1/2GG,32	34.5(5)	20.4(0.5)	718	2.55	Fire not suppressed
Fpc 60	1/2GG,25	34.5(5)	23.2(0.57)	955	2.7	Fire not suppressed
Fpc 61	1/2GG,25	69(10)	18.3(0.45)	657	3.05	Fire not suppressed
Fpc 62	1/2GG,25	103(15)	17.5(0.43)	459	3.08	Fire suppressed at 100 s
Fpc 63	1/2GG, 25	138(20)	22.4(0.55)	333	3.19	Fire suppressed at 75 s
Fpc 64	1/2GG, 25	172(25)	20.4(0.5)	317	3.49	Fire suppressed at 30 s
Fpc 65	1/2GG, 25	206(30)	16.7(0.45)	264	3.69	Fire suppressed at 4 s
Fpc 66	Spraco 110620-01	345(50)	3.3(0.08)	116	2.61	Fire not suppressed
Fpc 67	Spraco 110620-01	517(75)	4.5(0.11)	115	3.37	Fire not suppressed

Test no.	Nozzle type	Water pressure, kPa(psi)	Water density, mm/min (gpm/ft^2)	Water drop size (μm)	Water drop mean velocity (m/s)	Remark
Fpc 71	3/8GG,15	69(10)	14.3(0.35)	415	2.57	Fire not suppressed
Fpc 72	3/8GG,15	138(20)	15.9(0.39)	360	2.7	Fire not suppressed
Fpc 73	3/8GG,15	206(30)	17.1(0.42)	242	3.5	Fire suppressed at 45 s
Fpc 74	3/8GG, 15	276(40)	17.5(0.43)	237	3.63	Fire suppressed at 4 s
Fpc 75	3/8GG, 15	345(50)	18.3(0.45)	202	4.66	Fire suppressed at 4 s
Fpc 76	3/8GG, 15	414(60)	20(0.49)	186	5.28	Fire suppressed at 4 s
Fpc 77	1/2GG,29SQ	34.5(5)	23.2(0.57)	830	2.35	Fire not suppressed
Fpc 78	1/2GG,29SQ	69(10)	16.7(0.41)	613	2.44	Fire not suppressed
Fpc 79	1/2GG,29SQ	103(15)	17.5(0.43)	441	2.66	Fire suppressed at 119 s

Test no.	Nozzle type	Water pressure, kPa(psi)	Water density, mm/min (gpm/ft^2)	Water drop size (μm)	Water drop mean velocity (m/s)	Remark
Fpc 80	1/2GG,29SQ	138(20)	22.4(0.55)	373	2.74	Fire suppressed at 95 s
Fpc 81	1/2GG,29SQ	172(25)	20.4(0.5)	341	4.19	Fire suppressed at 65 s
Fpc 82	1/2GG,29SQ	206(30)	16.7(0.41)	296	4.43	Fire suppressed at 35s

8.2 Cooking oil fire suppression tests

Fire suppression tests started by heating the cooking oil with the ring burner for 9 min, and then removing the burner to allow unobstructed water spray to discharge onto the burning oil, as shown in Figure 8.10 to Figure 8.13. The fire flared up to about 5 ft high in the early stage of the test for 4 or 5 seconds as shown in Figure 8.11 because the hot liquid surface caused a lot of hot oil splattering by water spray to intensify the cooking oil fire. The flashpoint of cooking oil 291° C (556° F) is much higher than the water vaporization temperature of 100° C (212° F). The large temperature difference between these caused water boiling to splash up a lot of oil to intensify the fire. The flame height eventually was reduced as shown in Figure 8.12 because the water spray cooled the oil and also enhanced the mixing and heat transfer between hot and cold oil to help minimize the fire. The fire was extinguished 25 seconds after the water spray was initiated on the cooking oil fire as shown in Figure 8.13. Experiments have been conducted with different nozzles operating at various water pressures as shown in Table 8.2. Little water was collected at the bottom of the pan after the fire suppression tests because the water vaporized in the early stage and the fire was quickly suppressed.

Thermocouples installed above and below the oil surface provided temperature data before and during water spray discharge. Temperature data for a fire suppression test with the Spraying System 3/8GG, 22 nozzle pressure of 69 kpa (10 psi) are shown in Figure 8.14. The propane ring burner fire was pushed down to the liquid surface because the holes in the ring were 30 degree downward from the horizontal and the ring burner located at 1.27 cm (½ in) above the edge of the pan. The temperature of thermocouple at 1.9 cm (¾ in.) above the oil was 600° C because it exposed to propane ring burner. Propane ring burner fire was stopped at 547 seconds and removed from above the pan. Water began discharging at 577 seconds, and the flame was extinguished within 25 seconds as indicated by the steep drop in the temperature above the oil surface. The temperature at 1/2 in. below the surface raised quickly because the water spray provided good cooling and very good oil mixing and heat transfer between hot oil and cold oil to enhance the fire suppression. The temperature of the surface of the cooking oil was well below its flash point if enough water discharged into the fire and the fire was extinguished.

The fire flared up and sustained during the entire fire non-suppression test of cooking oil. Temperature data for a non-suppression fire test with a nozzle pressure of 345 kpa(50 psi) of Spraco 11-0620-01 are shown in Figure 8.15. The propane fire was stopped at 547 seconds and removed from above the pan. The water spray was discharged into fire at 577 seconds and sustained for 180 seconds. The fire flared up when water spray was discharged into the fire as shown in Figure 8.16. Visual observations show the flame intensifying at water application in this test. The temperature of the surface of the cooking oil was 350° C when the water discharged into the oil fire and the spray reduced the surface temperature to 300° C, which is slightly above the flash point. The water spray enhanced the fire size and a greater flame height was observed during these tests, depending on drop size and water density. The larger drop size causes higher flame height when water sprays discharge into a cooking oil fire.

The cooking oil was also preheated to 270° C and ignited by a propane ring burner from above. AM24 nozzle at 175 psi water spray could suppress the fire but the drop size and velocity were not measured at this pressure. The drop size is 68 micrometer from the correlation obtained in chapter 4. This preheated oil fire is more difficult to extinguish and smaller droplet spray or mist is suggested to use for preheated fire.

All 10 fire tests are as shown in Table 8.2 for cooking oil. 7 tests provided fire suppression and 3 tests did not.

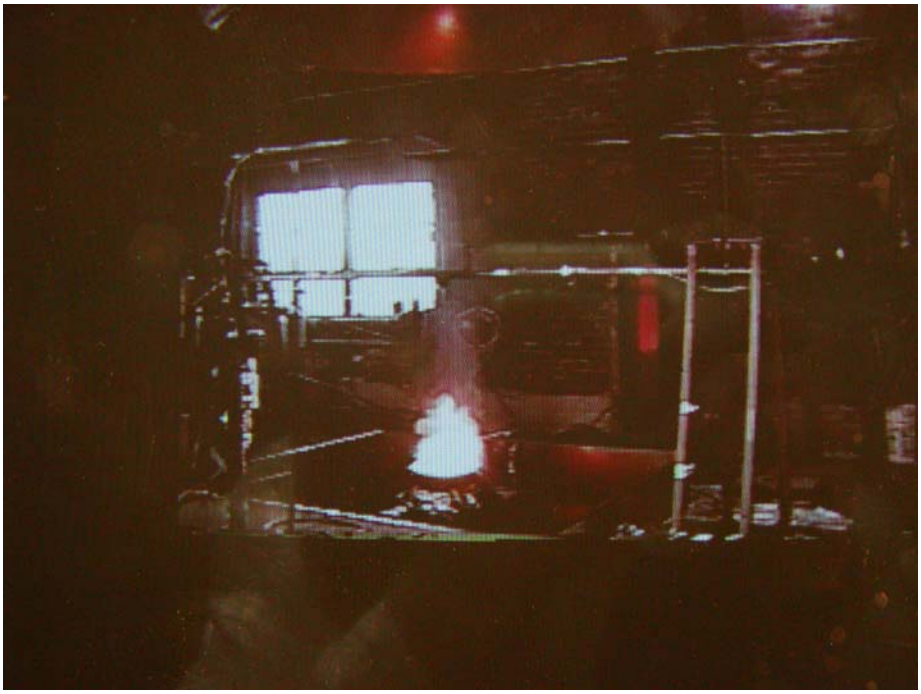

Figure 8.10 cooking oil free burn without water spray.

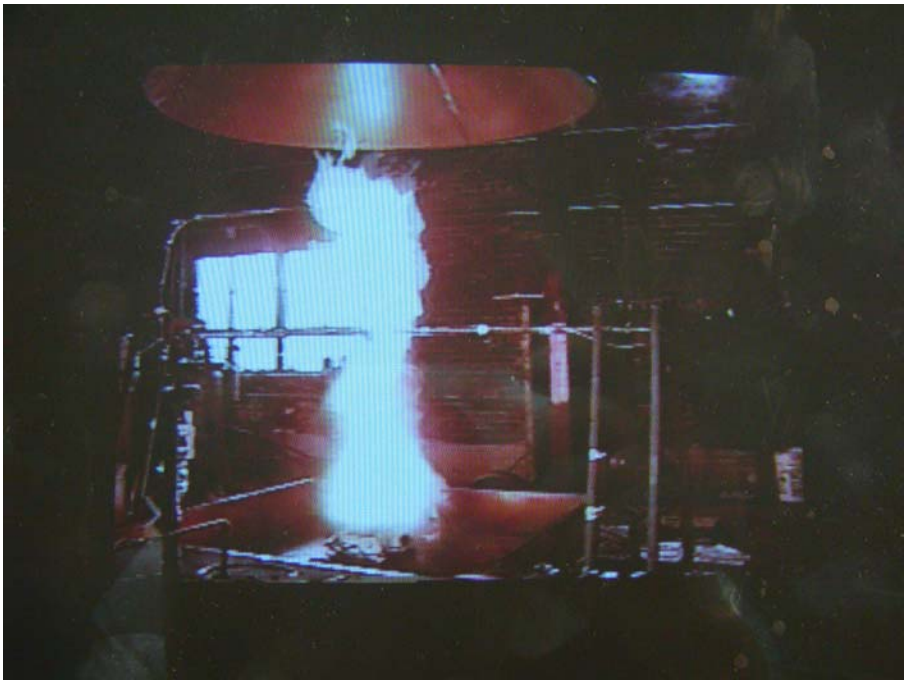

Figure 8.11 Cooking oil with water spray of 10 psi 3/8GG,22 nozzle at 2 second discharge.

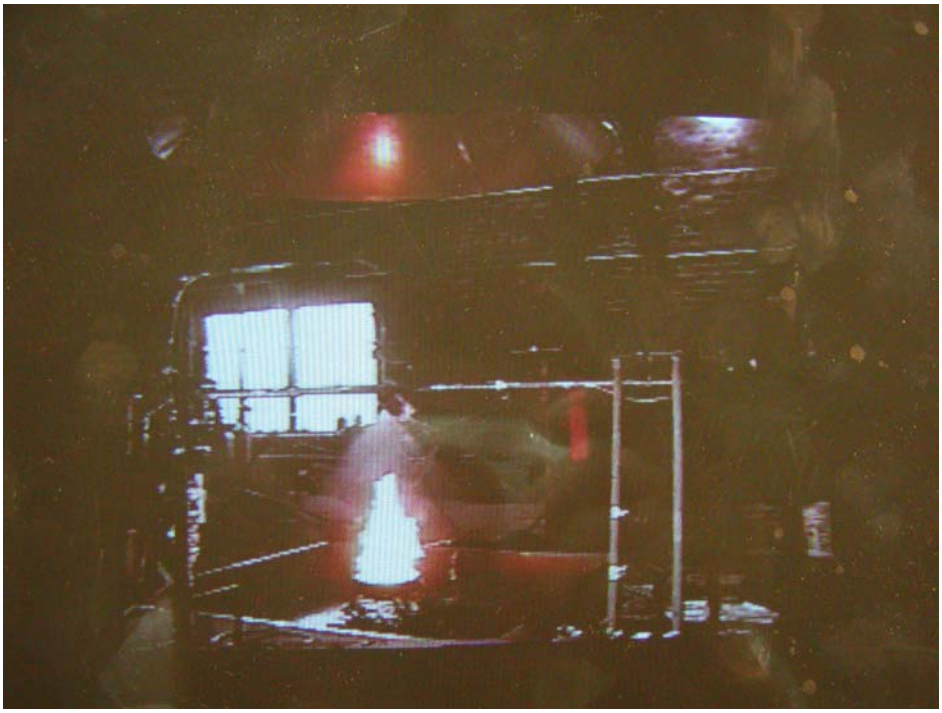

Figure 8.12 Cooking oil with water spray of 10 psi 3/8GG,22 nozzle at 21 second discharge.

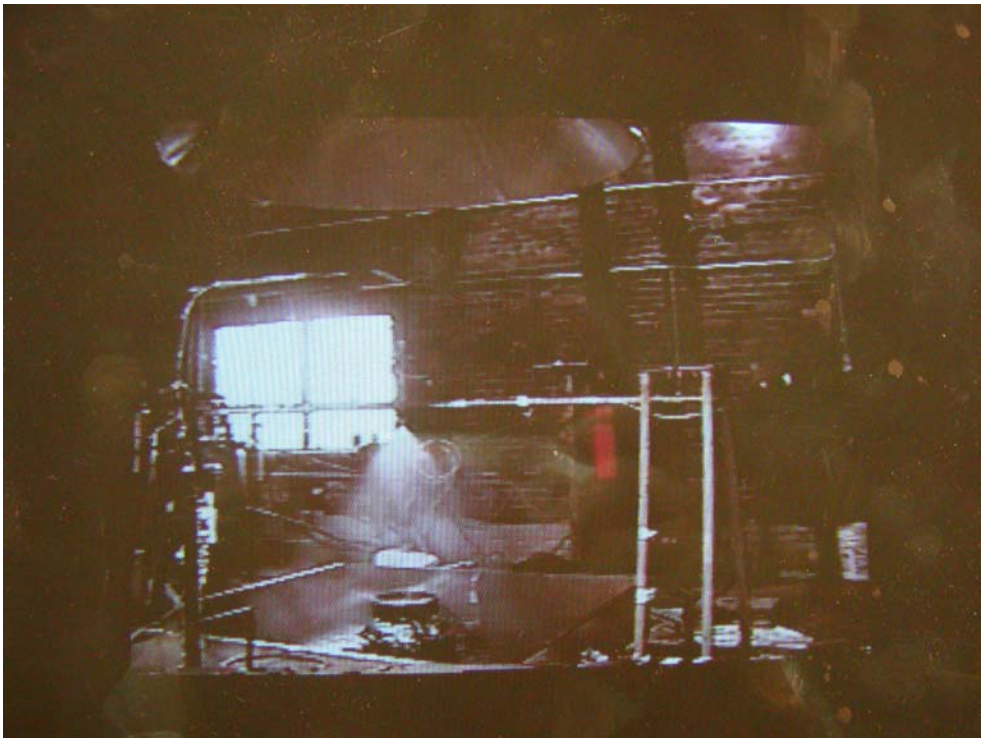

Figure 8.13 Cooking oil with water spray of 10 psi 3/8GG,22 nozzle at 25 second discharge.

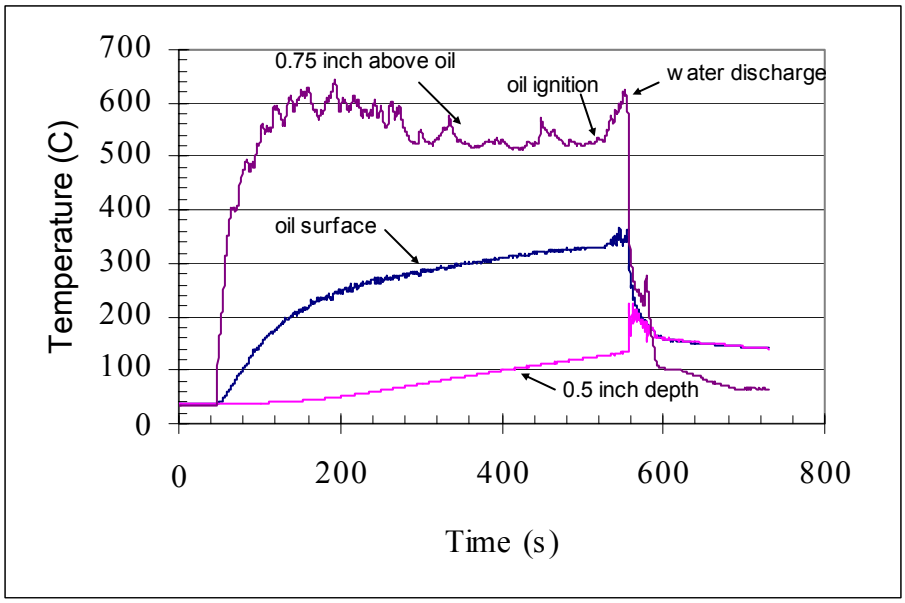

Figure 8.14 The Temperature of Suppression Test of Cooking Oil for 3/8GG,22 Nozzle (test #: FPC 123).

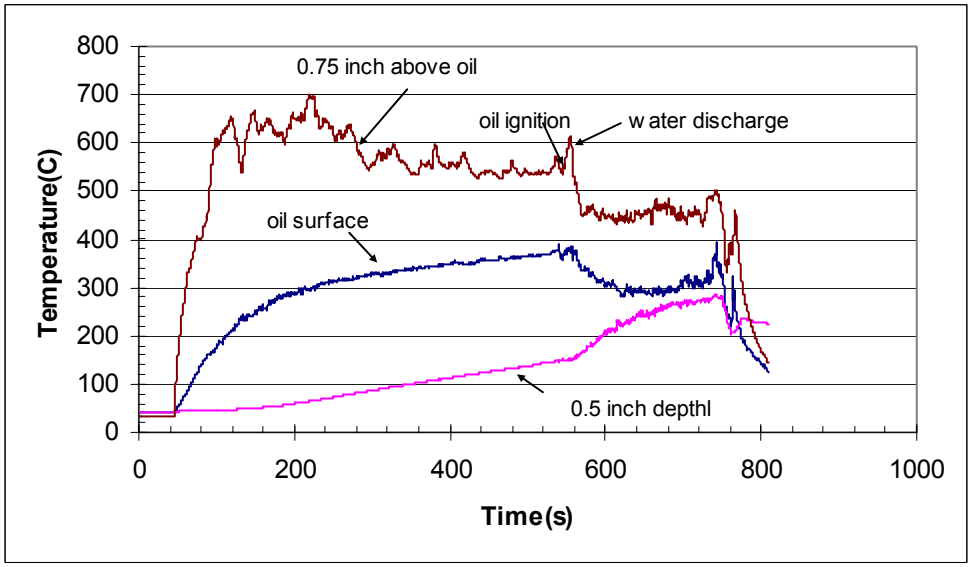

Figure 8.15 The Temperature of Non-suppression Test of Cooking Oil for Spraco11-0620-10 Nozzle (test #: FPC 121).

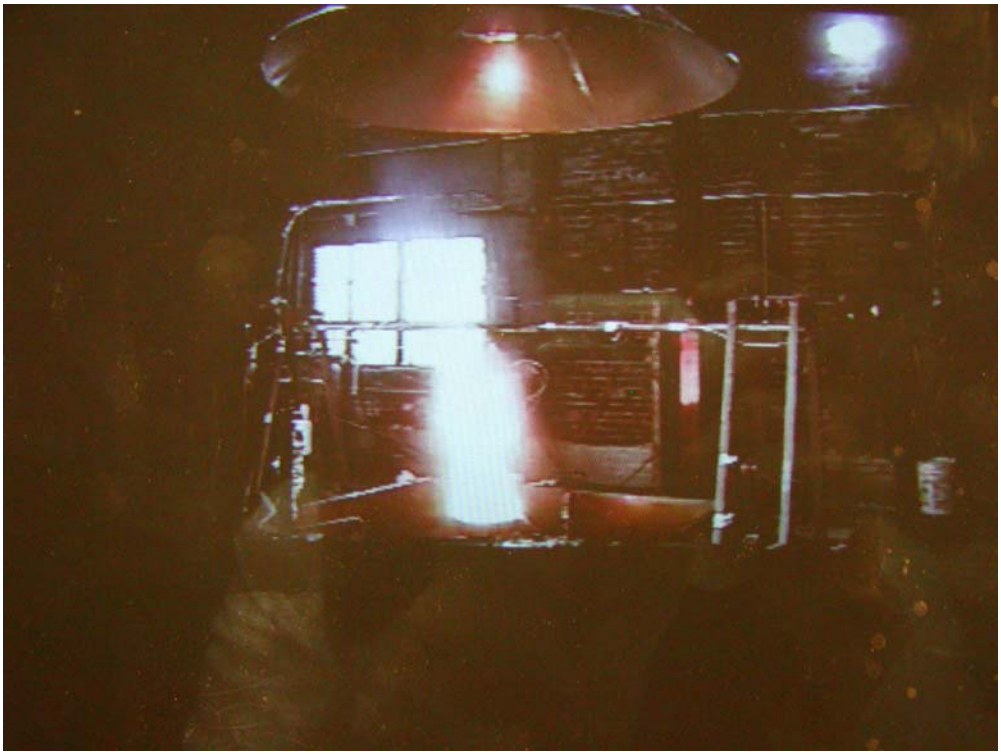

Figure 8.16 Water spray intensify the fire for cooking oil non-suppression test.

Table 8.2 Fire suppression tests for cooking oil.

Test no.	Nozzle type	Water pressure, kpa(psi)	Water density, mm/min (gpm/ft^2)	Water drop size (μm)	Water Velocity (m/s)	Remark
Test 26	AM24	172(25)	17.5(0.43)	1056	2.4	Fire suppression at 5 sec
Fpc 118	1/8HH-1.5	517(75)	2.85(0.07)	143	3.12	Fire not suppression
Fpc 119	1/8GG,6SQ	138(20)	6.1(0.15)	243	3.72	Fire suppression at 27 sec
Fpc 120	Bete WL 1 ½	172(25)	2.85(0.07)	189	3.2	Fire not suppression
Fpc 121	Spraco 11-0620-01	345(50)	3.3(0.08)	116	2.61	Fire not suppression
Fpc 122	Spraco 11-0620-01	690(100)	4.5(0.11)	115	4.3	Fire suppression at 68 sec
Fpc 123	3/8GG,22	69(10)	4.9(0.12)	425	2.3	Fire suppression at 27 sec

8.3 Cooking oil fire test with a 6 in. off-set water spray

The pan was moved 15.2 cm (6 in.) from the center of the nozzle and maintained 91 cm (3 ft.) below the nozzle as shown in Figure 8.17. The fire flared up and was blown to the side of the pan and more easily extinguished at 20 seconds than when the pan was directly under 3/8GG, 22 nozzle at 10psi. This was because the sprays pushed the flame sideways and the drops did not become heated in the flame and had a greater cooling capacity when they reached the liquid. It also could be because the entrained air velocity was higher at this particular radial distance.

Figure 8.17 Cooking oil fire suppression test for pan 15.2 cm (6 in.) from the center of the nozzle and 91 cm (3 ft) below the nozzle.

8.4 Summary

The temperature of the surface of the mineral seal oil was below its flash point after water spray was discharged into the oil fire. The oil splattering plays an important role to enhance the fire if the fire can be sustained below its flash point. The higher water density and smaller drop size can extinguish the mineral seal oil fire more easily. It makes sense that higher water density provides better oil and flame cooling and smaller drop size have a better flame cooling and less oil splattering.

The temperature of the surface of the cooking oil was close to its flash point after water spray was discharged into the cooking oil fire and the fire was not extinguished. The water spray enhanced the fire size and a higher flame height was observed during tests depending on particle size. The larger drop size caused higher flame height when water sprays discharge into the cooking oil fire. The temperature of the surface of the cooking oil was below its flash point if enough water was discharged into the fire and the fire was extinguished. The water spray cooled the oil and also enhanced the mixing and heat transfer between hot and cold oil to help extinguish the fire, which is shown by the fact that the amount of water collected under the oil after the tests was not significant.

Substantial oil spattering was observed during several tests depending on drop size of water spray. Larger droplets caused a flaming fire and smaller droplets had less oil splattering flame. The fire was extinguished quickly if no oil splattering was obtained during tests.

The horizontal 6 in. shift nozzle showed a better fire suppression for cooking oil because the sprays pushed the flame sideways and the drops did not become heated in the flame and had a greater cooling capacity when they reached the liquid. It also could be because the entrained air velocity was higher at this particular radial distance.

9 Criteria to Predict Suppression versus Intensification

Rasbash conducted a series of pool fire tests. He[58] found that the size and velocity of the spray drops mainly affects the heat transfer to flame and fuel but they also affect the tendency of drops to enhance the burning rate of liquids by causing splashing and sputtering at the fuel surface. A large upsurge of flame in the first 1- 2 seconds was observed for diesel oil (fire point 104-115 $^\circ$C) and transformer oil (175-180 $^\circ$C) fires at sprays of flow rate 267 $g/m^2 s$ (0.4 gpm/ft^2) and drop size 0.28 mm, 0.38 mm, and o.49 mm. The fires were eventually extinguished at these conditions. The critical water spray density for vertically downward application for a 30 cm diameter fire was about twice that for horizontal water spray application for transformer oil fires[55]. His correlation for critical spray density for high flash point fire suppression was based on spray cooling of oil below its fire point. He[54] also found the fire continued to burn for some time after the indicated temperature was reduced to below the fire point in a number of tests, particularly for transformer oil tests. This could be the unevenness in the water spray pattern to cool different parts of the liquid surface he described. Three mechanisms may be suggested by Rasbash to account for the cooling of the burning liquids: (1) heat transfer from the hot oil to the water drops; (2) mixing between hot oil and cold oil below the surface; (3) the formation of oil-in-water emulsion. The fire extinguishment time was obtained as Equation 9-1 by Rasbash. The longer extinction times were obtained when sprays were of 'central' type than when they were of the 'non-central ' type.

$$t_{ext} = 6800(d_w / \dot{R}''_w)(Y/(T_{fp} - T_w)^{1.75}) \qquad 9\text{-}1$$

where: d_w : mass median water drop size of the spray in mm

T_{FP} : fire point ($^\circ C$)

T_w : water temperature($^\circ C$)

t_{ext} : fire extinguishment time, sec

$\dot{R}''_w$: applied water density ($\frac{gpm}{ft^2}$)

Y: preburn time in minutes

In this research the results of fire suppression tests show that the water drop size is very important factors for high flash point pool fire suppression. The following will discuss their influence and quantify the criteria to predict suppression and intensification of high flash point pool fires for mineral seal oil and cooking oil.

9.1 Suppression criteria for Mineral seal oil

For 49 mineral seal oil fire tests, 32 tests resulted in suppression and 17 tests did not. Appendix E shows $D_{v,0.1}$, $D_{v,0.5}$, and $D_{v,0.9}$ in different operating pressures for different nozzles. Figure 9.1 to Figure 9.3 show that less water density is required for fire extinguishment as the water drop size decreases. $D_{v,0.5}$ is used for further analysis as shown in Figure 9.2, because it is more often used to characterize water spray particle size in fire tests. The critical suppression water density of mineral seal oil is as equation 9-2, based on test data curve fit. The result shows that the smaller water drop size requires less water for suppression. The critical water density is obtained as follows from Figure 9.2 for less conservative test data curve fit.

$$\dot{m}''_{cr,w} = 25.2 - 43.5e^{-\frac{d_w}{218}} \qquad (150\mu m < d_w < 1000\mu m) \tag{9-2}$$

Where: $\dot{m}''_{cr,w}$ is critical water density (mm/min)

d_w is the water drop size (μm)

When the water density of water spray to extinguish fires is larger than 25.2 mm/min ($0.61\ gpm/ft^2$), the water density is large enough to suppress the fire and the drop size is no longer important for mineral seal oil fire suppression. If the water density is smaller than 25.2 mm/min, the fire suppression of mineral seal oil is controlled by oil cooling, oil splattering, and oil surface cooling. Figure 9.4 shows the multiple of drop size and velocity that relate to Weber number or Reynolds number are not an appropriate criterion for fire suppression and non-suppression of mineral seal oil. The velocity may increase the liquid surface cooling, but it also increases the oil splattering to increase the burning rate. The overall effect of velocity to fire suppression is not clear because of competing these effects. The critical water density is proportional to the drop size the same way that Rasbash's correlation as equation 2-1 is only available for very small water drop size here.

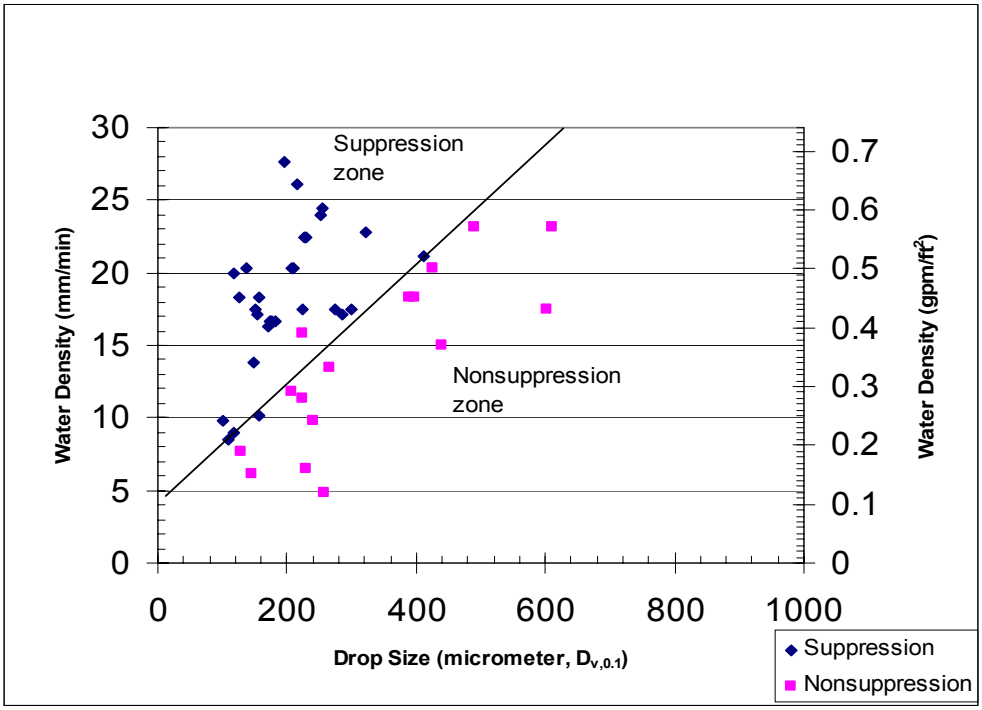

Figure 9.1 Mineral seal oil Fire Suppression Tests for Different Water Density and 10% volume fraction Particle Size ($D_{v,0.1}$).

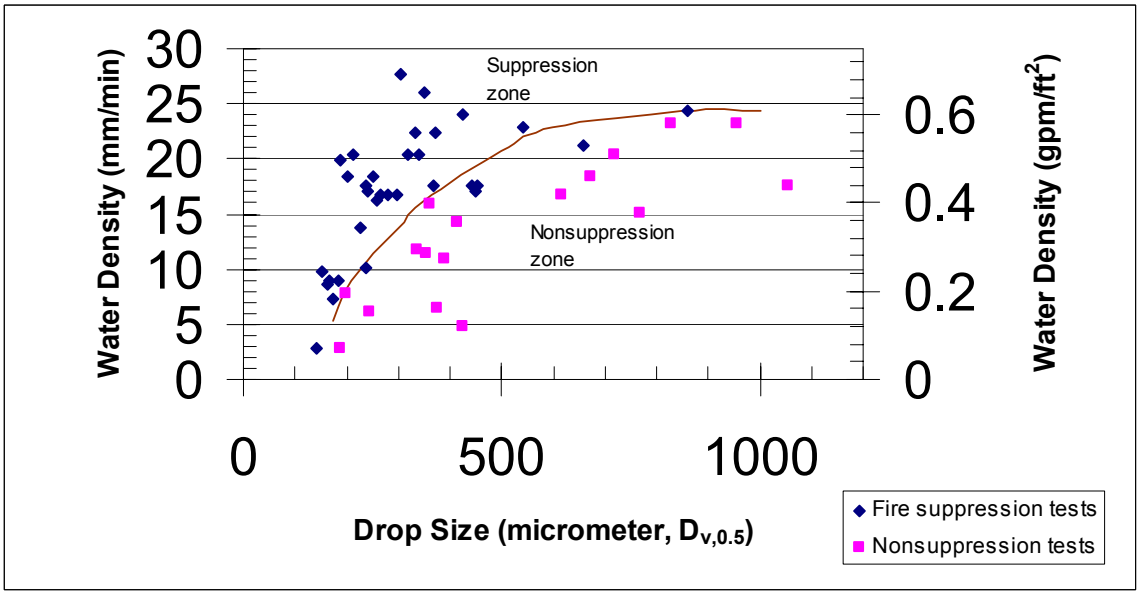

Figure 9.2 Mineral seal oil Fire Suppression Tests for Different Water Density and 50% volume fraction Particle Size ($D_{v,0.5}$).

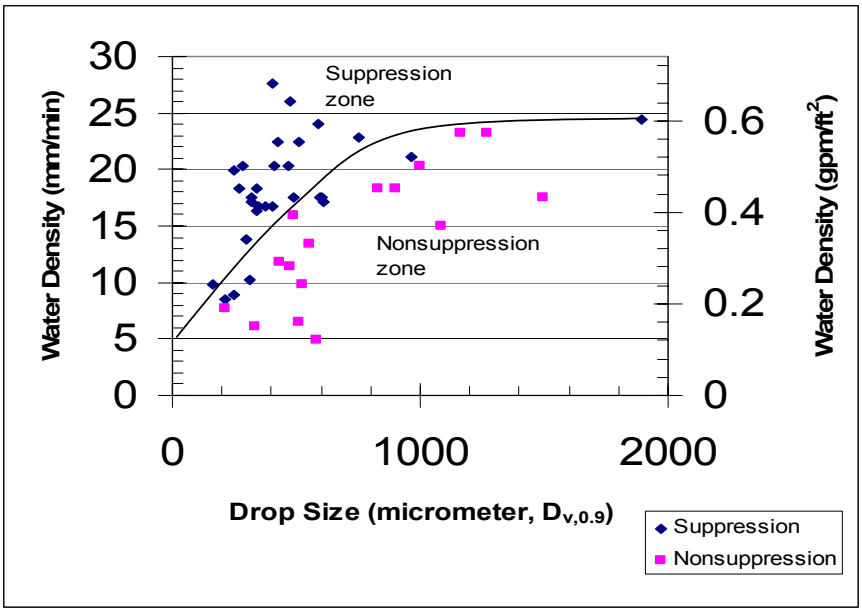

Figure 9.3 Mineral seal oil Fire Suppression Tests for Different Water Density and 90% volume fraction Particle Size ($D_{v,0.9}$).

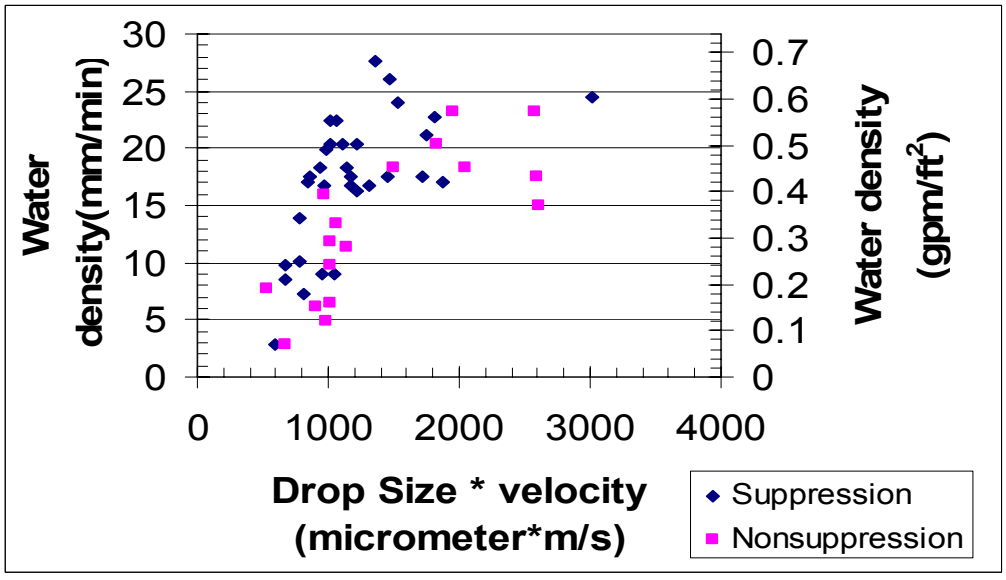

Figure 9.4 Mineral seal oil Fire Suppression Tests for Different Water Density and the Multiple of 50% Volume Fraction Particle Size ($D_{v,0.5}$) and Velocity.

9.2 Suppression criteria for cooking oil

For cooking oil fire suppression tests, 7 tests were suppression tests and 3 tests were non-suppression tests. The suppression of cooking oil fires only relates to water density and the water drop size does not matter as seen in Figure 9.5 because the water spray cooled the oil and disturbed and exchanged the heat between the cold oil below the surface and surface heated hot oil to enhance the fire suppression. The suppression criterion of cooking oil is 4.07 mm/min ($0.1 gpm/ft^2$) when water drop size is smaller than 500 μm from test data. The water sprays with water densities close to 4.07mm/min and volume median drop size larger than 500 μm were not tested. Therefore, the suppression scenario is still unknown in this area.

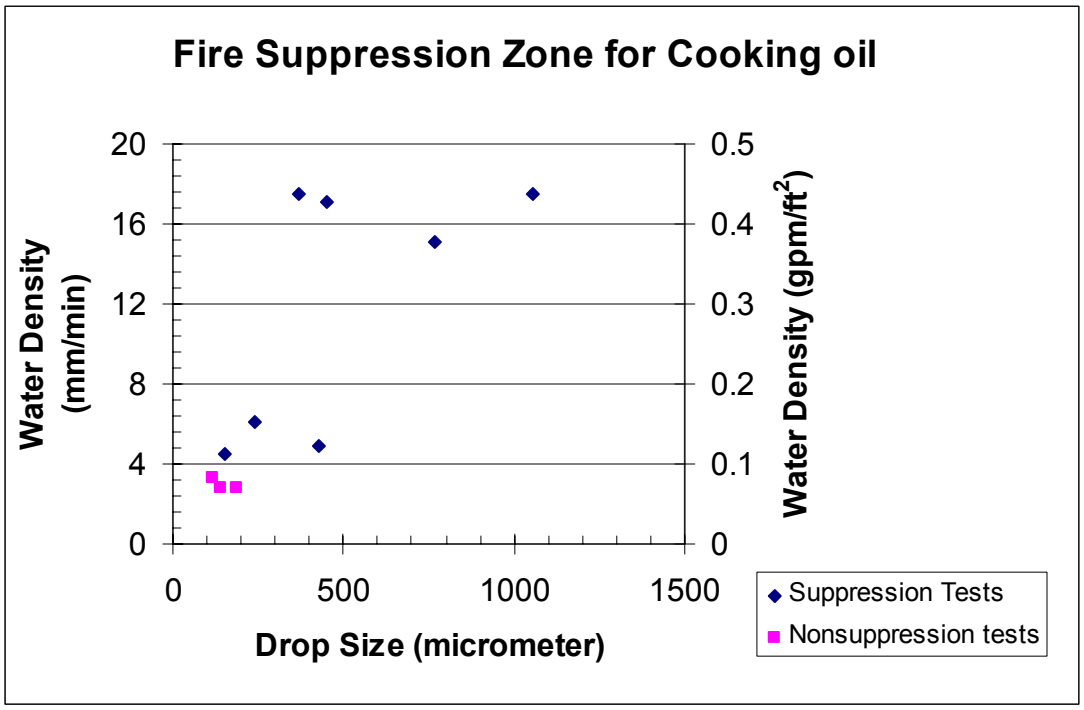

Figure 9.5 Fire suppression tests criteria for cooking oil.

9.3 Application of criteria of high flash point fire suppression tests

The critical water densities of water spray to extinguish fires of mineral seal oil and cooking oil are as shown in Figure 9.6. The required water density of water spray to extinguish fires of high flash point oil fire is 12.2 mm/min ($0.3\ gpm/ft^2$) in NFPA 15. This is enough for cooking oil if the drop size is less than $500\ \mu m$. It is only true for mineral seal oil when the volume median water drop size is smaller than 300 micrometers according to data in this research. The water densities of water spray to extinguish fires of mineral seal oil ($T_{FP} = 137^\circ C$) and cooking oil ($T_{FP} = 291^\circ C$) are also reproduced in Figure 9.6 based on Rasbash's correlation as shown in equation 2-1. These densities are below the results of this research from Figure 9.6. This could be because Rasbash's correlation is based on the oil being cooled below its fire point and the fire was only assumed to be suppressed. However the fire could be maintained even though the oil temperature was below its fire point in this research as observed here in the mineral seal oil tests. This required more water densities to extinguish the fire.

The critical water densities are as shown in equations 9-2 and 9-3 for mineral seal oil and cooking oil from this research if the oil heated from the surface and ignited.

$$\dot{m}''_{cr,w,m} = 25.2 - 43.5e^{-\frac{d_w}{218}} \qquad (150\mu m < d_w < 1000\mu m) \qquad \text{mineral seal oil} \qquad 9\text{-}2$$

$$\dot{m}''_{cr,w,c} = 4.07 \qquad (150\mu m < d_w < 500\mu m) \qquad \text{cooking oil} \qquad 9\text{-}3$$

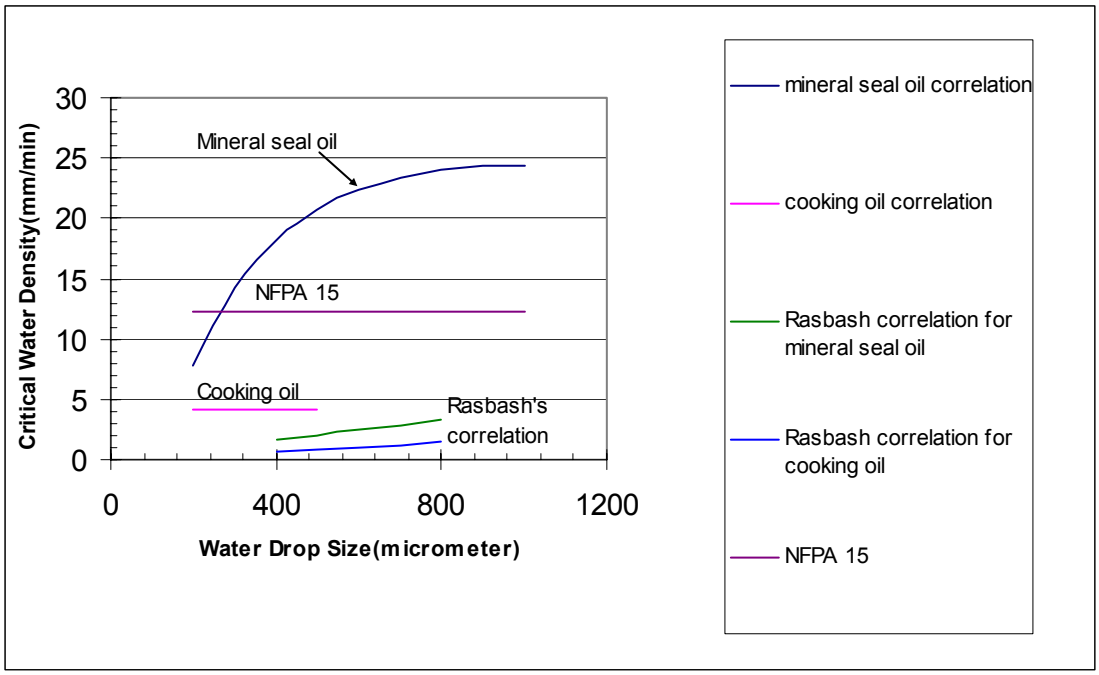

Figure 9.6 The critical water density comparison for different tests and codes.

The energy balance at the surface when the flame extinction is reached due to surface cooling is shown in equation 9-4 from Tewarson's chapter in SFPE Handbook [61].

$$\dot{m}''_{cr,b} = \frac{\varphi \Delta H_T \dot{m}''_{cr,b} - \dot{q}''_{rr} - \dot{q}''_{agent}}{\Delta H_g} = \frac{\varphi \Delta H_T \dot{m}''_{cr,b} - \dot{q}''_{rr} - \varepsilon_w \dot{m}''_{cr,w} \Delta H_w}{\Delta H_g} \qquad 9\text{-}4$$

$$\dot{m}''_{cr,w} = \frac{\varphi \Delta H_T \dot{m}''_{cr,b} - \dot{q}''_{rr} - \dot{m}''_{cr,b} \Delta H_g}{\varepsilon_w \Delta H_w} \qquad 9\text{-}5$$

Where: $\dot{m}''_{cr,b}$ is the critical burning rate of oil without splattering

$\dot{m}''_{cr,w}$ is the critical water density

ΔH_T is the total heat of combustion

φ is the maximum fraction of combustion energy that the flame reactions may loss to the sample surface by convection without flame extinction

ΔH_g is the heat of gasification

$\dot{q}''_{rr}$ is the surface re-radiation loss

ε_w is the water application efficiency

ΔH_w is the heat of gasification of water

Experiments were conducted in the FMGlobal advanced flammability measurements apparatus by Beaulieu [2] to obtain heats of gasification and critical burning rates to sustain a flame of mineral seal oil and cooking oil. The critical burning rates per unit area are 2.1 $\frac{g}{m^2 s}$ and 4.6 $\frac{g}{m^2 s}$ for cooking oil and mineral seal oil, respectively, and the heats of gasification of cooking oil and mineral seal oil are 0.8 kJ/g and 0.7 kJ/g. The parameter φ can be expressed as equation 9-6 by Tewarson [62] and Drysdale [15] based on Spalding mass transfer theory.

$$\varphi = \frac{Y_O \Delta H_O^*}{\Delta H_T (\exp(\dot{m}''_{cr,b} C_p / h) - 1)} \qquad 9\text{-}6$$

Where: Y_O is the oxygen mass fraction

ΔH_O^* is the net heat of complete combustion per unit mass of oxygen consumed (kJ/g)

C_P is the specific heat of air $(kJ / g - K)$

h is the convective heat transfer coefficient $(kW / m^2 - K)$

The parameter φ is the energy back to the fuel surface that is calculated to be 0.12 and 0.36 for mineral seal oil and cooking oil from equations 9-7 and 9-8. Using Equation 9-5, the critical water density for mineral seal oil and cooking oil fire suppression are calculated as equations 9-9 and 9-10.

$$\varphi_m = \frac{Y_O \Delta H_O^*}{\Delta H_T (\exp(\dot{m}''_{cr,b} C_p / h) - 1)} = \frac{3\frac{kJ}{g}}{42\frac{kJ}{g}(\exp(4.6\frac{g}{m^2 s}\times 10^{-3}\frac{kJ}{gK}/10^{-2}\frac{kJ}{m^2 s}) - 1)} = 0.12 \qquad 9\text{-}7$$

$$\varphi_c = \frac{Y_O \Delta H_O^*}{\Delta H_T (\exp(\dot{m}''_{cr,b} C_p / h) - 1)} = \frac{3\frac{kJ}{g}}{36\frac{kJ}{g}(\exp(2.1\frac{g}{m^2 s}\times 10^{-3}\frac{kJ}{gK}/10^{-2}\frac{kJ}{m^2 s}) - 1)} = 0.36 \qquad 9\text{-}8$$

$$\dot{m}''_{cr,w,m} = \frac{(0.12\times 42\frac{kJ}{g} - 0.7\frac{kJ}{g})\times 4.6\frac{g}{m^2 s} - 5.67\times 10^{-11}\times(410^4 - 298^4)\frac{kJ}{m^2 s}}{\varepsilon_w \times 2.58\frac{kJ}{g}} = \frac{0.45mm/\min}{\varepsilon_w}$$

for mineral seal oil 9-9

$$\dot{m}''_{cr,w,c} = \frac{(0.36\times 36\frac{kJ}{g} - 0.8\frac{kJ}{g})\times 2.1\frac{g}{m^2 s} - 5.67\times 10^{-11}\times(564^4 - 298^4)\frac{kJ}{m^2 s}}{\varepsilon_w \times 2.58\frac{kJ}{g}} = \frac{0.46mm/\min}{\varepsilon_w}$$

for cooking oil 9-10

Using the data correlations for $\dot{m}''_{cr,w,m}$ the efficiencies of water spray are calculated 11% to 2% for mineral seal oil at water drop size from 150 μm to 1000 μm and 11% for cooking oil at water drop size from 150 μm to 500 μm as shown in Figure 9.7. More than 89% water did not contribute effectively to fire suppression. These water droplets could be bouncing away from the fire zone or sank into the bottom of the oil without absorbing enough heat. Cooking oil had higher water efficiency to extinguish the fire because the high temperature difference between the oil and water spray. However more splattering oils were caused by water spray when water

discharged onto the cooking oil fire because it has higher temperature on the surface than mineral seal oil. The oil cooling, the oil splattering, and oil surface cooling for high flash point fire suppression affect the fire extinguishment.

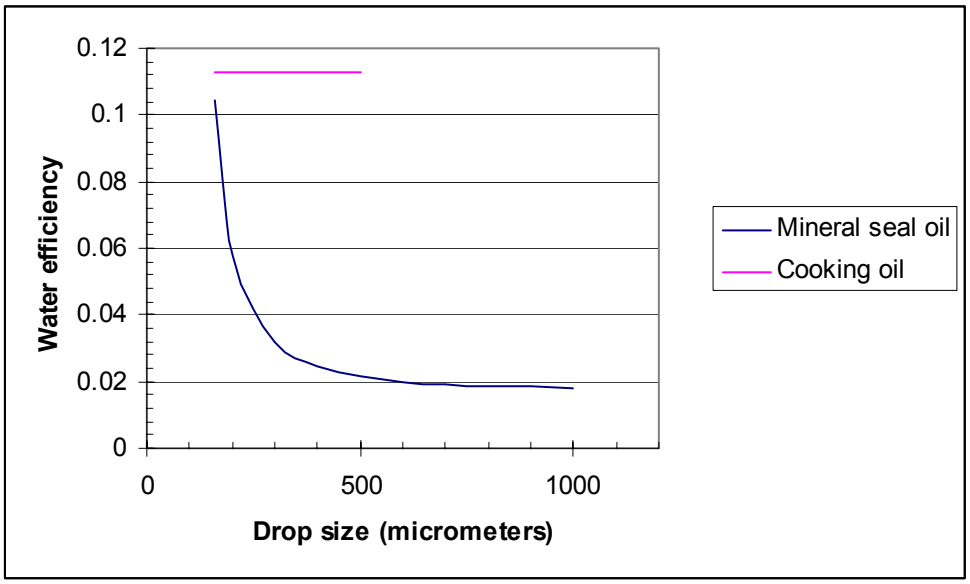

Figure 9.7 Water efficiency for mineral seal oil and cooking oil.

The four factors that can affect the water efficiency of high flash point pool fire are: surface impingement cooling, oil convective cooling, water in oil emulsion, and oil splattering as shown in Figure 9.8 to Figure 9.11. Figure 9.8 shows surface impingement cooling. Smaller water droplets impinging on the hot oil surface absorb some heat and bounce back to the environment. The drop sizes become smaller because they absorb heat and vaporize. Figure 9.9 shows oil convective cooling. If the water drop size is large and penetrates into the oil, the water vaporization is small on the oil surface and the oil heat is removed by convective heat transfer between oil and water droplet. The temperature profile in the oil is thermally thick because the oil is heated from above the surface. Figure 9.10 shows water-in-oil emulsion formation. Some water droplets penetrate into the oil and mixed with the oil to form an emulsion. Water-in-oil emulsion needs more heat flux to sustain the fire. Figure 9.11 shows the oil splattering. The oil splattering is caused in part by water impingement and boiling, and in part by some oil

rebounding with water droplets at surface. Larger water droplets cause more oil splattering and also intensify the fire.

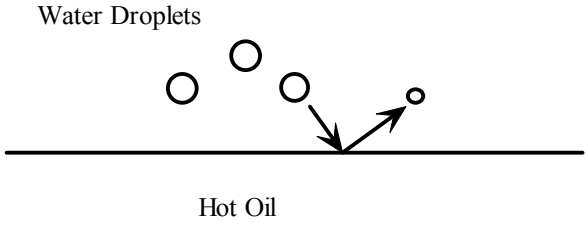

Figure 9.8 Surface impingement cooling.

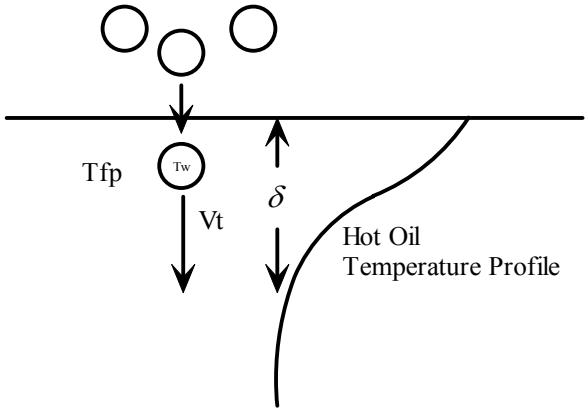

Figure 9.9 Convective cooling.

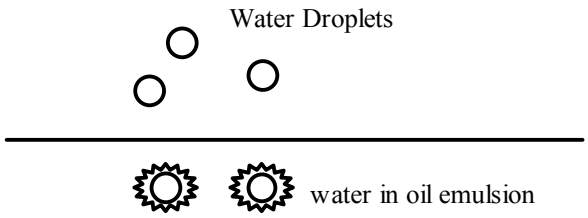

Figure 9.10 Water in oil emulsion.

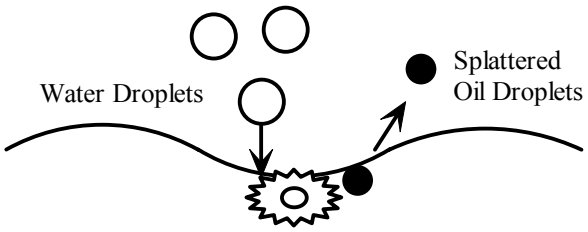

Figure 9.11 Oil splattering.

9.3.1 Surface impingement cooling

The surface impingement cooling is the water hitting on hot oil surface and vaporizing to absorb heat from the hot oil surface. Mcginnis [0] et al found the heat transfer per splattering drop satisfied the correlation as equation 9-11 when water, acetone, or alcohol droplets bounced from a heated plate.

$$\frac{Q}{\rho_{w,L} d_w^3 \Delta h_g} = 8.44\times10^{-4}\left(\frac{\rho_{w,L}^2 u_w^2 d_w}{\rho_{w,v}\sigma_w g_c}\right)^{0.341} f(\Delta T) = 8.44\times10^{-4}\left(\frac{\rho_{w,L} We}{\rho_{w,v}}\right)^{0.341} f(\Delta T) \qquad 66^\circ C < \Delta T < 260^\circ C \qquad 9\text{-}11$$

Where : Q is heat transfer per drop (Btu/drop)

$\rho_{w,L}$ is water density (lb/ft^3)

$\rho_{w,v}$ is water vapor density (lb/ft^3)

u_w is water drop velocity (ft/s)

σ_w is water drop surface tension (lbf/ft)

g_c is constant of proportionality in Newton's second law

$\Delta T = T_s - T_w$ is the temperature difference between the hot plate and water drop

$f(\Delta T)$ is between 0 and 1

Δh_g is modified water heat of gasification ($\Delta h_g = \Delta H_w + C_{pv}(T_{FP} - T_{sat})$)

The right hand side of equation 9-11 is the water efficiency per impinging water drop on the heated plate. The larger Weber number drops have a higher efficiency to cool the surface. The total droplets per unit area and per unit time on the pool surface calculated are as equation 9-12. The equations 9-11and 9-13 can be used to calculate the removed heat from the surface. If the $f(\Delta T)$ is used as 1, the maximum removed heat is calculated as $27\,kW/m^2$ when the drop size

is 174 μm and the water density is 7.3 mm/min. $f(\Delta T)$ is 1 only when ΔT is 167 ^{o}C. The removed heat in this case should be less than 27 kW/m^2. Other removed heat rates are listed in Table 9.1. The higher water density and larger drop spray is overestimate from this method because the most larger drops should penetrate into the oil to absorb heat and not absorb heat from the surface.

$$\dot{n}\frac{\pi}{6}d_w^3 = \dot{m}_w'' A \qquad 9\text{-}12$$

$$\dot{n}'' = \frac{\dot{m}_w''}{\frac{\pi}{6}d_w^3} \qquad 9\text{-}13$$

Where: $\dot{n}$ is the average number of water droplets on the surface per unit time

A is pan area

d_w is drop size

$\dot{m}_w''$ is water density

$\dot{n}''$ is the number of water droplets in contact with liquid surface per unit liquid surface area per unit time

Table 9.1 Heat removed rates for mineral seal oil and cooking at specific water spray condition.

Oil	Drop size (μm)	Velocity (m/s)	Water density (mm/min)	$\dot{n}''$	$Q_{\max}$	$\dot{n}''Q$ $(\frac{Btu}{m^2 s})$	$\dot{n}''Q$ $(\frac{kW}{m^2})$
Mineral seal oil	174	4.63	7.3	4.4×10^{7}	5.8×10^{-7}	26	27
	237	3.32	10.2	2.4×10^{7}	1.3×10^{-6}	32	33
	368	4.68	17.5	1.1×10^{7}	7.1×10^{-6}	80	84
	543	3.34	22.8	4.5×10^{6}	2.1×10^{-5}	94	99
Cooking oil	115	3.37	4.5	9.4×10^{4}	4.4×10^{-7}	11	12
	425	2.3	4.9	2×10^{3}	7.1×10^{-6}	14	15

9.3.2 Oil convective cooling

The energy transfer between oil and water is as shown in equation 9-14 for water droplets pass through the hot oil.

$$n'' h \frac{\pi d_w^2}{4} (T_{FP} - T_w) = \varepsilon_w \dot{m}_w'' \Delta H_w \qquad 9\text{-}14$$

where: n'' is the number of water droplets in contact with liquid surface per unit liquid surface area

h is convective heat transfer coefficient between water drops and hot oil

Equation 9-16 can be modified to equation 9-15.

$$\frac{\dot{m}_w''}{\rho_w u \frac{\pi d_w^2}{4}} h \frac{\pi d_w^2}{4} (T_{FP} - T_w) = \varepsilon_w \dot{m}_w'' \Delta H_w \qquad 9\text{-}15$$

and $Nu = \frac{h d_w}{\lambda}$, equation 9-15 can be rewritten as equation 9-16

$$\frac{\dot{m}_w''}{\rho_w u} \frac{(Nu)\lambda}{d_w} (T_{FP} - T_w) = \varepsilon_w \dot{m}_w'' \Delta H_w \qquad 9\text{-}16$$

$$\varepsilon_w = \frac{\lambda}{\rho_w C_{p,o} d_w u} \frac{C_{p,o}(T_{FP} - T_w)}{\Delta H_w} Nu \qquad 9\text{-}17$$

If the cooling is forced convection, equation 9-17 can rewrite as equation 9-18.

$$\varepsilon = \frac{\lambda}{\rho_w C_{p,o} d_w u} \frac{C_{p,o}(T_{FP} - T_w)}{\Delta H_w} \{2 + (0.4\,\mathrm{Re}_D^{1/2} + 0.06\,\mathrm{Re}_D^{1/2})\,\mathrm{Pr}^{0.4} [\frac{\mu_\infty}{\mu_s}]^{1/4}\}$$

$$= \frac{0.001367 \frac{kW}{mK}}{0.000543m \times 1000 \frac{kg}{m^3} \times 3.3 \frac{m}{s}} \times \frac{(137-25)K}{2580 \frac{kJ}{kg}}$$

$$(2 + (0.4 \times (\frac{1000 \frac{kg}{m^3} \times 3.3 \frac{m}{s} \times 0.000543m}{0.001 \frac{kg}{ms}})^{1/2} + 0.06 \times (\frac{1000 \frac{kg}{m^3} \times 3.3 \frac{m}{s} \times 0.000543m}{0.001 \frac{kg}{ms}})^{2/3}) \times 100^{0.4} \times 1^{1/4})$$

$$= 0.0003$$

9-18

The efficiency is calculated as 0.0003 from equation 9-18 for forced convection cooling of mineral seal oil when the drop size, velocity and water density are 543 μm, 3.3 m/s, and 22.8 mm/min. This overestimates the cooling effect, because the velocity is on the oil surface, but it is usually smaller inside the oil with drag force. It is small contribution to the overall fire suppression efficiencies shown in Figure 9.7.

9.3.3 Water in oil emulsion

Walavalkar[67] found that the critical flame heat flux necessary to cause sustain fire increases with increasing water content of the emulsion. For the same starting emulsion thickness less oil was burned when the water content of the emulsion increased from 20% to 80%. The separation time for water-in-oil increased with increasing the water fraction of the emulsion. The emulsion in these tests was observed as shown in Figure 9.12 when 10 psi water sprays discharged onto mineral seal oil fires from 3/8GG 18SQ and 3/8GG 15 nozzles. The emulsion fractions were measured as 0.2% and 0.5% of the total volume that remained in the pan after these tests with mineral seal oil. Few emulsions were found in cooking oil tests. Emulsion formation does not seem to be an important factor to extinguish the high flash point fires.

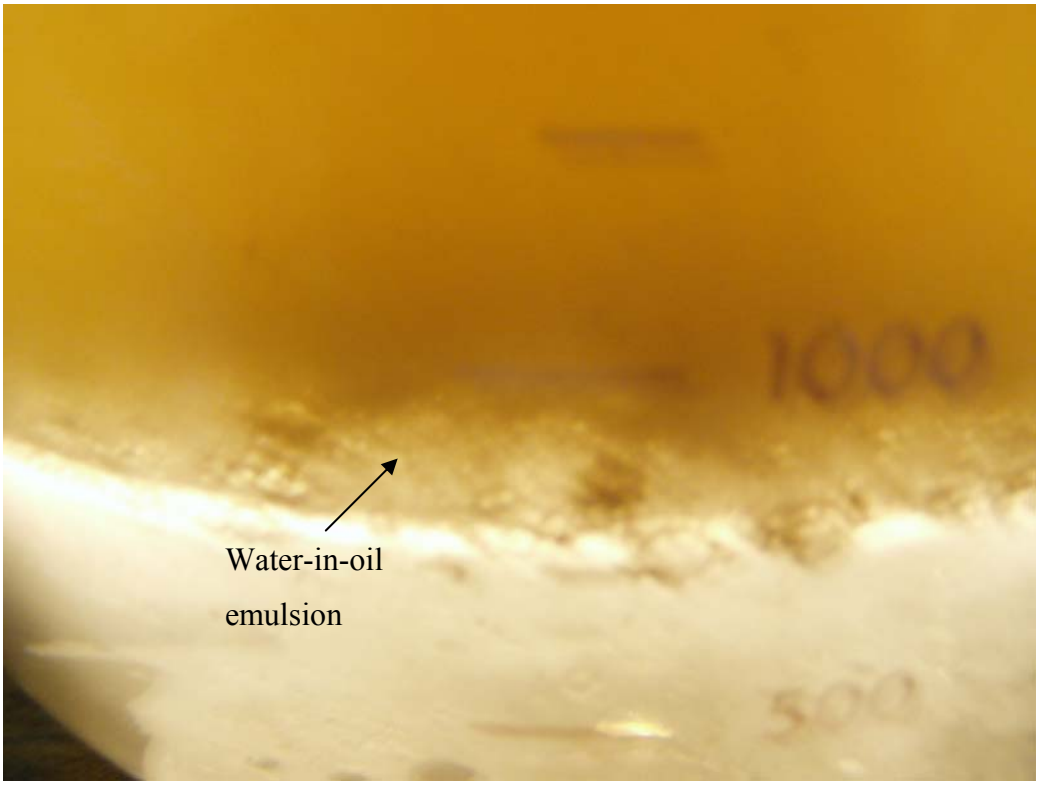

Figure 9.12 Water-in-oil emulsion between oil and water.

9.3.4 Oil splattering

Oil splattering was measured and discussed in chapters 6 and 7. The heat release rates contribution were calculated as 40 kW, 50 kW, and 54 kW at 15 psi water spray from 1/2GG29SQ nozzle, 10 psi water spray from 1/2GG32 nozzle, and 15 psi water spray from 1/2GG32 nozzle, respectively for 110 $^{\circ}C$ mineral seal oil. The fires were suppressed for these spray nozzle conditions in the fire suppression tests of fpc79, fpc55, and fpc56 as shown in Table 8.1. For 270 $^{\circ}C$ cooking oil, the heat release rates were calculated as 205 kW and 416 kW at 75 psi water from spraco110620-01 nozzle and 10 psi water from 3/8GG22 nozzle, respectively. The fires were also suppressed for these spray nozzle conditions in the fire suppression tests of fpc122 and fpc123 as shown in Table 8.2.

From these mechanism discussions, the surface cooling and oil splattering are the most important factors when water sprays discharge onto the oil fire. The surface temperature of the oil could be cooled to reduce its contribution to the fire. However the fire could not be extinguished for the oil splattering contribution. Water spray enhanced mixing between the hot oil and cold oil should be also important for the fire suppression since the sub-surface heat convective cooling from droplets is so small from the analysis of this research. This is also supported by only little water penetrated into the cooking oil but the temperature 1/2 in. below the surface rose up so quickly from the cooking oil suppression test.

9.3.5 Generalized criteria for oil suppression

The oil splattering is affected by Weber number and Ohnesorge number as describe by Cossaii, [9] and controlled by oil temperature and Weber number of the water spray in this research and Manzello [34]. The surface cooling is controlled by Weber number and temperature difference between oil surface and ambient. Larger Weber number water sprays cause more oil splattering to intensify the fires but increase the surface cooling to reduce the fire size and also enhance the mixing between the hot oil and cold oil to reduce the surface oil temperature. In this research, the critical water density does not have the relationship with Weber number of the water spray from the analysis of chapters 9-1 and 9-2 but it does depend on drop size. The efficiency of ε_w can be the function of the dimensionless factor $\frac{C_{pl}(T_{FP}-T_w)}{\Delta H_{chem}}$ and Ohnesorge number $(\frac{\mu_{oil}}{(\rho_{oil}\sigma_{oil}d_w)^{1/2}})$ for high flash point of hydrocarbon fuel fire from above analysis.

$$\varepsilon_w = f_1(\frac{C_{pl}(T_{FP}-T_w)}{\Delta H_{chem}}, Oh_{oil}) \qquad 9\text{-}19$$

From equations 9-2 and 9-3, the critical water density depends on two items and only one is related to drop size. The ε_w can be expressed as equation 9-20.

$$\frac{1}{\varepsilon_w} = f_2(\frac{C_{pl}(T_{fp}-T_w)}{\Delta H_{chem}}) - f_3(\frac{C_{pl}(T_{fp}-T_w)}{\Delta H_{chem}})e^{-k_1/Oh_{oil}^m} \qquad 9\text{-}20$$

where : $oh_{oil} = \frac{\mu_{oil}}{(\rho_{oil}\sigma_{oil}d_w)^{1/2}}$

Equations 9-5 and 9-20 can be generalized as equation 9-21.

$$\dot{m}''_{cr,w} = \frac{\varphi \Delta H_T \dot{m}''_{cr,b} - \dot{q}''_{rr} - \dot{m}''_{cr,b} \Delta H_g}{\Delta H_w} \left(f_2 \left(\frac{C_{pl}(T_{fp} - T_w)}{\Delta H_{chem}} \right) - f_3 \left(\frac{C_{pl}(T_{fp} - T_w)}{\Delta H_{chem}} \right) e^{-k_1 / Oh^m} \right) \quad 9\text{-}21$$

For mineral seal oil, equation 9-21 can be modified to equation 9-22 based on equations 9-2 and 9-9.

$$\dot{m}''_{cr,w,m} = 0.45 mm / \min \left(f_2 \left(\frac{C_{pl}(T_{fp} - T_w)}{\Delta H_{chem}} \right) - f_3 \left(\frac{C_{pl}(T_{fp} - T_w)}{\Delta H_{chem}} \right) e^{-k_1 / Oh^m} \right) = 25.2 - 43.5 e^{-\frac{d_w}{218}} \quad 9\text{-}22$$

For cooking oil, equation 9-21 can be modified to equation 9-23 based on equations 9-3 and 9-10.

$$\dot{m}''_{cr,w} = 0.46 mm / \min \left(f_2 \left(\frac{C_{pl}(T_{fp} - T_w)}{\Delta H_{chem}} \right) - f_3 \left(\frac{C_{pl}(T_{fp} - T_w)}{\Delta H_{chem}} \right) e^{-k_1 / Oh^m} \right) = 4.07 mm / \min \quad 9\text{-}23$$

The data indicate that $\dot{m}''_{cr,w}$ decreases with increasing $(T_{fp} - T_w)$. If $f_2 \left(\frac{C_{pl}(T_{fp} - T_w)}{\Delta H_{chem}} \right)$ is assumed to be $\frac{k_2}{\left(\frac{C_{pl}(T_{fp} - T_w)}{\Delta H_{chem}} \right)^n}$ and equations 9-24 and 9-25 can be obtained from equations 9-22 and 9-23.

$$\frac{k_2}{\left(\frac{C_{pl}(T_{fp,m} - T_w)}{\Delta H_{chem}} \right)^n} = \frac{25.2}{0.45} = \frac{k_2}{\left(\frac{1.92(137 - 25)}{32200} \right)^n} \quad \text{mineral seal oil} \quad 9\text{-}24$$

$$\frac{k_2}{\left(\frac{C_{pl}(T_{fp,cooking} - T_w)}{\Delta H_{chem}} \right)^n} = \frac{4.07}{0.46} = \frac{k_2}{\left(\frac{2.5(291 - 25)}{35300} \right)^n} \quad \text{cooking oil} \quad 9\text{-}25$$

The k_2 and n are 0.007 and 1.8 from equations 9-24 and 9-25.

For mineral seal oil, equation 9-26 can be obtained from equation 9-22.

$$f_3\left(\frac{C_{pl}(T_{fp}-T_w)}{\Delta H_{chem}}\right)=\frac{43.5}{0.45} \qquad 9\text{-}26$$

For cooking oil, equation 9-27 can be obtained from equation 9-23.

$$f_3\left(\frac{C_{pl}(T_{fp}-T_w)}{\Delta H_{chem}}\right)=0 \qquad 9\text{-}27$$

$f_3\left(\frac{C_{pl}(T_{fp}-T_w)}{\Delta H_{chem}}\right)$ is assumed to be exponential function of $\frac{C_{pl}(T_{fp}-T_w)}{\Delta H_{chem}}$ as equation 9-28.

$$Ae^{-k_3\frac{C_{pl}(T_{fp}-T_w)}{\Delta H_{chem}}} \qquad 9\text{-}28$$

Equations 9-29 and 9-30 can be obtained from the function of f_3 of mineral seal oil and cooking oil and equation 9-28.

$$96.7 = Ae^{-k_3\frac{1.92(137-25)}{32200}} \qquad \text{mineral seal oil} \qquad 9\text{-}29$$

$$0 = Ae^{-k_3\frac{2.5(291-25)}{35300}} \qquad \text{cooking oil} \qquad 9\text{-}30$$

The A is 2243 and k_3 is 500 from equations 9-2and 9-30.

The power of the exponential can be related together as equation 9-31 from equation 9-23. The m and k_1 is obtained as 2 and 0.28 for equation 9-31.

$$\frac{d_w}{218} = \frac{k_1}{Oh_{oil}^m} = k_1 d_w^{m/2} \times \left(\frac{(822\frac{kg}{m^3} \times 0.03\frac{N}{m})^{m/2}}{(38.8\frac{kg}{m \cdot s})^m}\right) \quad 9\text{-}31$$

Where

$$Oh_{oil} = \frac{\mu_w}{(\rho_w \sigma_w d_w)^{1/2}}$$

ρ_w is the oil density (kg/m^3)

σ_w is the oil surface tension (N/m)

d_w is the water drop size (μm)

μ_w is the oil viscosity (kg/ms)

The critical water spray density to extinguish fires of high flash point hydrocarbon oil can now be expressed as equation 9-32 from the above discussion.

$$\dot{m}''_{cr,w} = \frac{\varphi \Delta H_T \dot{m}''_{cr,b} - \dot{q}''_{rr} - \dot{m}''_{cr,b} \Delta H_g}{\Delta H_w} \times \left(\frac{0.007}{\left(\frac{C_{pl}(T_{fp} - T_w)}{\Delta H_{chem}}\right)^{1.8}} - (2243 e^{-500\frac{C_{pl}(T_{fp}-T_w)}{\Delta H_{chem}}}) e^{-\frac{0.28}{Oh_{oil}^2}}\right) \quad 9\text{-}32$$

Figure 9-13 shows that the requirement of critical water density to extinguish transformer oil fire and lubricating oil fire based on equation 9-32. These are consistent with Rasbash [56] and Kokkala's [28] tests. Rasbash used 16 mm/min water densities with 0.28mm, 0.38mm, and .48mm drop sizes to extinguish transformer oil fires of flash point 175 to 180$^{\circ}C$ and Kokkala used 8 mm/min water density (unspecified drop size) to extinguish lubricating oil fire of flash point 234$^{\circ}C$. Figure 9.13 also shows that the requirement critical water density to extinguish high flash point fire in NFPA 15 (12.2 mm/min) is only valid when the flash point of the oil is higher than 190^{o}C from equation 9-32.

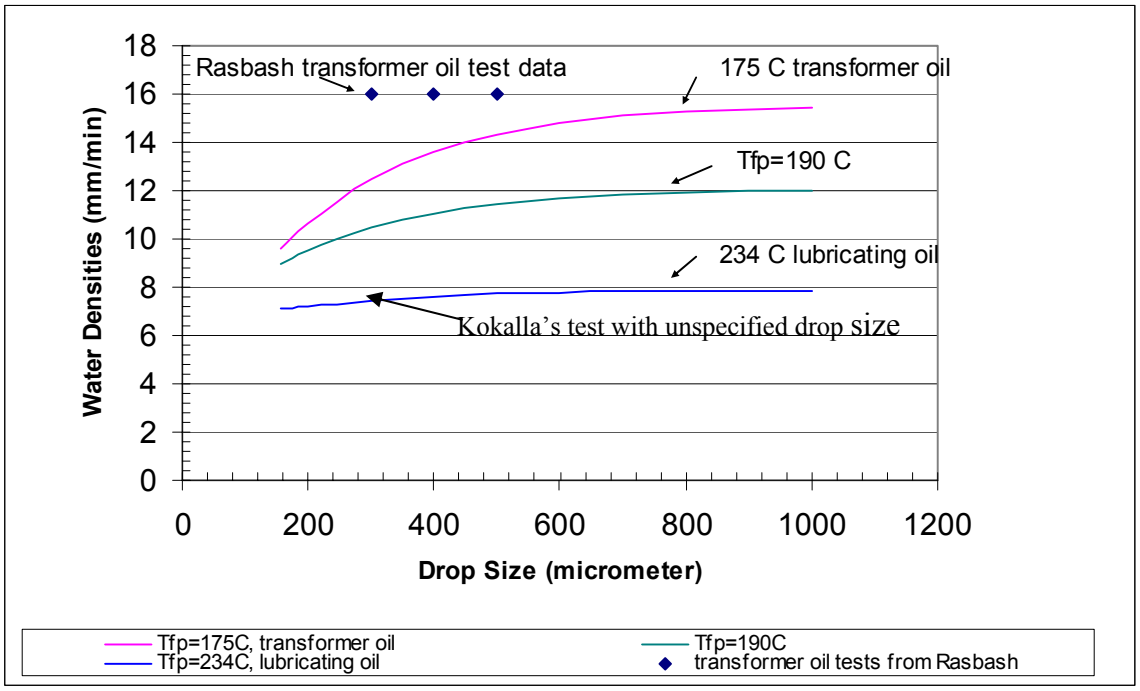

Figure 9.13 The critical water density prediction of flash point 175^{o}C, 190^{o}C, 234^{o}C for equation 9-32.

9.4 Extinguishment time analysis

Extinguishing time decreased with increased water pressure for specific nozzles in the mineral seal oil fire suppression tests. The results are shown as in Figure 9.14. The fire was extinguished at about 4 seconds when the pressure was larger than a critical point for a specific nozzle. Figure 9.15 shows the extinguishment times overestimated using Nash's extinguishment time correlation. His correlation is as shown in equation 2-2. The critical water density of water spray to extinguish obtained from this research is higher than Nash's [39]. A modified correlation should be developed to predict the extinguishment time for the test data in this research. From the Nash's correlation the water density, drop size and temperature difference between fire point and water temperature should be included in the dimensionless analysis as in equation 9-33. The constants k, m, and n are solved as 0.28, -2.1 and 0.6 based on the test data of mineral seal oil and cooking oil in this research. The critical water densities can be obtained from equations 9-2 and 9-3 from mineral seal oil and cooking oil tests. The equation 9-33 can be rewritten to equation 9-34. A better fire extinguishment time prediction can be obtained from this correlation as shown in Figure 9-15. The equations 2-2 and 9-34 are similar relations among the extinguishment time, water density, drop size, and excess temperature difference. Higher water densities, smaller drop size and higher fire point oils have smaller extinguishment time for high flash point oil fire suppression.

$$t_{ext} = 6.7\times10^{5} \times \dot{R}_{w}''^{-\frac{3}{2}} d_{w}^{\,0.85} (T_{FP} - T_{w})^{-\frac{5}{3}} \qquad 2\text{-}2$$

$$\frac{t_{ext}\dot{R}_{w}''}{d_{w}} = k\left(\frac{C_{p,o}(T_{FP} - T_{w})}{\Delta H_{w}}\right)^{m}\left(\frac{\dot{R}_{w}''}{\dot{R}_{w,c}''}\right)^{n} \qquad 9\text{-}33$$

$$\frac{t_{ext}\dot{R}_{w}''}{d_{w}} = 0.28\left(\frac{C_{p,o}(T_{FP} - T_{w})}{\Delta H_{w}}\right)^{-2.1}\left(\frac{\dot{R}_{w}''}{\dot{R}_{w,c}''}\right)^{0.6}$$

$$t_{ext} = 0.28 \times (\frac{C_{p,o}}{\Delta H_w})^{-2.1} \times \dot{R}_w''^{-\frac{2}{5}} \frac{d_w}{\dot{R}_{w,c}''^{0.6}} (T_{FP} - T_w)^{-2.1} \qquad 9\text{-}34$$

Where: d_w : water drop size (mm)

T_{FP} : fire point ($^\circ$C)

T_w : water temperature($^\circ$C)

t_{ext} : fire extinguishment time (min)

$\dot{R}_w''$: applied water density (mm/min)

$\dot{R}_{w,c}''$: critical water density (mm/min)

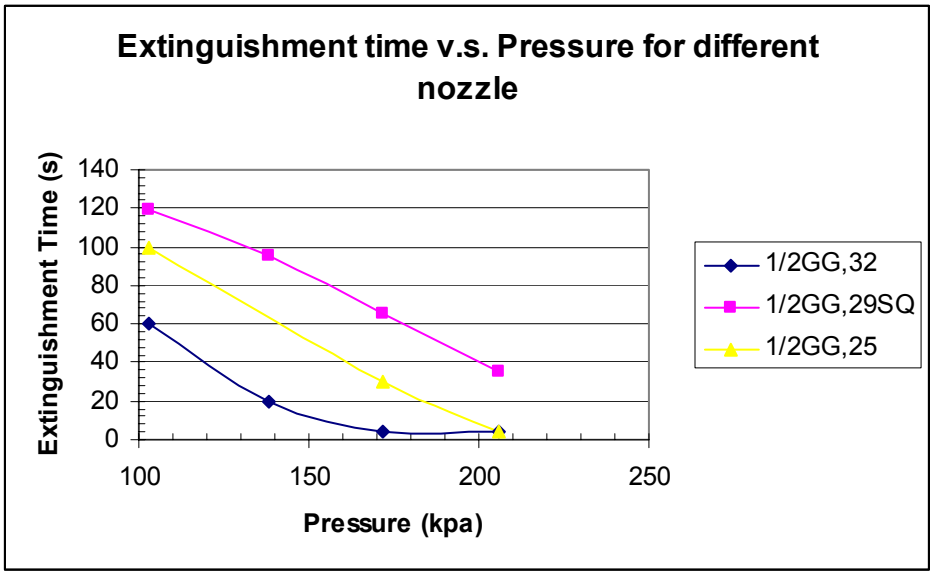

Figure 9.14 Extinguishment time v.s Pressure of Different Nozzle for surface heated mineral seal oil.

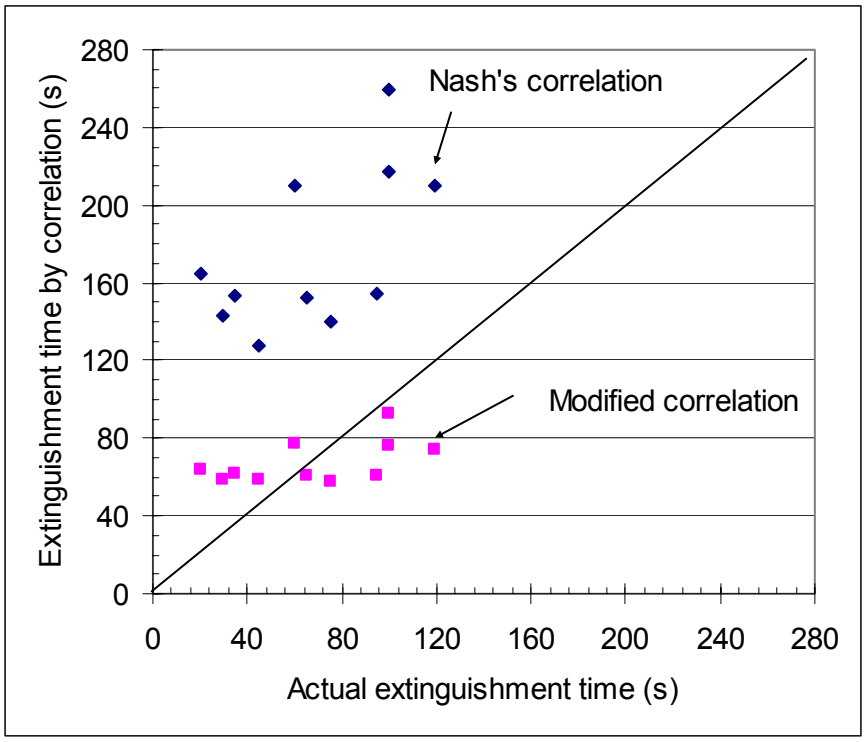

Figure 9.15 Prediction time by Rasbash's Correlation and Modified Correlation v.s Actual Extinguishment Time.

9.5 Summary

The critical water spray densities for water spray to extinguish fires are obtained from correlations for fire suppression tests for mineral seal oil and cooking oil. The critical water densities of water spray to extinguish fires of mineral seal oil and cooking oil are higher than the predictions of Rasbash's correlation. His correlation is based on the oil being cooled below its fire point and the fire was only assumed to be suppressed. However some of the tests reported here show that the fire could be maintained even though the oil temperature was below its fire point. The critical water density of mineral seal oil is also higher than the requirement of NFPA 15 for high flash point oil when the water drop size is larger than 300 micrometers. The critical water density of 4.07 mm/min obtained here for cooking oil is lower than the requirement of NFPA 15, 12.2 mm/min.

Oil splattering is an important factor when water sprays discharge onto the oil fire. The surface temperature of the oil could be cooled to reduce its contribution to the fire. However the fire could not be extinguished for the oil splattering contribution. The water spray enhancing the mixing between the hot oil and cold oil should be also important for the fire suppression if the heat convective cooling is so small from the analysis of this research. This is also supported by only little water penetrated into the cooking oil but the temperature 1/2 in. below the surface rose up so quickly from the cooking oil suppression test.

A generalized correlation is also developed to predict critical water density of different flash point oils besides mineral seal oil and cooking oil based on their test data. From this generalized correlation, the required critical water density of 12.2 mm/min in NFPA 15 is only valid when the flash point of oil is higher than $190\,^{o}C$ for large drop spray.

Extinguishment time decreased with increasing water pressure for specific nozzles at mineral seal oil fire suppression tests. The extinguishment times of mineral seal oil fires are overestimated by Rasbash's correlation. A modified correlation is used to predict a better extinguishment time based on dimensionless analysis and test data. Equations 2-2 and 9-34 are

similar relations in terms of the effects of water density, drop size, and excess temperature difference. Higher water densities, smaller drop size and higher fire point oils produce smaller extinguishment time for high flash point oil fire suppression.

10 Conclusions

Conclusions are presented under the headings spray drop size measurements, oil heating and spray cooling tests, fire suppression criteria, and spray induced fire intensification.

Water Spray Drop Size Measurements

Water spray drop size distributions from numerous nozzles tested fit the Rosin-Rammler distribution function. Except for the BETE nozzle, the volume median drop size, d_w, for nozzle orifices, D, smaller than 3mm can be correlated as $\frac{d_w}{D} = \frac{C}{We^{1/3}}$, where We is the Weber number based on nozzle orifice diameter and nozzle velocity. This correlation should be modified to $\frac{d_w}{D} = \frac{C}{We^{3/4}}$ when the orifice size is larger than 3 mm and the operating pressure is smaller than 30 psi for Spraying System 1/2GG, 25, 1/2GG,29SQ, 1/2GG,32 and Grinnell AM24 nozzles. These correlations from this research are applicable when the measurement site was located at 0.91m (3ft) under the centerline of the nozzle. This site was selected because it is where the oil pan was located during the water spray fire suppression/intensification tests.

Oil Heating and Spray Cooling Tests

The propane ring burner developed during this dissertation can provide a uniform heat flux over the surface of mineral seal oil to ignite it. Heat fluxes of 7.6 KW/m^2, 14.5 KW/m^2, and 24.5 KW/m^2 were obtained when the ring burner was 10.2 cm (4in.), 7.62 cm (3in.) and 5.08 cm (2in.), respectively, above the fuel surface. Liquid temperatures during the oil heating period up to ignition (at a surface temperature of 137 ^oC) are predicted well using a thermally thick heat conduction model.

Water spray discharge onto the heated oil completely disrupts the thin layer of heated oil below the oil surface. Even at relatively low water spray densities, the water spray not only cooled the oil surface, it also mixed and enhanced the heat transfer between the hot oil and cold oil below to rapidly reduce the oil temperature near the surface. Another important effect observed during water spray discharge is water drop splashing and oil splattering. This effect is increased at high spray drop Weber numbers.

Fire Suppression Criteria

Higher water spray density and smaller drop size promotes extinguishment of mineral seal oil fires. Higher water density provides better oil and flame cooling, and smaller drop size is better for flame cooling and less oil splattering. The fires were extinguished quickly if no oil splattering occurred upon spray discharge. Oil splattering did not necessarily prevent extinguishment, but it did significantly delay it.

The water spray densities needed to extinguish 30-cm diameter mineral seal oil fires are significantly larger than the densities predicted by Rasbash's correlation. This could be because Rasbash's correlation is based on the assumption that if the spray cools the oil below its fire point, then the fire is suppressed. However results obtained here demonstrate that the fire could be maintained via splattering even though the oil temperature was below its fire point. This required a larger water spray density to extinguish the fire. Fire suppression tests conducted with high flash point (291^{o}C) soybean cooking oil ignited by the ring burner showed that spray densities greater than 0.10 gpm/ft^2 (4 mm/min) suppressed the fire. The volume median drop size at this density was in the range 100 to 500 μm. This density is substantially lower than the spray density required to suppress the lower flash point mineral seal oil fires. The temperature of the surface of the cooking oil was close to its flash point when water spray was discharged onto the oil fire and the fire was not extinguished.

A generalized data correlation has been developed to predict the relationship between spray density and median drop size required to suppress pool fires of hydrocarbons with flash points in the range 130^{o}C to 300 ^{o}C. The required densities are more sensitive to drop size when the oil flash point is in the lower portion of this range.

The time it took to extinguish the fire decreased with increasing water pressure for specific nozzles in the mineral seal oil fire suppression tests. The extinguishment time of mineral seal oil is overestimated by Rasbash's correlation. A modified correlation is used to predict a better extinguishment time based on dimensionless analysis and test data. The lower extinguishment time was obtained in this research, probably because the critical water density is higher in this research than Rasbash's result.

Locating the spray nozzle at a horizontal 6 in. offset shift from the axis of the fire showed better fire suppression than centrally located nozzles for cooking oil fires. This is probably

because the sprays pushed the flame sideways (away from the oil surface) and had a greater cooling capacity when they reached the liquid. It also could be because the entrained air velocity was higher at this particular radial distance.

Spray-Induced Pool Fire Intensification

If the water spray density is not sufficient to suppress the oil pool fire, and if the spray drop Weber number is sufficiently high, oil splattering plays an important role in enhancing the fire size. Correlations of oil splattering rate, combustion fraction, vaporization rate, and heat release rate for water sprayed onto oil heated close to its flash point were developed based on fire heat release and vaporization/burning rate data obtained during this dissertation. These correlations can be used for prediction if the water drop size, velocity, and water density for a specific nozzle or sprinkler head are known as well as the oil temperature at the time of spray actuation.

The ratio of oil splattering to water spray density increases with the oil temperature and Weber number. The fraction of the vaporization rate to the total oil burning rate of mineral seal oil is between 1% and 1.7%, and this fraction for cooking oil is less than 1% from the test data, because the oil splattering is much greater for the higher flash point oil.

The heat release rate is enhanced by factor from 2.12 to 5.55 compared to the heat release rate of free burning cooking oil. For mineral seal oil, this ratio is only of 0.92 to 1.25. The oil splattering of cooking oil is much larger than the oil splattering of mineral seal oil with the same water density discharge because the flashpoint of the cooking oil ($291\,^{o}C$) is much higher than the flash point ($137\,^{o}C$) of the mineral seal oil.

11 Appendix A: Basic Theory of Particle Size and Velocity Measurement for PDA

The Dantec Particle Dynamic Analyzer (PDA) was used to measure the spray drop size distribution and drop velocity. Its basic theory is phase Doppler anemometry. There are two laser beams crossing together and reflection, refraction, or 2nd refraction will be received from a receiver when the water drops pass through the control volume in the beam-crossing section. The two crossing beams will form a couple of fringes as shown in Figure A.1. The particle velocity can be measured when the particles pass through the fringe. The frequency can be detected and related to velocity of the particles. Two detectors are used to receive the reflection, refraction, or 2nd refraction laser signals, and their phase difference is used to determine the particle size.

Equation A-1 can be used to calculate the particle velocity, but it cannot be used to distinguish whether the velocity is positive or negative as shown in Figure A.2. A modification should be made for this, and the 40 MHz is added to make a shift as shown in Figure A.3. The velocity can be measured from –57.6 m/s to 256 m/s for the 30 MHz to 75 MHz range.

$$U_x = \frac{\lambda}{2\sin(\theta/2)} f_D \qquad \text{A-1}$$

where:

U_x = the particle velocity

λ = the wave length of the laser beam

θ = two beam cross angle

f_D = detected frequency

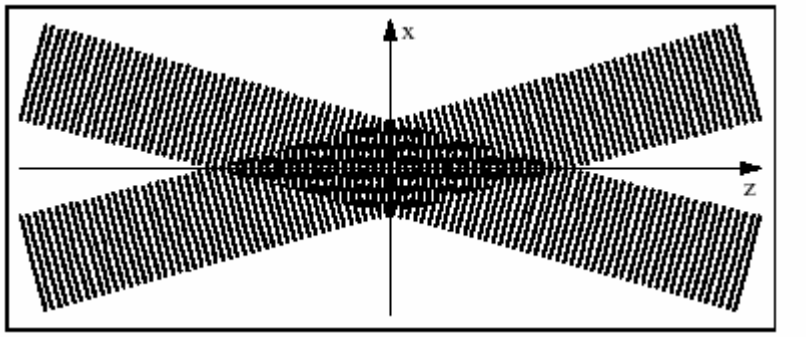

Figure A.1 Fringes form where two coherent laser beams cross. (From Dantec PDA Manual).

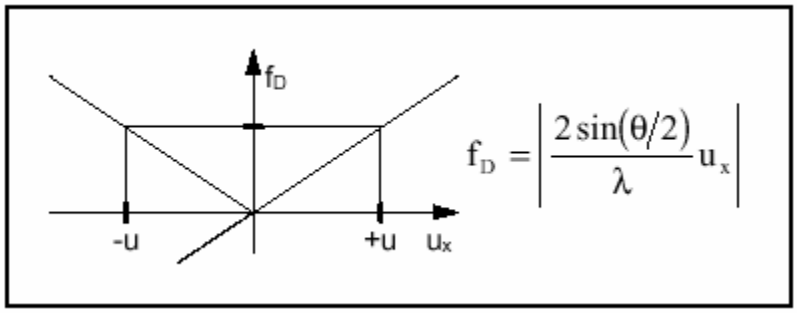

Figure A.2 Directional ambiguity without frequency shift. (From Dantec PDA Manual).

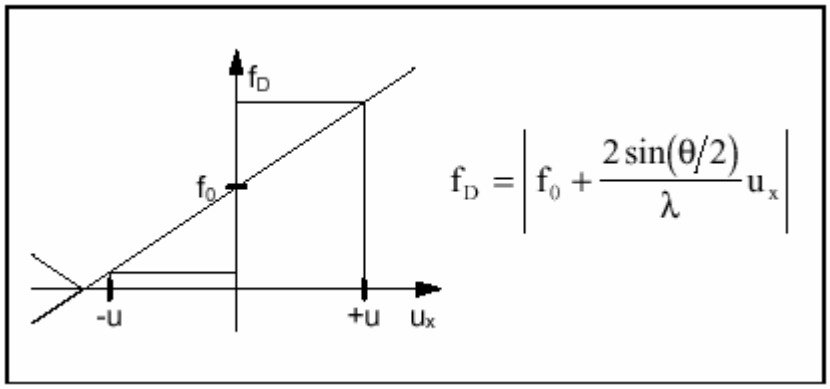

Figure A.3 Resolving directional ambiguity using frequency shift. (From Dantec PDA Manual).

The particle size is measured by the phase difference from different detectors as shown in Figure A.4, and can be calculated from equation A-2. According to Mie theory [15], the particle size and the phase difference have the following relationship.

$$\phi_i = \pi \frac{n_1}{\lambda} D\beta_i \qquad \text{A-2}$$

Where:

n_1 = refractive index of the scattering medium.

λ = laser wavelength in vacuum.

D = particle diameter.

β_i = geometric factor

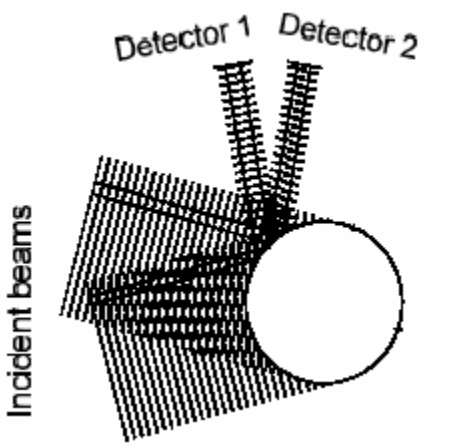

Figure A.4 The interference patterns differ at the two photo-detector surfaces. (From Dantec PDA Manual).

12 Appendix B: Test Photos

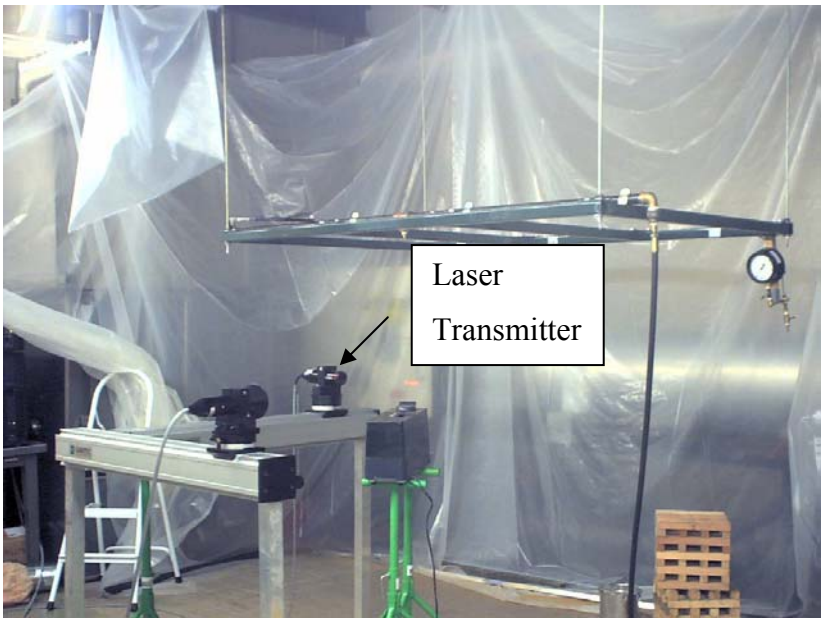

Figure B.1 Laser Transmitter and Signal Receiver for Dantec PDA.

Figure B.2 Laser Producer, Detector Unit, and Processor for Dantec PDA.

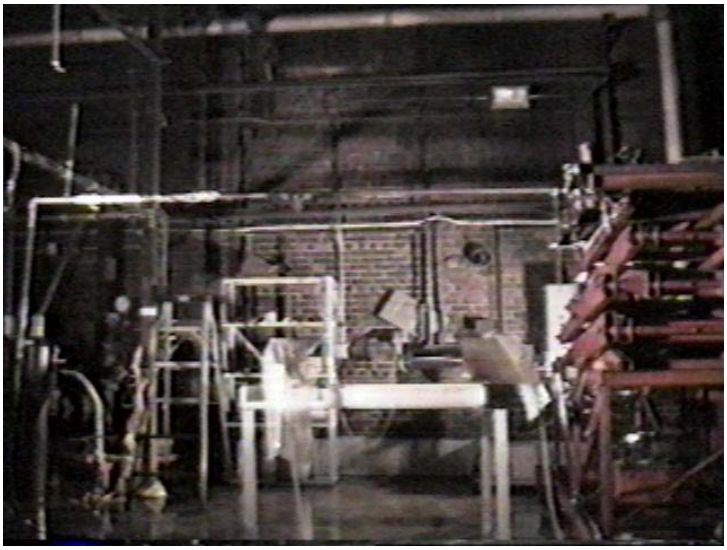

Figure B.3 The layout of PDA for water drop size measurement without water spray.

Figure B.4 The layout of PDA for water drop size measurement with water spray.

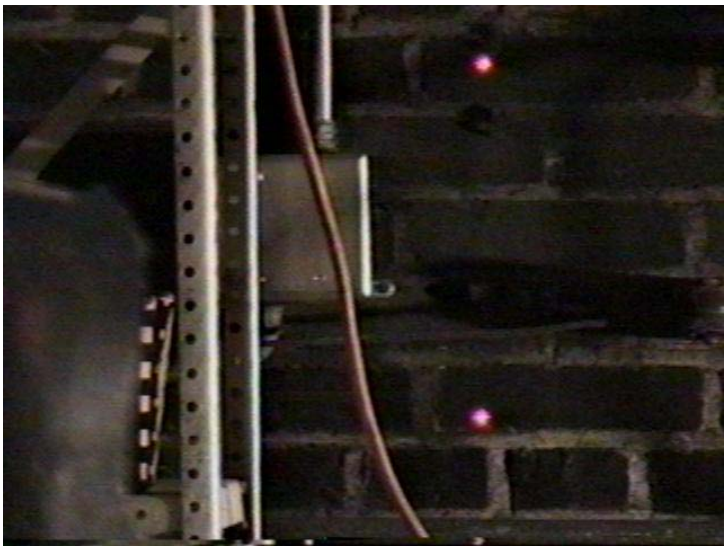

Figure B.5 The close view layout of PDA for water drop size measurement without water spray.

Figure B.6 The close view layout of PDA for water drop size measurement without water spray.

Figure B.7 The oil splattering test equipment with load cell (the same setup as FigureB.5).

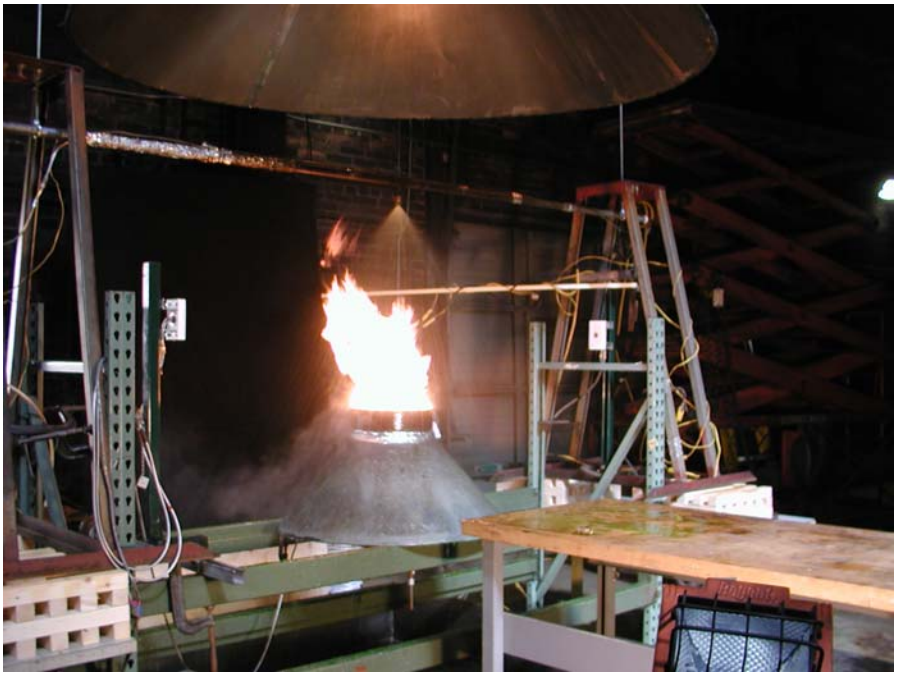

Figure B.8 Splattering oil burning test (10psi water for 3/8GG,18SQ nozzle on 110C heated oil).

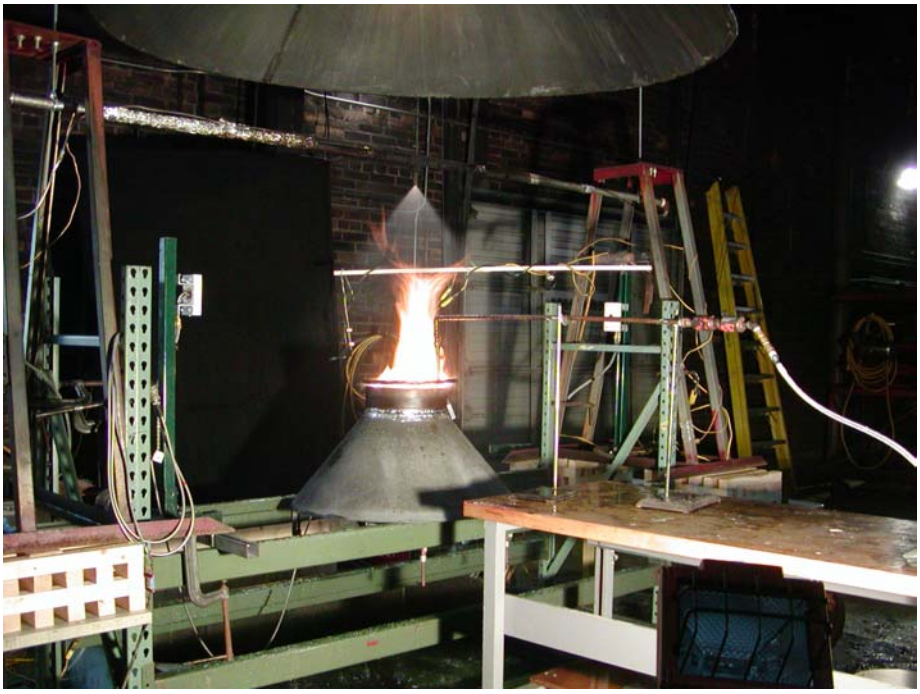

Figure B.9 Delivery Density test for 3/8GG 18SQ nozzle using 10psi water on 1.70 m^3 / hr (60 ft^3 / min) propane fire.

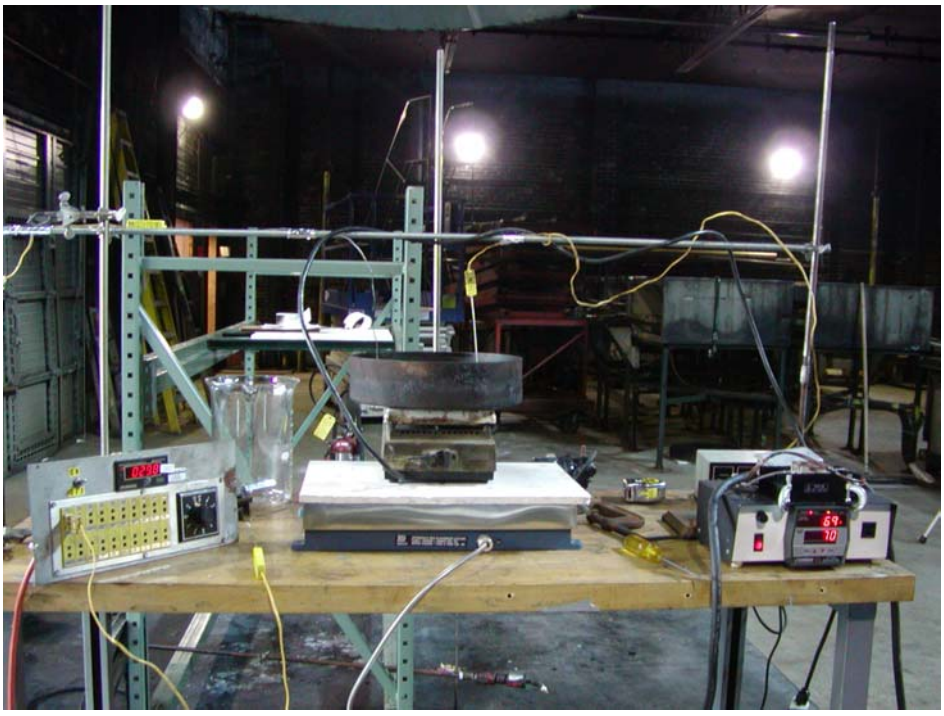

Figure B.10 Vaporization Rate Measurement of Mineral Seal Oil without wind velocity.

13 Appendix C: Heat Release Rate Measurement in Fire Product Collector

The chemical heat release rate and convective heat release rate measurement using a fire products collector.

The chemical heat release rate is obtained from C-1 in the test section duct per ASME E2058" Standard Test Methods for Measurement of Synthetic Polymer Material Flammability Using a Fire Propagation Apparatus".

$$\dot{Q}_{chem} = 13300(\dot{G}_{CO2} - \dot{G}_{CO2}{}^{0}) + 11100(\dot{G}_{CO} - \dot{G}_{CO}{}^{0}) \quad \text{C-1}$$

Where:

$\dot{G}_{CO2}$ and $\dot{G}_{CO}$ = the generation rates (kg/s) of CO_2 and CO, respectively, and

$\dot{G}_{CO2}{}^{0}$ and $\dot{G}_{CO}{}^{0}$ = the corresponding measurements before ignition of the specimen.

The generation rates of CO_2 and CO are derived as equations C-2 and C-3.

$$\dot{G}_{CO2} = A_d K (P_\infty / 101000)^{1/2} (2 \times 353 \Delta P / T_{gas})^{1/2} \times 1.52 X_{CO2} \quad \text{C-2}$$

$$\dot{G}_{CO} = A_d K (P_\infty / 101000)^{1/2} (2 \times 353 \Delta P / T_{gas})^{1/2} \times 0.966 X_{CO} \quad \text{C-3}$$

Where:

A_d = test section duct cross sectional area (m^2)

K = flow coefficient of the averaging Pitot tube

P_∞ = the actual atmospheric pressure (Pa)

ΔP = pressure differential across the averaging Pitot tube in the test section duct (Pa)

T_{gas} = gas temperature in the test section duct, measured by a thermocouple (K)

X_{CO2} = the measured volume ratio or mole fraction of CO_2

X_{CO} = the measured volume ratio or mole fraction of CO

The convective heat release rate is obtained as equation C-4.

$$\dot{Q}_{conv} = \dot{G}\int C_P dT = A_d K (P_\infty / 101000)^{1/2} (2 \times 353 \Delta P / T_{gas})^{1/2} \times \int C_P dT \qquad \text{C-4}$$

Where

$$C_P = 1 + 1.34 \times 10^{-4} T - 2590 / T^2$$

The A_d and K should be obtained from the specific measurements for the fire products collector. They were obtained by Yu for this collector in this research. The correlations of chemical heat release rate and convective heat release rate were modified as equations C-5 and C-6.

$$\dot{Q}_{chem} = [7.434 \times 10^{-2} (X_{co_2} - X_{co_{2,\infty}}) + 6.764 \times 10^{-3} (X_{co} - X_{co,\infty})](\frac{P_\infty \Delta P}{T_{gas}})^{1/2} \qquad \text{C-5}$$

$$\dot{Q}_{conv} = 3.3876(\frac{P_\infty \Delta P}{T_{gas}})^{1/2} (H_{(T_{gas})} - H_{(T_{amb})}) \qquad \text{C-6}$$

14 Appendix D: Water Drop Size , Velocity and Water Spray Density

Nozzle Type	Pressure, kpa (psi)	Drop Size ($D_{v,0.1}, \mu m$)	Drop Size ($D_{v,0.5}, \mu m$)	Drop Size ($D_{v,0.9}, \mu m$)	Water Density mm/min (gpm/ft^2)	Velocity (m/s)
1/8GG,2 (Spraying System)	172 (25)	128	197	214	7.7 (0.19)	2.71
1/8GG,2 (Spraying System	345 (50)	108	164	215	8.6 (0.21)	4.08
1/8GG,2 (Spraying System	517 (75)	100	152	165	9.8 (0.24)	4.47
1/8GG,6SQ (Spraying System	138 (20)	147	243	334	6.1 (0.15)	3.72
1/8GG,6SQ (Spraying System	345 (50)	118	184	250	9 (0.22)	5.16
1/4GG,10SQ (Spraying System	138 (20)	206	335	432	11.8 (0.29)	3.05
1/4GG,10SQ (Spraying System	345 (50)	170	260	338	16.3 (0.4)	4.69
3/8GG,18SQ (Spraying System	69 (10)	242	389	527	11 (0.27)	2.61
3/8GG,18SQ (Spraying System	172 (25)	223	354	475	11.4 (0.28)	3.21
3/8GG,18SQ (Spraying System	276 (40)	173	279	378	16.7 (0.41)	4.19

Nozzle Type	Pressure, kpa (psi)	Drop Size ($D_{v,0.1}, \mu m$)	Drop Size ($D_{v,0.5}, \mu m$)	Drop Size ($D_{v,0.9}, \mu m$)	Water Density mm/min (gpm / ft^2)	Velocity (m/s)
3/8GG,18SQ (Spraying System	345 (50)	156	250	337	18.3 (0.45)	4.59
3/8GG,18SQ (Spraying System	414 (60)	137	213	282	20.4 (0.5)	4.74
3/8GG,15 (Spraying System	69 (10)	265	415	550	14.3 (0.35)	2.57
3/8GG,15 (Spraying System	138 (20)	224	360	486	15.9 (0.39)	2.7
3/8GG,15 (Spraying System	206 (30)	154	241	322	17.1 (0.42)	3.5
3/8GG,15 (Spraying System	276 (40)	157	237	318	17.5 (0.43)	3.63
3/8GG,15 (Spraying System	345 (50)	127	202	270	18.3 (0.45)	4.66
3/8GG,15 (Spraying System	414 (60)	117	186	249	20 (0.49)	5.28
3/8GG,22 (Spraying System	69 (10)	259	425	582	4.9 (0.12)	2.3
3/8GG,22 (Spraying System	138 (20)	229	375	514	6.5 (0.16)	2.7

Nozzle Type	Pressure, kpa (psi)	Drop Size ($D_{v,0.1}, \mu m$)	Drop Size ($D_{v,0.5}, \mu m$)	Drop Size ($D_{v,0.9}, \mu m$)	Water Density mm/min (gpm / ft^2)	Velocity (m/s)
3/8GG,22 (Spraying System	206 (30)	225	330	435	7.3 (0.18)	2.8
3/8GG,22 (Spraying System	276 (40)	179	268	339	8.6 (0.21)	2.9
3/8GG,22 (Spraying System	345 (50)	151	237	309	10.2 (0.25)	3.32
3/8GG,22 (Spraying System	414 (60)	149	227	296	13.9 (0.34)	3.46
1/2GG,25 (Spraying System	5 (34.5)	612	955	1268	23.2 (0.57)	2.7
1/2GG,25 (Spraying System	10 (69)	398	672	903	18.3 (0.45)	3.05
1/2GG,25 (Spraying System	103 (15)	295	459	590	18.3 (0.45)	3.08
1/2GG,25 (Spraying System	138 (20)	227	333	426	22.4 (0.55)	3.19
1/2GG,25 (Spraying System	172 (25)	211	317	412	20.4 (0.5)	3.49
1/2GG,25 (Spraying System	206 (30)	177	264	345	16.7 (0.41)	3.69

Nozzle Type	Pressure, kpa (psi)	Drop Size ($D_{v,0.1}, \mu m$)	Drop Size ($D_{v,0.5}, \mu m$)	Drop Size ($D_{v,0.9}, \mu m$)	Water Density mm/min (gpm / ft^2)	Velocity (m/s)
1/2GG,29SQ (Spraying System	34.5 (5)	490	830	1161	23.2 (0.57)	2.35
1/2GG,29SQ (Spraying System	69 (10)	389	617	833	16.7 (0.41)	2.44
1/2GG,29SQ (Spraying System	103 (15)	275	441	595	17.5 (0.43)	2.66
1/2GG,29SQ (Spraying System	138 (20)	230	373	510	22.4 (0.55)	2.74
1/2GG,29SQ (Spraying System	172 (25)	207	341	467	20.4 (0.5)	3.59
1/2GG,29SQ (Spraying System	206 (30)	183	296	402	16.7 (0.41)	4.43
1/2GG,32 (Spraying System	34.5 (5)	427	718	999	20.4 (0.5)	2.55
1/2GG,32 (Spraying System	69 (10)	411	657	965	21.2 (0.52)	2.66
1/2GG,32 (Spraying System	103 (15)	323	543	754	22.8 (0.56)	3.34
1/2GG,32 (Spraying System	138 (20)	253	425	592	24 (0.59)	3.6

Nozzle Type	Pressure, kpa (psi)	Drop Size ($D_{v,0.1}, \mu m$)	Drop Size ($D_{v,0.5}, \mu m$)	Drop Size ($D_{v,0.9}, \mu m$)	Water Density mm/min (gpm / ft^2)	Velocity (m/s)
1/2GG,32 (Spraying System	172 (25)	217	350	475	26.1 (0.64)	4.21
1/2GG,32 (Spraying System	206 (30)	195	305	406	27.7 (0.68)	4.47
AM24 (Grinnell)	172 (25)	603	1056	1495	17.5 (0.43)	2.45
AM24 (Grinnell)	345 (50)	439	769	1088	15.1 (0.37)	3.39
AM24 (Grinnell)	517 (75)	285	450	612	17.1 (0.42)	4.18
AM24 (Grinnell)	690 (101)	224	368	489	17.5 (0.43)	4.68
BETE1/4WL 1 1/2	172 (25)	130	189	251	2.85 (0.07)	3.2
BETE1/4WL 1 1/2	517 (75)	119	174	219	7.3 (0.18)	4.63
BETE1/4WL 1 1/2	862 (125)	111	168	210	9 (0.22)	6.26
Sprayco 110620	345 (50)	79	116	150	3.3 (0.08)	2.61
Sprayco 110620	517 (75)	76	115	147	4.5 (0.11)	3.37
1/8HH 1.5 (Spraying System)	345 (50)	111	161	205	2.85 (0.07)	3
1/8HH 1.5 (Spraying System)	517 (75)	95	143	182	2.85 (0.07)	3.12

15 Appendix E: Temperature profile for fire suppression tests

The following graphs show the temperatures measured in tests listed in Tables 8.1 and 8.2, with the measurements at the following locations.

TCS = surface temperature

TCB1/2 = temperature 1/2-inch below surface

TCB1 = temperature 1-inch below surface

TCA1/4 = temperature 1/4 above surface

TCA1/2 = temperature 1/2-inch above surface

TCA3/4 = temperature 3/4-inch above surface

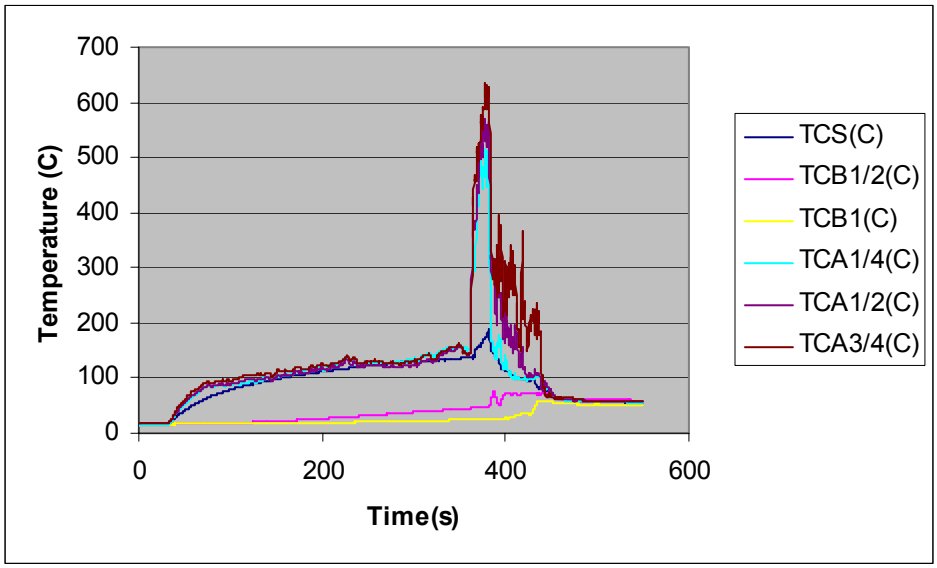

Figure E.1 Temperature profile in test 19

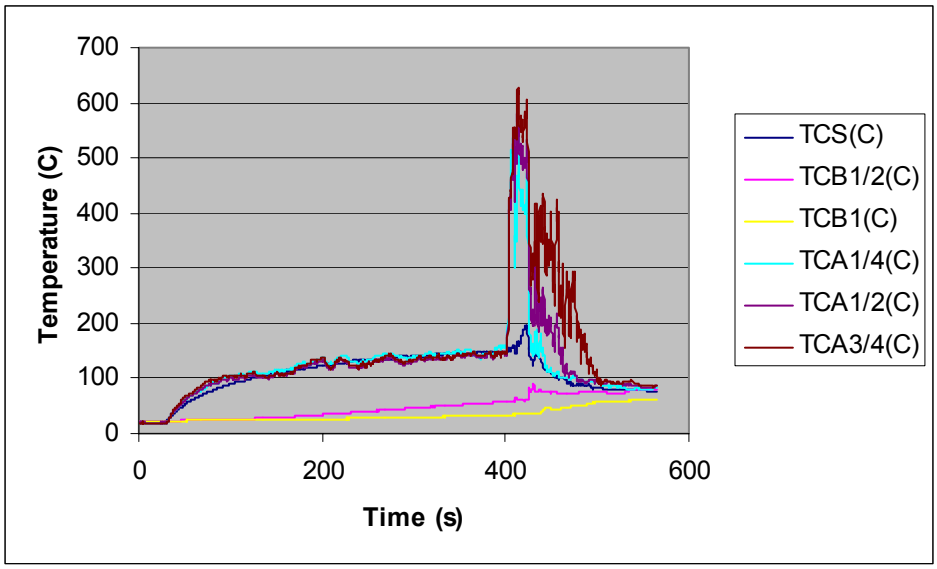

Figure E.2 Temperature profile in test 21

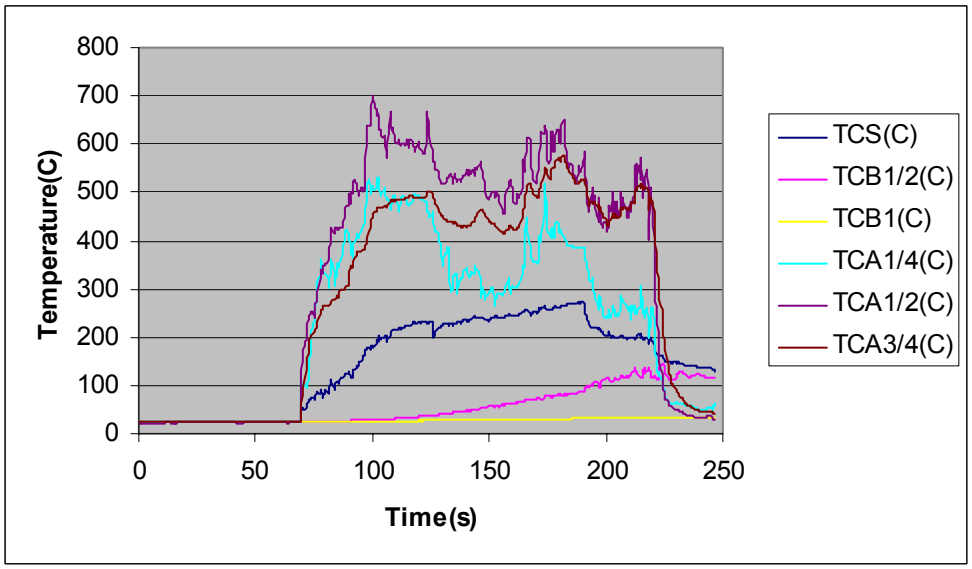

Figure E.3 Temperature profile in Fpc 20

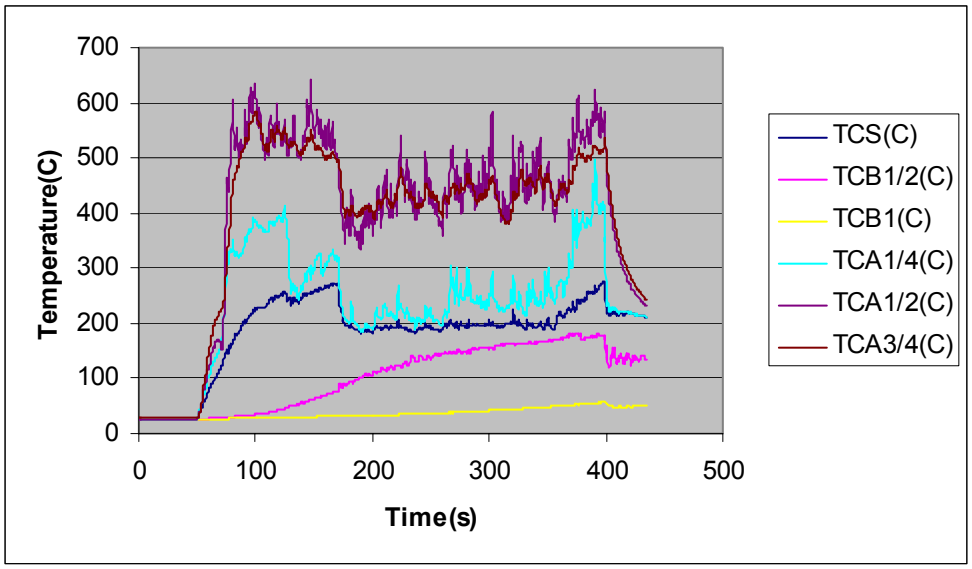

Figure E.4 Temperature profile in test 21

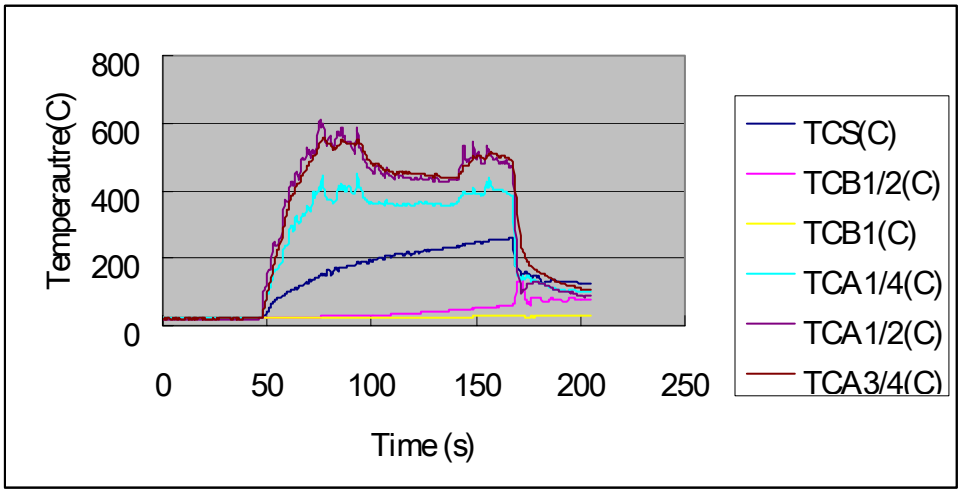

Figure E.5 Temperature profile in Fpc22

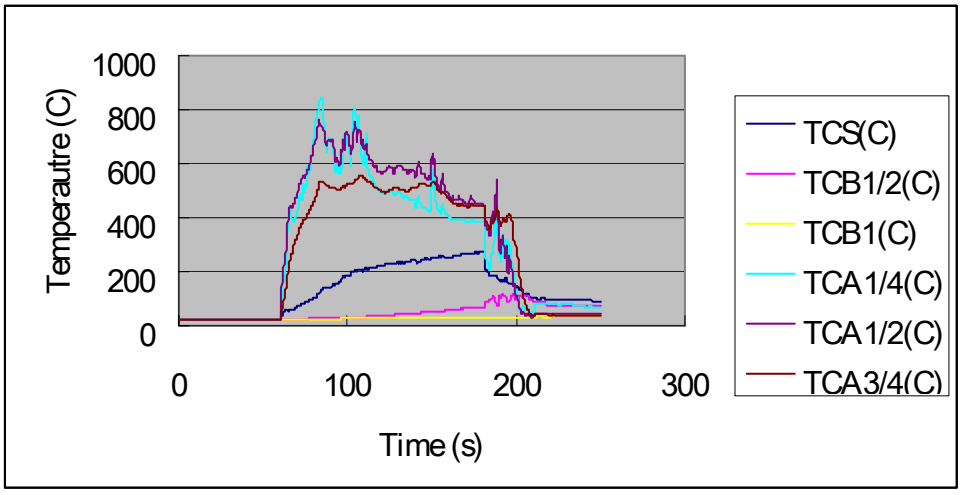

Figure E.6 Temperature profile in Fpc23

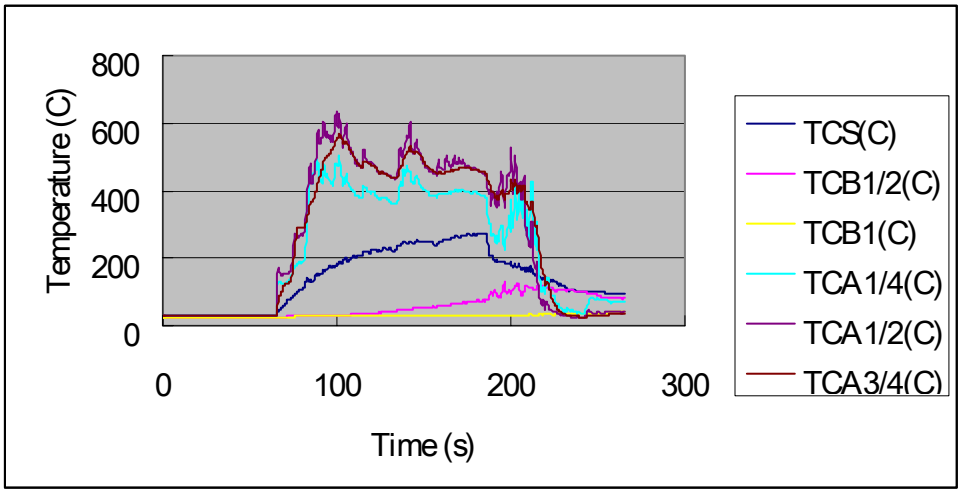

Figure E.7 Temperature profile in Fpc24

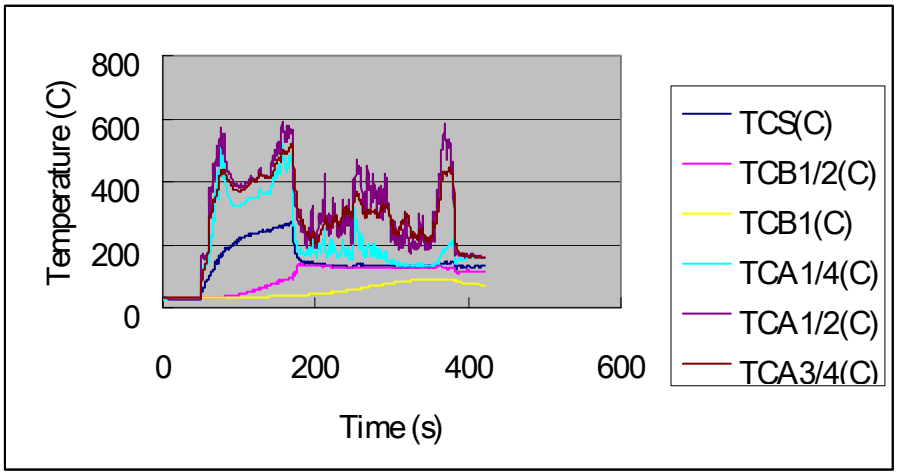

Figure E.8 Temperature profile in Fpc26

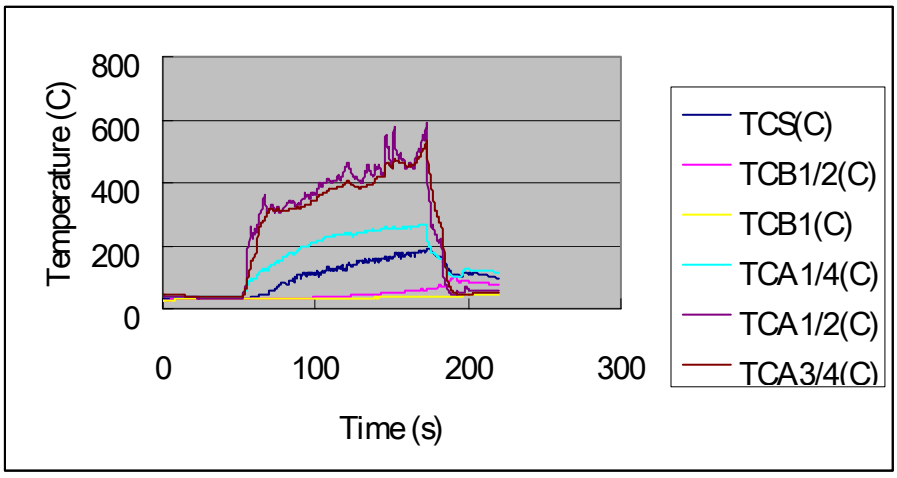

Figure E.9 Temperature profile in Fpc27

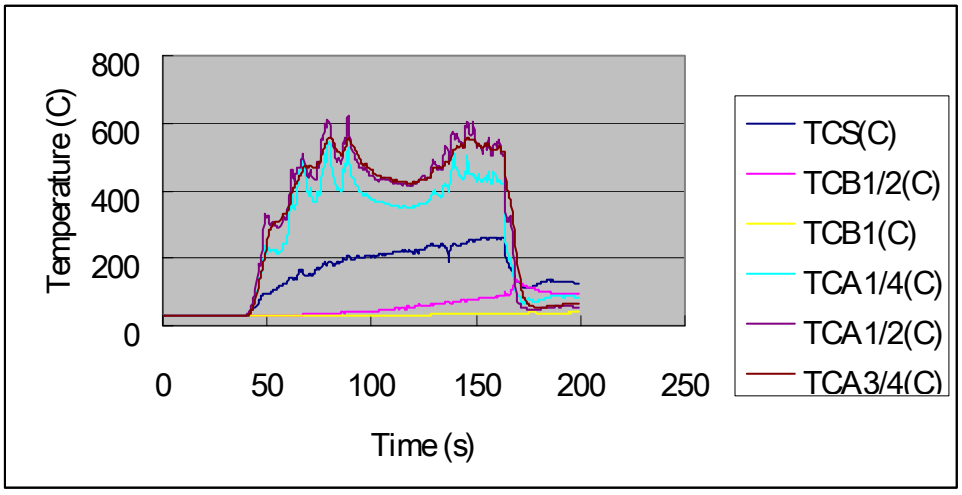

Figure E.10 Temperature profile in Fpc28

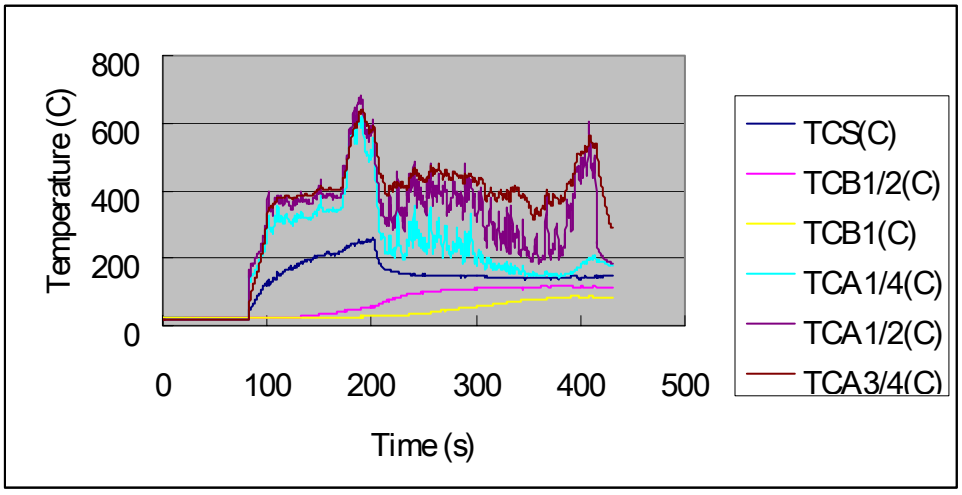

Figure E.11 Temperature profile in Fpc30

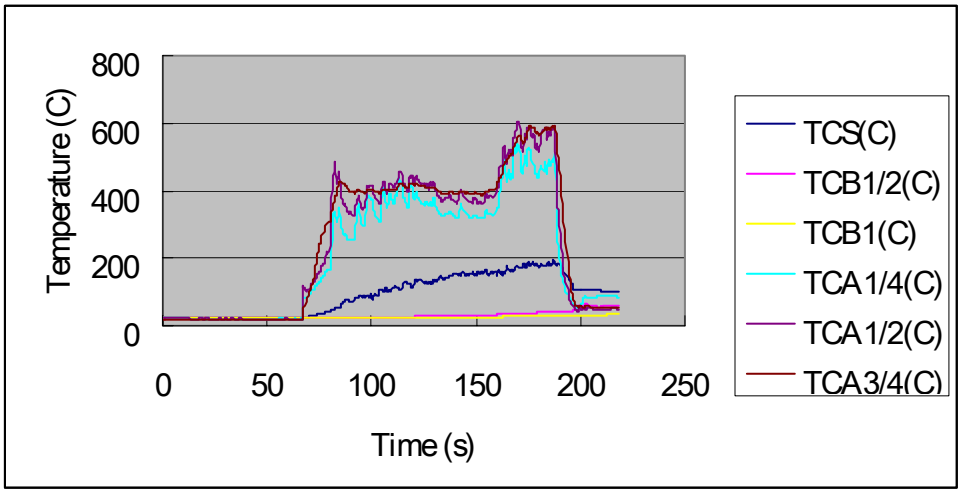

Figure E.12 Temperature profile in Fpc33

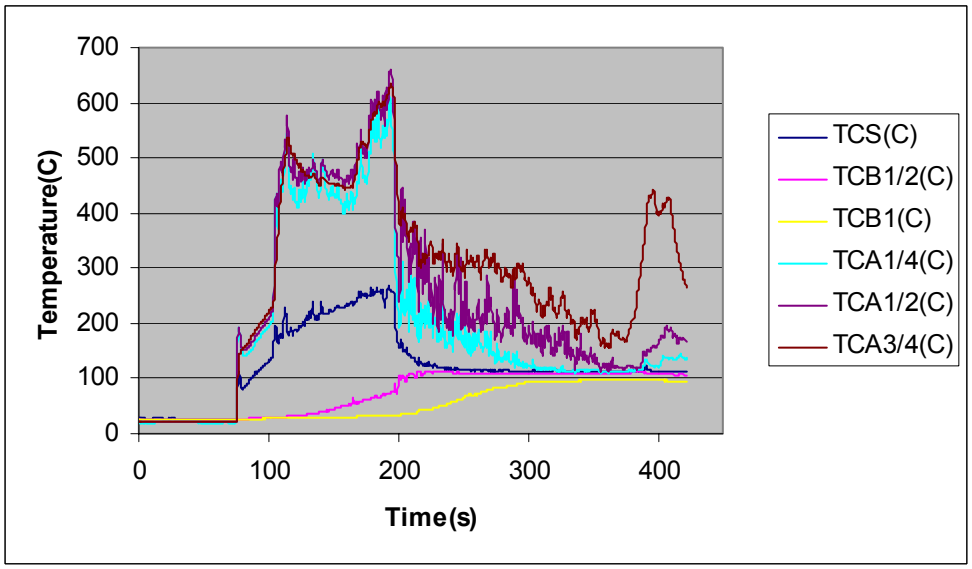

Figure E.13 Temperature profile in Fpc36

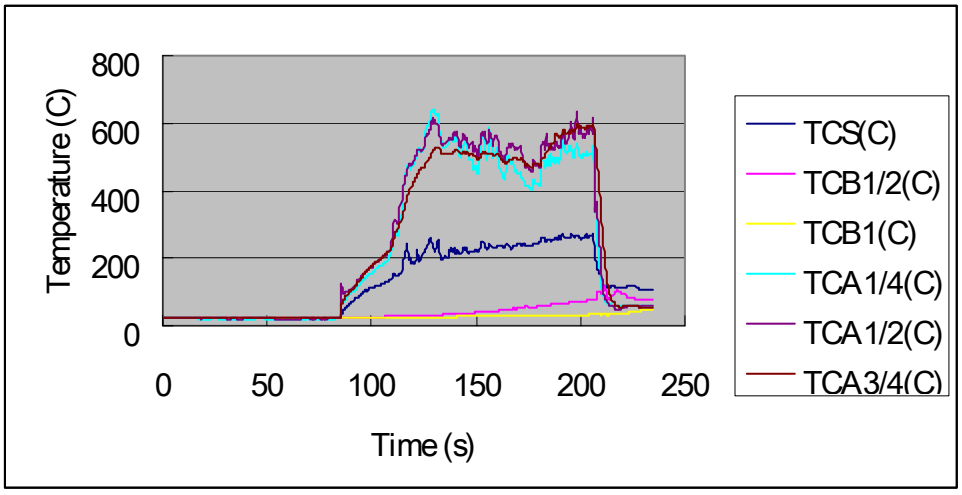

Figure E.14 Temperature profile in Fpc39

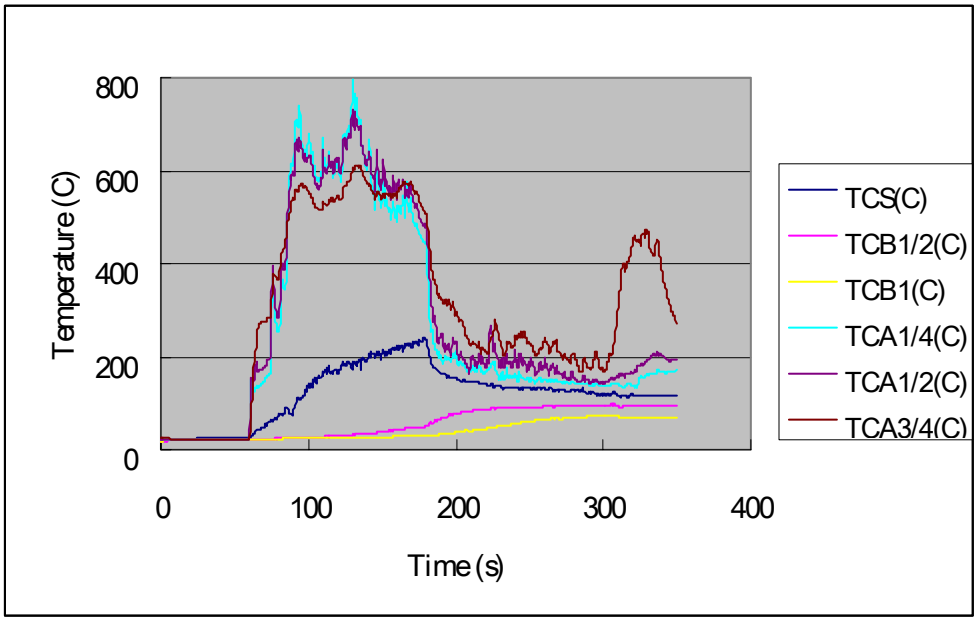

Figure E.15 Temperature profile in Fpc42

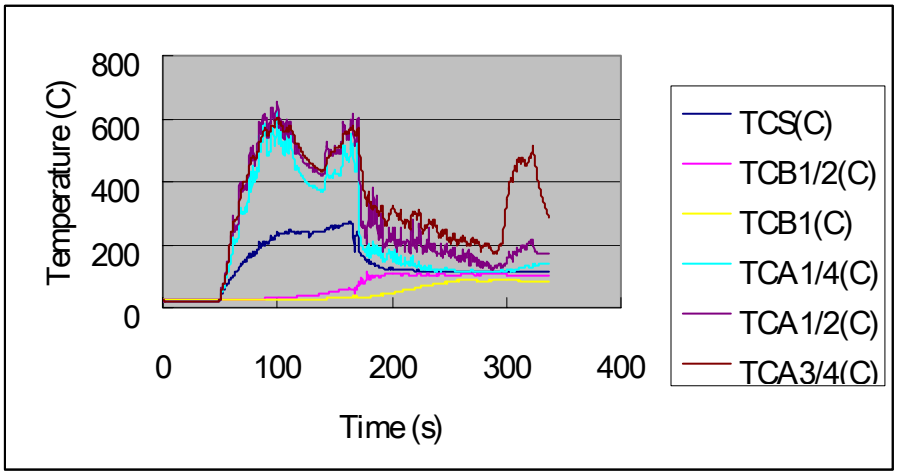

Figure E.16 Temperature profile in Fpc44

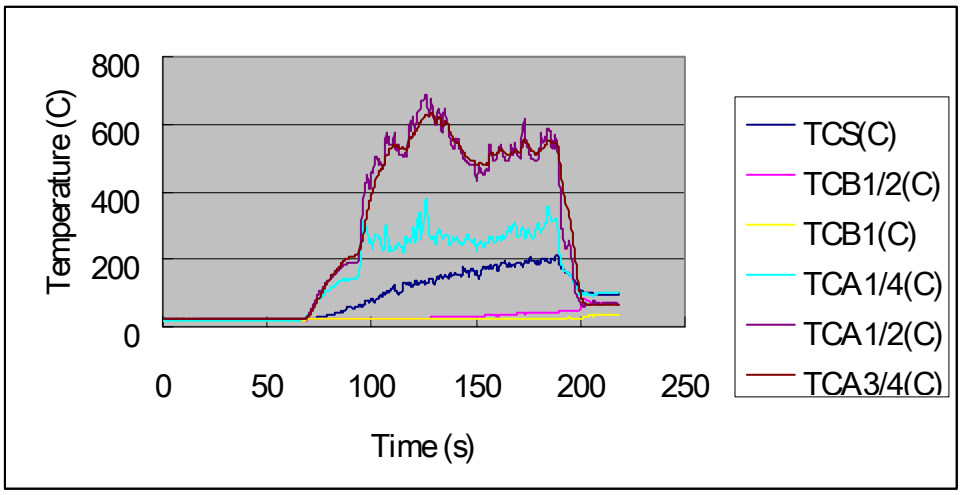

Figure E.17 Temperature profile in Fpc83

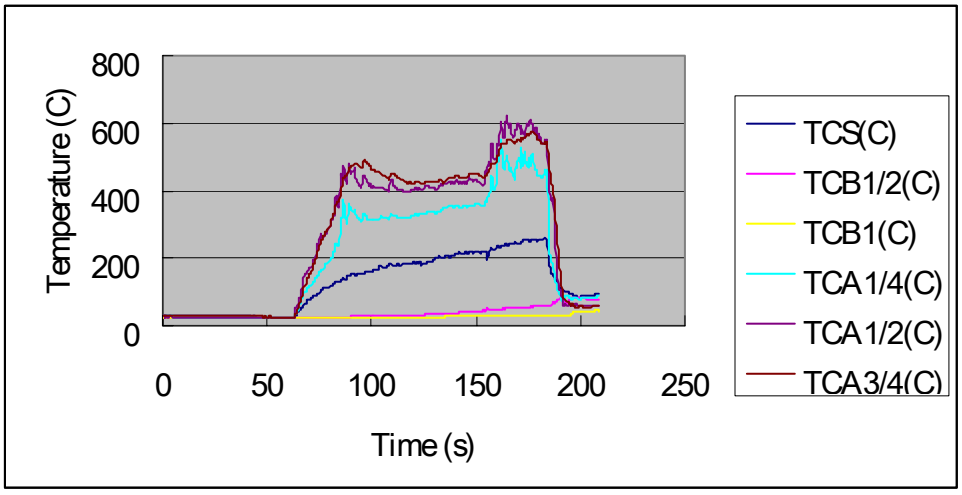

Figure E.18 Temperature profile in Fpc84

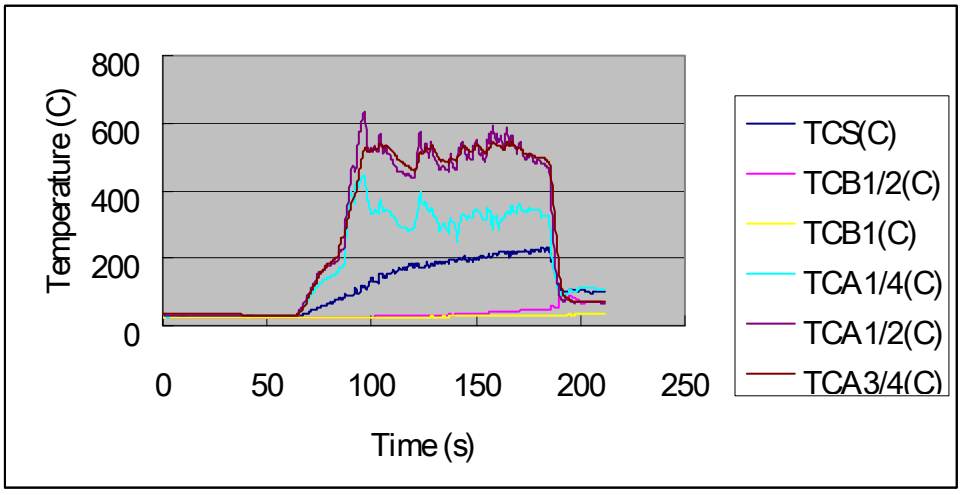

Figure E.19 Temperature profile in Fpc85

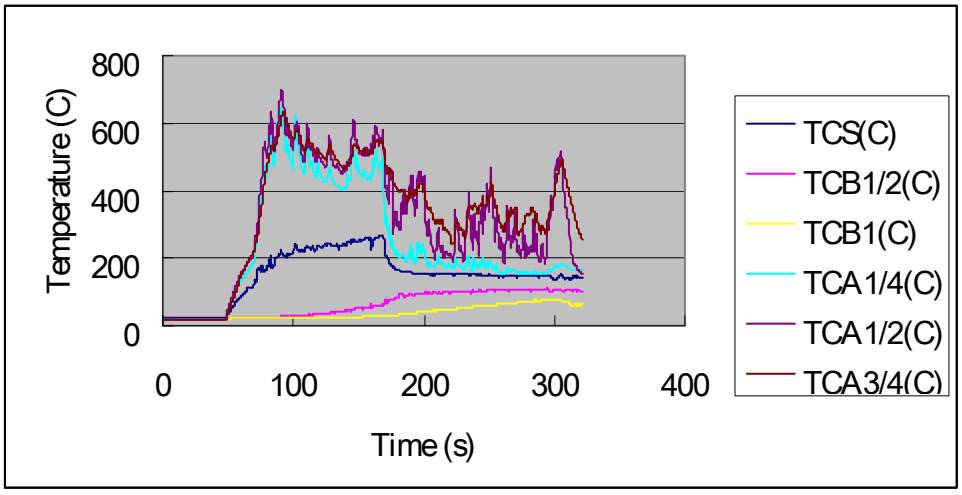

Figure E.20 Temperature profile in Fpc48

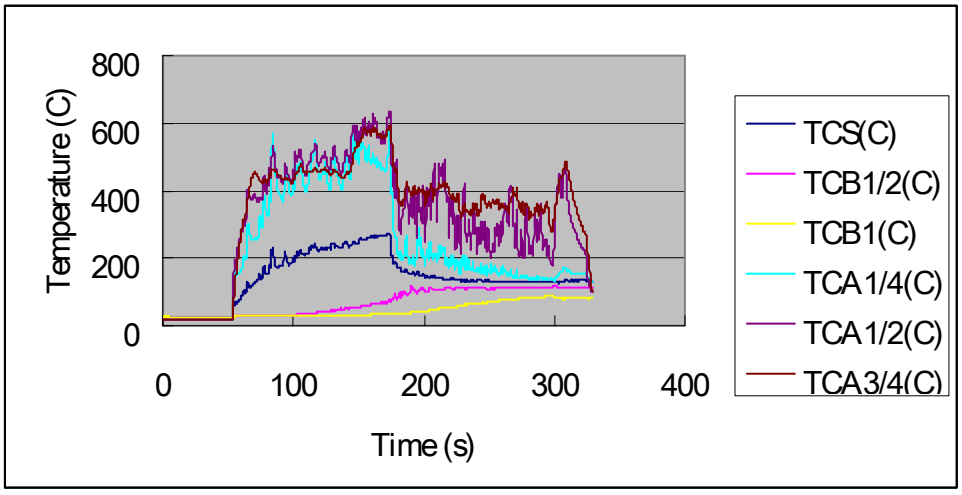

Figure E.21 Temperature profile in Fpc50

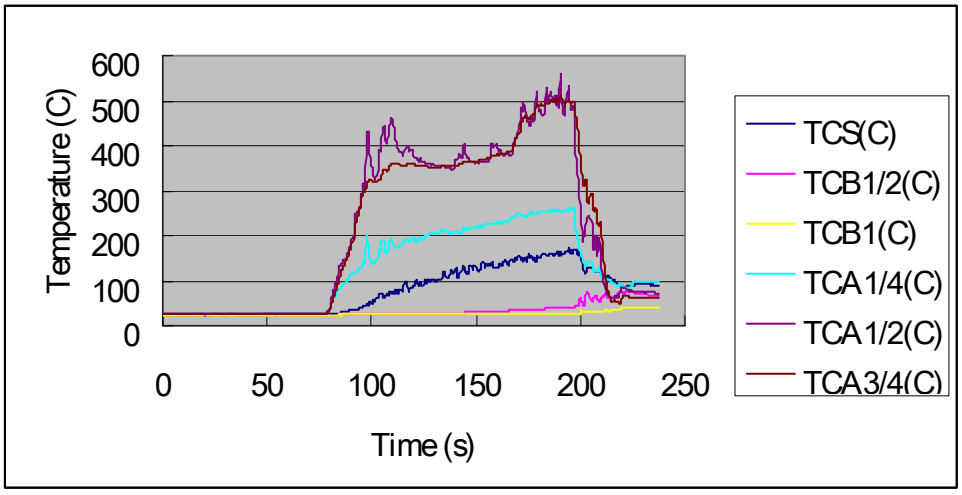

Figure E.22 Temperature profile in Fpc86

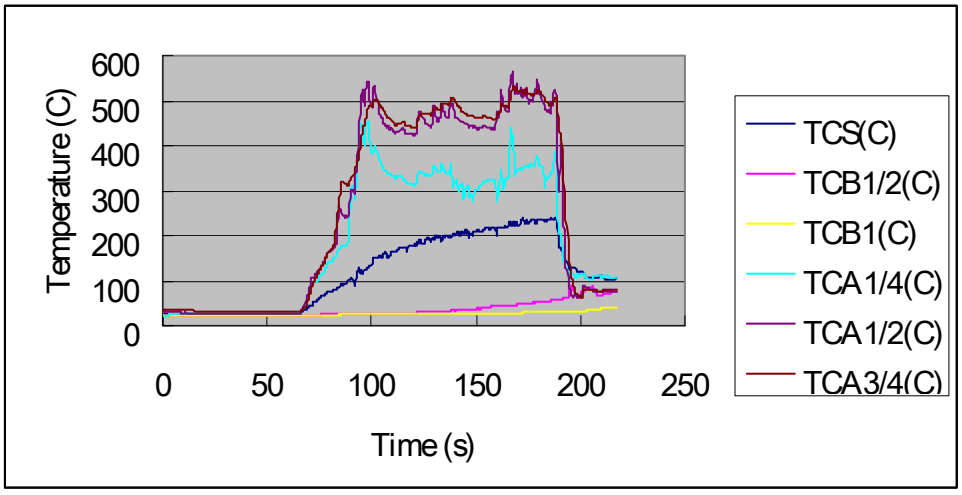

Figure E.23 Temperature profile in Fpc87

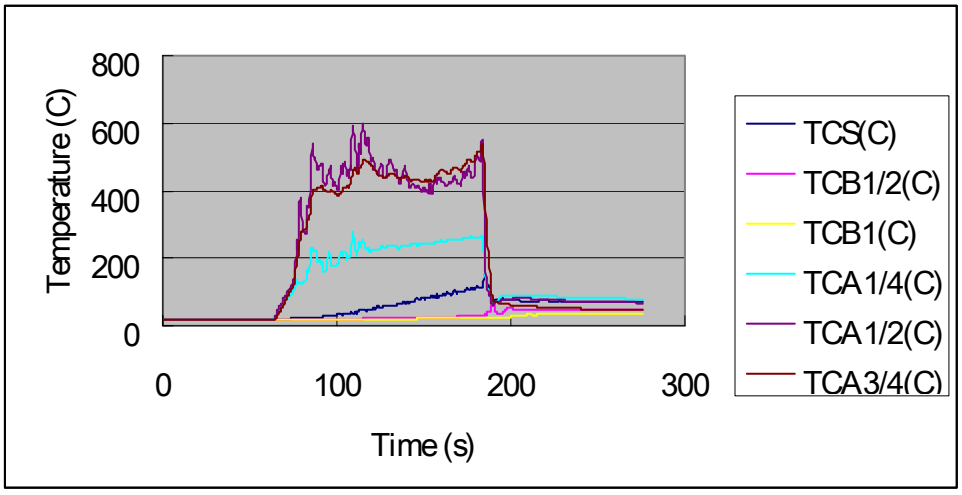

Figure E.24 Temperature profile in Fpc53

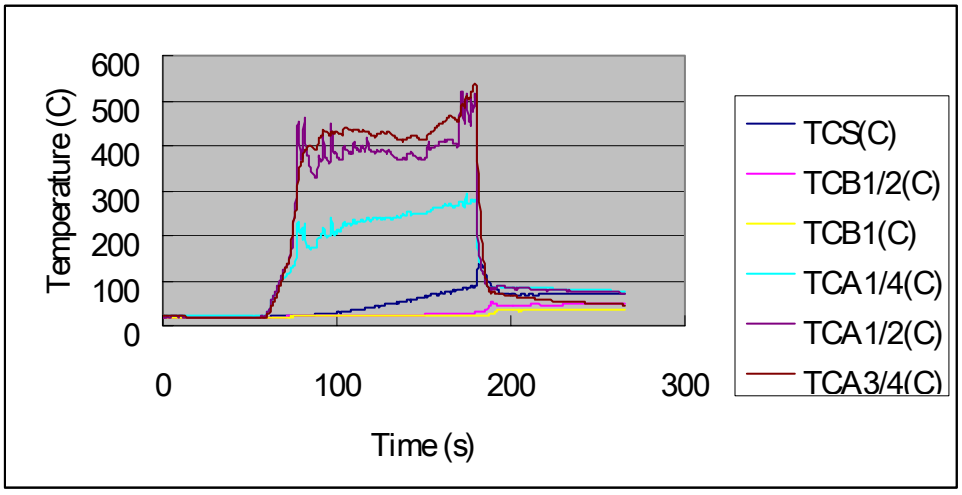

Figure E.25 Temperature profile in Fpc54

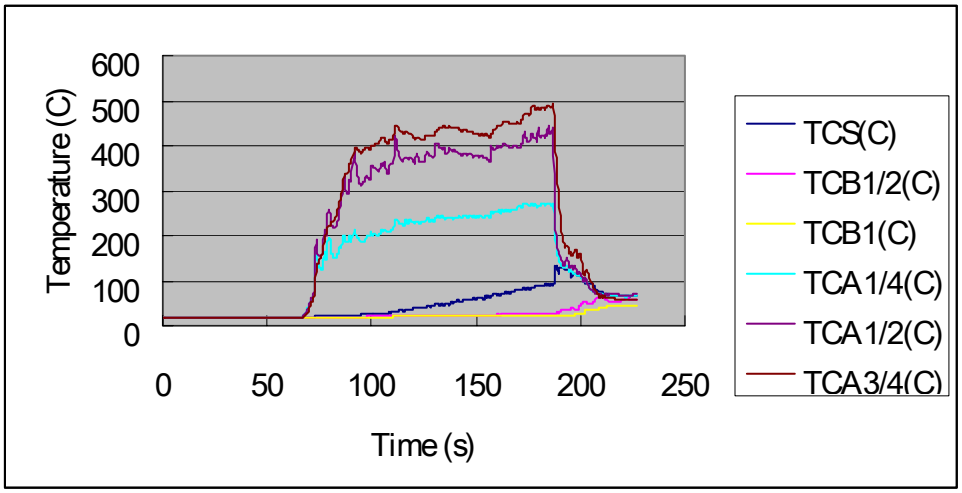

Figure E.26 Temperature profile in Fpc55

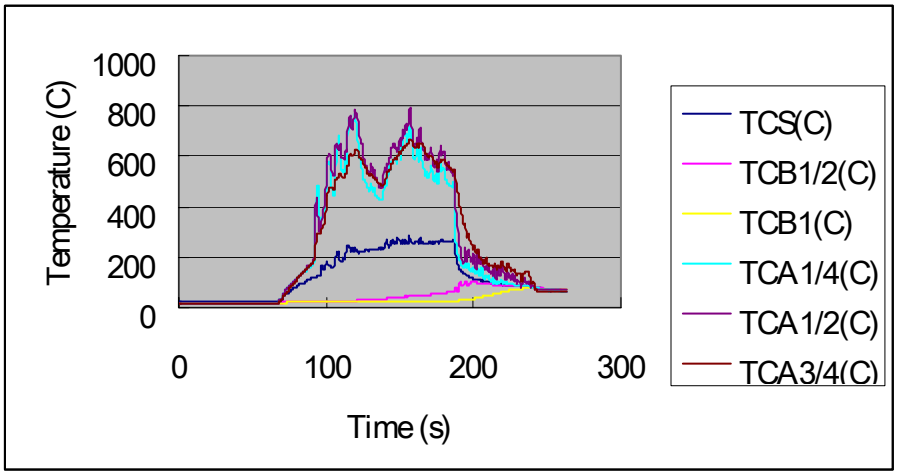

Figure E.27 Temperature profile in Fpc56

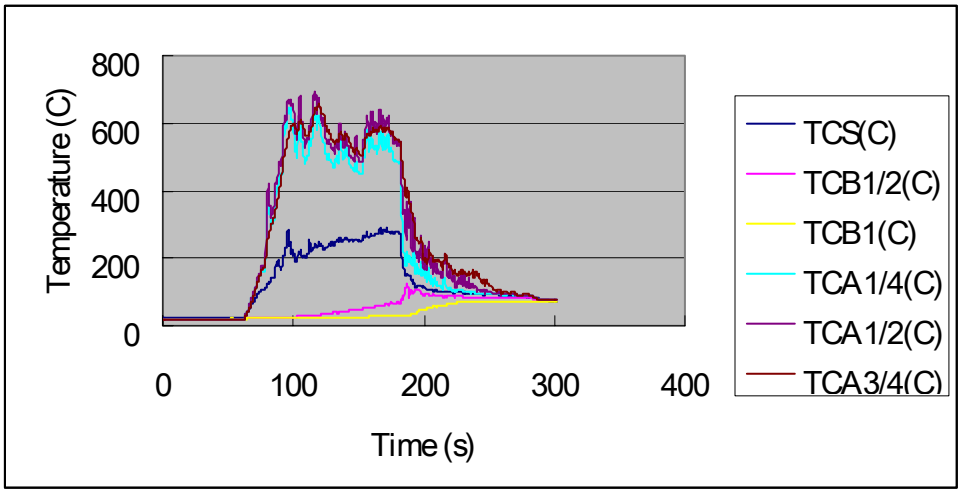

Figure E.28 Temperature profile in Fpc58

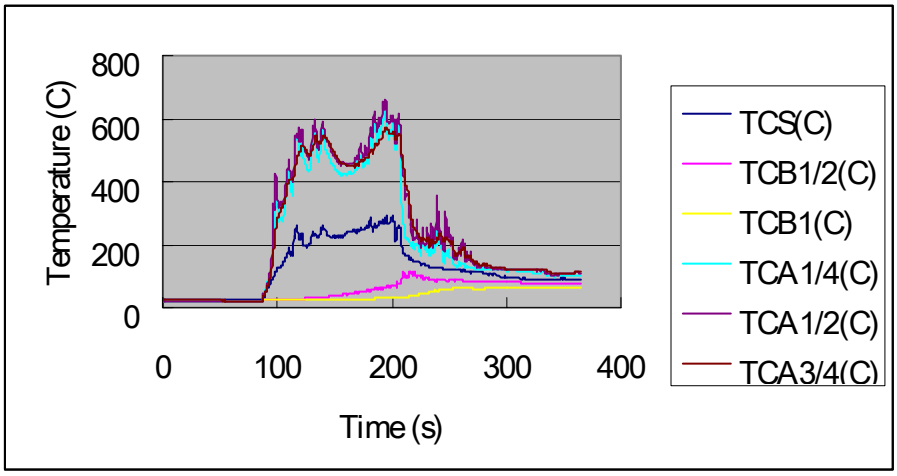

Figure E.29 Temperature profile in Fpc59

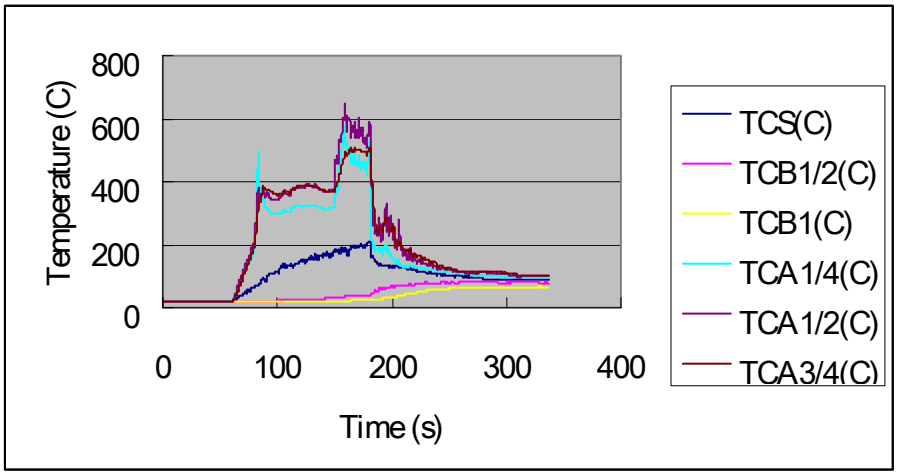

Figure E.30 Temperature profile in Fpc60

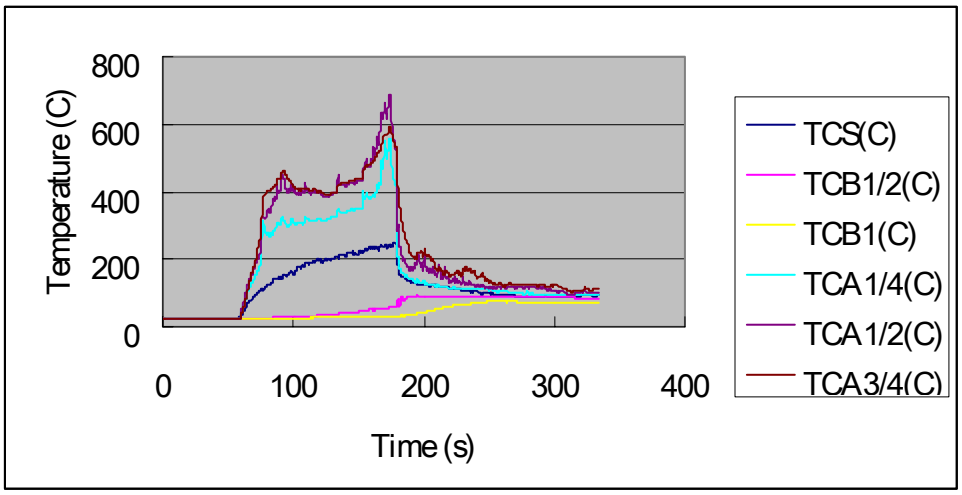

Figure E.31 Temperature profile in Fpc61

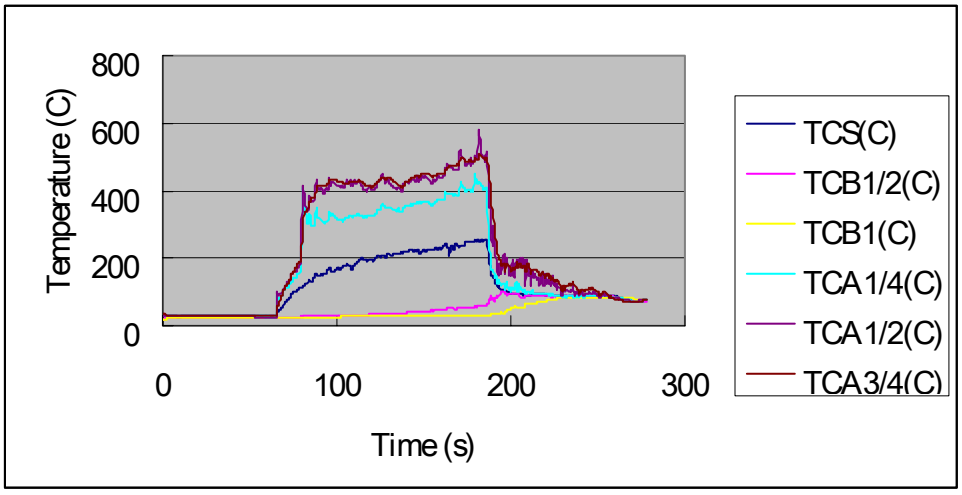

Figure E.32 Temperature profile in Fpc62

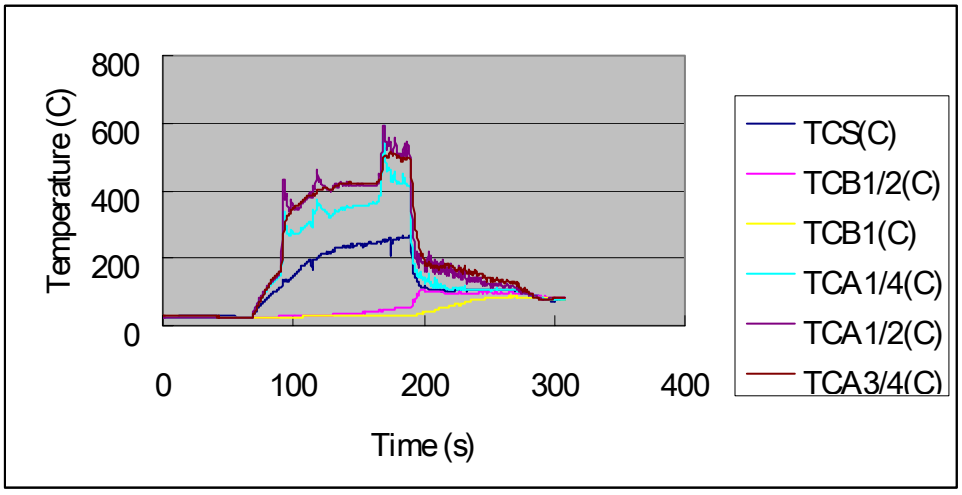

Figure E.33 Temperature profile in Fpc63

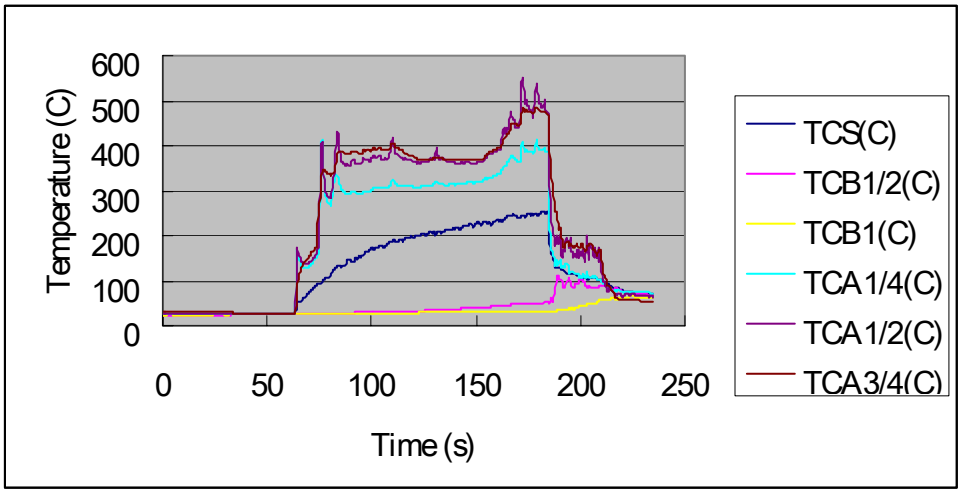

Figure E.34 Temperature profile in Fpc64

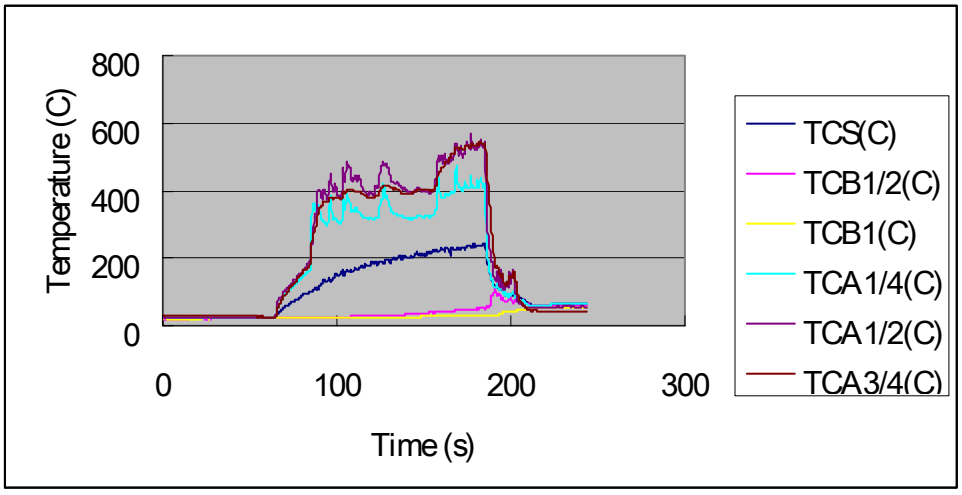

Figure E.35 Temperature profile in Fpc65

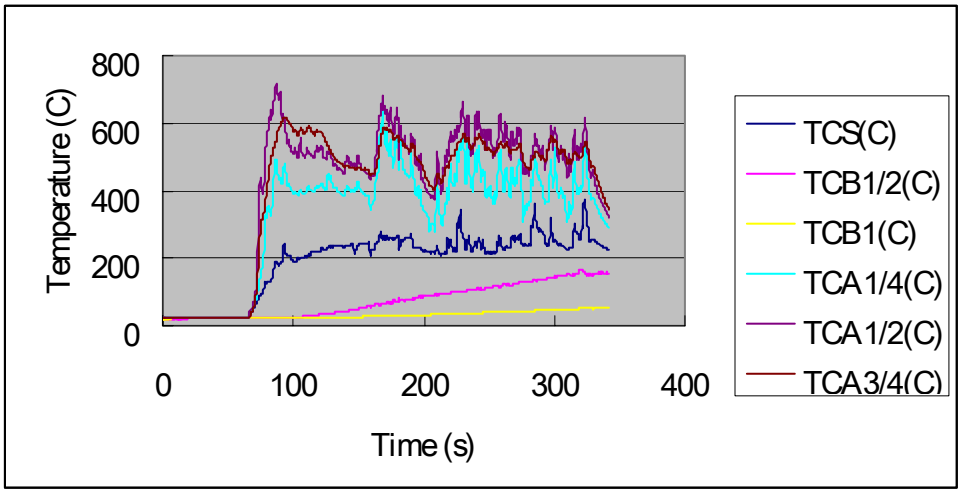

Figure E.36 Temperature profile in Fpc66

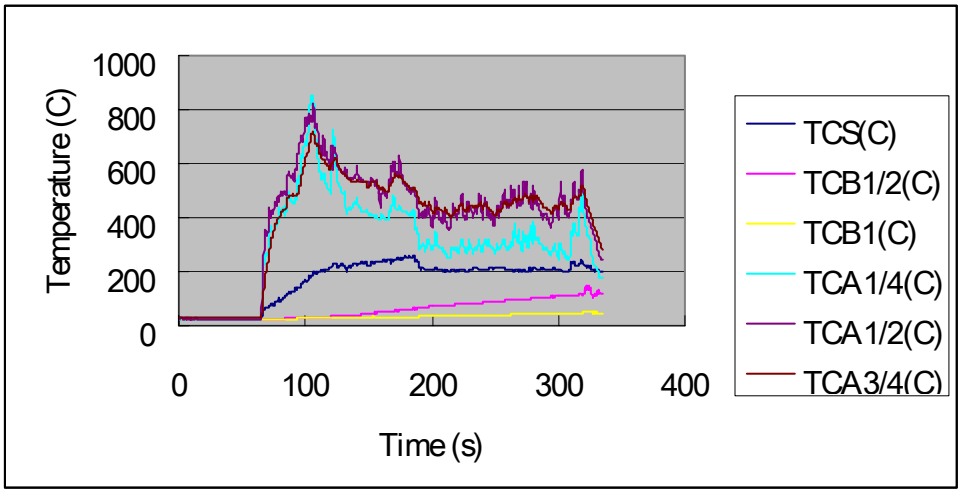

Figure E.37 Temperature profile in Fpc67

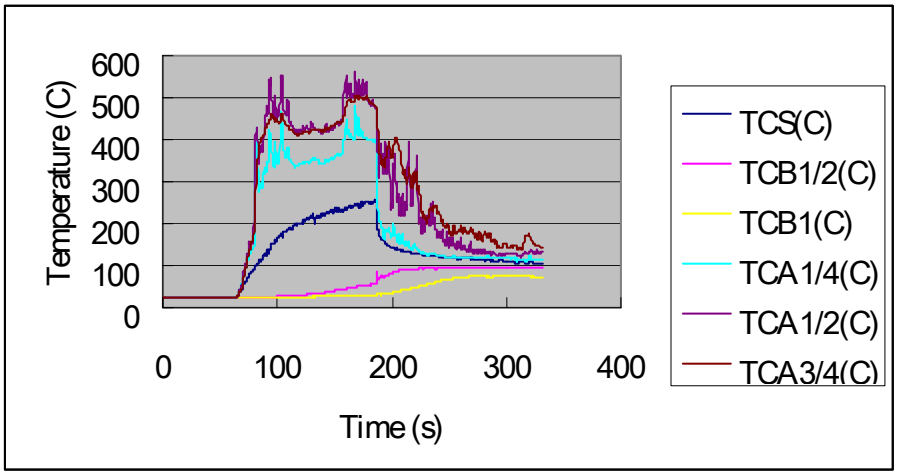

Figure E.38 Temperature profile in Fpc71

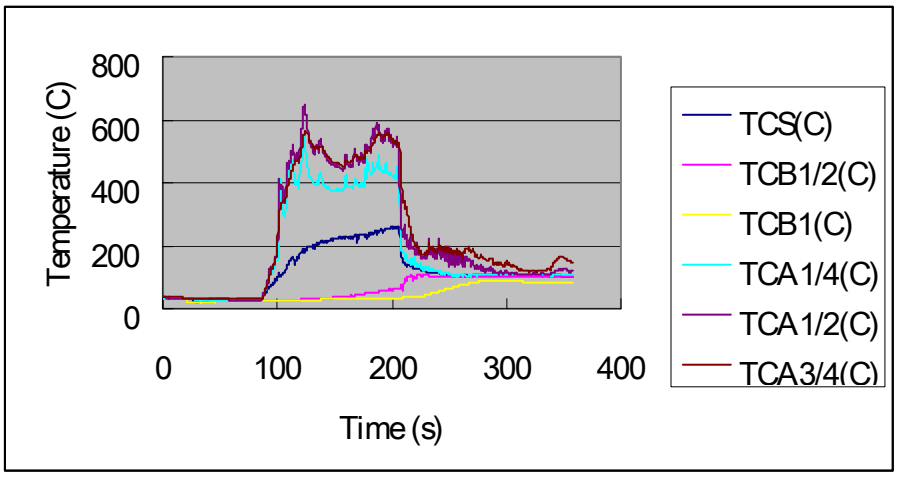

Figure E.39 Temperature profile in Fpc72

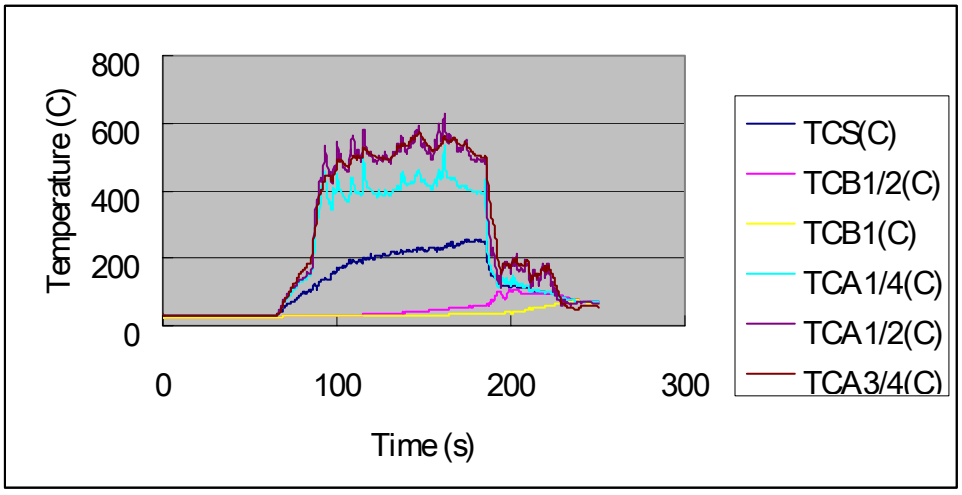

Figure E.40 Temperature profile in Fpc73

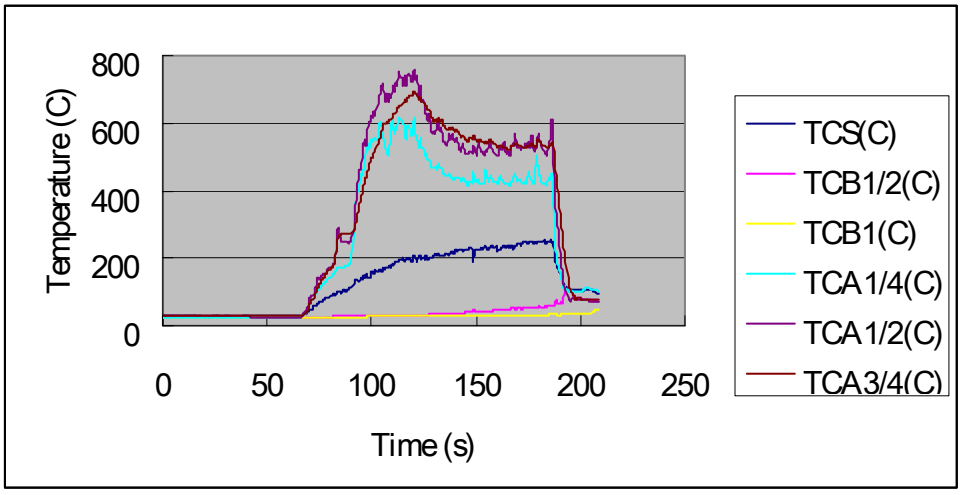

Figure E.41 Temperature profile in Fpc74

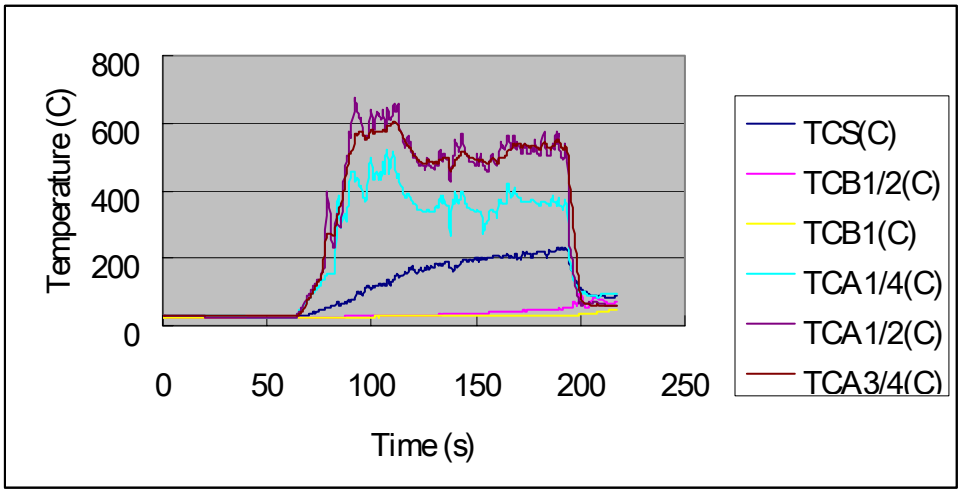

Figure E.42 Temperature profile in Fpc75

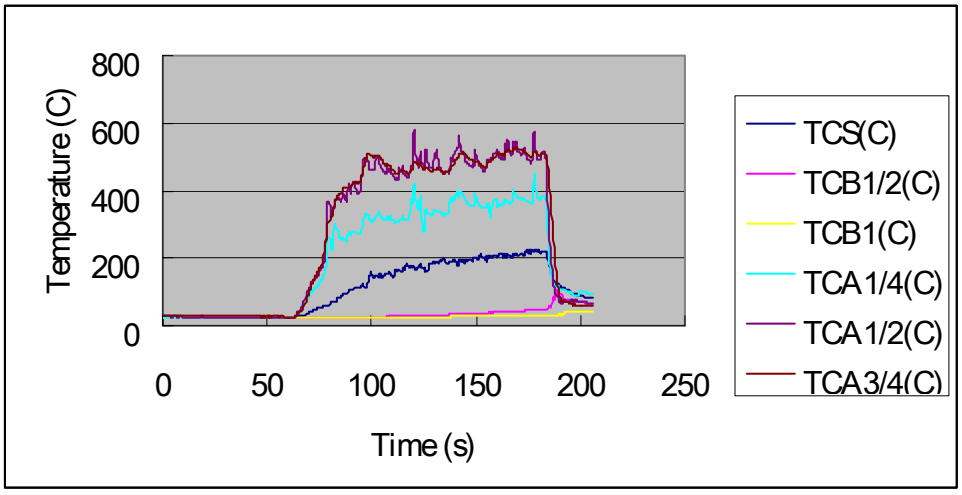

Figure E.43 Temperature profile in Fpc76

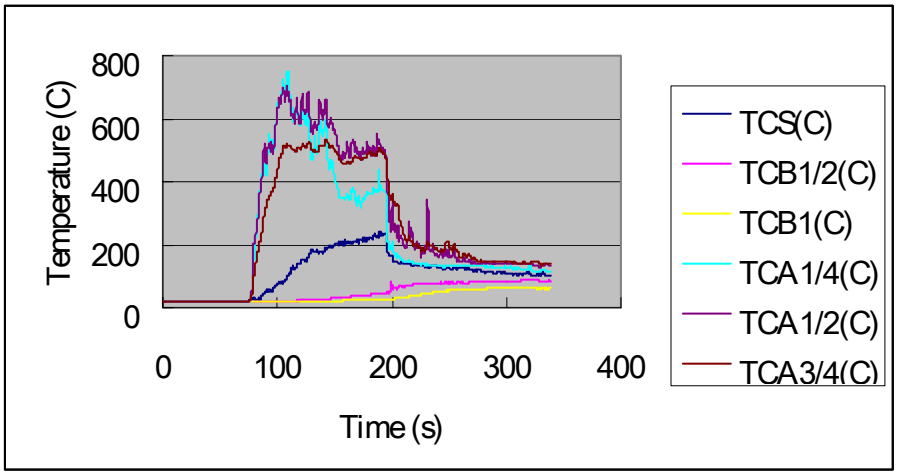

Figure E.44 Temperature profile in Fpc77

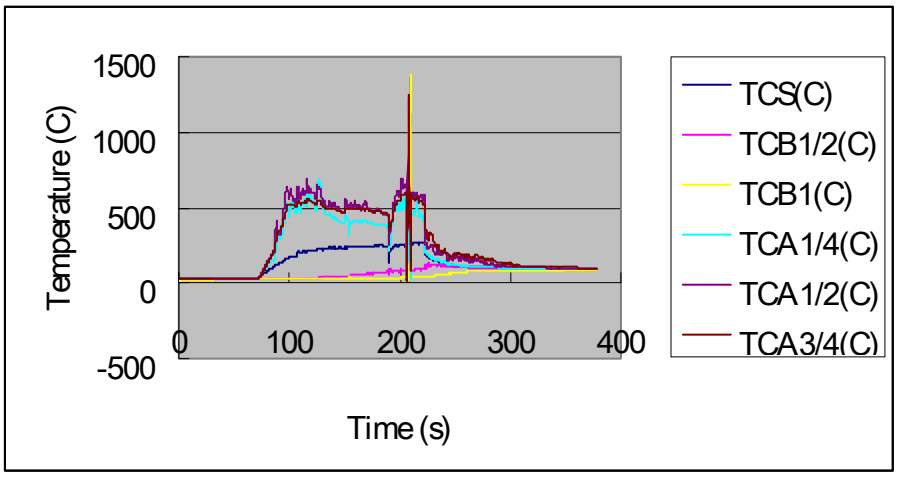

Figure E.45 Temperature profile in Fpc78

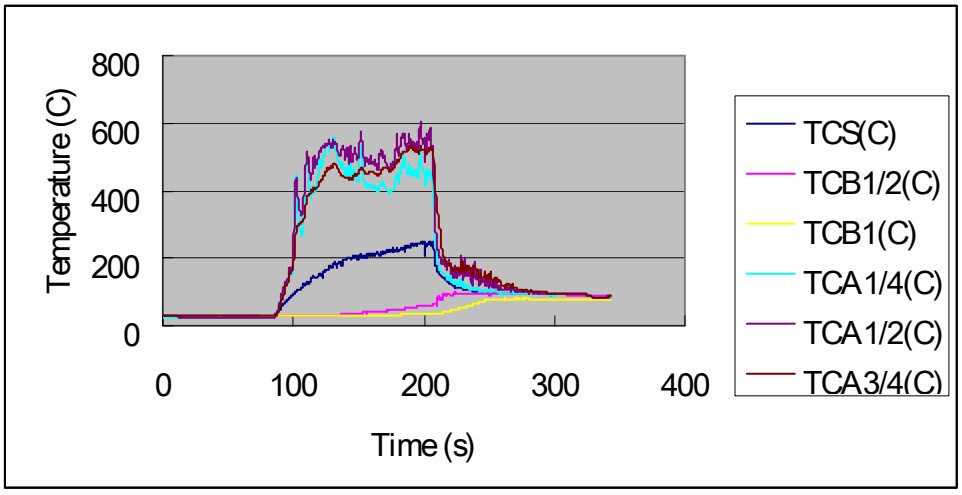

Figure E.46 Temperature profile in Fpc79

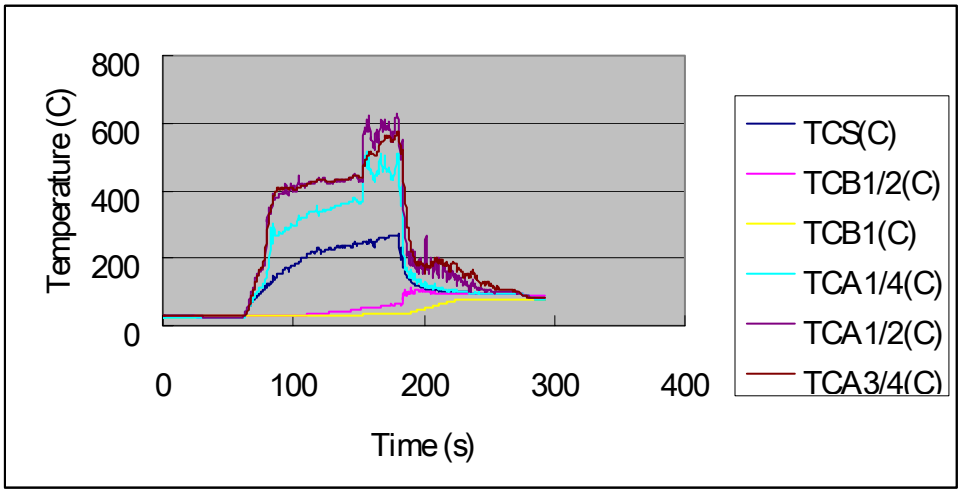

Figure E.47 Temperature profile in Fpc80

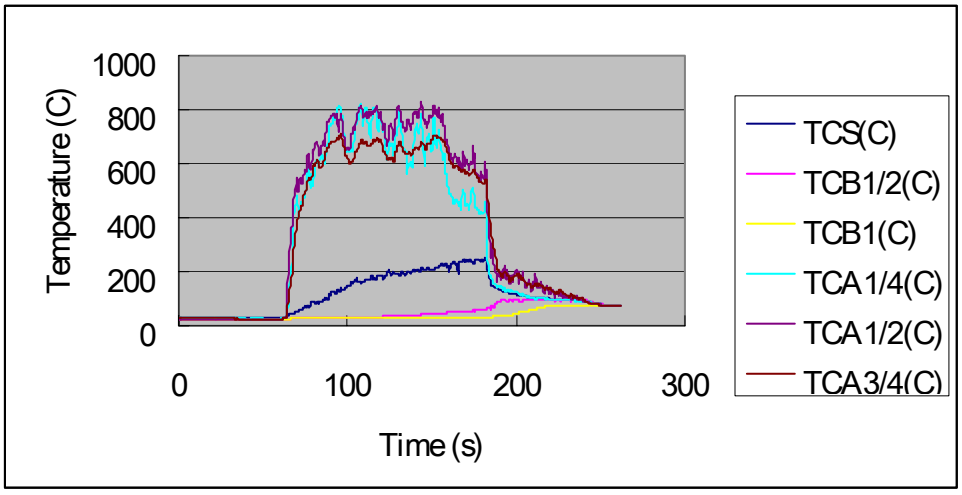

Figure E.48 Temperature profile in Fpc81

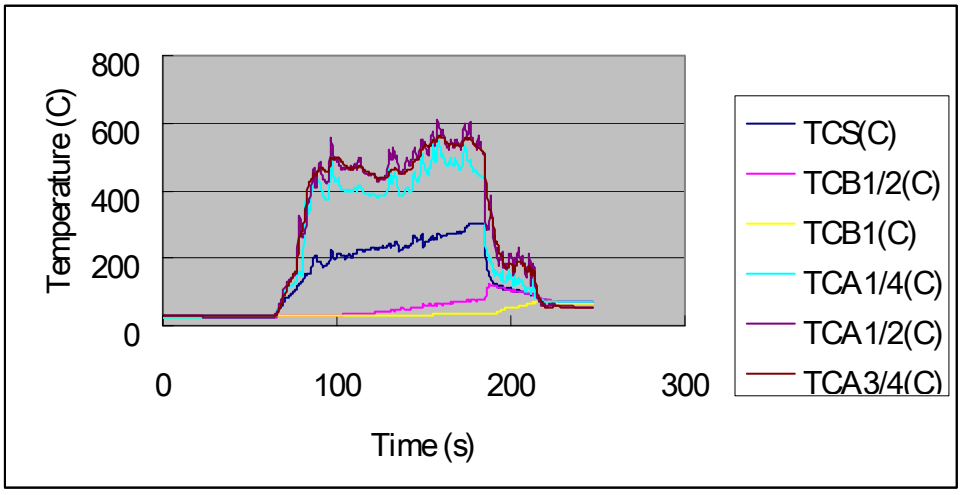

Figure E.49 Temperature profile in Fpc82

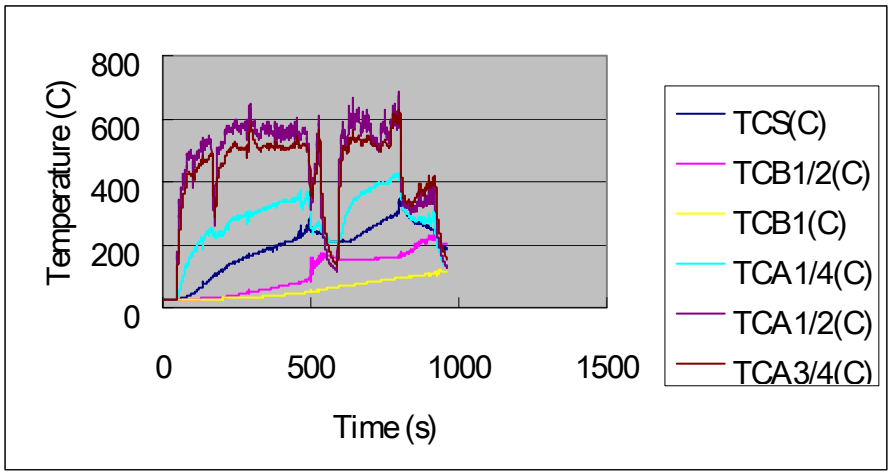

Figure E.50 Temperature profile in Fpc118

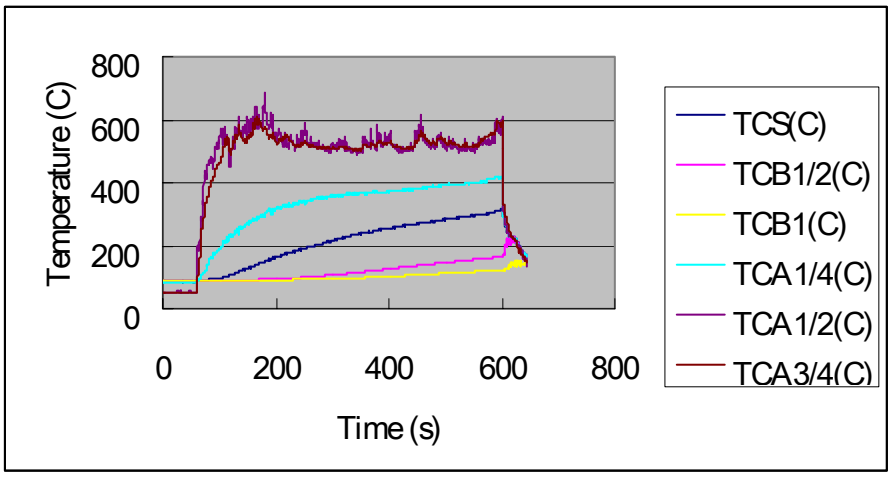

Figure E.51 Temperature profile in Fpc119

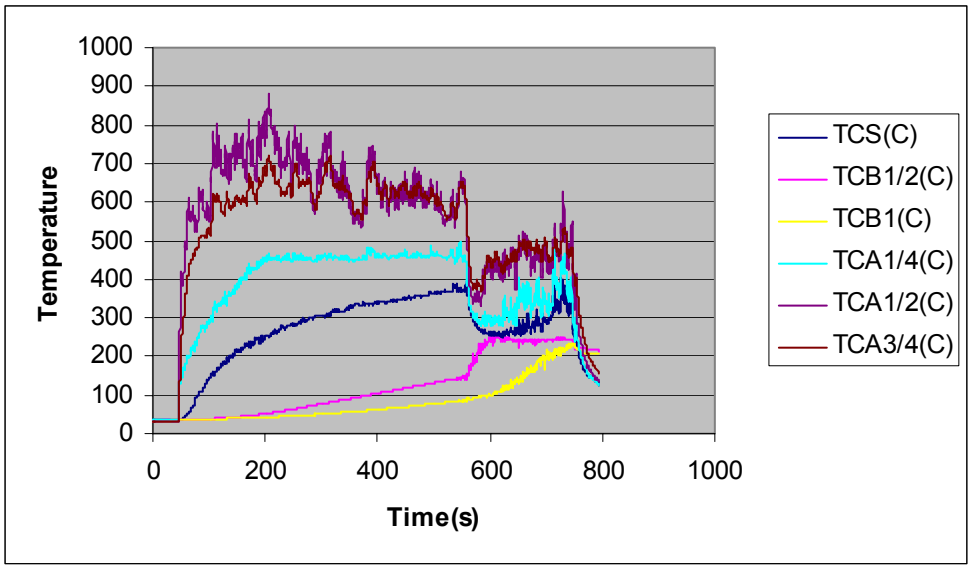

Figure E.52 Temperature profile in Fpc120

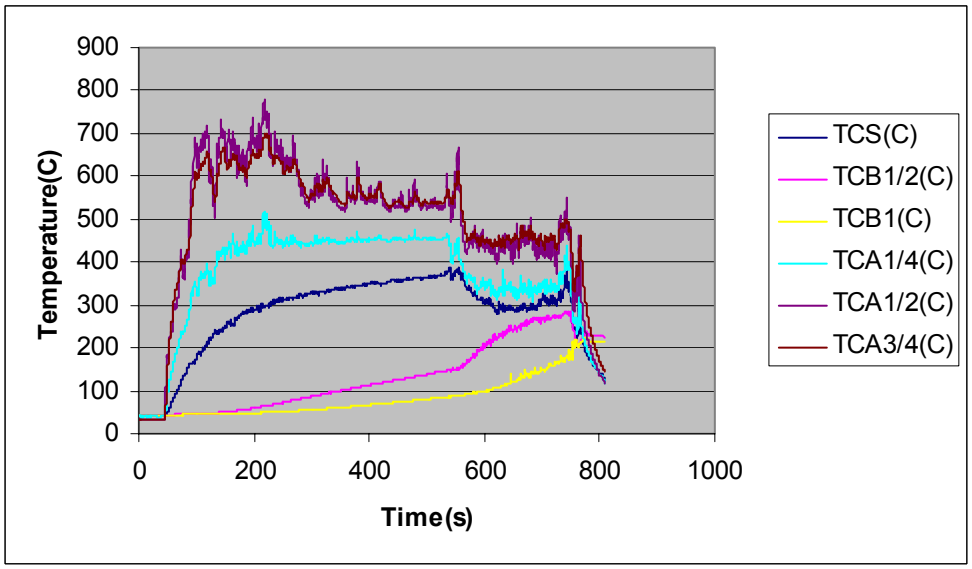

Figure E.53 Temperature profile in Fpc121

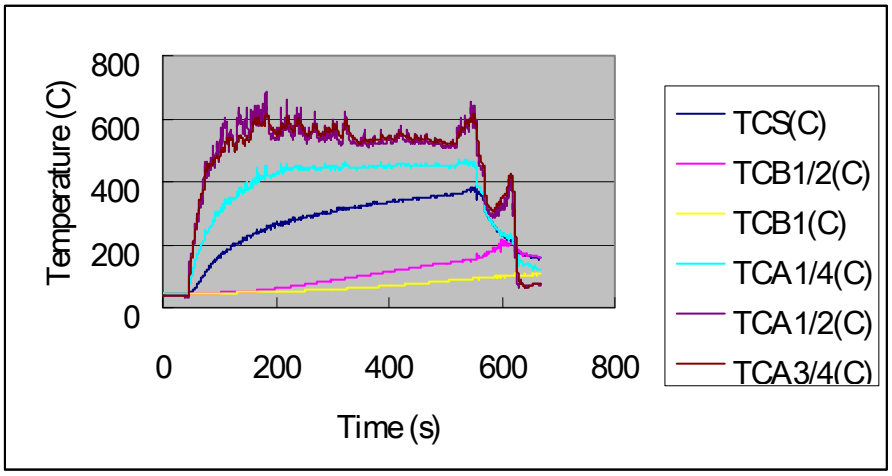

Figure E.54 Temperature profile in Fpc122

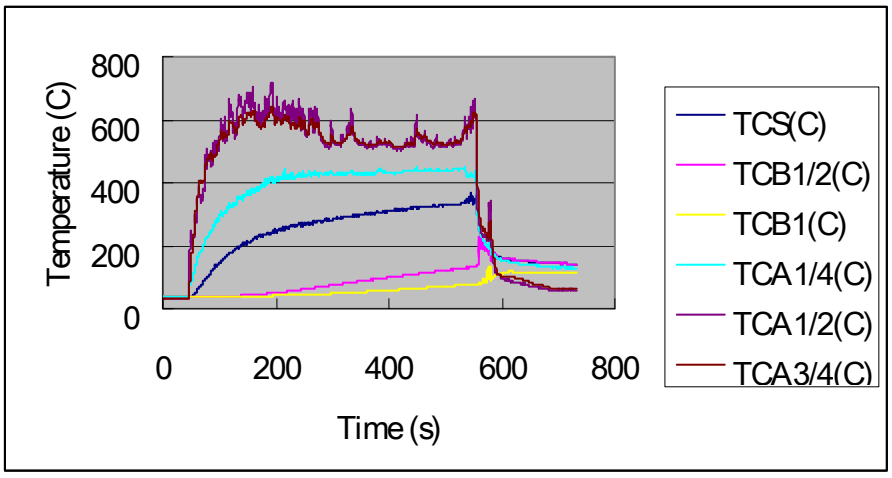

Figure E.55 Temperature profile in Fpc123

NOMENCLATURE

α alpha (kW/m^2)

β beta (g/m^2s)

k thermal conductivity ($kW/m^2\,K$)

$\dot{R}''_{cr,w}$: spray density required to cool the liquid surface to its flash point (gpm/ft^2)

d_w: water mass median diameter $(mm, d_w > 0.4mm)$

T_{FP}: flash point (^0C)

T_w: water temperature (^0C)

t_{ext}: fire extinguishment time (s)

$\dot{R}''_w$: applied water density (gpm/ft^2)

d_w: water drop size (mm)

D: nozzle diameter (mm)

We_n: Weber number in the nozzle based on nozzle velocity

d_w is drop size (mm)

D is the orifice diameter (mm)

C is constant

We_n is Weber number based on nozzle velocity

V_c is the percentage of volume fraction of water droplet

x , n are Rosin- Rammler constants from each test data

$\dot{q}''_e$ is external heat flux on the oil

k is thermal conductivity

ρ_{oil} is oil density

C is heat capacity

h_c is convective heat transfer coefficient

T_{fp} is the fire point of oil

$\dot{m}''_s$ is the oil splattering rate per unit area

$\dot{m}_v''$ is the oil vaporization burning rate per unit area without splattering

A is cross section pan area

χ_s is the combustion fraction of the splattering oil, relative to that oil vapor

ΔH_{chem} is the chemical heat of combustion for mineral seal oil ($\Delta H_{chem} = \chi_v \Delta H_T$)

$\dot{Q}_{chem}$ is chemical heat release rate measured in the fire products collector

$\dot{m}_v''$ is vaporization rate ($\frac{g}{s \cdot m^2}$)

u is vertical wind velocity (m/s)

M_v is the vapor molecular weight (kg/kg-mole)

k_g is the mass transfer coefficient (m/min)

P_{sat} is the liquid saturation vapor pressure (Pa) at T_L

R is the ideal gas constant

T_L is the liquid temperature (^0K)

k_g is the mass transfer coefficient (m/s)

N_{sc} is the Schmidt number ($\frac{\nu}{D}$)

u is the wind velocity 10 m off the ground (m/s)

d_P is the diameter of the pool (m)

ν is the kinematic viscosity (m^2/s)

D is the diffusivity (m^2/s)

X_{co_2} the carbon dioxide concentration in the exhaust (ppm)

$X_{co_{2,\infty}}$ the carbon dioxide concentration in the atmosphere (ppm)

X_{co} the carbon monoxide concentration in the exhaust (ppm)

$X_{co,\infty}$ the carbon monoxide concentration in the atmosphere (ppm)

P_∞ the atmosphere pressure (in. Hg)

ΔP the differential pressure in the exhaust (mmHg)

T_{gas} the temperature in the ambient (K)

T_{amb} the temperature in the exhaust (K)

$\dot{Q}_{chem}$ the chemical heat release rate (kW)

$\dot{Q}_{conv}$ the convective heat release rate (kW)

$H_{(T)}$ The enthalpy (kJ/kg) ($H_T = T + 6.7 \times 10^{-5} T^2 - 2590 / T$)

$\dot{m}''_{dd}(\dot{Q})$ is the water delivered density at $\dot{Q}$ using the same nozzle and flow rate.

$\dot{m}_{w,s}$ is water gain rate in the pan

$\dot{m}_{pan}$ is mass change rate in the pan

$\dot{m}_{loss}$ is the oil loss rate in the pan

d_w : mass median water drop size of the spray in mm

T_{FP} : fire point ($^\circ C$)

T_w : water temperature($^\circ C$)

t_{ext} : fire extinguishment time, sec

$\dot{R}''_w$: applied water density ($\frac{gpm}{ft^2}$)

Y: preburn time in minutes

$\dot{m}''_{cr,w}$ is critical water density (mm/min)

d_w is the water drop size (μm)

$\dot{m}''_{cr,b}$ is the critical burning rate of oil

$\dot{m}''_{cr,w}$ is the critical water density

ΔH_T is the total heat of combustion

φ is the maximum fraction of combustion energy that the flame reactions may loss to the sample surface by convection without flame extinction

ΔH_g is the heat of gasification

$\dot{q}''_{rr}$ is the surface re-radiation loss

ε_w is the water application efficiency

ΔH_w is the heat of gasification of water

Y_O is the oxygen mass fraction

ΔH_O^* is the net heat of complete combustion per unit mass of oxygen consumed (kJ/g)

C_P is the specific heat of air $(kJ/g-K)$

h is the convective heat transfer coefficient (kW/m^2-K)

Q is heat transfer per drop (Btu/drop)

$\rho_{w,L}$ is water density (lb/ft^3)

$\rho_{w,v}$ is water vapor density (lb/ft^3)

u_w is water drop velocity (ft/s)

σ_w is water drop surface tension (lbf/ft)

g_c is constant of proportionality in Newton's second law

$\Delta T = T_s - T_w$ is the temperature difference between the hot plate and water drop

$f(\Delta T)$ is between 0 and 1

Δh_g is modified water heat of gasification ($\Delta h_g = \Delta H_w + C_{pv}(T_{FP} - T_{sat})$)

$\dot{n}$ is the average number of water droplets on the surface per unit time

A is pan area

d_w is drop size

$\dot{m}_w''$ is water density

$\dot{n}''$ is the number of water droplets in contact with liquid per unit liquid surface area per unit time

$$Oh_{oil} = \frac{\mu_w}{(\rho_w \sigma_w d_w)^{1/2}}$$

ρ_w is the oil density (kg/m^3)

σ_w is the oil surface tension (N/m)

d_w is the water drop size (μm)

μ_w is the oil viscosity (kg/ms)

d_w: water drop size (mm)

T_{FP}: fire point ($^\circ$C)

T_w: water temperature($^\circ$C)

t_{ext} : fire extinguishment time (min)

$\dot{R}''_w$: applied water density (mm/min)

$\dot{R}''_{w,c}$: critical water density (mm/min)

U_x = the particle velocity

λ = the wave length of the laser beam

θ = two beam cross angle

f_D = detected frequency

n_1 = refractive index of the scattering medium.

λ = laser wavelength in vacuum.

D = particle diameter.

β_i = geometric factor

$\dot{G}_{CO2}$ and $\dot{G}_{CO}$ = the generation rates (kg/s) of CO_2 and CO, respectively, and

$\dot{G}_{CO2}{}^0$ and $\dot{G}_{CO}{}^0$ = the corresponding measurements before ignition of the specimen.

A_d = test section duct cross sectional area (m^2)

K = flow coefficient of the averaging Pitot tube

P_∞ = the actual atmospheric pressure (Pa)

ΔP = pressure differential across the averaging Pitot tube in the test section duct (Pa)

T_{gas} = gas temperature in the test section duct, measured by a thermocouple (K)

X_{CO2} = the measured volume ratio or mole fraction of CO_2

X_{CO} = the measured volume ratio or mole fraction of CO

$C_P = 1 + 1.34 \times 10^{-4} T - 2590 / T^2$

REFERENCES

[1] AICHE, " Guidelines for Use of Vapor Cloud Dispersion Models", 2nd Edition, 1996.

[2] Back III, Gerard G., Beyler, Craig L., and Hansen, Rich, " A Quasi-Steady-State Model for Predicting Fire Suppression in Spaces Protected by water Mist Systems", Fire Safety Journal, 2000, Volume 35, pp 327-362.

[3] Beaulieu, P., Dembsey, N. and Alpert, R.,"A New Material Flammability Apparatus and Measurement Techniques," Proceedings of SAMPE 2003, Long Beach, CA, May 2003.

[4] Bernardin, John D., Stebbins, Clinton J. and Mudawar, Issam, " Mapping of Impact and Heat Transfer Regimes of Water Drops Impinging on a Polished Surface", International Journal of Heat Mass Transfer. , Volume 40, No.2, pp 247-267,1997.

[5] Bill Jr, R. G., Hansen, R. L. and Richards, K., " Fine Spray (Water Mist) Protection of Shipboard Engine Rooms", Fire Safety Journal, 1997, Volume 29, pp 317-336.

[6] Brenn, G., and Frohn, A., "Collision and Coalescence of Droplets of Various Liquids", J. Aerosol Sci., 1989, Vol. 20, No. 8, PP. 1027-1030.

[7] Chan, Tak-Sang, Kung, Hsiang-Cheng, Yu, Hong-Zeng and Brown, William R.," Experimental Study of Actual Delivered Density for Rack-Storage Fires" International Symposium on Fire Safety Science (1994), pp.913-924

[8] Chandra, S., Marzo, M. di, Qiao, Y. M., and Tartarini, P., " Effect of Liquid-Solid Contact Angle on Droplet Evaporation", Fire Safety Journal, 1996, vol27, pp141-158.

[9] Cossaii, G.E., Coghe, A., Marengo, M.," The Impact of a Single Drop on a Wetted solid Surface", Experiments in Fluids, Volume 22, pp 463-472, 1997.

[10] Dantec Measurement Technology, Fiber PDA Flow and Particle Software Installation and User's Guide, 2000.

[11] Dantec Measurement Technology, Fiber PDA Installation and User's Guide, 2000.

[12] Dombrowsky, N., F., F.Inst., and Wolfsohn, D.L., " The Atomisation of Water by Swirl Spray Pressure Nozzles", TRANS INSTN CHEM. ENGRS, Vol. 50, 1972.

[13] Derevich, I.V., " Statistical Modeling of Mass Transfer in Turbulent Two Phase Dispersed Flows-1. Model Development" International Journal of Heat and Mass Transfer, 2000,Vol. 43, pp 3709-3723.

[14] Derevich, I.V., " Statistical Modeling of Mass Transfer in Turbulent Two Phase Dispersed Flows-2. Calculation Results" International Journal of Heat and Mass Transfer, 2000,Vol. 43, pp 3725-3734.

[15] Drysdale, D." An Introduction to Fire Dynamics 1st edition", Wiley.
"

[16] Dundas, P. H., "Optimization of Sprinkler Fire Protection – Progress Report No. 10 - The Scaling of Sprinkler Discharge: Prediction of Drop Size", Technical Report, FMRC RC73-T-40, June 1974

[17] Eisenberg, Jon, Gilda, Brian, and Till, Bernie, Engineering Evaluation of Fire Hazards and Consequences, WPI FP573 Project.

[18] Ewing, Curtis T. and Beyler, Craig L.,"Extinguishment of Class B Flames by Thermal Mechanism; Principles Underlying a Comprehensive Theory; Prediction of Flame Extinguishing Effectiveness" Journal of Fire Protection Engineering, 1994,pp23-54.

[19] FMGlobal, "Transformers " FM DATA SHEET 5-4.

[20] FMGlobal, “Oil cookers” FM DATA SHEET 7-20.

[21] FMGlobal,”Lack of Dissolved-Gas-in-Oil Analysis for Transformers”, Understanding of Hazard, December 2001.

[22] Heskestad, Gunner and Dobson, Paul H., “ Pool Fires of Transformer Oil Sinking into a Rock Bed”, Fire Safety Journal, 1997, Volume 28, pp 33-46.

[23] Hemstreet, R. A., Flammability Tests of Askarel Replacement Transformer Fluids, Technical Report, FMRC RC78-T-43, August, 1978.

[24] Hung, Ling-Shun, Investigations of the Transport and Dynamics of Droplets Impacting on Complex Objects, PhD Dissertation, Department of Mechanical Engineering, Carnegie Mellon University, April 1998.

[25] Kang, Myeong-Gie, “Effect of Surface Roughness on Pool Boiling Heat Transfer”, International Journal of Heat and Mass Transfer, 2000,Vol. 43, pp 4073-4085.

[26] Kim, Myung Bae, Jang, Yong Jae and Kim, Jin Kook, “ Burning Rate of a Pool Fire with Downward-directed Sprays”, Fire Safety Journal, 1996, Volume 27, pp 37-48.

[27] Kim, Myung Bae, Jang, Yong Jae and Kim , Jin Kook, “ Extinction Limit of a Pool Fire With a Water Mist”, Fire Safety Journal, 1997, Volume 28, pp 295-306.

[28] Kokkala, Matti A.,” Fixed Water Sprays Against Open Liquid Pool Fires”, VTT.

[29] Kung, Hsiang-Cheng and Stavrianidis, Paraskevas, Plume Behavior of Large-Scale Pool Fires, Technical Report, FMRC J.I. 0C0E6. RA 070 (A), November, 1982.

[30] Liter, Scott G., and Kaviany, Massoud, "Pool-boiling CHF Enhancement by Modulated Porous-layer Coating: Theory and Experiment", International Journal of Heat and Mass Transfer, 2000,vol. 44, pp 4287-4311.

[31] Liu, W., Nariai, H., and Inasaka, F., " Prediction of Critical Heat Flux for Subcooled Flow Boiling" International Journal of Heat and Mass Transfer, 2000,vol. 43, pp3371-3390.

[32] MacKay, D., and R.S. Matsuga (1973), "Evaporation of Liquid Hydrocarbon Spills on Land and Water." The Canadian Journal of Chemical Engineering, Vol. 51, August, pp.434-439.

[33] Macklin, WC, Metaxas GJ (1976) Splashing of Drops on Liquid Layers. Journal of Applied Physics 47:3963.

[34] Manzello, Samuel L. and Yang, Jiann C., "The Influence of Liquid Pool Temperature on the Critical Impact Weber Number for Splashing", Physics of Fluids, Vol 15, Number 1, pp257-260, January 2003.

[35] Marzo, M. DI and Tinker S., "Evaporative Cooling Due to a Sparse Spray", Fire Safety Journal 27 (1996) 289-303.

[36] Nam, Soonil, " Application of Water Sprays To Industrial Oil Cooker Fires, FMRC J.I.0003005113, August 2001.

[37] Nam, Soonil, " Development of a Computational Model Simulating the Interaction Between a Fire Plume and a Sprinkler Spray", Fire Safety Journal, 1996, Volume 26, pp 1-33.

[38] Nam, Soonil, " Numerical Simulation of the Penetration Capability of Sprinkler Sprays", Fire Safety Journal, 1999, Volume 32, pp 307-329.

[39] Nash, P., “The Fire Protection of Flammable Liquid Storages with Water Sprays”, International Chemical Engineering Symposium No.39 (1974), pp1-18

[40] Ndubizu, C.C., Ananth, R., Tatem, P. A., and Motevalli, V., “ On Water Mist Fire Suppression Mechanisms in a Gaseous Diffusion Flame”, Fire Safety Journal, 1998, Volume 31, pp 253-276.

[41] Newman, Jeffrey S.,”Determinationof Theoretical and Chemical Heats of Combustion of Chemical Substances”, FM Report, JANUARY 1994.

[42] NFPA 15, Standard for Water Spray Fixed Systems for Fire Protection, 2001 edition, National Fire Protection Association.

[43] NFPA 30, Flammable and Combustible Liquids Code, 1996 edition, National Fire Protection Association.

[44] NFPA 34, Standard for Dipping and Coating Processes Using Flammable or Combustible liquids, 1995 edition, National Fire Protection Association.

[45] Notarianni, Kathy A., “ Water Mist Suppression Systems”, Proceedings of Technical Symposium on Halon Alternatives, June 27-28, 1994.

[46] Nyankina, K. and Turan, O.F., “ Optimal Droplet Diameter and Relative Sprinkler Location in Fire Sprinkler Interation”, International Symposium on Fire Safety Science (1999), pp.421-432

[47] Pasandideh-Fard, M., Bhola, R., Chandra, S., and Mostaghimi, J., “ Deposition of Tin Droplets on a Steel Plate: Simulations and Experiments”, International Journal of Heat and Mass Transfer, 1998,Vol. 41, pp 2929-2945.

[48] Prasad, Kuldeep, Li, Chiping, and Kailasanath, K., " Simulation of Water Mist Suppression of Small Scale Methanol Liquid Pool Fires" Fire Safety Journal, 1999, Volume 33, pp 185-212.

[49] Putorti, "Application of the critical radiative ignition flux methodology to high viscosity petroleum fractions." WPI thesis, 1994.

[50] Qiao, Y. M., and Chandra, S., " Boiling of Droplets on a Hot Surface in Low Gravity", International Journal of Heat and Mass Transfer, 1996,Vol. 39, pp 1379-1393.

[51] Qian, J., and Law, C. K., "Regimes of Coalescence and Separation in Droplet Collision", J. Fliud Mech. (1997), vol. 331. pp59-80.

[52] Rasbash, D.J. and Rogowski, Z. W., "The Extinction of Open Fires with Water Sprays ", Fire Research Note No. 58, 1953

[53] Rasbash, D.J., "The Properties of Sprays Produced by Batteries of Impinging Jets", Fire Research Note No. 181, 1955

[54] Rasbash, D.J. and Rogowski, Z. W., "Extinction of Fire in Liquids by Cooling with Water Sprays", Cobustion and Flame, (1957), vol 1, pp.453-466.

[55] Rasbash, D.J., Rogowski, Z. W., and Stark, G.W.V., "Mechanisms of Extinction of Liquid Fires with Water Sprays", Combustion and Flame 4, 223-334, 1960

[56] Rasbash, D.J., "The Extinction of Fire by Water Sprays", Fire Research Abstracts and Reviews 4: 1 and 2, 28-52, 1962

[57] Rasbash, D. J., A.R.C.S., D.I.C. and Stark, G.W.V., "Some Aerodynamic Properties of Sprays", the Chemical Engineer, December, 1962.

[58] Rasbash, D.J., "The Extinction of Fire with Plain Water: A Review", International Symposium on Fire Safety Science (1985), pp.1145-1163

[59] Roberts, A. F. and Quince, B. W., "A Limiting Condition for the Burning of Flammable Liquids", Combustion and Flame 20, 245-251 (1973)

[60] Sharma, T.P., Badami, G. N., LAL, B. B., and Singh, Jagbir," A New Particulate Extinguishant for Flammable Liquid Fires", International Symposium on Fire Safety Science (1988), pp.667-677

[61] Shiraz, D. Aziz, and Chandra, Sanjeev, " Impact Recoil and Splashing of Molten Metal Droplets", International Journal of Heat and Mass Transfer, 2000,Vol. 43, pp 2841-2857.

[62] Tewarson,A., "Generation of Heat and Chemical Compounds in Fires", The SFPE Handbook of Fire Protection Engineering 2nd Edition, Chapter 3 pp 53-124.

[63] Tewarson, A., Lee J.L. and Pion, R.F.,"The influence of Oxygen Concentrarion on Fuel Parameters for Fire Modeling", Eighteenth Symposium on Combustion, 563-570 (1981)

[64] Toda, Saburo,"A Study of Mist Cooling (1st Report: Investigation of Mist Cooling)", Heat Transfer Janpan Research, Vol 1, Issue 3, pp 39-55, 1972

[65] Toda, Saburo,"A Study of Mist Cooling (2st Report: Theory of Mist Cooling and Its Fundamental Experiments)", Heat Transfer Japan Research, Vol 3, Issue 1, pp 1-44, 1974

[66] Unoki, Juzo, " Fire Extinguishing Time by Sprinkler", International Symposium on Fire Safety Science (1985), pp.1187-1196

[67] Walavalkar, A. Y. and Kulkarni, A. K.," Combustion of Water-in-Oil Emulsion Layers Supported on Water", Combustion and Flame 125, pp1001-1011, (2001)

[68] Wang, Xishi, Liao,Guangxuan, Qin , Jun and Fan, Weicheng," Experimental Study on the Effectiveness of the Extinction of a Pool Fire with Water Mist", Journal of Fire Sciences, Vol. 20, July 2002, pp.279-295

[69] Wang, Weining, " Mathematical Method of Vaporization during Gasline Spills", WPI thesis, 1997.

[70] Widmann, John F., " Characterization of a Residential Fire Sprinkler using Phase Doppler Interferometry", Fire Safety Journal, 2001, Volume 36, pp 545-567.

[71] Wighus, Ragnar," Extinguishment of Enclosed Gas Fires with Water Spray", International Symposium on Fire Safety Science (1991), pp.997-1006

[72] Worthington, A. M., A Study of Splash, September, 1907.

[73] Yao, Bin, Fan, Weicheng, and Liao, Guangxuan, " Interaction of water Mists with a Diffusion Flame in a Confined Space", Fire Safety Journal, 1999, Volume 33, pp 129-139.

[74] Yao, C., and Kalelkar, A.S., Effect of Drop Size on Sprinkler Performance, FMRC Technical Report, Series No. 18792, May 1970.

[75] Yu, Hong-Zeng, " Investigation of Spray Patterns of Selected Sprinklers with the FMRC Drop Size Measuring System", International Symposium of Fire Safety Science (1985), pp.1165-1176.

[76] Yu, Hong-Zeng, Sprinkler Drop Size Measurement Part II: An Investigation of The Spray Patterns of Selected Commercial Sprinklers with The FMRC PMS Droplet Measuring System, Technical Report, FMRC J. I. 0G1E7. RA070(A), May 1983.

[77] Zalosh, G. R.” Industrial Fire Protection Engineering”, Wiley, 2003.

[78] Zhang, H., “ Theoretical Analysis of Spreading Solidification of Molten Droplet During Thermal Spray Deposition”, International Journal of Heat and Mass Transfer, 1999,Vol. 42, pp 2499-2508.

[79] Zhang, H., Wang, X. Y., Zheng, L.L., and Jiang, X.Y., “ Study of Splat Morphology and Rapid Solidification during Thermal Spraying”, International Journal of Heat and Mass Transfer, 2001,Vol. 44, pp 4579-4592.